



THE HONG KONG  
POLYTECHNIC UNIVERSITY

香港理工大學

Pao Yue-kong Library

包玉剛圖書館

---

## Copyright Undertaking

This thesis is protected by copyright, with all rights reserved.

**By reading and using the thesis, the reader understands and agrees to the following terms:**

1. The reader will abide by the rules and legal ordinances governing copyright regarding the use of the thesis.
2. The reader will use the thesis for the purpose of research or private study only and not for distribution or further reproduction or any other purpose.
3. The reader agrees to indemnify and hold the University harmless from and against any loss, damage, cost, liability or expenses arising from copyright infringement or unauthorized usage.

### IMPORTANT

If you have reasons to believe that any materials in this thesis are deemed not suitable to be distributed in this form, or a copyright owner having difficulty with the material being included in our database, please contact [lbsys@polyu.edu.hk](mailto:lbsys@polyu.edu.hk) providing details. The Library will look into your claim and consider taking remedial action upon receipt of the written requests.

**SMART ACOUSTIC LEAK DIAGNOSIS IN WATER  
DISTRIBUTION NETWORKS: LEVERAGING  
MACHINE LEARNING APPROACHES**

**RONGSHENG LIU**

**PhD**

**The Hong Kong Polytechnic University**

**2025**

**The Hong Kong Polytechnic University**

**Department of Building and Real Estate**

**Smart Acoustic Leak Diagnosis in Water Distribution  
Networks: Leveraging Machine Learning Approaches**

**Rongsheng Liu**

**A thesis submitted in partial fulfilment of the  
requirements for the degree of Doctor of Philosophy**

**Sep 2024**

## **CERTIFICATE OF ORIGINALITY**

I hereby declare that this thesis is my own work and that, to the best of my knowledge and belief, it reproduces no material previously published or written, nor material that has been accepted for the award of any other degree or diploma except where due acknowledgement has been made in the text.

\_\_\_\_\_ (Signed)

Rongsheng LIU (Name of student)

# Abstract

Water leakage in the water distribution network (WDN) is a significant issue leading to infrastructure damage, economic loss, and potential health hazards, emphasizing effective solutions. Among the various leak detection and localization methods, acoustic-based approaches are widely employed for their comprehensive capabilities. However, their effectiveness depends heavily on signal quality and is susceptible to external factors, requiring substantial prior knowledge. Given the remarkable performance of machine learning (ML) techniques, they have been introduced into leak diagnosis, offering significant benefits while also introducing new challenges.

This study aims to propose an acoustic ML leak diagnosis framework and complete the following objectives: 1) Propose a generative approach that augments the leak detection dataset, addressing the data scarcity-related problems for WDNs. 2) Establish an explainable leak detection model, enhancing the interpretability and entailing comprehensive analysis of collected signals. 3) Develop an effective and robust time-series leak detection model for WDN, and facilitate smart leak detection in real scenarios. 4) Develop a robust time-delay estimation deep learning leak localization model for WDN.

The key findings can be concluded as four points. First, an innovative data augmentation approach has been proposed to enhance the vibroacoustic datasets. The generated samples have been demonstrated to have similar acoustic features to real samples, contributing to improving leak detection accuracy. Second, an explainable deep learning framework has been proposed to enhance interpretability during leak detection

modeling and deepen the understanding of the decision-making mechanism of deep learning models.

Third, the Time-Transformer leak detection model has been proposed to enhance detection accuracy. The proposed model utilizes the attention mechanism, capturing the temporal patterns inherent in signals. The empirical results demonstrate that the Time-Transformer outperforms alternative models, achieving 88.46% accuracy in out-of-sample validation. Fourth, a time-delay-based leak localization model has been proposed. The model harnesses the complex pattern recognition capabilities of deep learning techniques to deduce the time delay of signal pairs. The deep learning leak localization model exhibits reduced prediction error compared to basic cross-correlation, particularly in low signal-to-noise ratio (SNR) conditions.

This study contributes to the development of ML-based acoustic leak diagnosis. Theoretically, it expands the knowledge of water leak diagnosis by providing a comprehensive review of ML applications in acoustic leak detection and proposing advanced data augmentation techniques for acoustic data. Additionally, this study is the first to reveal the underlying mechanisms of acoustic leak detection models, thereby enhancing their interpretability. The experiments validate the effectiveness of one- and two-dimensional data for leak detection and introduce a novel deep-learning model to estimate the time delay of signal pairs for leak localization. Practically, this study contributes to developing a smart acoustic leak detection system, improving the accuracy and reliability of leak diagnosis, reducing maintenance costs and resource waste, advancing the understanding and acceptance of ML techniques for leak detection, and facilitating the progress of smart leak management systems.

## **Publications arising from the thesis**

### **Referenced Paper:**

[1] R. Liu, T. Zayed, R. Xiao, Advanced Acoustic Leak Detection in Water Distribution Networks Using Integrated Generative Model, *Water Research* (2024) 121434. <https://doi.org/10.1016/j.watres.2024.121434>.

[2] R. Liu, T. Zayed, R. Xiao, Q. Hu, Time-Transformer for acoustic leak detection in water distribution network, *Journal of Civil Structural Health Monitoring* (2024) 1–17. [10.1016/j.watres.2024.122600](https://doi.org/10.1016/j.watres.2024.122600)

[3] R. Liu, T. Zayed, R. Xiao, Acoustic leak localization for water distribution network through time-delay-based deep learning approach, *Water Research* 268 (2025) 122600. <https://doi.org/10.1016/j.watres.2024.122600>.

### **Related Paper:**

[4] R. Liu, T. Zayed, R. Xiao, Contrastive learning method for leak detection in water distribution networks, *Npj Clean Water* 7 (2024) 118. <https://doi.org/10.1038/s41545-024-00406-6>.

[5] R. Liu, S. Tariq, I.A. Tijani, A. Fares, B. Bakhtawar, H. Fan, R. Zhang, T. Zayed, Data-Driven Approaches for Vibroacoustic Localization of Leaks in Water Distribution Networks, *Environ. Process.* 11 (2024) 14. <https://doi.org/10.1007/s40710-024-00682-x>.

## **Acknowledgements**

I want to extend my gratitude to the Department of Building and Real Estate at The Hong Kong Polytechnic University for providing financial support and equipment for my Ph.D. study.

I want to express my deepest gratitude to my supervisor, Prof. Tarek Zayed, for his unwavering support, invaluable guidance, and continuous encouragement throughout my research and the writing of this thesis. His expertise and insights were instrumental in shaping this work.

I would also like to acknowledge the financial support provided by the Innovation and Technology Fund (Innovation and Technology Support Programme (ITSP)), Hong Kong, and the Water Supplies Department, Hong Kong, under grant number ITS/067/19FP, which made this research possible.

Meanwhile, I am immensely grateful to Dr. Hu Qian for her encouragement and Dr. Xiao Rui for his academic guidance. Furthermore, I sincerely thank Mr. Liu Zhuqi and Mrs. Chi Biyu for their decades of selfless support.

Lastly, I am grateful to all those who contributed, directly or indirectly, to the successful completion of this thesis. Your support has been invaluable and deeply appreciated.

# Table of Contents

Abstract.....	I
Publications arising from the thesis.....	III
Acknowledgements .....	IV
Table of Contents.....	V
List of Figures.....	IX
List of Tables .....	XII
Nomenclature.....	XIII
CHAPTER 1 Introduction .....	1
1.1 Introduction .....	1
1.2 Background .....	1
1.3 Research Scope and Problem Statement.....	5
1.4 Research Objectives .....	7
1.5 Research Methodology.....	8
1.6 Structure of The Thesis .....	11
CHAPTER 2 Literature Review .....	13
2.1 Introduction .....	13
2.2 Overall Development Trend.....	13
2.3 Leak Signal Management and Enhancement.....	16
2.3.1 Leak Signal Collection .....	16
2.3.2 Data Preprocessing .....	17
2.4 Leak Pattern Extraction and Analysis.....	25
2.4.1 Leak Feature Extraction.....	25
2.4.2 Feature Selection .....	35
2.5 Acoustic-based Water Leak Detection Models.....	39
2.5.1 Development of HFB Models.....	39
2.5.2 Development of Deep Learning Model .....	46
2.6 Research Gaps .....	53
2.6.1 Limitation and Gaps .....	54

2.6.2 Future Directions .....	59
2.7 Chapter Summary.....	67
CHAPTER 3 Research Design and Methodology.....	68
3.1 Introduction .....	68
3.2 The Framework of Methodology .....	68
3.3 Research Method.....	71
3.3.1 Machine Learning Model .....	71
3.3.2 Analytical and Process Tools.....	85
3.4 Chapter Summary.....	92
CHAPTER 4 Generative Approach for Data Augmentation and Enhancement.....	93
4.1 Introduction .....	93
4.2 The framework for the generative model for data augmentation .....	93
4.2.1 Data Collection .....	95
4.2.2 LSTM-GAN for Enhancing Acoustic Dataset.....	97
4.2.3 Generative Result Evaluation .....	100
4.3 Generative Results Evaluations and Discussion .....	104
4.3.1 t-SNE Results.....	104
4.3.2 Acoustic Characteristics Analysis Results .....	106
4.3.3 Model Augmentation Validation Analysis .....	107
4.4 Model Comparison.....	111
4.5 Chapter Summary.....	115
CHAPTER 5 Model Explanation and Interpretation .....	117
5.1 Introduction .....	117
5.2 Development of Time-Frequency Spectrum Visualization Framework.....	117
5.2.1 Data Preprocessing .....	118
5.2.2 Leak Detection Modeling .....	120
5.2.3 Grad-CAM Interpretation .....	121
5.3 Model Results Evaluation and Interpretability Discussion.....	122

5.3.1 Experiment Setup and Data Preparation.....	122
5.3.2 Performances of the Proposed CNNs .....	123
5.3.3 Grad-CAM Interpretation Results .....	127
5.4 Chapter Summary.....	136
CHAPTER 6 Time-series-based Deep Learning Model for Leak Detection.....	138
6.1 Introduction .....	138
6.2 Development of Transformer-based Leak detection Framework .....	138
6.2.1 Data Collection & Processing.....	139
6.2.2 Time-series Leak Detection Modeling .....	140
6.2.3 Model Performance Evaluation .....	142
6.3 Leak Detection Evaluation and Discussion .....	143
6.3.1 Parametric Experiment .....	143
6.3.2 Model Identification Results.....	145
6.3.3 Feature Vectors Visualization.....	149
6.3.4 Discussion.....	151
6.4 Chapter Summary.....	152
CHAPTER 7 Time-delay-based Leak Localization Model for WDNs.....	154
7.1 Introduction .....	154
7.2 Framework for Time-Delay Estimation Deep Learning Model .....	154
7.2.1 Data Preparation .....	156
7.2.2 Leak Localization Model Development .....	158
7.2.3 Model Experiments.....	161
7.3 Leak Localization Experiments & Evaluation .....	165
7.3.1 Model Parametric Experiments .....	165
7.3.2 Comparison of Techniques .....	166
7.3.3 Sensitivity Analysis .....	169
7.4 Case Study for Leak Localization .....	182

7.5 Discussion .....	184
7.6 Chapter Summary.....	186
CHAPTER 8 Conclusions and Recommendations .....	187
8.1 Introduction .....	187
8.2 Summary of Findings.....	187
8.3 Contribution of the Research .....	189
8.4 Limitations and Future Research .....	191
8.4.1 Limitations .....	191
8.4.2 Future Studies .....	193
References .....	195

## List of Figures

Figure 1.1 Research objectives, methods, and outcome.....	12
Figure 2.1 The trend of published ML-based acoustic leak diagnosis papers .....	14
Figure 2.2 Mapping of mainstream journals in the domain of ML-based water leak detection.....	15
Figure 2.3 The number of studies applied field measurements and laboratory experiments (a) The trend of annual published papers (b) The proportion for all published papers .....	17
Figure 2.4 Applied HFB models for water pipe leak detection.....	40
Figure 2.5 General workflow of cnn for water pipe leak detection .....	49
Figure 2.6 Summary of limitations and potential future directions .....	53
Figure 3.1 Framework of the overall research methodology .....	70
Figure 3.2 Typical framework for CNN.....	71
Figure 3.3 The typical model structure of AlexNet.....	72
Figure 3.4 The typical model structure of VGGs.....	73
Figure 3.5 The typical structure of Residual blocks.....	74
Figure 3.6 A concept diagram for the long short-term memory model .....	76
Figure 3.7 A typical structure of the generative adversarial neural network .....	78
Figure 3.8 A concept diagram for the LSTM-GAN model.....	80
Figure 3.9 The main components of the time-series tokenizer .....	81
Figure 3.10 A typical structure of multi-head attention .....	83
Figure 4.1 The framework of the proposed method.....	94
Figure 4.2 Phase I: Data Collection and Preprocessing Roadmap .....	95
Figure 4.3 Spectrogram images of the acoustic signals from leak statues (a) leak signals; (b) noleak signals.....	97
Figure 4.4 The neural structures of GAN (a) Discriminator (b) Generator .....	99
Figure 4.5 Data split for model testing and validation .....	103
Figure 4.6 t-SNE results for comparing generated and original datasets (a) Comparison among leak, noleak, and generated data (b) Comparison between leak and generated data.....	105

Figure 4.7 KDE results for acoustic characteristics of original and enhanced datasets .....	106
Figure 4.8 Sensitivity analysis of generated samples through t-SNE results .....	108
Figure 4.9 The testing and validation results of models trained with various enhanced dataset .....	110
Figure 4.10 t-SNE results from various generative methods .....	111
Figure 4.11 The model performances on testing and validation dataset .....	113
Figure 5.1 Proposed framework of explainable leak detection for WDNs. ....	117
Figure 5.2 A typical Grad CAM result from the leak detection model for demonstration. ....	121
Figure 5.3 The performance of CNN models in the testing dataset. ....	125
Figure 5.4 The model performance comparison between testing and out-of-sample results. ....	126
Figure 5.5 Grad-CAM visualization results comparison among various models based on leak signal (i). ....	128
Figure 5.6 Grad-CAM visualization compares various models based on leak signal (ii). ....	129
Figure 5.7 Grad-CAM visualization results in comparison among various models based on noleak signal (i). ....	130
Figure 5.8 Grad-CAM results for leak signals (iii) and (iv). ....	132
Figure 5.9 Grad-CAM results for leak signal (v) and (vi). ....	133
Figure 5.10 Grad-CAM results for leak signal (vii) and (viii). ....	134
Figure 5.11 Grad-CAM results for noleak signal (ii) and (iii). ....	135
Figure 6.1 The structures of other time-series DL models .....	146
Figure 6.2 The performances of models on the testing dataset .....	147
Figure 6.3 The performances of models on the out-of-sample validation dataset ....	148
Figure 6.4 t-SNE results of the feature vectors extracted from DL models (a) Origin samples, (b) Transformer, (c) 1D-CNN, (d) CNN-LSTM .....	150
Figure 7.1 Overall framework for deep-learning-based leak localization modeling .	155
Figure 7.2 The structure of the Res1D-CNN leak localization model .....	160
Figure 7.3 Framework for model experiments and discussion. ....	161

Figure 7.4 The scatter plot of the time-delay result based on clean data .....	167
Figure 7.5 The distribution of MAE of time-delay results .....	168
Figure 7.6 The distribution of RMSE of time-delay results .....	169
Figure 7.7 The scatter plot of the time-delay results under WGN .....	171
Figure 7.8 The performance metrics of time-delay results under WGN .....	172
Figure 7.9 The scatter plot of time-delay results for mixed datasets under WGN.....	173
Figure 7.10 The distribution of RMSE and MAE based on the mixed dataset under WGN.....	174
Figure 7.11 The leak distance error under WGN .....	175
Figure 7.12 The scatter plot of the time-delay results under alpha-stable noise .....	176
Figure 7.13 The performance metrics of time-delay results under alpha-stable noise .....	178
Figure 7.14 The scatter plot of time-delay results for mixed datasets under alpha-stable noise .....	179
Figure 7.15 The distribution of RMSE and MAE based on the mixed dataset under Alpha-stable noise .....	181
Figure 7.16 The leak distance error under alpha-stable noise .....	182
Figure 7.17 The deployment diagram of field experiments .....	183

## List of Tables

Table 2.1 Applied filter in ML-based leak diagnosis studies .....	21
Table 2.2 Summary of signal decomposition methods in acoustic water leak diagnosis .....	24
Table 2.3 The applied features for ML-based modeling .....	26
Table 2.4 Applied Multi-Dimension Representation Processing for Leak Detection Studies .....	32
Table 2.5 The applied feature selection indicator .....	38
Table 2.6 A summary of HFB models for water leak detection using acoustic signals .....	45
Table 2.7 Applied optimization techniques and improved structure for CNN .....	47
Table 4.1 Pseudocode of LSTM-GAN for generating leak signals .....	100
Table 6.1 The volume of datasets for model evaluation .....	139
Table 6.2 Parameters for the Proposed Time-Transformer .....	141
Table 6.3 Influence of the hyperparameters on Time-Transformer .....	144
Table 7.1 Influence of the hyperparameters on Res1D-CNN .....	166

## Nomenclature

WDN	:	Water distribution network
ML	:	Machine learning
SNR	:	Signal-to-noise ratio
RMS	:	Root mean square
BCC	:	Basic-cross-correlation
DL	:	Deep learning
STFT	:	Short-time fourier transform
CWT	:	Continuous wavelet transform
GAN	:	Generative adversarial network
t-SNE	:	T-Distributed Stochastic Neighbor Embedding
Grad-CAM	:	Gradient-weighted Class Activation Mapping
CNN	:	Convolutional neural network
VMD	:	Variational mode decomposition
LSTM	:	Long-short-term-memory
SMOTE	:	Synthetic minority oversampling technique
SVD	:	Singular value decomposition
WT	:	Wavelet transform
EMD	:	Empirical mode decomposition
VMD	:	Variational mode decomposition
IMFs	:	Intrinsic mode function
WT	:	Wavelet transform
ZCR	:	Zero crossing rate
MIE	:	Monitor index efficiency
ApEn	:	Approximate entropy
SampEn	:	Sample entropy
MLE	:	Maximum Lyapunov exponent
SHAP	:	Shapley Additive explanations
HFB	:	Handcrafted feature-based
ANN	:	Artificial neural network
SVM	:	Support vector machine
KNN	:	K-nearest neighbors

GMM	:	Gaussian mixture model
DT	:	Decision tree
RF	:	Random forest
VGG	:	Visual geometry group
TL	:	Transfer learning
CAE	:	Convolutional autoencoders
VAE	:	Variational autoencoder
RNN	:	Recurrent neural network
ReLU	:	Rectified linear unit
GeLU	:	Gaussian error linear unit
MLP	:	Multi-layer perceptron
KDE	:	Kernel distribution estimation
BCE	:	Binary cross-entropy
MSE	:	Mean squared error
MAE	:	Mean absolute error
RMSE	:	Root mean squared error
$R^2$ .	:	Coefficient of determination
GCC-SCOT	:	Generalized cross-correlation - Smoothed Coherence Transform

# **CHAPTER 1 Introduction**

## **1.1 Introduction**

This chapter lays down the foundational aspects of the present research. Initially, the research background is presented, followed by the definition of the research scope and problem statement. Subsequently, the research objectives and methodologies are depicted. Lastly, an overview of the thesis design and structure is provided.

## **1.2 Background**

Water resources are essential to human life, influencing food supply, economic development, and ecosystems (Taylor et al., 2013; Yin et al., 2017; H. Zhao et al., 2020). With the increasing urban population and climate change, water shortages have become increasingly prominent (J. Li et al., 2017), and more than half of human-inhabited areas are suffering from water scarcity problems (Boretti & Rosa, 2019). However, a third of the water provided by the water distribution system (WDS) has been wasted because of pipe leaks (Puust et al., 2010; Vrachimis et al., 2021). Meanwhile, leakages in the water network have also caused enormous resource and economic loss, becoming a challenging problem for city development (Rajani & Kleiner, 2001). Therefore, accurate leak diagnosis methods are necessary to minimize these issues and ensure efficient water management.

Leak diagnosis involves a systematic approach divided into two problems: leak detection and localization. Leak detection is widely acknowledged as the foundation for developing effective leak detection systems (El-Zahab et al., 2016), distinguishing leaks from other potential noise that could affect the identification. In contrast to the binary

classification task of leak detection, leak localization is more complex and involves predicting the exact leak location by determining its distance along the WDN.

Several approaches have been applied to achieve effective leak detection and localization, including mass/volume equilibrium, transient-based methods, and acoustic methods. Measurements from the traditional hydraulic balance method and minimum flow method obtained in district meter areas facilitate proactive strategies for leak detection and localization. Farah and Shahrour (2017) utilized real-time sensor recordings and hydraulic parameters to estimate water loss and locate pipe faults by generating leakage alarms based on flow thresholds. Li et al. (2022) adopted the data-driven approach utilizing hydraulic models to identify the precise location of the leakage effectively. Meanwhile, the transient analysis relies on the pressure transient wave reflection principle. Srirangarajan et al. (2010) presented a wavelet-based and local search to accurately determine the arrival time of the pressure front, which was verified through leak-off experiments on the test bed in Singapore. Jara-Arriagada et al. (2024) tackled the challenge of uncertain network connectivity in localizing pressure transient sources. The findings demonstrate a significant enhancement in accurately detecting and localizing the source of a transient, even when faced with unknown valve closures or pipe blockages.

Compared to other techniques, the acoustic methods employed in leak detection and localization have demonstrated comprehensive capabilities regarding sensitivity, accuracy, false alarm rate, and response time (Hu et al., 2021; LI & LIU, 2017). Due to these benefits, acoustic-based approaches have garnered widespread attention and interest in the field.

The acoustic method is achieved based on the vibration sound waves generated by leaks, and then leak detection and localization analysis are performed based on the collected signal (X. Cui et al., 2022). Conventional acoustic methods for water leak detection involve establishing reference indexes and utilizing statistical indicators from signals to identify leaks. Martini et al. (2017) introduced the Monitoring Index Efficiency, which utilized the standard deviation of the signal to differentiate between leak and non-leak status. Yazdekhashti et al. (2018) proposed a leak detection index based on changes in cross-spectral density caused by leaks. Fabbiano et al. (2020) employed the Root Mean Square (RMS) to indicate signal energy content for leak detection. Similarly, Gong et al. (2020) employed RMS and median frequency as indicators, incorporating smart technologies for detecting leaks from the urban level. Furthermore, Ahmad et al. (2023) developed a multiscale Mann-Whitney test for fluid pipe, and the output is regarded as the indicator for pipeline leak states. However, these statistical indicators heavily rely on signal information, and the complexities of real-world water distribution networks and ambient noise levels influence their effectiveness.

For localization, the cross-correlation-based acoustic methods are the most widely applied (X. Cui et al., 2023), primarily deducing the leak distance considering time delay. Gao et al. (2004) developed an analytical model of the cross-correlation function. Then, they used it to study the impact of bandpass filtering on detecting leaks in buried plastic water pipes. Ozevin and Harding (2012) introduced geometric connectivity into the cross-correlation function to determine the time-of-arrival difference, which facilitated the localization of leak points within the two-dimensional pipeline network configuration, thereby enhancing the applicability scope of the technique. Building

upon this, Almeida et al. (2018) proposed a method to compensate for the time delay error caused by resonant behavior. They demonstrated its superior performance compared to the basic-cross-correlation (BCC) function-based approach. Nevertheless, the BCC is heavily dependent on the quality of the collected signals and is vulnerable to degradation by noise and signal distortion,

In recent years, the emergence of ML has promoted the development of novel methods for water leak diagnosis, presenting significant advantages over conventional approaches (Kammoun et al., 2022). The ML-based techniques exhibit rapid processing capabilities and advanced pattern recognition (Nikos Fakotakis et al., 2023), effectively recognizing specific sound or vibration patterns associated with leaks and analyzing these patterns. ML-based methods demonstrate enhanced accuracy and efficiency in leak diagnosis operations (Tariq et al., 2022; Tijani & Zayed, 2022). These approaches possess remarkable adaptability and the capacity to continuously learn from newly acquired data, augmenting their performance over time (Vanijjirattikhan et al., 2022). Such adaptability ensures their efficacy across diverse water distribution systems, thus facilitating effective water management practices and contributing to substantial cost savings for water utilities while promoting environmental sustainability by conserving invaluable water resources (Mwelase, 2016).

Therefore, with the capabilities of ML, it has been introduced into the field of leak diagnosis, which has not only promoted effective and rapid leak diagnosis but also brought new challenges.

### 1.3 Research Scope and Problem Statement

However, ML-based acoustic leak diagnosis research remains in its early stages. Previous studies have yet to comprehensively explore the full potential of ML methodologies and have largely overlooked the challenges associated with applying ML techniques to acoustic leak diagnosis in WDNs.

First, though machine learning has offered several advantages and significantly influenced various research areas, building a comprehensive training dataset for leakage detection model training in practical engineering projects is challenging. Collecting leakage data consumes significant time and resources and requires authorization from local authorities (Sousa et al., 2023; Tariq et al., 2021). Although several studies employ laboratory-based data collection, the data do not represent actual engineering practice in leak detection. It has been observed that field leak signals are influenced by various factors, including pipe characteristics (e.g., diameter, thickness, and material) (Abdulshaheed et al., 2018; J. D. Butterfield et al., 2017, 2018; Khulief et al., 2012a), pipe topology (e.g., bends and branches) (M. Liu et al., 2021; Yazdekhashti et al., 2018), hydraulic parameters (e.g., pipe pressure and flow rate) (R. A. Cody & Narasimhan, 2020; Khulief et al., 2012a), and properties of the surrounding soil (Brennan et al., 2018a; Scussel et al., 2023; Shukla et al., 2020). Besides, leak signals experience significant attenuation as they propagate along the pipes, further complicating the detection process.

Simulating all conditions in the lab is impractical, and collecting signals from real WDNs requires substantial effort. The limited test site attributes result in a subset of data that may not fully capture leak pattern diversity, affecting model capacity for new

sites. Consequently, models developed based on such datasets may have limited capacity when applied to signals collected from new sites that have not been previously encountered. Therefore, it is urgent to utilize generative techniques to augment the dataset, providing an economical and effective solution to enhance the dataset for water leak diagnosis.

Second, despite deep learning models potentially improving leak detection performance, they are often regarded as ‘black box’ models due to their inherent opacity in internal operations and decision-making processes (Guidotti et al., 2019). As a result, comprehending the specific variables and features that drive the model's predictions becomes a challenge (Q. Zhang et al., 2018). The lack of interpretability poses a significant obstacle to understanding the underlying mechanisms and justifications behind the model's outputs. The inability to explain how and why the leak detection model arrives at its predictions hinders the trust and acceptance of these models by maintenance companies. Therefore, the model's interpretability needs to be enhanced through explainable techniques.

Third, two primary types of inputs are commonly employed when implementing deep learning (DL) algorithms for water leak detection: two-dimensional data in the form of time-frequency spectrograms and one-dimensional data represented as time-series signals. For two-dimensional data, techniques such as the Short-Time Fourier Transform (STFT) (G. Guo et al., 2021a), Continuous Wavelet Transform (CWT) (Sitaropoulos et al., 2023a), and recurrence plots (Y. Nam et al., 2021) are utilized to convert the input signal into image representations. However, it is essential to acknowledge that a part of the information may be lost during the signal transformation

process. In contrast, the application of time-series models specifically for water leak detection remains an underexplored area. Consequently, there is a need to investigate the effectiveness of time-series models in leak detection within water distribution networks.

Fourth, the traditional acoustic method for water leak localization relies on the analysis of vibration sound waves generated by leaks, followed by the estimation of leak location based on the time delay of wave arrival (X. Cui et al., 2022). However, the accuracy of this method is heavily dependent on the quality of the acquired signals and is susceptible to degradation caused by noise and signal distortion, necessitating improvement (Azaria & Hertz, 1984). Despite the promising potential of machine learning techniques in water leak detection, their application in leak localization remains largely unexplored. Consequently, it is worthwhile to explore using deep learning algorithms to estimate the time delay of signals collected by the correlator, enhancing robustness and requiring less prior knowledge than existing techniques.

#### **1.4 Research Objectives**

This research is motivated by the growing significance and rapid development of leak diagnosis management systems and the promising potential of ML in revolutionizing leak diagnosis practices. The study aims to explore the benefits and address the challenges of integrating ML into leak diagnosis systems while establishing robust and effective leak detection and localization models for WDN, thereby facilitating sustainable development in water management practices.

The research objectives include:

- i. Proposed a generative approach to augment the dataset, effectively addressing data scarcity issues while enhancing the quality, volume, and diversity of the leak dataset.
- ii. Establish an explainable leak detection model, enhancing the model interpretability and entailing a comprehensive analysis of collected signals to discern significant features that distinguish different leak conditions.
- iii. Develop an effective time-series leak detection model for WDN based on vibroacoustic signals. The model leverages advanced time-series analysis and attention mechanisms to enhance robustness and generalization, improve performances across various leak scenarios, and facilitate effective leak detection in real scenarios.
- iv. Develop a robust time-delay deep learning leak localization model for WDN. By incorporating temporal characteristics of signal pair, the time-delay estimation deep learning models have the potential to enhance leak localization accuracy, enabling prompt maintenance of leaks in WDNs.

By addressing these research objectives, this research aims to advance the field of water leak diagnosis by applying comprehensive ML-based leak diagnosis techniques, ultimately contributing to an accurate, efficient, and sustainable water distribution network management system.

## **1.5 Research Methodology**

According to Figure 1.1, the following methodologies have been adopted to achieve the previous objectives.

- i. A systematic review of studies that utilize ML-related methods to enhance leak diagnosis in WDN is conducted. The research development trend and main research theme are pointed out by conducting content and bibliometrics of relevant previous works. Next, the limitations of current studies and corresponding future directions were analyzed and discussed. The result points out the potential research direction and methods that form the foundations for subsequent analysis.
  
- ii. A generative adversarial network is established to enrich the leakage dataset. The generative adversarial network (GAN) is a machine-learning-based generative approach that enables in-depth analysis of the collected signals and generates customized amounts of signals. First, an initial dataset was collected and established to train the generative adversarial network, consisting of two submodels, the generator and the discriminator. The model is trained through competition between the generator and the discriminator. After training, the generator enables capturing the acoustic pattern of input samples and generates new samples. The quality and validity of generated samples were evaluated through different perspectives, including t-distributed stochastic neighbor embedding (t-SNE), acoustic features, and model augmentation validation. The research outcome assists in establishing a comprehensive leak dataset for further analysis and provides insights to solve the data scarcity in the vibroacoustic domain. (Objective 1)
  
- iii. The Gradient-weighted Class Activation Mapping (Grad-CAM) algorithm and two-dimensional Convolutional Neural Network (CNN) were incorporated to propose an explainable deep-learning model for leak detection. Initially, the Variational Mode Decomposition (VMD) was employed to denoise the signals, mitigating the

impact of external noise. Subsequently, a series of CNNs were utilized for the leak detection. During the evaluation phase, the Grad-CAM was integrated to visualize the gradient flow, elucidating the model's decision-making process. By comparing these visualization results, the underlying workings of the model were revealed, offering valuable insights into the analysis of leak-related signal components. (Objective 2)

iv. A time-series modeling approach (Time-Transformer) was devised to enhance model accuracy and robustness to address the complexities and practicality of leak scenarios. Initially, a comprehensive training dataset was meticulously assembled, incorporating data samples from field experiments and employing data augmentation algorithms. Furthermore, VMD was used to denoise the samples, effectively mitigating the influence of outliers. Subsequently, the Time-transformer model was developed specifically to cater to leak detection tasks. The performance of the Time-transformer model was then compared with other prevalent time-series models 1D-CNN and long-short-term-memory CNN (Conv-LSTM), and the features were visualized using t-SNE. The proposed model's validation and practicality were assessed through various evaluations and case studies, ultimately providing a robust and effective alternative for accurately identifying the leak point. (Objective 3).

v. To enable robust and efficient leak localization in WDNs, a residual 1D-CNN (Res1D CNN) is employed to infer the time delay between signal pairs. By incorporating the physical principles of wave propagation and considering various physical factors such as diameter and material properties, leak samples from two

sites are simulated to train the model. The performance of the proposed model is subsequently compared to basic cross-correlation from diverse perspectives to validate its capabilities for accurate leak localization. (Objective 4).

## **1.6 Structure of The Thesis**

Chapter 1 introduces and highlights the whole research picture, including the background, overall research aim, and specific objectives and significance. Chapter 2 reviews the existing literature on water pipe leak research, establishing the foundation for the current study. Chapter 3 introduces the present research framework, including methods and algorithms applied in this research. Chapter 4 presents the details of the proposed generative adversarial network for enriching the data for deep learning modeling. Chapter 5 describes the procedures for developing explainable CNN models for leak detection, revealing leak fault-related features and working mechanisms. Chapter 6 proposes the time-series-based deep learning model for facilitating robust and effective leak detection for WDN. Chapter 7 proposes the time-delay-estimation deep learning model for localizing leak points within WDN. Chapter 8 summarizes the main research findings, discusses limitations, provides recommendations for future work, and highlights the research's significance and contributions.

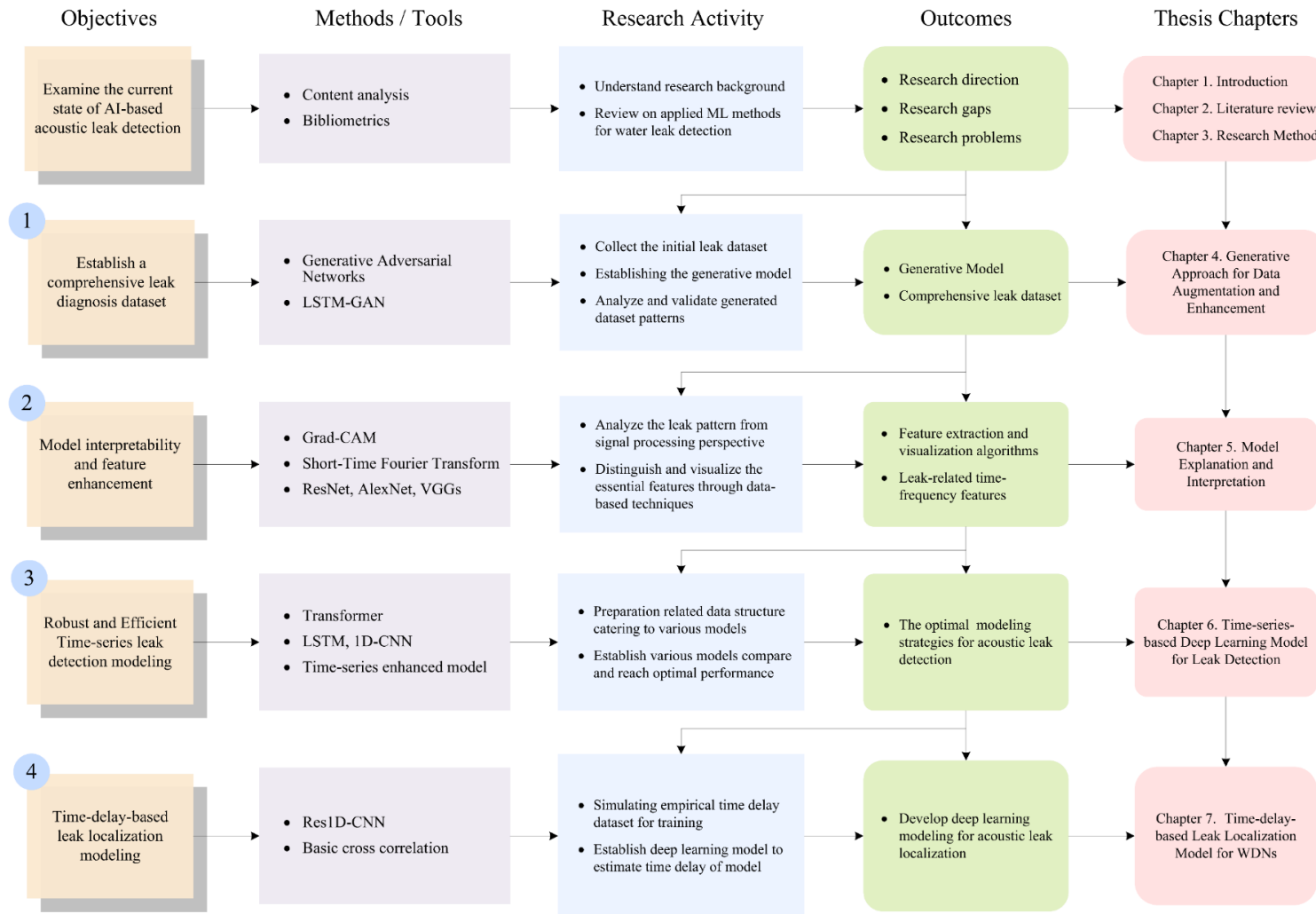


Figure 1.1 Research objectives, methods, and outcome

## **CHAPTER 2 Literature Review**

### **2.1 Introduction**

This chapter provides a holistic and comprehensive literature review of leak diagnosis research utilizing ML techniques. The chapter starts by reviewing studies on current applied data augmentation approaches for enriching leak signals. Then, the feature analysis approach for leak pattern identification was discussed. Furthermore, previous efforts to improve the leak diagnosis performance have been compared and analyzed. Finally, the chapter highlights research gaps and proposes future direction.

### **2.2 Overall Development Trend**

The literature review concentrated on ML-based acoustic water pipe leak diagnosis using Scopus and WoS (Web of Science) databases. These databases are widely regarded as comprehensive, multidisciplinary research literature repositories, indexing a vast number of academic articles across various fields, especially for natural sciences and engineering (Falagas et al., 2008; Mongeon & Paul-Hus, 2016). By utilizing these databases, this review ensures access to a rich and diverse range of academic resources to provide a thorough examination of the field.

The search targeted engineering subjects, including peer-reviewed journals and conference proceedings using artificial intelligence techniques for acoustic water pipe leak diagnosis. Considering related review studies (Dawood et al., 2020; Fan et al., 2022; Hu et al., 2021), an extensive search was conducted with the following search query:

**TITLE-ABS-KEY**(( 'accelerometer' OR 'noise logger' OR 'acoustic sensor') **AND** ('pipe\*' OR 'supply\*' OR 'distribut\*' OR 'main\*') **AND** ('Leak\*' OR 'Failure' OR 'Crack\*' OR 'break' OR 'burst' OR 'defect') **AND** ('water') **AND** ('machine

learning' OR 'artificial intelligen\*' OR 'deep learning' OR 'ANN' OR 'neur\*' OR 'random forest' OR 'decision tree' OR 'KNN' OR 'Support vector machine' OR 'SVM' OR 'Data driven' OR 'supervisi\*' OR 'unsupervisi\*' OR 'CNN' OR 'RNN') ).

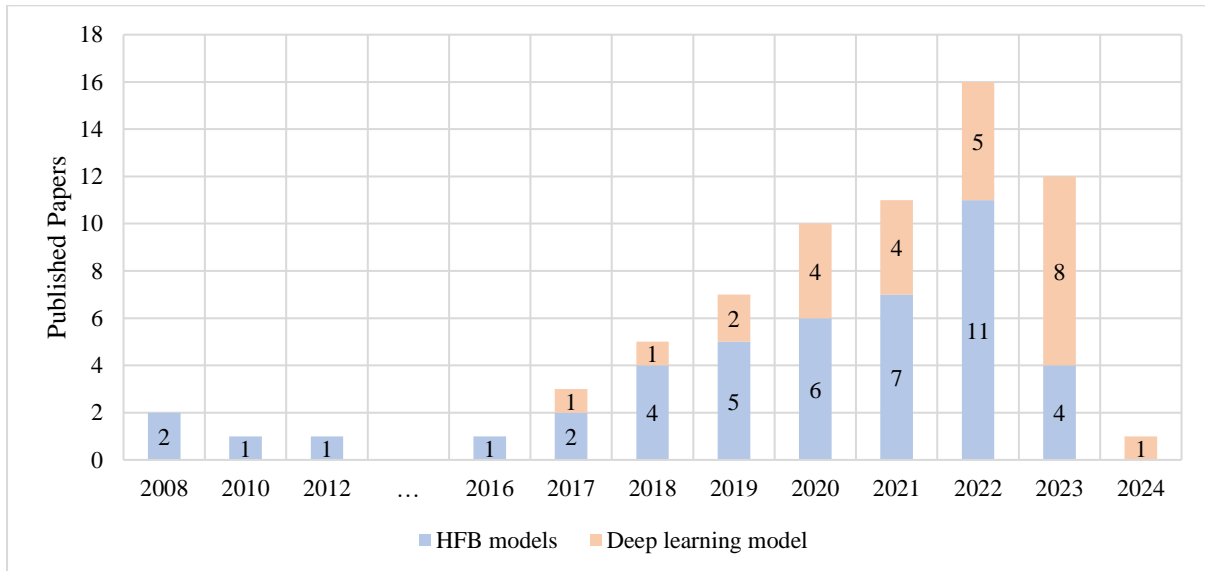


Figure 2.1 The trend of published ML-based acoustic leak diagnosis papers

The selected publications were academic papers published between 2000 and Jan 2024. After the initial search, irrelevant documents were excluded. This review included articles with data collected from non-acoustic instruments and research from other fields, such as gas or oil pipeline detection applications. Ultimately, 57 journal articles and 13 conference articles were collected for further analysis. Figure 2.2 demonstrates the growth trend in published papers within a specific domain, with a significant surge since 2017, showcasing the increase in conventional and deep learning model-based studies. The popularity of deep learning models has gradually increased, resulting in a shift towards more sophisticated models in recent years, while conventional model-based studies remain prevalent.

A bibliographic analysis was conducted on journals using information extracted from a database with the aid of VOSviewer (van Eck & Waltman, 2010). Figure 2.2 visualizes



## **2.3 Leak Signal Management and Enhancement**

This section will examine the methods used to obtain data from different sources, including sensor networks, and outline the necessary steps for data preparation before analysis. It will focus on preprocessing techniques such as data balance, filtering, and decomposition.

### **2.3.1 Leak Signal Collection**

The ML-based innovative diagnostic system was widely applied to classify and predict the leak status of the water supply distribution, which is a data-driven methodology that requires a certain amount of data for training, testing, and validation. The most commonly used sensors for data collection are accelerometers, hydrophones, geophones, and acoustic emission sensors (Hu et al., 2021). Herein, hydrophones are used to measure the acoustic waves propagated in the water column inside the pipe (Khulief et al., 2012b), while the other three devices sense the vibration of the pipe wall (F. Almeida et al., 2014a; R. Li et al., 2015). Considering the portability and installation requirements, accelerometers and AE sensors are used the most.

The data collection practices can generally be divided into field measurements and laboratory experiments. Figure 2.3 depicts the trend of various types of experiments over time. In the initial stage, field measurements-based studies are more prevalent. At the same time, laboratory experiments show an increasing proportion as time progresses. The rising proportion of laboratory experiments over time suggests their growing popularity. However, selecting the research method should depend on the research question and the phenomenon under study, considering the pros and cons of field measurements and laboratory experiments.

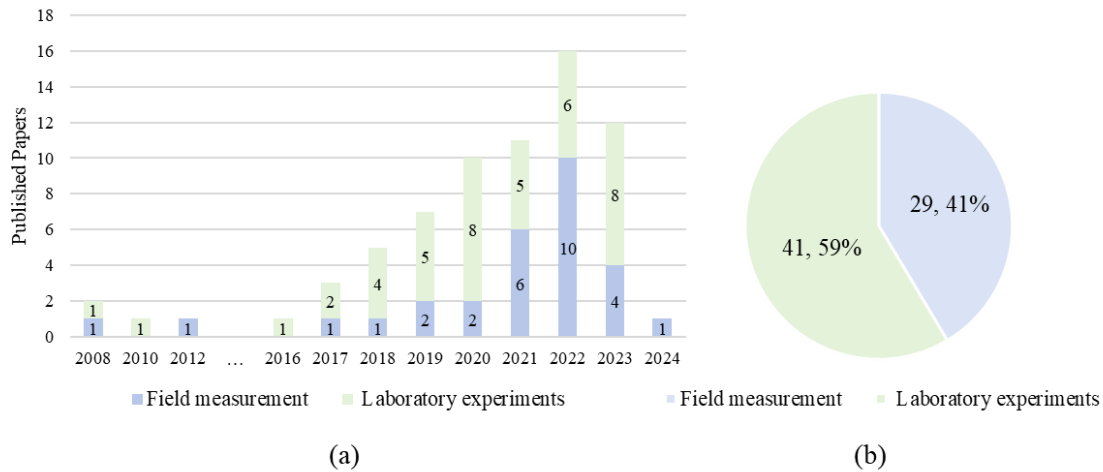


Figure 2.3 The number of studies applied field measurements and laboratory experiments (a)

The trend of annual published papers (b) The proportion for all published papers

The laboratory experiments were applied due to 1) cost efficiency, 2) control influence factors, and 3) accessibility. However, laboratory experiments have a limited experiment scale, and it is hard to reveal the impacts of background noise and the complex structure of the water pipe system on collected signals. In comparison, field measurements are the most promising means of developing practical models for leak diagnosis in water pipes and helping to verify the performance of various technologies. Likewise, field measurements face several constraints in practical application. For example, the government or authorized enterprises maintain urban water distribution networks that are inaccessible to the public. Additionally, background noise, such as traffic, construction, and street noise, are collected simultaneously, which might interfere with identifying water leaks. In this case, advanced signal processing techniques are needed to remove unwanted noise.

### 2.3.2 Data Preprocessing

The measured signals generally need to be preprocessed for subsequent analysis. One prevalent issue is the imbalance in data, as leak signals are typically less frequent than

non-leak signals. Consequently, specific techniques need to be performed to address this challenge. Besides, filtering and signal decomposition are two essential techniques commonly used for preprocessing collected signals in acoustic leak diagnosis, aiming to remove unwanted noise from signals before ML modeling.

### **2.3.2.1 Data Balance**

The performance of the ML model hugely relied on the quality of training data (Chuang et al., 2019). Since water leaks occur infrequently, leak signals are significantly less than non-leak signals, resulting in an imbalanced dataset. The imbalanced datasets are often challenging for almost all machine learning algorithms, as they ignore minority cases (López et al., 2013). Therefore, it is necessary to perform appropriate techniques on imbalanced data to generate a class-balanced dataset (Tariq et al., 2022). For most imbalanced data sets, sampling techniques aid in improved performance and can be roughly divided into two main categories: undersampling and oversampling (Haibo He & Garcia, 2009a).

#### **i. Undersampling**

Primarily, undersampling tackles the problem of imbalanced datasets by aiming to achieve balance within the dataset and enhance its capacity for generalization. It is accomplished by eliminating some data from the more abundant class (Haibo He & Garcia, 2009b). However, data is always valuable, and discarding it might lead to partial information loss. Therefore, this method is not widely used and is only used in the study by Yu et al. (2023) to address the imbalance of the dataset.

## ii. Oversampling

Oversampling is mainly used to enhance data by generating new data based on existing data. One example of oversampling is bootstrapping, which is used by Ravichandran et al. to generate acoustic instances using sampling with a replacement representative of the original sample distribution (Ravichandran, Gavahi, Ponnambalam, Burtea, & Mousavi, 2021). It is easy to operate but suffers from the overfitting problem and requires rigorous statistical assumptions to ensure accuracy. The synthetic minority oversampling technique (SMOTE) uses random oversamples. It aims to interpolate a new data sample between a specific actual sample and one of its nearest neighbors (Chawla et al., 2002). SMOTE can capture the signal's inherent distribution; therefore, the non-linear transformation-based augmentation can simulate signals that fit the actual scenario (G. Guo et al., 2020; Harmouche & Narasimhan, 2020). In literature, Tariq et al. (2022) applied SMOTE to increase the vibration dataset and address the class imbalance problem. Other studies have also used interpolation methods, such as bicubic interpolation, which considers the influence of neighboring points on the sampling point's value to increase data. Nam et al. (2021) applied bicubic interpolation to enhance leak data and transform one-dimensional data into two-dimensional recurrence plots of  $64 \times 64$  dimensions.

However, undersampling and oversampling might lead to the over-fitting problem and decrease the applicability of developed models. Undersampling might not cater to the context of data scarcity of water leak diagnosis, while oversampling might not consider the minority class distribution and can generate synthetic samples that are not representative of the original minority class distribution. Overall, sampling techniques

contribute to establishing a water leak dataset. It is essential to carefully consider its limitations and use them in combination with influence factors, such as selected features or model characteristics, to improve the performance of a machine learning model.

### **2.3.2.2 Signal Filtering**

Filtering refers to removing specific frequency components while retaining the interesting components from signals. In acoustic leak diagnosis, filters can remove noise and interference from collected signals. Several filters are commonly used, including high-pass, low-pass, band-pass, and notch filters classified based on the frequency response (F. Almeida et al., 2014b; Zeng et al., 2022).

Generally, leak signals exhibit variations in frequency distribution patterns, fluctuations, and internal pressure, which can be attributed to diverse conditions arising from factors such as pipeline structures, materials, sizes, leak openings, fluid flow rates, etc. When selecting a specific filter, signal pre-analysis is often implemented as the basis for subsequent analysis. For example, spectral analysis was performed first to determine the main frequency range of water leak signals, which was found to be within 0-10 kHz, followed by introducing a low-pass filter below 15 kHz to preprocess the raw signals in the study by Li et al. (S. Li et al., 2018). Alternatively, reference can be made to other studies on applying filters in acoustic leak diagnosis.

Table 2.1 summarizes the filters used in ML-based leak diagnosis research for consideration. Filters should be selected based on the frequency information of leak signals to avoid unnecessary signal distortion and over-filtering by the filter. Note that filters are not effective in handling non-stationary and transient data (Basu & RoyChaudhuri, 2016)

Table 2.1 Applied filter in ML-based leak diagnosis studies

Ref	Pipe characteristics	Device/ Sensor	Sensor placement	Sample Frequency (Hz)	Filter type
(T. Yu et al., 2023)	DN15 to DN 500 Galvanized steel, Steel, Ductile cast iron, Cast iron; De 2 to De 200 PE, PPR, UPVC, PVC	Accelerometer	Valve	8192	Band-pass filter 100 to 1500 Hz
(Y. Nam et al., 2021)	Ductile Iron Pipe, Vinyl Lined Steel Pipe, Unplasticized Vinyl Chloride Pipe, Polyethylene Pipe, Lead Pipe	Correlator	Fire hydrant gate valve	1×e4	Low-pass filter 1500 Hz
(G. Guo et al., 2021b)	DN50 to DN 300 Cast iron pipe and steel pipe	Accelerometer	Pipe surface in the chamber	4800	Band-pass filter 100 to 2000 Hz
(Harmouche & Narasimhan, 2020)	Grey Scale 80 PVC pipes with a 6-inch inner diameter	Hydrophone	Fire hydrant	2048	High-pass filter 2 Hz
(S. Li et al., 2018)	200 mm inside diameter ductile iron pipe	AE sensor	Pipe surface	1×e6	Low-pass filter 15 kHz
(Kang et al., 2018)	DN 80 to DN 300 ductile iron	Accelerometer	Valve	2048	Band-pass filter 100 to 800 Hz
(J. Butterfield et al., 2018)	DN80 to DN 300 ductile cast iron pipe	Accelerometer	Pipe surface close to valve	2500	4th Order Butterworth bandpass filter 10 to 1,000 Hz

### 2.3.2.3 Signal Decomposition

Signal decomposition is a powerful technique separating a signal into components or modes, each representing a specific physical phenomenon or source. In leak diagnosis, signal decomposition techniques have been widely used to separate leak signals from background noise or interference signals. However, proper signal decomposition techniques should be selected based on signal characteristics and modeling

requirements. To date, Singular Value Decomposition (SVD), Wavelet Transform (WT), Empirical Mode Decomposition (EMD), and Variational mode decomposition (VMD) have been widely used in ML-based water pipe leak diagnosis research.

#### i. Singular Value Decomposition

SVD is a linear transformation of the data to the reduced eigenarray space where data are diagonalized. It can be applied to a wide range of signal and data types, but its noise reduction ability is limited as it does not consider signal nonlinearity and non-stationarity (Klema & Laub, 1980). For water leak diagnosis, R. Cody et al. (2018) and Tijani & Zayed (2022) used SVD to decompose and reconstruct acoustic data collected by hydrophones and noise loggers for denoising.

#### ii. Wavelet Transform

Wavelet Transform (WT) is a signal processing technique that simultaneously explores signals in both time and frequency domains by breaking down the signal into different frequency components at varying scales. It has many applications in image processing, data compression, and noise reduction (Daubechies, 1992; Mallat, 2009). Luong and Kim (2020) applied wavelet packet transform to decompose leak signals, and Shannon entropy was used as the basis to select interested sub-bands. Tijani et al. (2022) used Haar wavelet and applied threshold-based denoising techniques to the signal, choosing the best wavelet denoising level based on standards such as SNR and RMSE. However, the choice of inappropriate wavelet functions may lead to information overlap and redundancy, affecting the effectiveness of signal processing. Kumar et al. (2017) investigated the significance of selecting the mother wavelet to extract the features in

leak acoustic signals, and the “Morlet” mother wavelet exhibited the maximum correlation and robustly localized the leak signal features.

### iii. Empirical Mode Decomposition

EMD is used to decompose a signal into a set of intrinsic mode functions (IMFs), which represent the different frequency components of the original signal without assuming any predefined basis functions based on the local characteristics of signals, and it is widely used in analyzing non-stationary and nonlinear data (N. E. Huang et al., 1998). In literature, Pan et al. (2018) used both EMD and WT to denoise measured signals to improve the accuracy of subsequent correlation analysis. Feature extraction is mainly performed on the IMFs decomposed by EMD. For example, Y. Liu et al. (2019) used EMD to decompose the signal and calculated the mean power spectrum of each IMF as the frequency domain feature of leak signals. Similarly, Butterfield et al. (J. Butterfield et al., 2018) extracted features such as RMS and Shannon entropy from IMF obtained by the decomposition. Furthermore, Guo et al. (2021b). transformed IMFs into time-frequency representations, similar to the RGB image, facilitating two-dimensional data recognition by CNN.

### iv. Variational Mode Decomposition

VMD decomposes a signal into a set of narrowband frequency components with time-varying amplitudes and frequencies, and the decomposition is achieved by minimizing a cost function using a set of essential functions adaptively (Dragomiretskiy & Zosso, 2014a). In literature, Diao et al. (2020) integrated the particle swarm optimization algorithm with VMD to optimize the governing parameters, i.e., the penalty term and the number of IMFs, and features were extracted from sub-modes for leak diagnosis.

Similarly, Wang et al. (2022) selected the top four correlated IMFs based on signal energy and correlation, respectively, and features were extracted from these key IMFs. Xu et al. (2021) decomposed signals collected by a spherical detector inside the water pipe using VMD to remove low-correlated noise based on the correlation coefficient. Table 2.2 summarizes the specialities of decomposition techniques, along with corresponding references. In signal analysis, careful consideration of signal characteristics is crucial when selecting appropriate filters and signal decomposition techniques. Factors such as signal non-stationarity, noise levels, and desired decomposition accuracy should be taken into account when making this selection. Each signal decomposition technique has unique advantages and limitations, as the table outlines, and should be chosen based on specific application scenarios. Moreover, in practical applications, it is imperative to thoroughly validate and optimize the chosen techniques to ensure the reliability and accuracy of the obtained results.

Table 2.2 Summary of signal decomposition methods in acoustic water leak diagnosis

Decomposition techniques	Specialties	References
SVD	<ul style="list-style-type: none"> <li>• Use for dimension reduction</li> <li>• Not useful in problems that require adaptive procedures</li> <li>• Computationally expensive</li> </ul>	SVD (R. Cody et al., 2018; Tijani & Zayed, 2022)
WT	<ul style="list-style-type: none"> <li>• Simultaneous localization ability for covering the time domain and frequency domain</li> <li>• Multiresolution capability to separate the fine detail in signals</li> <li>• Depending on the decomposition structure formed by wavelet function and decomposition levels</li> </ul>	WT (Kumar et al., 2017; Luong & Kim, 2020; Tijani et al., 2022)
EMD	<ul style="list-style-type: none"> <li>• Suitable for analyzing nonlinear and non-stationary signals</li> <li>• Lack of theoretical basis and limitation of frequency resolution</li> <li>• Phenomenon of endpoint and mode mixing</li> </ul>	EMD (G. Guo et al., 2021b; Y. Liu et al., 2019), EEMD (J. Butterfield et al., 2018),

	<ul style="list-style-type: none"> <li>Improved versions, such as EEMD and CEEMD, were proposed to solve the mode-mixing and suppress the residue</li> </ul>	EMD+WT (Pan et al., 2018)
VMD	<ul style="list-style-type: none"> <li>Solid theoretical foundation and good noise robustness</li> <li>Allow adaptive decomposition of signals into various modes</li> <li>Suffer from the limitation of the Fourier spectrum</li> </ul>	VMD (Z. Wang et al., 2022; T. Xu et al., 2021), PSO-VMD (Diao et al., 2020)

## 2.4 Leak Pattern Extraction and Analysis

Feature extraction improves detection accuracy by extracting relevant information, reducing noise and dimensionality, and selecting meaningful features. Feature engineering includes two main parts: feature extraction and feature selection. Feature extraction involves transforming signals into more valuable forms and choosing the most relevant information for leak diagnosis, while feature selection involves eliminating irrelevant and redundant information. The goal of feature selection is to find a compact and informative set of features that can represent the original signal meaningfully.

### 2.4.1 Leak Feature Extraction

ML-based studies on acoustic leak diagnosis face challenges due to the high dimensionality of raw acoustic signals (H. Jin et al., 2014). Before developing ML-based models for leak diagnosis, one of the tasks is to extract useful features from measured acoustic signals, which are high-dimensional time series. It is performed to compress original signals and keep important target information, aiming to speed up model training and yield better results. Generally, Table 2.3 summarizes the extracted features that can be divided into two categories: 1) Statistical features, typically the time

and frequency domain features and 2) Model/technique-based features, for example, the fitted parameters of the time series models or time-frequency feature are obtained from decomposition results using EMD or WT.

Table 2.3 The applied features for ML-based modeling

		Feature	Ref
Statistical Feature	Time Domain	Maximum	(R. Cody et al., 2017; Fares et al., 2022; S. Li et al., 2018; Luong & Kim, 2020)
		Minimum	(J. Butterfield et al., 2018; R. Cody et al., 2017)
		Mean	(J. Butterfield et al., 2018; Fares et al., 2022; G. Guo et al., 2021b; S. Li et al., 2018; Pan et al., 2018; T. B. Quy et al., 2019; T. Quy & Kim, 2019; Singh et al., 2021; Tijani et al., 2022; Tijani & Zayed, 2022; W. Xu et al., 2022)
		Standard Deviation	(J. Butterfield et al., 2018; R. Cody et al., 2017; S. Li et al., 2018; T. Quy & Kim, 2019)
		Root Mean Square	(J. Butterfield et al., 2018; R. Cody et al., 2017, 2018; G. Guo et al., 2021b; S. Li et al., 2018; Luong & Kim, 2020; Muller et al., 2021; Pan et al., 2018; T. B. Quy et al., 2019; T. Quy & Kim, 2019; Singh et al., 2021; Tijani et al., 2022; W. Xu et al., 2022; T. Yu et al., 2023; C. Zhang et al., 2022)
		Skewness	(J. Butterfield et al., 2018; S. Li et al., 2018; Luong & Kim, 2020; Tijani et al., 2022; Tijani & Zayed, 2022; W. Xu et al., 2022)
		Kurtosis	(J. Butterfield et al., 2018; Diao et al., 2020; S. Li et al., 2018; Luong & Kim, 2020; T. Quy & Kim, 2019; Tijani et al., 2022; Tijani & Zayed, 2022; Z. Wang et al., 2022; W. Xu et al., 2022; T. Yu et al., 2023)
		Margin Factor	(Luong & Kim, 2020)
		Clearance Factor	(Diao et al., 2020; Luong & Kim, 2020)
		Shape Factor	(Luong & Kim, 2020)
		Crest Factor	(J. Butterfield et al., 2018; S. Li et al., 2018; Luong & Kim, 2020; Tijani et al., 2022; Tijani & Zayed, 2022)
		ZCR	(G. Guo et al., 2021b; Muller et al., 2021; T. Quy & Kim, 2019; T. Yu et al., 2023; C. Zhang et al., 2022)
		Skewness	(J. Butterfield et al., 2018; S. Li et al., 2018; Luong & Kim, 2020; Tijani et al., 2022; Tijani & Zayed, 2022; W. Xu et al., 2022)
	Frequency	Frequency Centroid	(S. Li et al., 2018; Luong & Kim, 2020; Muller et al., 2021; T. Quy & Kim, 2019; Tijani et al., 2022; Tijani & Zayed, 2022; Z. Wang et al., 2022; W. Xu et al., 2022; C. Zhang et al., 2022)
		Spectral Roll-Off	(Muller et al., 2021; C. Zhang et al., 2022)
		Spectral Flatness	(Muller et al., 2021; T. Quy & Kim, 2019; C. Zhang et al., 2022)
		Spectral Spread	(T. Quy & Kim, 2019; Tijani et al., 2022; Tijani & Zayed, 2022; C. Zhang et al., 2022)
		Energy	(R. Cody et al., 2017; S. Li et al., 2018; Luong & Kim, 2020; Pan et al., 2018; T. B. Quy et al., 2019; T. Quy &

		Other	MIE	Kim, 2019; Singh et al., 2021; Tijani et al., 2022; Tijani & Zayed, 2022; W. Xu et al., 2022)	
Model/Technique-based Features				(El-Zahab et al., 2018, 2022; Tariq et al., 2022)	
	Entropy		Shannon entropy	(J. Butterfield et al., 2018; R. Cody et al., 2018; G. Guo et al., 2021b; Luong & Kim, 2020)	
			Approximate Entropy		(Y. Liu et al., 2019; Yang et al., 2008, 2013)
			Sample Entropy		(Z. Wang et al., 2022; W. Xu et al., 2022; T. Yu et al., 2023)
	Autocorrelation		MLE		(Fares et al., 2022; Tijani et al., 2022)
			Autocorrelation		2023/6/25
		Autocorrelation MLE		(Tijani et al., 2022)	

### 2.4.1.1 Statistical Features

Statistical features and other features are mainly extracted from time or frequency domains.

#### i. Time Domain Features

In the time domain, the typical features are maximum and minimum values, mean value, standard deviation, and RMS. The minimum and maximum values provide information about the lowest and highest values in the signal. The mean value provides a central value that reflects the signal trend in time. The standard deviation measures the distribution of data around the mean. RMS characterizes the variation of the instantaneous signal amplitude within a sampling period and is a time-averaged value. The above features are universal and can be applied to various signals and signal types. Moreover, these features are straightforward and can assist in quickly and easily understanding a part of the characteristics of the signal, and therefore, have been commonly used for leak diagnosis in water pipes (Fan et al., 2022).

The water leak might induce variations in the signal waveform or shape, which can be depicted by several features, including skewness, kurtosis, margin factor, clearance factor, shape factor, crest factor, and Zero Crossing Rate (ZCR). Skewness and kurtosis

can indicate the presence of non-Gaussian noise, which can help to detect the leak status. The margin factor can reveal the "flatness" or lack of kurtosis of the signal, which helps distinguish the leak sound from other ambient sounds. The clearance factor can help detect the duration and pulse width of the leak sound, respectively. The shape factor can indicate the symmetry of the sound waveform, which can aid in identifying the leak source (Luong & Kim, 2020). The crest factor is effective for measuring the dynamic range or peaks of the signal. ZCR measures the number of times a signal crosses the zero axis in a unit of time, which can be used to distinguish leak and non-leak signals based on their temporal behavior. Based on waveform or shape features, the variations of acoustic signals induced by water leaks can be better described, potentially increasing the performance of developed water leak diagnosis models.

## ii. Frequency Domain

In the frequency domain, features such as frequency centroid, spectral roll-off, and spectral flatness provide information about the harmonic structure, fundamental frequency, and energy distribution of the signal. The frequency centroid is commonly used to estimate the primary frequency of leak signals. At the same time, spectral roll-off measures the shape of the sound signal, indicating the frequency below which a specified percentage of the total spectral energy lies. Spectral spread is calculated as the difference between the upper and lower frequency limits that contain a specified percentage of the total signal power, which provides the components of signals that assist models in differentiating leak signals from normal signals. Spectral flatness measures the relative balance of the energy across the frequency spectrum of a signal. It is calculated as the ratio of the geometric mean to the arithmetic mean of the power

spectrum. Energy refers to the power or strength in a signal over a given period. Severe leaks produce more energy and stronger sound waves than normal conditions or minor leaks. Thus, energy as the feature can assist in distinguishing the leak and non-leak signals.

### iii. Other Features

Apart from the traditional statistical features, several studies proposed new features based on the statistical analysis of leak signals. For example, Martini et al. (Martini et al., 2015) established a feature called Monitor Index Efficiency (MIE), a vital tool in determining the proper operation of water pipes. It collects acoustic data during standard pipe operations and establishes a baseline for normal conditions. The ratio between the measured signal and the baseline is analyzed to identify any irregularities or abnormal behavior in the pipe (El-Zahab et al., 2018, 2022; Tariq et al., 2022).

Statistical features used in ML-based models for water leak diagnosis are summarized in Table 2.3. In short, traditional features may not fully capture the dynamic range of signal behavior nor provide a complete picture or other aspects of the signal. Meanwhile, they have difficulty describing complex signals and are sensitive to outliers, which can be significantly affected by signal spikes or sudden drops.

#### **2.4.1.2 Model/Technique-based Features**

Model/technique-based features are parameters of time-series models or the new indicator derived from specific techniques. For example, the degree of chaos in a signal refers to the level of disorder or randomness in the signal and can be described using the concept of entropy. Shannon entropy will increase as the level of disorder and randomness in a system increases. Leak signals within pipelines typically exhibit

instability, complexity, and non-linearity (Sun et al., 2016). Guo et al. (G. Guo et al., 2021b) and Butterfield et al. (J. Butterfield et al., 2018) considered that chaotic signals are more likely to be associated with leaks and applied Shannon entropy to detect leaks. In addition, the level of chaos in sound signals was considered to provide information about the size and severity of leaks. Approximate Entropy (ApEn) quantifies the likelihood of similar data point patterns repeating, which is robust to low-level noise that can extract meaningful information from certain data points (Pincus, 1995). Yu et al. (T. Yu et al., 2023) and Liu et al. (Y. Liu et al., 2019) applied ApEn to measure irregularity in acoustic signals. Meanwhile, Sample entropy (SampEn) is proposed based on ApEn. It has the advantage of data length independence and is less noise-sensitive (Richman & Moorman, 2000). The maximum Lyapunov exponent (MLE) is another tool to determine chaos. In the leaked state, MLE is generally positive and belongs to chaotic systems (J. Liu et al., 2018) and has proven to be a practical feature for ML-based models (Fares et al., 2022; Tijani et al., 2022).

Autocorrelation analyzes the periodicity or regularity of the sound signal. It shows a high correlation between the repeated signal pulses in the presence of a leak. Conversely, autocorrelation is reduced in a non-leak signal that exhibits more random or irregular fluctuations. It serves as the basis for a characteristic feature applied by Yang et al. (Yang et al., 2013) and incorporated with ApEn to capture the leaks in the presence of non-leak noise inside and outside the pipeline. The autocorrelation energy ratio, which is the energy in a certain range divided by the total energy of the autocorrelation function, was also adopted by Guo et al. (G. Guo et al., 2021b) for water leak diagnosis.

The signal decomposition technique introduced above is commonly used in signal preprocessing, the decomposition results of which can be used to propose features, which will be discussed in the following section. Similarly, the above traditional features can be extracted from the decomposed sub-components. To avoid confusion, such features are included in this category. For instance, RMS was extracted from IMFs of acoustic features decomposed using EMD to enhance the accuracy (J. Butterfield et al., 2018; G. Guo et al., 2021b), kurtosis vector and the frequency information were extracted from IMFs of VMD, then recombined into a new feature vector to enrich acoustic information (Z. Wang et al., 2022). In addition, several studies proposed new features based on the decomposition results. For instance, the “Morlet” wavelet coefficients were used by Luong and Kim (Luong & Kim, 2020) to establish machine learning models for leak diagnosis. Other features include the energy ratio and entropy-based features based on decomposed components.

#### **2.4.1.3 Multi-Dimension Representation Data**

Although one-dimensional features have the advantages of simplicity and lower computational complexity, they may not fully capture the complexity and structure of audio data. In comparison, multi-dimensional features can provide comprehensive information and representation of audio data. Table 2.4 highlights the use of multi-dimensional data with CNN models in existing research, attributed to the superior processing capabilities of CNN for such data.

Time-frequency domain analysis merges time and frequency-domain analysis to represent changing signals and locate frequency components over time, which is suitable for scrutinizing non-stationary signals from leak diagnosis. Time-frequency

domain techniques such as STFT, WT, and Mel plot are commonly used in leak diagnosis to extract relevant features from the signal.

Table 2.4 Applied Multi-Dimension Representation Processing for Leak Detection Studies

Plot	Advantage	Limitation	Model	Ref
Short Time Fourier Transform	<ul style="list-style-type: none"> <li>• Easy to implement and interpret.</li> <li>• Suitable for stationary signals.</li> </ul>	<ul style="list-style-type: none"> <li>• Fixed time-frequency resolution, is not optimal for non-stationary signals.</li> <li>• Require window function selection, affecting the representation</li> </ul>	CNN-VAE	(R. A. Cody et al., 2020)
			CNN	(T. Yu et al., 2023)
			CNN	(G. Guo et al., 2021b)
Continuous Wavelet Transform	<ul style="list-style-type: none"> <li>• Variable time-frequency resolution and improvement of the representation of non-stationary signals.</li> <li>• Suitable for detecting transient features in acoustic signals.</li> </ul>	<ul style="list-style-type: none"> <li>• Computationally intensive, making it slower for real-time applications.</li> <li>• Require selection of the mother wavelet, affecting the representation.</li> </ul>	Not given	(Shukla & Piratla, 2020b)
			CNN	(Shukla & Piratla, 2019, 2020a)
Mel plot	<ul style="list-style-type: none"> <li>• Mimic human auditory perception, emphasizes frequency bands relevant to human hearing.</li> <li>• Reduce dimensionality while preserving relevant information.</li> </ul>	<ul style="list-style-type: none"> <li>• Information loss when dimensionality reduction</li> <li>• Require selection of parameters such as window size and Mel filter bank.</li> <li>• Fixed time resolution, misses the rapid changing of signals occurring over the short time scale</li> </ul>	CNN	(Chuang et al., 2019)
			DCAE	(Muller et al., 2021)
			CNN	(Tsai et al., 2022)
			Siamese CNN	(C. Zhang et al., n.d.)
Recurrence plot	<ul style="list-style-type: none"> <li>• Reveal underlying dynamics and chaos in acoustic signals.</li> <li>• Applicable to both stationary and non-stationary signals.</li> </ul>	<ul style="list-style-type: none"> <li>• Require parameter tuning, affecting the representation</li> <li>• Interpretation can be subjective.</li> </ul>	CNN	(Y. Nam et al., 2021)
RGB format plot	<ul style="list-style-type: none"> <li>• Represent up to three dimensions of data simultaneously using color channels.</li> <li>• Visually intuitive, easier to interpret the data.</li> </ul>	<ul style="list-style-type: none"> <li>• Limited to three dimensions.</li> <li>• Require normalization and color mapping, which may result in information loss.</li> </ul>	CNN	(Vankov et al., 2020)
			CNN	(P. Liu et al., 2023)

\*CNN-convolutional neural network; VAE-Variational Autoencoder; DCAE-Deep Convolutional Auto Encoder; RGB image - Red, green and blue image

### 2.4.1.3.1 Short-Time Fourier Transform

STFT enables the analysis of time-varying signals in the frequency domain and involves dividing a signal into overlapping short segments, computing the Fourier Transform

(FT) of each segment, and then stitching them together to obtain a time-frequency representation of the signal (Boashash, 2016). In leak diagnosis, STFT can be used to analyze the frequency components of the sound signal captured from the pipeline, which generates a spectrogram as the input for a CNN, allowing the extraction of multi-dimensions features from the data. Related studies include R. A. Cody et al. (2020) and Yu et al. (2023), who used STFT to decompose acoustic signals into time-varying spectral components and extract the overall features of the 2D data, which can then be fed into a CNN for subsequent modeling.

#### **2.4.1.3.2 Continuous Wavelet Transform**

Unlike WT used in conventional machine learning models to denoise signals or extract features, WT referred to here is the Continuous Wavelet Transform (CWT) that simultaneously enables the analysis of non-stationary signals in both time and frequency domains. It involves convolving a signal with a family of scaled and translated wavelets to obtain a representation of the signal as a function of time and scale (Mallat, 2009). CWT offers improved time-frequency resolution compared to STFT and allows variable frequency resolution by decomposing signals into wavelet coefficients at different scales, making it useful for detecting and analyzing transient events. It is mainly applied in studies of Shukla & Piratla's research team (Shukla & Piratla, 2019, 2020a, 2020b), where Morse Wavelet was utilized to convert and analyze acoustic signals with complex structures.

#### **2.4.1.3.3 Mel Spectrogram**

Mel Spectrogram is a signal processing technique that accounts for the non-linear human perception of frequency. It involves transforming a signal into the frequency

domain using the Short-Time Fourier Transform and mapping the resulting spectrogram onto a Mel-frequency scale. This scale emphasizes important acoustic features of the audio, allowing for more effective analysis and interpretation (M. Xu et al., 2005). The representation is often more effective than traditional Fourier analysis because it can capture the nonlinearity of human hearing, emphasizing lower-frequency signals, which is essential for detecting subtle changes in acoustic signals that may indicate leaks. Chuang et al. (Chuang et al., 2019) and Muller et al. (Muller et al., 2021) have shown that the Mel spectrogram can extract multi-dimensional data for improved models. However, Mel spectrograms may lose some high-frequency information in the acoustic signals.

#### **2.4.1.3.4 Other Techniques**

Several techniques can be used to transform time series into multi-dimensional data beyond time-frequency analysis. One simple transformation method is to convert one-dimensional time-series data into a matrix format based on time steps (J. Choi & Im, 2023). However, this approach may result in loss of frequency and time-frequency information and may not perform better than one-dimensional signals. A recurrence plot is expressed on a multi-dimensional plane to visualize the characteristics of time series data (ECKMANN et al., 1995). Nam et al. (Y. Nam et al., 2021) used recurrence plots to find patterns in time series data. However, RP loses the components of high-frequency information, which STFT and CWT can detect. In addition, for RGB space, Vankov et al. (Vankov et al., 2020) utilized the characteristics of experimental instruments to construct multi-dimensional data. They arranged the data into a matrix according to the regularity of time and used a vibration transducer to collect the

vibration data of the x and y axes. The values from the x-axis, y-axis, and timestamp represent the red, green, and blue channels in an RGB image. Meanwhile, Liu et al. (P. Liu et al., 2023) also proposed an innovative transformation approach. It first transforms the one-direction signal to a two-dimensional grayscale image based on time series, then converts the greyscale to three-channel RGB. This approach minimizes reliance on expert knowledge. However, the former approach has particular prerequisites for the data acquisition instrument. Furthermore, as the multi-dimensional data is organized in rows and columns based on time series, there is a risk of information loss during the transformation process.

Overall, time-frequency domain analysis is essential for analyzing non-stationary signals like those encountered in leak diagnosis. STFT, CWT, and Mel spectrogram are commonly used techniques to extract signal features. These techniques have broad applicability in signal analysis, can extract multi-dimensional data for CNN and improved models, provide valuable insights into leak diagnosis, and contribute to developing more accurate and efficient detection methods. It is also important to note that intrinsic patterns of leak acoustic signals need to be considered when choosing the appropriate processing technique to enhance the information representation.

### **2.4.2 Feature Selection**

Feature selection is crucial in creating robust pattern recognition or leak detection classifiers. Redundant features can impede classifier efficiency and accuracy and increase the computational burden and expense if the input features cannot distinguish between samples. The process of feature selection involves identifying relevant features

and discarding irrelevant ones. Feature selection methods can generally be categorized into three types: wrapper, embedded, and filter methods (Chandrashekar & Sahin, 2014).

#### i. Filter Methods

Filter methods use a suitable ranking criterion to score variables and a threshold to remove irrelevant ones. These ranking methods, applied before classification, are effective in practical applications and filter out variables with low feature relevance, which is a fundamental property of unique features in the data. One of the conventional filter methods employed in ML-based water leak diagnosis is the Kullback-Leibler distance. This method evaluates the importance of features by analyzing their probability distribution in scenarios with and without water leaks (S. Li et al., 2018; T. B. Quy et al., 2019; Tijani & Zayed, 2022). Another typical method is Mutual Information (MI), which was applied by R. Cody et al. (R. Cody et al., 2017) to extract features as it measures the degree of mutual dependence between two variables. Additionally, correlation analysis was applied by Tijani et al. (Tijani et al., 2022) to evaluate the linear relationship between pairs of features, and it can further remove redundant features with high correlation values. Yu et al. (T. Yu et al., 2023) adopted the Analysis of variance (ANOVA) to calculate the variance of features between and within classes. The feature is statistically significant once the between-classes variance is higher than the within-class variance.

#### ii. Wrapper Methods

Wrapper approaches employ the performance of predictive models as a criterion to select subsets of variables. However, evaluating all possible subsets is computationally infeasible. Hence, search algorithms are implemented to identify optimal subsets

heuristically. Simplified algorithms such as sequential search or evolutionary algorithms (e.g., genetic algorithm and particle swarm optimization) are mainly utilized to produce computationally feasible and satisfactory results for large datasets. Several studies have used wrapper methods to select essential features for subsequent model development. For instance, Boruta, a wrapper method, uses a simple model to identify and remove irrelevant or redundant features from a dataset and iteratively compares the importance of original features with that of shadow features. The consistently more essential features than their shadow counterparts are considered significant and selected for further analysis. W. Xu et al. (W. Xu et al., 2022) used Boruta to classify acoustic features into tentative, confirmed and rejected. Meanwhile, Xu et al. (W. Xu et al., 2022) and Zhang et al. (C. Zhang et al., 2022) have used Shapley Additive explanations (SHAP), a game-theory-based and ‘select from model’ approach, to explain the contribution of features through outputs from machine learning models. The contribution can then be used as a basis for feature selection.

### iii. Embedded Methods and Others

Embedded methods seamlessly integrate feature selection into the training process of machine learning models, often by imposing regularization terms on the optimization objectives of classifiers. Upon completion of the training process, these methods automatically select relevant features. The computational demands, the complexity of implementation, and reliance on specialized models may limit their application across various detection techniques. Nevertheless, embedded methods offer the potential for improved performance and interpretability. Exploring these methods further in acoustic leak diagnosis could lead to more efficient and accurate algorithms in the future.

PCA has been employed in several studies, including those by Y. Liu et al. (2019), Ravichandran et al. (2021), and Terao & Mita (2008), to extract potential acoustic features from the data. PCA forms new features that retain the original information by projecting the data onto a hyperplane. However, interpreting the meaning of individual principal components is challenging, especially when faced with high-dimensional data. Table 2.5 summarizes the applied algorithms for selecting acoustic features and their limitations. In conclusion, feature selection is essential in creating robust classifiers for water leak diagnosis. Various algorithms have been developed to evaluate the quality of collected signal features and select relevant features for further analysis. Each of these methods has its advantages and limitations. Researchers should choose the appropriate feature selection method based on the data type, sample size, and research question. Current research does not have a vast data set and does not require high computing power. Therefore, it is recommended that performance- and accuracy-based methods, such as Boruta and SHAP, be used.

Table 2.5 The applied feature selection indicator

Applied study	Feature selection	Selection method	Limitation
(S. Li et al., 2018; T. B. Quy et al., 2019; Tijani & Zayed, 2022)	Filter method	Kullback-Leibler distance	<ul style="list-style-type: none"> <li>• Sensitive to outliers</li> <li>• Influenced by the comparison of probability distributions.</li> </ul>
(R. Cody et al., 2017)	Filter method	Mutual information algorithm	<ul style="list-style-type: none"> <li>• Sensitive to outliers</li> <li>• Computationally intensive</li> </ul>
(Tijani et al., 2022)	Filter method	Correlation analysis	<ul style="list-style-type: none"> <li>• Limited to linear relationships</li> <li>• No causation identification</li> </ul>
(T. Yu et al., 2023)	Filter method	ANOVA	<ul style="list-style-type: none"> <li>• Sensitive to outliers</li> <li>• Poor with missing data</li> </ul>
(W. Xu et al., 2022; C.	Wrapper	Shapley Additive exPlanations (SHAP)	<ul style="list-style-type: none"> <li>• Computationally expensive</li> <li>• Interpretation challenge</li> <li>• Correlated feature sensitivity</li> </ul>

Zhang et al., 2022)			
(W. Xu et al., 2022)	Wrapper	Boruta	<ul style="list-style-type: none"> <li>• Computationally intensive</li> <li>• Incomplete feature identification</li> <li>• No causation, only correlation</li> </ul>
(Y. Liu et al., 2019; Ravichandran, Gavahi, Ponnambalam, Burtea, & Mousavi, 2021; Yuriko Terao & Akira Mita, 2008)	Other	PCA	<ul style="list-style-type: none"> <li>• Interpretation challenge</li> <li>• Outlier sensitivity</li> <li>• Limited to linear relationships</li> <li>• Information loss possible</li> </ul>

---

## 2.5 Acoustic-based Water Leak Detection Models

Capitalizing on the advantages of ML models, including their interpretability, simplicity, and computational efficiency, these models play a critical role in data-driven water pipe leak detection. The modeling process primarily encompasses feature extraction, feature selection, and the implementation of various modeling techniques. This section examines the crucial models, including handcrafted feature-based (HFB) and deep learning models.

### 2.5.1 Development of HFB Models

ML-based acoustic leak detection models analyze sound waves emitted by leaks and provide accurate information to prevent environmental contamination and financial losses. In water leak detection, HFB models refer to ML models that utilize manually designed acoustic features extracted from the collected signals. It requires expertise in feature selection and design and offers competitive performance. These models have become increasingly crucial for establishing efficient water management. Figure 2.4

depicts the main categories of handcrafted feature-based (HFB) models for water leak detection. The following section provides a detailed discussion of the applied handcrafted feature-based models.

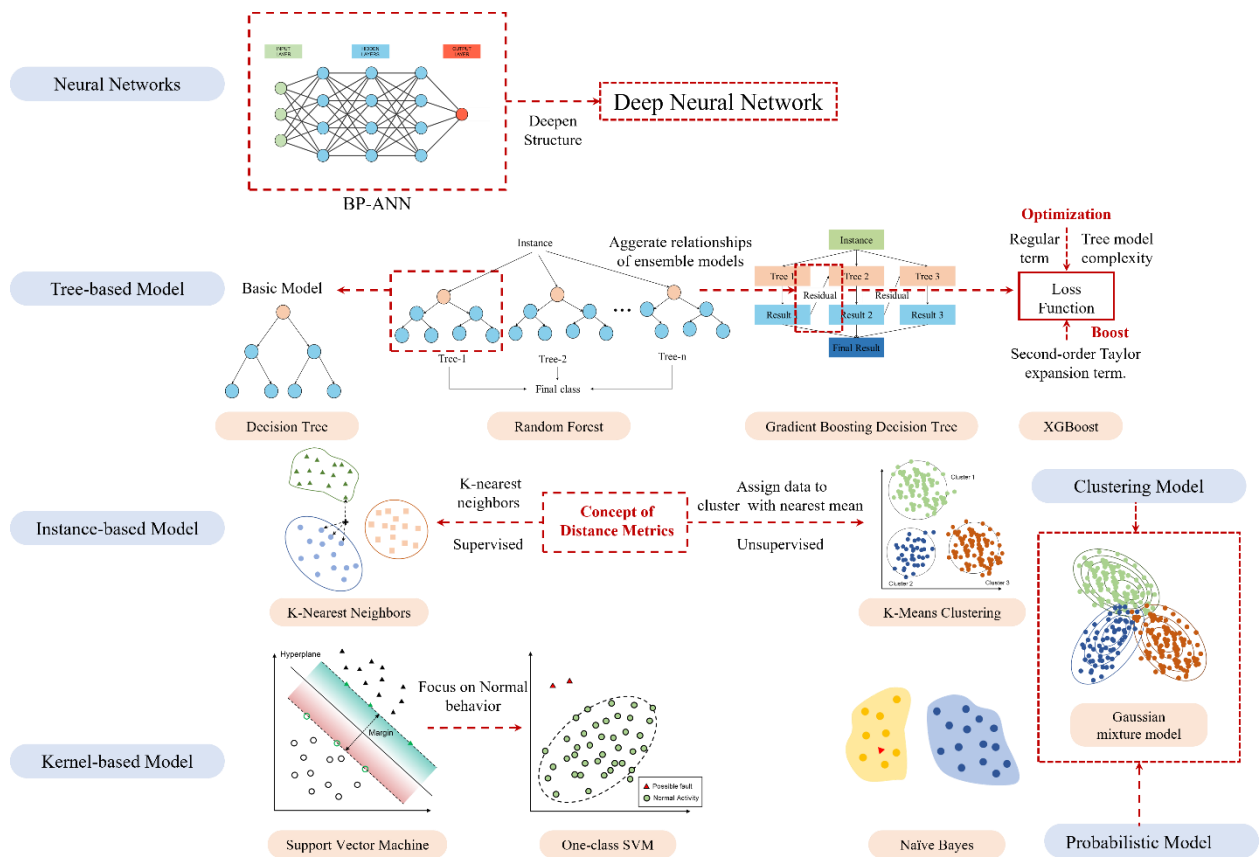


Figure 2.4 Applied HFB models for water pipe leak detection

### 2.5.1.1 Artificial Neural Network

Artificial Neural Network (ANN) is inspired by the human brain (McCulloch & Pitts, 1943). It consists of interconnected nodes processing information through weighted connections solving non-linear relationships by adjusting connections during training to minimize prediction error (Krogh, 2008). As illustrated in Equation (2.1), neurons of one layer connect only to neurons of the preceding and following layers, for the  $l$  th layer, the activation  $a_j^l$  of the  $j$  th neuron is a sum of the activations in the  $(l - 1)$  th layer.

$$a_j^l = \sigma \left( \sum_k \omega_{jk}^l a_k^{l-1} + b_j^l \right) \quad (2.1)$$

where  $b_j^l$  is the bias of the  $j$  th neuron,  $\omega_{jk}^l$  is the weight from the  $k$ -th neuron in the  $(l - 1)$  th layer to the  $j$  th layer, and  $\sigma$  is the activation function. The training of ANN involves adjusting the weights to improve the accuracy of the result by minimizing the observed errors.

In the literature, Kumar et al. (Kumar et al., 2017) early applied ANN to water pipe leak detection, using the maximum correlation between the leak signals and background noise and feeding the coefficients into an ANN for classification. Subsequent studies focused on enhancing the model by adopting various data inputs and modifying the model structure. For example, Wang et al. (W. Wang et al., 2021) utilized the attributes of ANN, directly inputting 1000 data points corresponding to 1000 input layer neurons into the ANN for anomaly recognition. Li et al. (S. Li et al., 2018) used acoustic features from time and frequency domains. Furthermore, El-Zahab et al. (El-Zahab et al., 2022) utilized MIE to extract the acoustic characteristics of leak signals and background noise in water pipes. Regarding model structure, various approaches have been taken to improve the overall performance of anomaly recognition models. For example, some researchers have focused on enhancing the network architecture using deep learning techniques such as CNN and DNN, which will be discussed in Section 2.5.2.

### **2.5.1.2 Support Vector Machine (SVM)**

SVM is a supervised ML algorithm commonly used for classification and regression tasks (Cortes & Vapnik, 1995). It aims to find the maximum margin separating the hyperplane by solving the optimization problem, as illustrated in Equation (2.2)

$$\begin{aligned} & \text{minimize} \cdot \frac{1}{2} \|\mathbf{w}\|^2 \\ & y_i(\mathbf{w}^T \mathbf{x}_i + b) \gg 1 \cdot \text{for} \cdot \text{all} \cdot i \end{aligned} \quad (2.2)$$

where  $\|\mathbf{w}\|$  is the L2 norm of the weight vector, and  $y_i$  is the class label of the  $i$  th data point.

Water leak detection works by finding the best decision boundary, called hyperplane, to separate the leak samples in the input data with the maximum margin. SVM is appropriate for solving leak detection problems with small sample sizes (Z. Wang et al., 2022). R. Cody et al. (R. Cody et al., 2017, 2018) introduced one-class SVM, a semi-supervision model that caters to anomaly detection. One-class SVM detects leak samples outside of the normal acoustic boundary. It can handle different leak signals but requires normal data of high quality. However, it cannot handle multiple-class problems and may generate false alarms due to noise.

### **2.5.1.3 K-Nearest Neighbors (KNN)**

KNN uses distance metrics to measure similarity among samples, classifying instances or performing regression based on the K closest neighbors in the feature space. The main advantages of KNN are simplicity, ease of implementation, and adaptability. However, according to the results of studies, its performance may be inferior to other methods and sensitive to the choice of parameters and the quality of training data. For instance, in the context of MEMS accelerometer data, KNN demonstrates the least identification capability compared to other methods, such as decision trees and random forests for both metal and non-metal material (Tariq et al., 2022). Meanwhile, KNN performed worse than SVM and DT in detecting leaks of different sizes in the study of Virk et al. (Virk et al., 2020).

#### **2.5.1.4 K-means Clustering**

Inspired by the concept of distance metrics and clustering of data points, K-means clustering is an unsupervised technique that partitions a dataset into K-clusters based on similarity (MacQueen, 1967). El-Zahab et al. (El-Zahab et al., 2019) applied it to clustering collected samples into different leak statuses. While it discovers data patterns without labeled examples, K-means struggles with scarce leak signals, unbalanced clustering sizes, and sensitivity to outliers, which may affect centroid locations and cluster assignments (Berkhin, 2006). Additionally, noise in acoustic signals from field experiments can influence model performance.

#### **2.5.1.5 Gaussian Mixture Model (GMM)**

As a family of probabilistic machine-learning algorithms, GMM is also a clustering algorithm. Compared to K-means clustering, GMM provides benefits such as adaptability in modeling diverse cluster shapes and sizes, increased outlier resilience, and enhanced fitting to the underlying data distribution. However, these advantages come with the trade-offs of higher computational complexity and susceptibility to parameter initialization issues. To strengthen model performance further, multi-scale Kolmogorov-Smirnov was applied to extract important features (Rai & Kim, 2021). Furthermore, Liu et al. (2022) proposed an ensemble model that generates several weights to reduce outlier sensitivities.

#### **2.5.1.6 Naive Bayes**

Naive Bayes classifiers, grounded in the Bayes theorem, are a family of probabilistic machine-learning algorithms that operate under the assumption of feature independence

(H. Zhang, 2004). As shown in Equation (2.3) the naive Bayes classifier predicts that  $\mathbf{x}$  belongs to the class that has the highest posterior probability

$$p(C_k|\mathbf{x}) = \frac{p(C_k)p(\mathbf{x}|C_k)}{p(\mathbf{x})} \quad (2.3)$$

where  $p(C_k)$  is the class prior probability,  $p(\mathbf{x}|C_k)$  is the likelihood, and  $p(\mathbf{x})$  is the predictor prior probability.

It is proposed based on the independence assumption, but the extracted acoustic features might correlate, potentially impacting the classification accuracy (Domingos & Pazzani, 1997). Thus, Naïve Bayes was not widely applied for water leak detection, even though it achieved good performance in leak detection (El-Zahab et al., 2018; Fares et al., 2022) and leak size identification (El-Zahab et al., 2018).

### **2.5.1.7 Tree-based Model**

Decision tree (DT) is a popular supervised learning algorithm for classification and regression. However, its performance in water leak detection is often inferior to other ML models (Tijani et al., 2022; T. Yu et al., 2023) due to its sensitivity to the dataset and overfitting.

To overcome this issue, ensemble methods were applied, including Random Forest (RF), Gradient boosting tree, and XGBoost have been proposed. These methods combine multiple decision trees to improve accuracy and robustness, making them practical for handling complex non-linear relationships between features and the target variable. Ensemble methods handle high-dimensional datasets with complex non-linear relationships and provide a measure of feature importance, making them widely used for various classification and regression tasks (Rayaroth & G, 2019). Therefore, they have been widely adopted for leak detection (J. Butterfield et al., 2018; G. Guo et al.,

2021b; Singh et al., 2021; Tariq et al., 2022; W. Xu et al., 2022), with studies showing excellent performance among different models. The details and advantages and disadvantages of each algorithm can be referred to following studies (T. Chen & Guestrin, 2016; Friedman, 2001; Tin Kam Ho, 1998).

### 2.5.1.8 Summary

Overall, the ML model selection should be based on the specific requirements and constraints of the problem rather than solely on the latest or best model available (Provost & Fawcett, 2013). Table 2.6 provides detailed adopted HFB leak detection models for water pipes, including advantages and disadvantages, for reference.

Table 2.6 A summary of HFB models for water leak detection using acoustic signals

Model	Advantages	Disadvantages	Ref
ANN	<ul style="list-style-type: none"> <li>Ability to model complex nonlinear relationships between inputs and outputs</li> <li>Be able to learn from large datasets and improve performance over time</li> </ul>	<ul style="list-style-type: none"> <li>Black box in nature and hard to explain</li> <li>Be prone to overfitting</li> <li>Be computationally intensive, particularly for large-scale applications</li> </ul>	<p>(Bohorquez et al., 2020; El-Zahab et al., 2022; Fares et al., 2022; Kumar et al., 2017; S. Li et al., 2018; Ravichandran, Gavahi, Ponnambalam, Burtea, &amp; Mousavi, 2021; Tijani et al., 2022; W. Wang et al., 2021)</p>
SVM	<ul style="list-style-type: none"> <li>Perform well in high-dimensional spaces</li> <li>Be robust to outliers in the data</li> <li>Ability to model nonlinear relationships between inputs and outputs using kernel technique</li> </ul>	<ul style="list-style-type: none"> <li>Sensitive to the choice of parameters</li> <li>The decision boundary created by SVMs can be difficult to interpret</li> </ul>	<p>(Ayati et al., 2022; Banjara et al., 2020; Chi et al., 2022; Chuang et al., 2019; R. Cody et al., 2017, 2018; Diao et al., 2020; Duong &amp; Kim, 2018; El-Zahab et al., 2018; Fares et al., 2022; G. Guo et al., 2021b; X. Guo et al., 2024; Y. Liu et al., 2019; Luong &amp; Kim, 2020; Pan et al., 2018; T. Quy &amp; Kim, 2019; Rashid et al., 2014; Saravanabalaji et al., 2023; Singh et al., 2021; Tijani et al., 2022; Vanijjirattikhan et al., 2022; Virk et al., 2020; Z. Wang et al., 2022; T. Xu et al., 2021; Yang et al., 2010; T. Yu et al., 2023; Yuriko</p>

			Terao & Akira Mita, 2008; C. Zhang et al., 2022; S.-L. Zhao et al., 2023)
KNN	<ul style="list-style-type: none"> <li>• Easy to understand and implement</li> <li>• No need to make any assumptions about the underlying data distribution</li> </ul>	<ul style="list-style-type: none"> <li>• Sensitive to the choice of distance metric</li> <li>• Struggle with imbalanced classes</li> </ul>	(Chuang et al., 2019; Levinas et al., 2021; T. B. Quy et al., 2019; Singh et al., 2021; Tariq et al., 2022; Tijani et al., 2022; Ullah et al., 2023; Virk et al., 2020; T. Yu et al., 2023)
K-means clustering	<ul style="list-style-type: none"> <li>• Simple and easy-to-implement</li> <li>• Computationally efficient and can converge quickly</li> </ul>	<ul style="list-style-type: none"> <li>• Sensitive to the initial choice of centroids and outliers</li> <li>• Require prior knowledge of the number of clusters</li> </ul>	(El-Zahab et al., 2019)
GMM	<ul style="list-style-type: none"> <li>• Able to model complex distributions by combining multiple Gaussian distributions</li> <li>• Ability to handle overlapping clusters</li> </ul>	<ul style="list-style-type: none"> <li>• Sensitive to the initial choice of parameters</li> <li>• The number of components in GMMs can be difficult to interpret</li> <li>• Require Prior Knowledge of the number of components</li> </ul>	(M. Liu, Yang, et al., 2022; Muller et al., 2021; Rai & Kim, 2021; Rashid et al., 2014)
Naïve Bayes	<ul style="list-style-type: none"> <li>• Easy to understand and implement</li> <li>• Require less training data</li> <li>• Robust to Irrelevant Features</li> </ul>	<ul style="list-style-type: none"> <li>• Assumption of the independence of features</li> <li>• Limited model flexibility and sensitivity to outliers</li> </ul>	(El-Zahab et al., 2018; Fares et al., 2022; T. Quy & Kim, 2019)
Decision Tree	<ul style="list-style-type: none"> <li>• Easy to interpret and visualize</li> <li>• Able to handle both categorical and numerical data</li> <li>• Ability to handle missing data</li> </ul>	<ul style="list-style-type: none"> <li>• Prone to overfitting</li> <li>• Sensitive to small changes in the data</li> <li>• Possible bias in imbalanced data.</li> </ul>	(El-Zahab et al., 2018; Fares et al., 2022; G. Guo et al., 2021b; Harmouche & Narasimhan, 2020; Tariq et al., 2022; Tijani et al., 2022; Virk et al., 2020; T. Yu et al., 2023)
Ensemble Tree Model	<ul style="list-style-type: none"> <li>• Able to handle non-linear and complex data</li> <li>• Provide a measure of feature importance</li> </ul>	<ul style="list-style-type: none"> <li>• Computation is expensive.</li> <li>• Interpretation can be challenging.</li> <li>• Possible bias in imbalanced data.</li> </ul>	(J. Butterfield et al., 2018; Fares et al., 2022; G. Guo et al., 2021b; Harmouche & Narasimhan, 2020; Saravanabalaji et al., 2023; Tariq et al., 2022; W. Xu et al., 2022)

## 2.5.2 Development of Deep Learning Model

In acoustic leak detection, HFB models, such as ANN, have been widely used to analyze acoustic data and identify leaks. However, deep learning models have emerged as an

advanced technique that handles large and high-dimensional datasets with complex patterns and features. As an illustration, Vanijjirattikhan et al. (2022) used deep neural networks (DNN) to process thousands of acoustic data samples from the leak detection system. They were incorporated with genetic algorithms to optimize their structure (Duong & Kim, 2018). Despite being a deeper iteration of ANN, DNN exhibits significantly higher complexity and demands substantial computational resources.

In contrast to DNN, CNN is a type of deep learning that automatically extracts and suppresses meaningful features from input data using convolutional layers. CNN has revolutionized the field of acoustic leak detection by capturing time-frequency features and local patterns in data, significantly improving the identification performance (LeCun et al., 2015). Therefore, the following section focuses on CNN and describes improvements to the applied model.

CNN is the most applied deep learning model for acoustic water leak detection, as it analyzes and extracts features from complex data such as spectrograms. Other deep learning models, such as RNN and LSTM, have been utilized in different applications but have not been widely explored for acoustic water leak detection. Therefore, this section describes the attempts applied on CNN, including the adopted optimizer and structures, as shown in Table 2.7.

Table 2.7 Applied optimization techniques and improved structure for CNN

		Details	Ref
Input Data	1-D CNN	<ul style="list-style-type: none"> <li>Analyzes time pattern characteristics</li> <li>Detects local time-series characteristics</li> <li>Less capable of capturing frequency</li> </ul>	(Z. Ahmad, Nguyen, & Kim, 2023; Bohorquez et al., 2020; Boujelben et al., 2023; Kang et al., 2018; Vanijjirattikhan et al., 2022; W. Wang & Gao, 2023; M. Zhou et al., 2021)
	2-D CNN	<ul style="list-style-type: none"> <li>Captures both time and frequency features</li> </ul>	(Bykerk & Valls Miro, 2022; J. Choi & Im, 2023; Chuang et al., 2019; R. A.

		<ul style="list-style-type: none"> <li>• Handles multi-dimensional input data</li> </ul>	Cody et al., 2020; G. Guo et al., 2021b; P. Liu et al., 2023; Y. Nam et al., 2021; Ravichandran, Gavahi, Ponnambalam, Burtea, Mousavi, et al., 2021; Shukla & Piratla, 2020a; Siddique, Ahmad, Ullah, et al., 2023; Tsai et al., 2022; Vankov et al., 2020; Wu et al., 2023; T. Yu et al., 2023; B. Zhou et al., 2020)
Main structure	LeNet-5	<ul style="list-style-type: none"> <li>• Suitable for small-scale 2-D data recognition.</li> <li>• Simple and effective structure.</li> <li>• Lightweight model with smaller size and parameters.</li> </ul>	(J. Choi & Im, 2023)
	Squeeze Net	<ul style="list-style-type: none"> <li>• Parameter compression reduces storage and computation.</li> <li>• Achieves a good balance between model size and accuracy</li> </ul>	(T. Yu et al., 2023)
	AlexNet	<ul style="list-style-type: none"> <li>• Introduces ReLU activation and GPU parallel computing.</li> <li>• Requires significant resources and training time.</li> </ul>	(Shukla & Piratla, 2020a)
	VGG	<ul style="list-style-type: none"> <li>• Simple and unified structure for easy implementation.</li> <li>• Uses small kernels and pooling for improved performance.</li> </ul>	(C. Zhang et al., 2023)
	Residual Network	<ul style="list-style-type: none"> <li>• Reduces vanishing gradient problem</li> <li>• Increase model complexity</li> <li>• Require more training data</li> </ul>	(G. Guo et al., 2021b; Mei et al., 2022; Peng et al., 2023); CS-ResNet (Mei et al., 2022); ResNet V2 (Vankov et al., 2020)
Optimizer	Transfer Learning	<ul style="list-style-type: none"> <li>• Faster training and higher robustness</li> <li>• Not suitable for a new task</li> <li>• Limited flexibility in modifying the architecture</li> </ul>	(G. Guo et al., 2021b; P. Liu et al., 2023; M. Zhou et al., 2021)
	Autoencoder	<ul style="list-style-type: none"> <li>• Extract features without labeled data</li> <li>• Reduce the dimensionality of data</li> <li>• Generate new data</li> </ul>	(R. A. Cody et al., 2020; Kingma & Welling, 2013; Ravichandran, Gavahi, Ponnambalam, Burtea, Mousavi, et al., 2021; Siddique, Ahmad, & Kim, 2023; Tsai et al., 2022)
	Data fusion	<ul style="list-style-type: none"> <li>• Utilize the signals from multiple sources to enhance validity and accuracy.</li> </ul>	(W. Wang & Gao, 2023)
	Siamese CNN	<ul style="list-style-type: none"> <li>• Identifies identical or different objects</li> <li>• Trains on a few samples</li> </ul>	(C. Zhang et al., 2023); Pseudo-siamese (P. Zhang et al., 2023)

**Figure 2.5** provides the comprehensive optimization efforts of studies that utilized CNN to detect water pipe leaks. According to the dimension of the input data, CNN leak detection models can be mainly divided into 2D-CNN and 1D-CNN. Many studies have adopted the structure of 2D-CNN, primarily extracting time-frequency information from the 2D data using convolutional kernels. Meanwhile, 1-D CNN

intends to directly analyze the time pattern characteristics and attributes in one-dimensional acoustic signals generated by water leakage. The input one-dimensional signals were obtained using an acoustic rod, AE sensors, and accelerometers deployed along the pipeline (Z. Ahmad, Nguyen, & Kim, 2023; Kang et al., 2018; Vanijjirattikhan et al., 2022). The proposed 1-D CNN can detect the local time characteristics for fault identification without signal transformation. Meanwhile, data fusion was adopted to enrich the information. Wang and Guo (2023) used pressure and acoustic to reconstruct the data matrix, providing more reliable data support for the diagnosis algorithm. However, 1-D CNN can capture fewer features in the frequency domain and time-frequency characteristics.

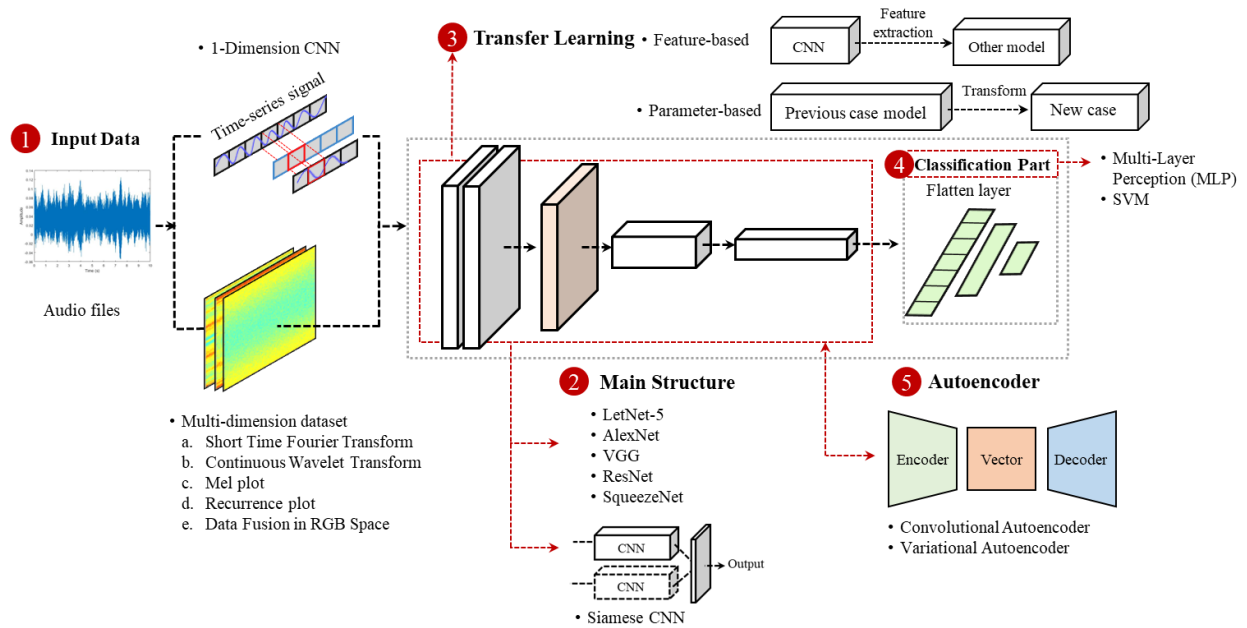


Figure 2.5 General workflow of cnn for water pipe leak detection

Researchers have adopted classic CNN models and explored various modifications to enhance model performance in acoustic data analysis for the main structure of CNN. LeNet-5 pioneered CNN for small-scale image recognition (LeCun et al., 1998). Choi and Im (2023) applied it to analyze short vectors, transforming the magnitude spectrum

vector of  $1 \times 512$  to a matrix of  $32 \times 16$  as input for the CNN detection model. AlexNet revolutionized image classification with its deep architecture (Krizhevsky et al., 2017), incorporating multiple convolutional and fully connected layers and introducing key techniques such as ReLU activation functions, local response normalization, and dropout to address training challenges and enhance generalization. Shukla and Piratla (2020a) utilized AlexNet to analyze the more complex scalogram with  $227 \times 227$  size, which might not be suitable for LeNet-5. Visual Geometry Group (VGG) is known for its simple, effective deep architecture with multiple convolutional layers (Simonyan & Zisserman, 2014). It uses small  $3 \times 3$  filters, allowing for variations by adjusting the network depth. It is acknowledged to be an effective tool for audio classification (Hershey et al., 2017). Thus, it has been used to process  $96 \times 64$  mel spectrogram for leak detection. ResNet is a deep neural network with skip connections designed to address the vanishing gradient problem (He et al., 2016), facilitating the training of deeper models. ResNet offers improved gradient flow, easier optimization, and enhanced performance in capturing complex signal patterns in acoustic-based water leak detection. However, ResNet is limited by increased architectural complexity and potential overfitting on small or unrepresentative datasets. To cover this, Mei et al. (2022) utilized compressed sensing to achieve relatively high leakage identification accuracy while significantly reducing model training time.

On the other hand, SqueezeNet achieved high accuracy while reducing the number of parameters, making it well-suited for resource-constrained environments like mobile devices (Iandola et al., 2016). Yu et al. (2023) compared SqueezeNet with other HFB

classifiers and found that SqueezeNet is an effective and powerful tool for identifying leaks in water pipe networks.

Meanwhile, the Siamese structure is incorporated with CNN to compare the similarity of input signals. It is more robust to the class imbalance in datasets because it focuses on learning pairwise relationships rather than class-specific features (Koch et al., 2015). When given the baseline, the model can determine whether the collected data relates to scheduled/unscheduled events. Zhang et al. (2023) adopted the Siamese CNN model, classifying acoustic files into anomalies, background, or environmental noise. When detecting anomalous status, a field investigation will be conducted if the waveform is classified as an anomaly unrelated to predetermined events. The model has been validated using data from Adelaide's recordings. Besides, Zhang et al. (2023) adopted the pseudo-siamese CNN that uses two parallel convolutional structures for processing the handcrafted features and collected signals, achieving feature fusion.

Transfer learning (TL) has also been introduced in the main structure of the CNN leak detection model to enhance performance. Research on water pipe leakage detection predominantly relies on parameter-based and feature-based transfers. Parameter-based TL is commonly utilized when applying classical CNN models. Liu et al. (2023) adopted several pre-trained models (e.g., ResNet, VGG) and replaced the final fully connected layers for fine adjustment. Similarly, Zhang et al. (2023) also conducted a similar TL process on VGG to establish Siamese models. Besides, Guo et al. (2021b) applied parameter-based TL, pre-trained the model parameters using water leakage data from Chengdu, and then transferred it to the cases in Changzhou. On the other hand, feature-based TL transfers feature representation from source to target data, enabling

traditional ML approaches to perform better. Liu et al. (2023) transferred the trained HFB networks as the feature layers for the subsequent classification model. The result reveals that the feature-based classification methods significantly outperform parameter-based and traditional CNN.

The previous convolutional layers or main structure can be regarded as performing feature extraction, wherein they extract relevant information and feed it into the classification part. In acoustic leak detection, most traditional CNN employs multi-layer perceptron (also known as a type of feedforward ANN (Haykin & Network, 2004)) for classification purposes. Shukla & Piratla (2020a) applied the typical 2-D CNN for fault identification. The proposed model captures the time-frequency characteristics and condenses them into each perceptron neuron, revealing the impact of external physical factors. Alternatively, Kang et al. (2018) proposed an ensemble classification method that respectively feeds the features from convolution into the MLP and SVM for cross-classification. The proposed CNN-SVM model improves the classification accuracy compared to one-dimensional feature extraction and traditional deep learning architectures.

Autoencoders compress and reconstruct data by minimizing the discrepancy between the original and reconstructed data, thereby enhancing flexibility and capabilities in the training process when combined with CNN. Convolutional autoencoder (CAE) is designed to handle grid-like data, applied by Tsai et al. (2022) to suppress multi-dimensions matrix, preserving the correlation between the timing information on the compression matrix and the sensor. Siddique et al. (2023) and Ahmad et al. (2022) utilized Convolutional Autoencoders (CAE) to extract global features, which were then

combined with the local features extracted by the traditional CNN structure. This fusion of global and local features offers a comprehensive information representation for accurate acoustic leak detection. Meanwhile, the variational autoencoder (VAE) is a probabilistic autoencoder that learns the parameters of latent space distribution, enabling new sample generation and unsupervised learning tasks (Kingma & Welling, 2013). In literature, Cody et al. (2020) insert VAE into CNN. The model is built based on the non-leak scenario, thus establishing a semi-supervision detection system. In acoustic leak detection, VAEs enable unsupervised learning and identify anomaly patterns. Meanwhile, CAE efficiently captures multi-dimensional patterns and relationships in acoustic data, making them suitable for feature extraction related to leak detection.

## 2.6 Research Gaps

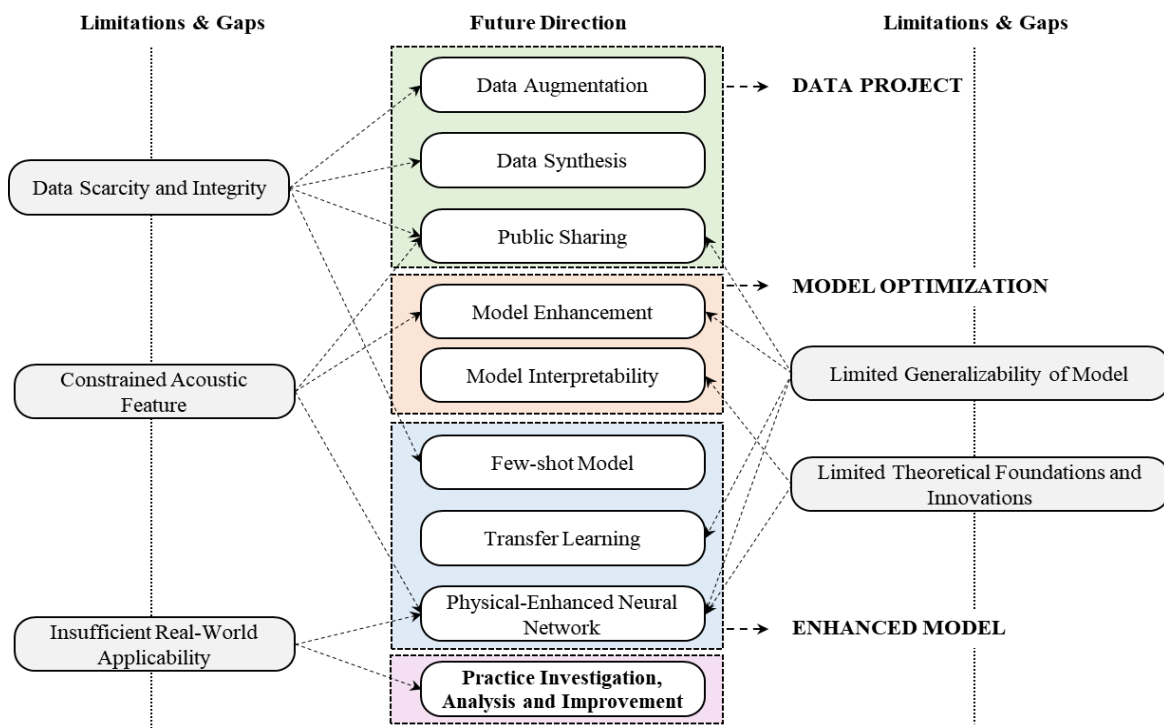


Figure 2.6 Summary of limitations and potential future directions

In addition to the progress reviewed in the previous sections, limitations and gaps still require further investigation. Figure 2.6 analyzes the principal limitations and gaps of the proposed approaches and outlines potential avenues for future research to mitigate them.

## **2.6.1 Limitation and Gaps**

### **2.6.1.1 Data Scarcity and Integrity**

Water leak diagnosis research needs to build a laboratory-simulated testbed or collect data from the field measurements, which requires a lot of capital investment and long-term experiments. Most existing research contains limited samples, especially when using complex models (e.g., CNN). In several studies (G. Guo et al., 2021b; Y. Nam et al., 2021; T. Yu et al., 2023), data segmentation or enhancement techniques were used to divide data samples into sub-samples with similar acoustic characteristics. A part of the experimental studies was based on data from a single location, and all data was generated in one location. During training, the sound recorded in a region was also used to verify the model's performance in the same area. Consequently, if data is present in both the training and testing sets, it may result in overfitting or inflated accuracy, violating the requirement for independence between training and testing sets (Y. Nam et al., 2021).

Notably, the authors noticed that data sharing was rare in the relevant research area, and there is no such open database similar to the one in computer vision. This implies that researchers who want to replicate or advance the studies should spend additional time on data collection, preprocessing, and labeling. It is also not feasible, and there is no benchmark to validate the performance of models developed by different researchers

on another water pipe network with distinct characteristics. Moreover, only Guo et al. (G. Guo et al., 2021b) shared the code for developing CNN, allowing other researchers to build on their work. A possible reason for the lack of data sharing is that researchers wanted to protect their intellectual property rights and competitive advantage in developing novel detection techniques (Stieglitz et al., 2020). It may lead to a research monopoly by a few researchers who have access to the data, which hinders the healthy development and progress of the field. Therefore, the authors encourage the researchers in this research area to establish an open dataset. For example, Aghashahi et al. (Aghashahi et al., 2023) provided the benchmarking dataset for leak diagnosis, properly facilitating relevant studies, which can contribute to academic and industrial development.

#### **2.6.1.2 Limited Generalizability of Model**

Although numerous studies have reported high accuracy, 90% or even 100% of the developed ML-based models for leak diagnosis in water pipes, the generality of current ML-based leak diagnosis models is limited due to their significant dependence on the training dataset. Generally, the acoustic signal induced by water leaks is associated with various factors, including pipe diameter, pipe thickness, pipe material, pipe pressure, leak size, backfill soil, and so on (J. Butterfield et al., 2018; Sitaropoulos et al., 2023b). It has been found that leaks generated different acoustic responses, even with the same flow rate and distance to the sensor but different topology (Sitaropoulos et al., 2023a). However, it is not practical to simulate all scenarios in laboratory conditions, not even in field measurements. The signals used for model development are a subset of the complete dataset, whose representativeness is limited, posing challenges in capturing

the true diversity of leak scenarios in water pipe signals. In addition, the attenuation of leak signals in the propagation from the leak source to the sensor locations leads to a loss of partial leak information. Therefore, the data collected at different locations are different. Existing studies have not treated the attenuation of leak signals in much detail in developing ML-based models. As a result, the developed models may exhibit poor performance in areas where data has not been collected, thereby hindering their generalizability to new employment sites. Clear evidence is the work conducted by Terao and Mita (Yuriko Terao & Akira Mita, 2008), who applied the newly collected data to the previous research, which only obtained 53.6% accuracy.

From the perspective of model complexity, a simple model may not be able to learn complex acoustic patterns in leak signals. In contrast, an overly complicated model may overfit the training data, leading to decreased performance in new areas (Goodfellow et al., 2016). Factors such as overfitting, underfitting, and inadequate model selection can contribute to poor generalization. In particular, for DNN and CNN, the numerous parameters and complex model structure might exacerbate the overfitting problem.

### **2.6.1.3 Constrained Theoretical Foundations And Innovations**

The limited theoretical foundation of ML models poses inherent limitations, leading to a greater emphasis on empirical rules and experimentation in water pipe leak models. Most studies rely on parametric studies to determine appropriate data segmentation methods and employ optimization methods such as grid search to optimize model parameters. The model lacks a solid theoretical basis and has poor interpretability. Therefore, the model may not be able to detect or correct its errors or biases, which may

lead to inaccurate, unfair, or harmful results. Users or stakeholders might not easily understand and accept ML techniques.

Meanwhile, the research on water leak diagnosis using ML is mainly based on applying existing models. The modeling phase of each study is almost similar, especially for the traditional machine learning models. At the same time, the innovation is mainly concentrated in the data preparation stage (for example, applying different data processing techniques), which is relatively similar. There is a lack of innovative research related to water leak diagnosis. Last, ML-based water leak diagnosis studies prioritize the development of intricate algorithms, overlooking the integration of sufficient domain knowledge, such as the generation of leak acoustic signals and their propagation characteristics along water pipes. Such oversights may result in models that fail to capture the core principles that govern the phenomena under study, thereby imposing limitations on both the theoretical foundation and innovation potential.

#### **2.6.1.4 Constraints in Acoustic Feature**

Most ML-based leak diagnosis models are based on insufficient features because the features of leak signals have not been fully understood. As mentioned, the acoustic signals collected under different conditions may have other acoustic characteristics. The difference is even more pronounced when considering the attenuation of leak signals in the propagation along water pipes. Evidence found by Hunaidi & Chu (Hunaidi & Chu, 1999) demonstrates that the acoustic noise generated by leaks in plastic pipes suffered rapid attenuation after propagating over long distances, and the frequency components of collected signals presented great variability. As a result, the leak noise signature could become indistinguishable from the acoustic characteristics of non-leak data.

Therefore, further research is needed to study and understand the features of leak signals and incorporate pipe characteristics and attenuation patterns into the feature engineering to explain the acoustic signal better.

### **2.6.1.5 Insufficient Real-World Applicability**

In the current body of ML-based modeling research, while models can differentiate between leaks and noleak signals, there is a lack of specifically developed leak diagnosis models for practical applications. Several studies (El-Zahab et al., 2022; S. Li et al., 2018) deployed sensors on the surfaces of pipes. However, this approach is less feasible in real-world situations, as water pipes are typically underground, making sensor attachment challenging. Optional deployment places are generally valves that can be opened and used to attach sensors, which are also used in practical applications (Kang et al., 2018; Tariq et al., 2022; Tijani & Zayed, 2022). Although ML models can determine leak status, they do not provide information about which pipe is experiencing the leak since the sensor can sense the possible leak noise propagated from all pipes that it is connected to, diminishing the practical value of ML detection models.

Furthermore, while some studies have examined the model's ability to identify varying leak sizes (Duong & Kim, 2018; W. Wang et al., 2021), there is limited information on the maximum detectable leak distance for ML-based models. It's been confirmed that leak signals attenuated much more quickly in plastic pipes than in steel pipes (J. M. Muggleton et al., 2004), and the attenuation pattern also differs in pipes with different characteristics (F. Almeida et al., 2014a; Brennan et al., 2018b). Consequently, during practical implementation, it is hard to optimally configure the detection network based on the model's performance or to efficiently schedule inspection and maintenance work,

ultimately affecting the effectiveness of the model. Therefore, much more effort is suggested to examine the detectable capability of developed models, which can help optimize the sensor deployment in the field water pipe network.

## **2.6.2 Future Directions**

### **2.6.2.1 Data Project**

To deal with the problem of data scarcity, techniques such as data augmentation and synthesis can be used to enrich the dataset. Meanwhile, data sharing is encouraged to establish a benchmark dataset for the research area.

#### **i. Data Augmentation**

Data augmentation is a technique used to increase the diversity and size of a dataset by creating new samples through various transformations applied to the existing dataset. Previous studies were mainly applied to the time domain, and future work can focus on frequency and time-frequency domains, including frequency masking and filter augmenting. Herein, frequency masking randomly obscures some frequency bands in the signals to emulate diverse acoustic environments and noises (Park et al., 2019), increasing the model's resilience to frequency variations. Filter augment randomly assigns different weights to frequency bands in the signals to imitate acoustic filters (H. Nam et al., 2022), which allows the model to extract relevant information from broader frequency regions.

#### **ii. Data Synthesis**

Data synthesis is used to generate new samples that can be used for data simulation and testing in acoustic water leak diagnosis. Various techniques can be employed to enhance

the comprehensiveness of a dataset, such as waveform concatenation, generative adversarial networks, Variational Autoencoders, and WaveNet.

Waveform concatenation refers to dividing time series into several segments and recombining them to generate new samples (Z. Meng et al., 2019). GAN involves a generator and a discriminator, working together in a competitive game-like manner to generate realistic data similar to the training data (Creswell et al., 2018). GAN can create approximately realistic and high-quality acoustic or vibration leak signals, augment existing datasets, and improve the performance of ML-based models.

VAE uses the encoder and decoder networks to learn and generate data while encouraging a learned latent distribution to follow a pre-defined probability distribution for diverse outputs (Doersch, 2016). VAE can model the underlying structure of acoustic data and generate new samples with similar characteristics (Nishizaki, 2017). Regarding water pipe leak diagnosis, VAE can be trained to reconstruct clean versions of noisy input signals with a denoising objective. WaveNet is a self-regressive model that generates one sample at a time and adjusts each new sample based on the previously generated samples (Oord et al., 2016). It employs dilated causal convolutions, which allow the model to capture both short-term and long-term dependencies in the audio waveform. Other cutting-edge methods for data synthesis are also suggested to be implemented, and a comparative study is worth carrying out to determine the appropriate approach for water leak diagnosis.

### *iii. Data Sharing*

To promote collaboration, establishing benchmark datasets is an effective solution to help academic studies by offering data that is hard or expensive to collect. This will also

support research in this area by allowing verification, replication, extension, and comparison of studies. Especially in the ML-based domain, the famed Neural Information Processing Systems, for example, will propose a dataset and establish competition annually, which promotes the invention of Transformer (Vaswani et al., 2017). For water leak diagnosis, Vrachimis et al. (Vrachimis et al., 2022) have publicized a dataset of pressure and flow signals collected from L-town and appealed to international institutions to detect and localize the defects. It promotes the development of techniques for defect detection using pressure or flow information. Therefore, it is urgent to establish a benchmark dataset of acoustic signals for water leak diagnosis, which facilitate the development of technologies in the research area. The public dataset is expected to contain sufficient information about physical characteristics of target water pipes and have massive validation data to test the proposed models thoroughly.

### **2.6.2.2 Model Enhancement and Interpretability**

#### **i. Model Enhancement**

Water pipe leaks change acoustic and pressure waves, temperature, and soil properties in the vicinity. Relying on a single type of signal provides limited information. Data fusion integrates data and knowledge from various sources, improving the reliability and robustness of models (Castanedo, 2013). Data fusion also includes the fusion of overlapping measurements obtained from the same sensor at different times to improve the model's representation, accuracy, certainty, and completeness (Bellot et al., 2002). In water pipe detection, current studies primarily use data fusion of multiple sensors of the same type. Fusion and utilizing the advantages of different sources of information,

such as pressure signals, ground penetrating radar, and electromagnetic induction sensors, might help to improve detection accuracy and reduce false alarms (Misiunas et al., 2005). In particular, hydraulic information is easier to obtain in water pipe networks through the equipped supervisory control and data acquisition system compared to other types of signals (Murvay & Silea, 2012), but fewer studies have integrated acoustic and hydraulic information for water leak diagnosis. Future research can use data fusion techniques in this direction to improve the robustness and accuracy of the model.

#### ii. Model Interpretability

Machine learning models are commonly considered a “black box”, and their results are hard to interpret, making it difficult for researchers or industrial practitioners to understand the model's inner workings and ensure its reliability.

Several techniques are proposed to improve interpretability and remove redundant features or data. SHAP and Boruta have been utilized to assign weights to each feature and enhance interpretability in machinery fault detection (Brito et al., 2022) and water pipe leak detection (W. Xu et al., 2022).

Local sensitivity analysis methods, such as individual conditional expectation plots (Goldstein et al., 2015) and partial dependence plots (Friedman, 2001), can be used to visualize and analyze interactions between the target response and input features of interest. Global sensitivity analysis, which involves changing multiple input features simultaneously and measuring the model's response, can also be applied. Techniques, including the Morris method and variance-based sensitivity analysis (Homma & Saltelli, 1996), can quantify the contribution of each input feature and its interaction with the model output variance. The intricate models, such as CNN, can be better understood by

visualizing filters and activation maps in future research. It is beneficial for detection models that rely on the time-frequency spectrum, as it can reveal the acoustic patterns or areas to which the model is sensitive.

### **2.6.2.3 Enhanced Model**

It is acknowledged that machine learning methods are still in rapid development, and new algorithms are constantly being proposed. No algorithm has been considered the most appropriate for water leak diagnosis. It is suggested to keep utilizing and comparing newly developed models for water leak diagnosis in the future. The following are some potential choices for future studies.

#### **i. Leak Localization Deep Learning Modeling**

Despite the promising potential of machine learning in water leak detection, its application in water leak localization has been largely unexplored. Only one study by El-Abbasy et al. (2016) has employed machine learning for water leak localization using the acoustic method. This study conducted experiments on a small-scale pipeline, utilizing noise loggers to measure signals. The noise levels were used as inputs to train an artificial neural network, treating leak localization as a regression problem. However, the feasibility of this method in practical engineering applications is uncertain due to susceptibility to interference from background noise and the non-linear behavior of leak signal attenuation along the pipeline. To address these challenges and leverage recent advances in deep learning for time series data, developing an ML-based approach for water leak localization would be a meaningful and promising endeavor, focusing on achieving efficient and reliable performance.

Furthermore, machine learning has found widespread application in sound source localization based on time delay. Vera-Diaz et al. (2021) combined a CNN with generalized cross-correlation to estimate a Gaussian shape function representing the time delay between signals received by a pair of microphones. Wang et al. (2018) utilized deep learning-based time-frequency masking to improve speaker localization algorithms in noisy and reverberant environments. Bai et al. (2018) employed sparsely distributed microphone arrays and artificial intelligent systems that utilized time difference of arrival-based localization and beamforming, followed by Conv-LSTM-based machine learning, for sound source localization. These studies demonstrate that machine learning models can effectively identify and extract time-delay-related features from pairs of signals.

By integrating the knowledge gained from these studies, it is possible to develop a deep learning-based approach for water leak localization that overcomes the limitations of traditional methods, improves accuracy, and enhances the efficiency and reliability of leak detection and localization in practical scenarios.

#### ii. Few-shot models

Few-shot models are a kind of machine learning model that can effectively learn from limited training examples, often called "shots". In the context of few-shot learning, "shot" denotes the number of available training examples or instances for a specific task or category. Few-shot learning is beneficial in acoustic-based or vibration-based detection because obtaining enough labeled defect or anomaly examples can be challenging.

Models based on metric learning focus on learning similarity measures between instances. Siamese models are a specific type of neural network architecture designed to learn similarity measures between input data. As a result, Siamese models only require one or a few samples within each class to identify new objects. Currently, there are models combining CNN with Siamese models; however, recurrent neural networks (RNN) can recognize sequential signals more effectively but have not been fully explored. Therefore, Siamese-RNN was used to capture the temporal structure of acoustic signals (Kong et al., 2019). To date, networks have also been improved from Siamese networks to triple networks (Hoffer & Ailon, 2015) to enhance the recognition accuracy of specific categories, and it is a potential alternative for water leak diagnosis. Meta-learning is a subfield of machine learning that focuses on developing models that can learn and adapt quickly to new tasks with limited datasets. It aims to understand the optimal learning strategy from multiple tasks or problems, allowing them to generalize and adapt to new, unseen functions with a small amount of training data. This is particularly useful in cases where acquiring labeled data is expensive or time-consuming (Y. Wang et al., 2020), as in the case of water leak diagnosis. Currently, meta-learning techniques have been used to learn from multiple defect types and quickly adapt to detect mechanical faults with only a few labeled examples (Y. Zhang et al., 2023). By learning generalizable feature representations and optimization strategies, meta-learning can perform better on novel tasks with limited data than traditional supervised learning methods.

### iii. Transfer Learning

Transfer learning is a machine learning technique that leverages knowledge from one problem or dataset to improve parameter-based and feature-based transfer learning.

To the authors' knowledge, transfer learning has been less used for water leak diagnosis and might be a solution in the future. Considering Guo et al. (2021b) have publicized their model, subsequent studies can utilize the developed model to improve its robustness using a benchmark dataset. Furthermore, transfer learning can be applied when there is some similarity or relationship between the source and target tasks or domains. Supposing the acoustic characteristics of gas leak signals are relevant to the water leak problem, the existing studies on gas leak diagnosis might provide many pre-trained models for water pipe leak diagnosis.

#### **2.6.2.4 Practice Investigation, Analysis, and Improvement**

In addition, existing research rarely examines the application of technologies or the practical needs of the water detection industry. Some hydraulic sensor companies, Gutermann (*Water Leak Detection Technology and Products*, 2023) and Aquarius Spectrum (*Leak Detection Systems Home*, 2023), have asserted that they can create intelligent acoustic leak diagnosis systems incorporating various novel technologies. The existing application systems may have already greatly improved detection efficiency. However, it is unclear what technologies are most needed by the industry and what aspects require breakthroughs. There is a need for more purposeful solutions to address the current problems. Hence, future research could benefit from surveying and reviewing the existing methods and patents in the market or industry, enabling them

to understand the current industry needs and design or refine models more specifically and effectively.

Future ML-based research should assess the performance boundaries of acoustic detection models by combining controlled experiments and field experiments. Controlled experiments can test the performance boundaries of fault detection models, including the maximum detection distance, the smallest detectable leak size, model performance under different pipeline pressure conditions, and so forth. Field experiments can test the model's robustness in complex situations. This comprehensive approach will provide valuable insights into the capabilities and limitations of acoustic detection models, guiding further improvements and refinements for real-world applications.

## **2.7 Chapter Summary**

This chapter thoroughly evaluates machine learning-based methodologies for leak diagnosis in WDNs. The primary objective is to elucidate the existing gaps and limitations within the ML modeling framework, thereby proposing future research avenues to expedite the advancement of leak diagnosis capabilities. This comprehensive review analyzed a corpus of 70 peer-reviewed publications on ML-based acoustic leak detection, spanning 2000 to 2024. The key research limitations and shortcomings are meticulously summarized following the in-depth review, complemented by the proposition of potential future research directions.

## **CHAPTER 3 Research Design and Methodology**

### **3.1 Introduction**

This chapter offers a comprehensive exposition of the research framework devised to accomplish the research objectives effectively. The framework represents the interconnections between the objectives and outlines the research methods employed to attain each specific purpose. Furthermore, this chapter provides an extensive elucidation of these methods, highlighting their integration and demonstrating their concerted application in achieving the intended aims of the study.

### **3.2 The Framework of Methodology**

Based on the specific research objectives outlined in Chapter 1, the ML-based water leak diagnosis research follows the process depicted in Figure 3.1. The research process can be summarized as follows:

- (1) The first step in the research process is thoroughly reviewing the current state of ML-based acoustic leak diagnosis. This involves examining existing literature, technologies, and methodologies used in this field. The goal is to understand the strengths and weaknesses of current ML-based water leak diagnosis approaches, identify existing knowledge gaps, and determine areas where further research could lead to improvements.
- (2) Following a thorough review of the current ML landscape, the subsequent step involves enhancing the dataset and assembling a comprehensive dataset of diverse acoustic leak signals. The dataset is enriched upon collection using an advanced model, generative adversarial networks, and long-and-short-term memory. The generative results are evaluated through t-SNE, acoustic feature, and model

enhancement testing. After validating the effectiveness of the proposed technique, it provides generated samples for subsequent modeling and tasks. (Objective I)

(3) Grad-CAM will be applied to visualize the working mechanism of deep learning to enhance the model's interpretability. The short-time Fourier transform has been used to transform the signals into the time-frequency spectrum and, therefore, fed into CNN-based models for leak detection. The visualization results provide insights into the underlying working mechanism and elucidate the critical regions of the leak detection process. These findings can deepen the understanding of CNN and guide the denoising procedures, enhancing overall denoising performance. (Objective II)

(4) A time-series-based approach will be applied to develop robust and accurate models. The transformer incorporating the Attention mechanisms will focus on relevant input data, allowing for selective processing and analysis. Time-series enhanced models will be leveraged to handle temporal data, effectively capturing crucial dynamics and dependencies. Combining these techniques aims to handle complex data structures and scenarios effectively. (Objective III)

(5) In parallel, deep learning techniques are employed to capture the temporal patterns present in the signal pairs. It enables the model to estimate the time delay between the signals accurately, which can be used to deduce the distance to the leak. By leveraging the capabilities of deep learning, the model can effectively analyze the temporal characteristics of the signals and provide valuable insights into the location and extent of the leak within the system. (Objective IV)

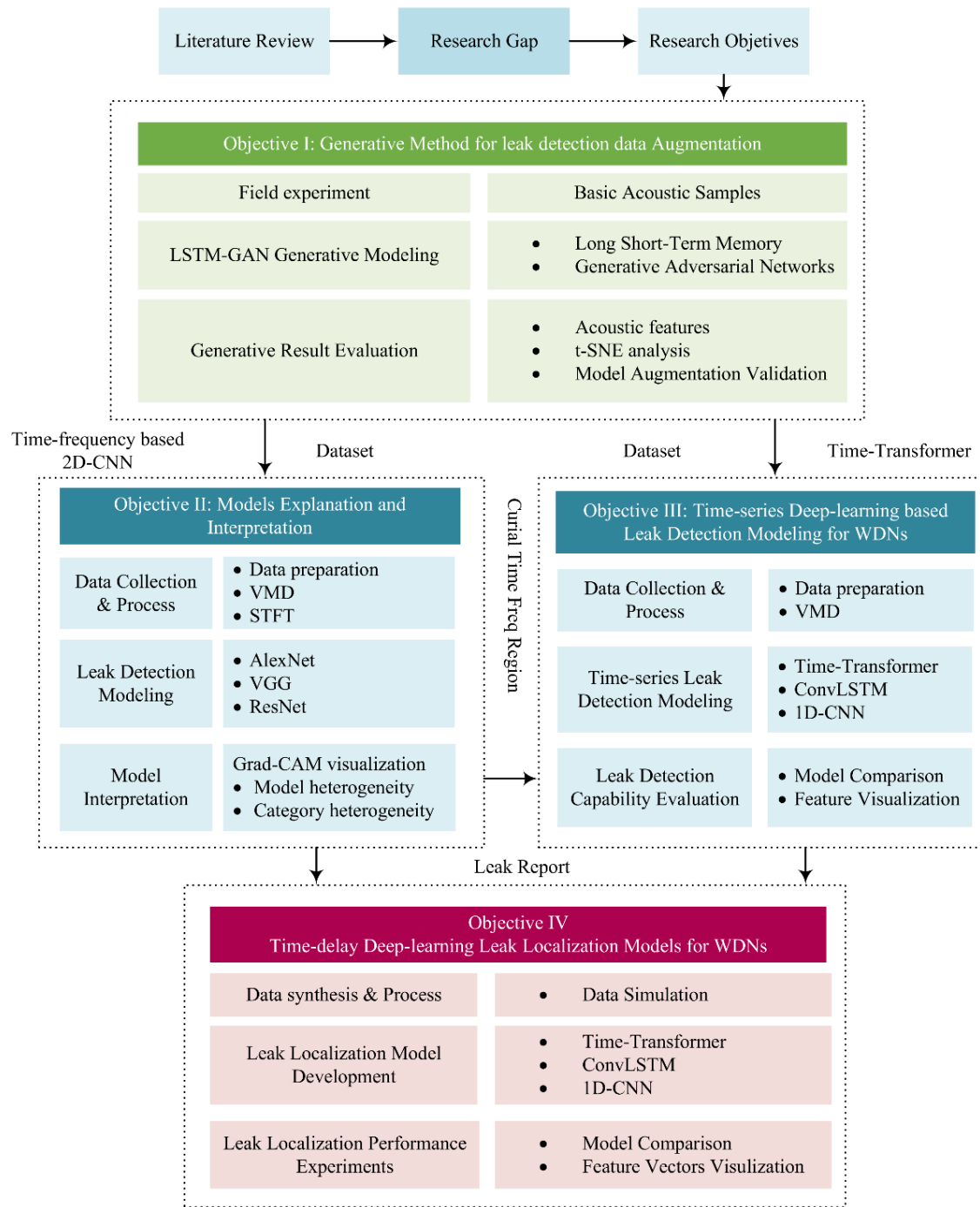


Figure 3.1 Framework of the overall research methodology

### 3.3 Research Method

This section provides an overview of the research methodologies employed in the study, which encompasses various research methods classified into two groups: machine learning modeling algorithms and analytical tools.

#### 3.3.1 Machine Learning Model

##### 3.3.1.1 Convolutional Neural Networks

CNN is a specialized deep learning model designed to effectively handle data, such as images and audio, with a grid-like structure. It has emerged as the prevailing structure for numerous computer vision tasks, primarily because it possesses the inherent capability to learn and extract features from two-dimensional data (Alzubaidi et al., 2021; T. Liu et al., 2023)

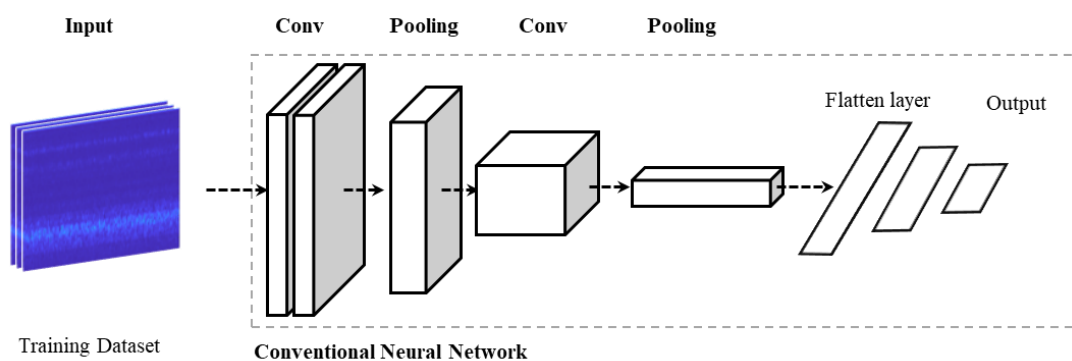


Figure 3.2 Typical framework for CNN.

The typical framework of CNN is illustrated in Figure 3.2. The convolutional layers enable CNN to capture spatial dependencies in the data. These layers apply a set of learnable filters to local regions of the input data, allowing the network to detect and extract relevant features at different spatial scales. Additionally, activation functions introduce non-linearities to the network, enabling it to learn intricate relationships between the input and output. By stacking multiple convolutional layers, CNN can learn

hierarchical representations of the input data, allowing them to capture both low-level and high-level features (Guidotti et al., 2016). Moreover, pooling layers are often placed after convolutional layers to reduce the spatial dimensions of the feature maps while retaining the essential features. Max pooling is the most common pooling operation, selecting the maximum value from each local region of the feature map and discarding the rest. This downsampling helps reduce the network's computational complexity and makes it more robust to minor spatial variations (Scherer et al., 2010). After several convolutional and pooling layers, the neural network extracts essential features from the input data. These features are then used for further processing and making predictions.

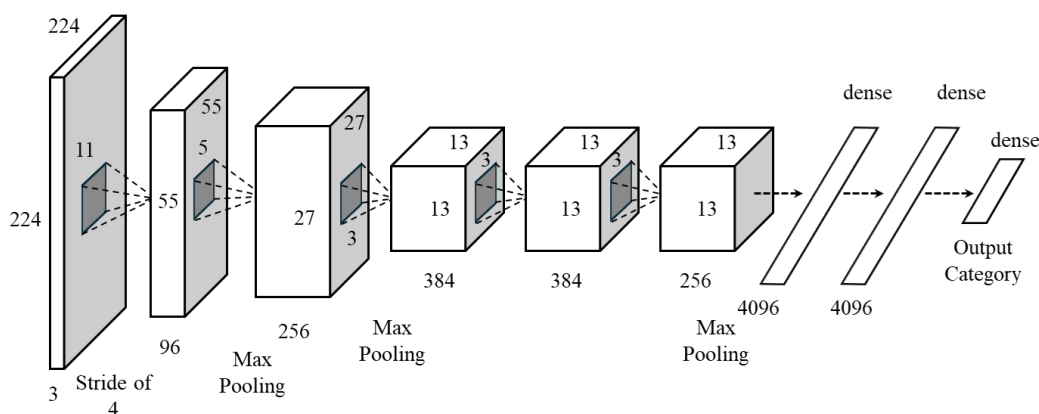


Figure 3.3 The typical model structure of AlexNet.

Figure 3.3 introduces the general structure of AlexNet, which was introduced in 2012 and revolutionized computer vision by introducing key architectural innovations (Krizhevsky et al., 2017), including increased depth, smaller receptive fields, Rectified Linear Unit (ReLU) activation, overlapping pooling, local response normalization, and dropout regularization. These advancements allowed the model to capture complex

hierarchical features, exploit spatial hierarchies, generalize better, and reduce overfitting.

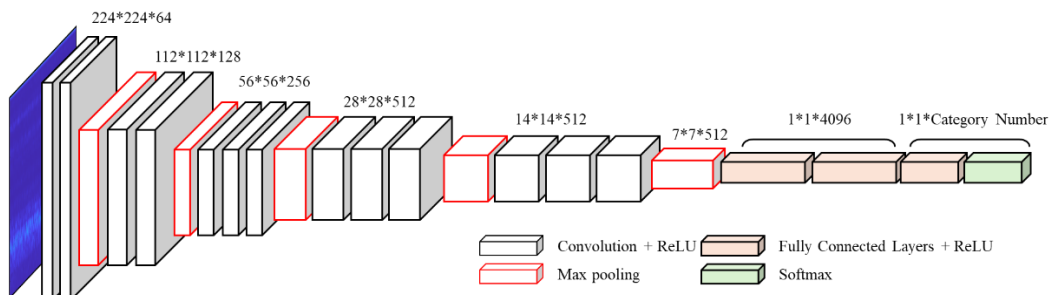


Figure 3.4 The typical model structure of VGGs.

The general structure of the Visual Geometry Group (VGG) is depicted in Figure 3.4. VGGs are another widely used CNN architecture emphasizing a more straightforward and uniform structure (Simonyan & Zisserman, 2014). It employs smaller convolutional kernels but deeper layers than AlexNet, which enhances its ability to capture complex nonlinear representations. VGG networks have shown excellent performance in grid-data classification tasks but require more computational resources due to their larger structure.

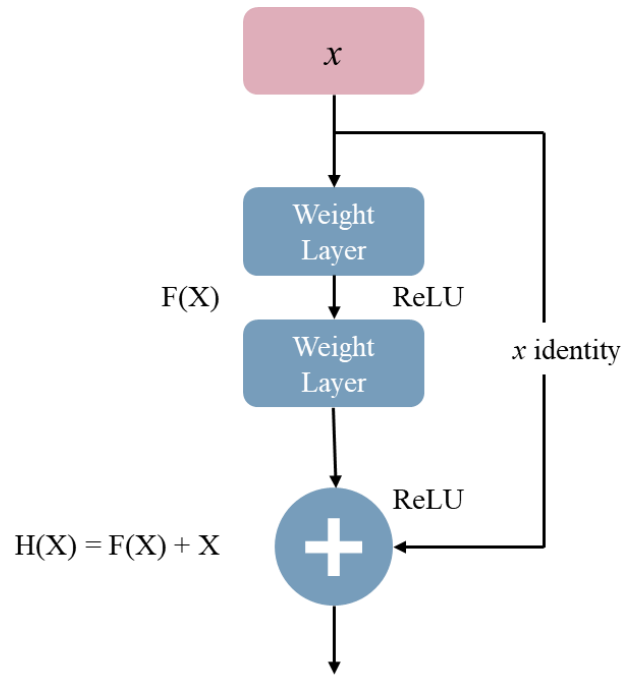


Figure 3.5 The typical structure of Residual blocks.

Residual Network (ResNet) introduces the concept of residual block, addressing the challenge of training intense networks (He et al., 2016). As illustrated in Figure 3.5, the optimal function is recorded as  $H(x)$ , then the objective function we fit is defined as  $F(x) := H(x) - x$ , and the function is defined as the residual function. ResNet assumes that the optimal function is similar to a linear function, allowing it to model the residual of the identity function, leading to faster training and easier optimization, as well as gradient vanishing and exploding that occur in deep neural networks. ResNet has been widely adopted for grid-data recognition tasks and has achieved state-of-the-art results in various benchmarks (Wen et al., 2020). However, it requires more computational resources and longer training times than shallower architectures.

In summary, CNNs have had a transformative impact on two-dimensional data analysis and have been successfully applied to various audio and signal tasks, including speech audio recognition (Hema & Garcia Marquez, 2023), machine fault diagnosis (Jiao et al.,

2020; Ruan et al., 2023), and also leak detection for WDNs (Y. Nam et al., 2021). Therefore, 1D-CNN functions as the backbone for generative modeling (Objective I) and leak localization (Objective IV) compared to other leak detection models for Objective II. Meanwhile, 2D-CNN is designated to process spectrograms and provide the basis for model interpretability enhancement (Objective III).

### **3.3.1.2 Long Short-Term Memory**

Time-series models analyze and predict time-dependent data by capturing temporal dependencies and trends, leveraging previous observations to make accurate predictions based on historical information. However, the traditional time series models, including ARIMA, exponential smoothing, and state-space models, have limitations in capturing non-linear relationships and might not have intricate dependencies and long-term patterns within time-series data (G. P. Zhang, 2003).

In contrast, LSTM, an improved variant of RNN, has emerged as a potent tool for modeling time-series data (Hochreiter & Schmidhuber, 1997). LSTM addresses the challenges of capturing long-term dependencies and mitigating vanishing gradients in RNN, making it well-suited for time-series analysis. It extends the theoretical foundation of RNN by incorporating memory cells with gate mechanisms to process sequential data effectively.



memory. Under the control of the forget gate and input gate, LSTM selectively incorporates the previous timestamp memory  $c_{t-1}$  and the new input  $c_t$ . The update of the state vector  $c_t$  is determined by Equation (3.1).

Similarly, the output gate  $g_o$  selectively determines which state vector components will be output, as shown in Equation (3.5).  $w_i$ ,  $w_c$ , and  $b_i$ ,  $b_c$  are parameter tensors of the forget gate. Ultimately, the output of LSTM is depicted in Equation (3.6).  $c_t$  passes through the tanh activation function and acts on the input gate to obtain the output of LSTM.

$$g_f = \sigma \left( w_f \begin{bmatrix} S_{t-1} \\ x_t \end{bmatrix} + b_f \right) \quad (3.1)$$

$$\hat{c}_t = \tanh \left( w_c \begin{bmatrix} S_{t-1} \\ x_t \end{bmatrix} + b_c \right) \quad (3.2)$$

$$g_i = \sigma \left( w_i \begin{bmatrix} S_{t-1} \\ x_t \end{bmatrix} + b_i \right) \quad (3.3)$$

$$c_t = g_f * c_{t-1} + g_i \hat{c}_t \quad (3.4)$$

$$g_o = \sigma \left( w_o [S_{t-1}, x_t] + b_o \right) \quad (3.5)$$

$$h_t = g_o \cdot \tanh(c_t) \quad (3.6)$$

As mentioned, LSTM models have proven their efficacy in capturing long-term dependencies in time-series data by incorporating memory cells and gate mechanisms. These mechanisms enable LSTM to learn complex patterns, handle noise, and make accurate predictions based on available information. The superiority makes LSTM a valuable tool that has been applied across various time-series tasks, including stock market prediction (Moghar & Hamiche, 2020), epidemic spread (Chimmula & Zhang,

2020), energy load forecasting (Bashir et al., 2022), biohazard prediction (M. Liu, He, et al., 2022) and anomaly detection (Lyu et al., 2020). Therefore, LSTM was utilized for data generation (Objective I) and was compared to other leak detection models (Objective III).

### 3.3.1.3 Generative Adversarial Network

GAN is a groundbreaking approach to machine learning that combines game theory, probabilistic modeling, and information theory (Goodfellow et al., 2014). The typical GAN structure consists of two neural networks, the generator and the discriminator, which are trained in an adversarial manner to generate realistic data.

As shown in Figure 3.7, the training process of GAN can be regarded as a minimax game. In this game, the generator and discriminator engage in a competitive and adversarial relationship (J. Wang et al., 2017). The generator aims to minimize the discriminator's ability to distinguish between real and synthetic samples, while the discriminator aims to maximize its discriminatory performance.

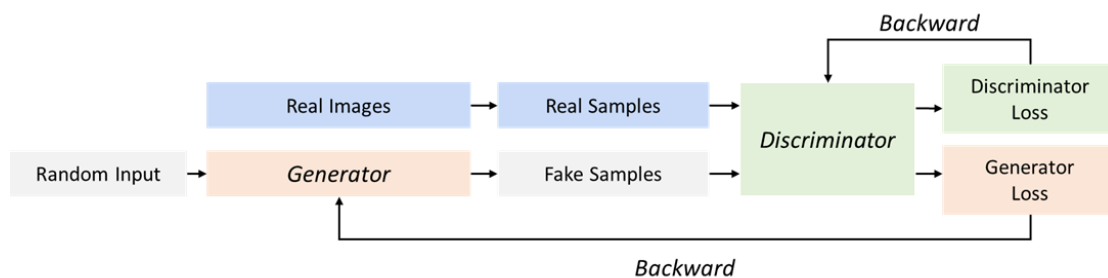


Figure 3.7 A typical structure of the generative adversarial neural network

The whole process can be summarized as Equation (3.7) (Goodfellow et al., 2014). The  $G$  and  $D$ , respectively, represent the generator and the discriminator. The  $S(D, G)$  refers to the disparity between the generated sample and the actual sample.  $P_{data}$  and  $P_z$  represents the actual samples and samples from Gaussian distribution.  $D(x)$  denotes the

probability that the input sample  $x$  is real. Meanwhile,  $G(z)$  represents the fake samples synthesized by the generator when inputting a noise vector  $z$ .

$$\min_G \max_D S(D, G) = E_{x \sim P_{data}} [\log D(x)] + E_{z \sim P_z} [\log (1 - D(G(z)))] \quad (3.7)$$

$$L_G = E_{z \sim P_z} [\log (1 - D(G(z)))] \quad (3.8)$$

$$L_D = E_{x \sim P_{data}} [\log D(x)] + E_{z \sim P_z} [\log (1 - D(G(z)))] \quad (3.9)$$

The generator and discriminator networks are trained iteratively, with the generator minimizing its loss function, as defined in Equation (3.8), while the discriminator maximizing its loss function, as defined in Equation (3.9). Through the adversarial processes between the generator and the discriminator, GAN enables mutual improvement, with the generator learning to generate realistic samples, and the discriminator enhances its ability to differentiate between real and generated data. This iterative process drives convergence and capturing higher-level features, resulting in a robust and effective generative model.

However, GAN is originally designated to process image data and is susceptible to pattern collapse when dealing with long-time series data. Specifically, it struggles to capture complex feature patterns and trends, and maintaining balance between the generator and discriminator during training becomes challenging (Brophy et al., 2023). LSTM-GAN represents an advanced iteration of the traditional GAN. Figure 3.8 illustrates the distinctive feature of LSTM-GAN, which sets it apart from conventional GAN architectures. LSTM-GAN incorporates Long Short-Term Memory units within its generator or discriminator networks. This integration of LSTM units enhances the

model's ability to generate coherent and realistic sequential data, surpassing the capabilities of standard GAN models.

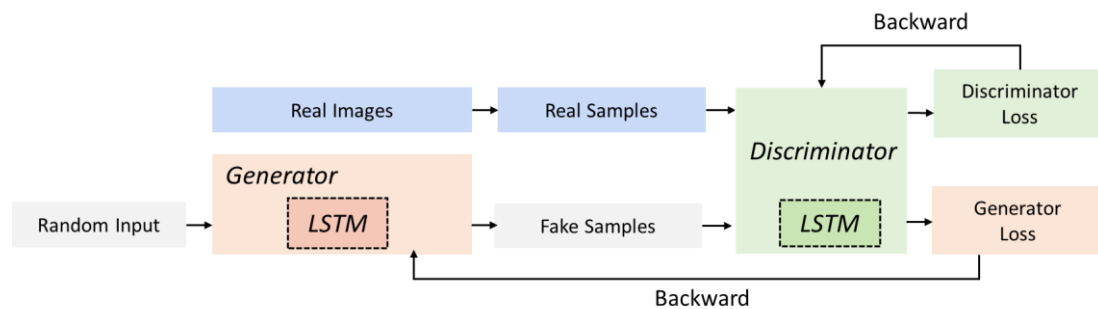


Figure 3.8 A concept diagram for the LSTM-GAN model

The LSTM-GAN exhibits broad applications in generating samples across domains with significant temporal dynamics and dependencies. It proves exceptionally advantageous in tasks involving time-series or sequential generative, including synthetic biomedical signals (Brophy et al., 2023), music composition (Y. Yu et al., 2021), and natural language processing (Y. Yu et al., 2021). Its exceptional capability to capture long-term dependencies makes it well-suited for generating acoustic leak signals. Therefore, it is employed as the training framework, capturing the distribution of input signals for data augmentation for Objective I.

### 3.3.1.4 Time-Series Transformer

Transformer is a DL model architecture that revolutionized the field of natural language processing (Vaswani et al., 2017). It has been widely adopted in various applications, including speech recognition (Dong et al., 2018), machine fault diagnosis (Ding et al., 2022), bioelectric signal recognition (L. Meng et al., 2022), and more. The Time-Transformer architecture is based on basic Transformer architecture and comprises several vital components, including time-series tokenizer, Transformer layer, and classification layer. Notably, in subsequent contents, the Time-Transformer employed

in this study is referred to as the 'Transformer', as it shares a majority of mechanisms and structures with the original Transformer model.

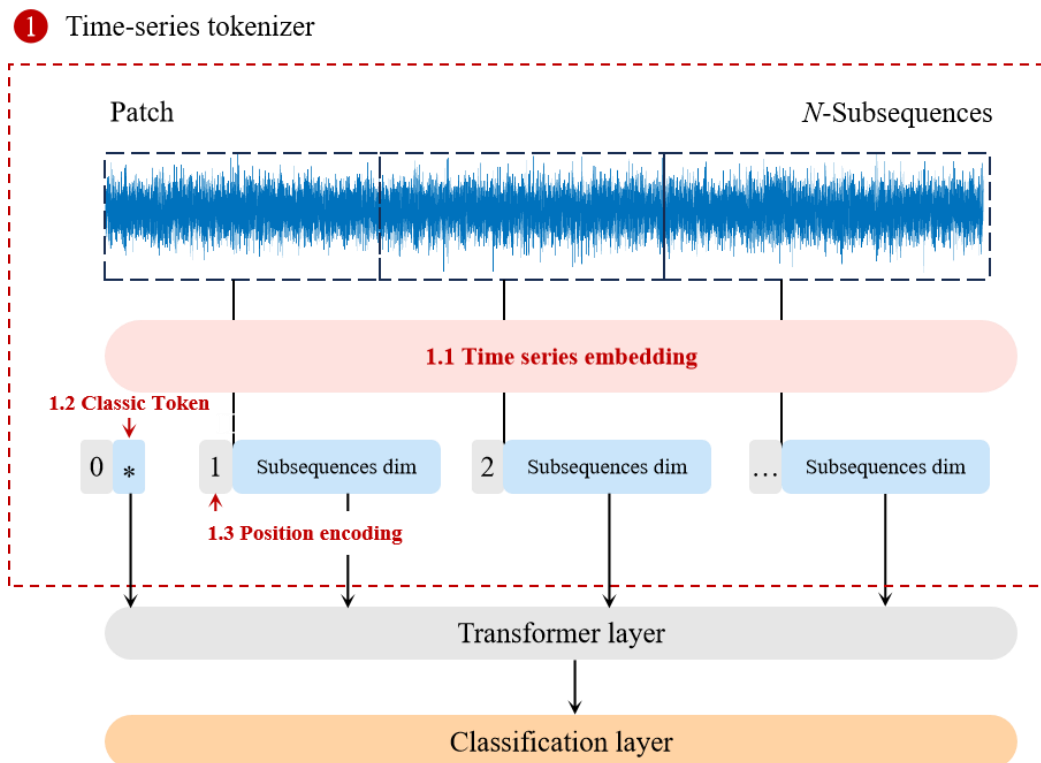


Figure 3.9 The main components of the time-series tokenizer

The time-series tokenizer is a fundamental component of the Transformer architecture, segmenting the input time-series signal into discrete tokens. This process involves breaking down the continuous time series into primary units, allowing for effective analysis and comprehension by the model. The tokenizer transforms the time-series data into a sequence of distinct tokens, facilitating the model in capturing and interpreting the underlying temporal patterns and dependencies inherent in the signal. As illustrated in Figure 3.9, the tokenizer consists of time-series embedding, class token, and position encoding.

Specifically, within the scope of this study, the linear layers are employed as the time series embedding, trimming the input time-series input into  $N_s$  distinct subsequences

and are denoted as  $s \in \mathbb{R}^{Batch \times N_s \times (L/N_s)}$ , where  $L$  is the length of the input acoustic signal. Subsequently, time series embedding adopted the linear projection  $W_{embedding}$ , mapping the sequence onto the dimension ( $dim$ ), which can be depicted as Equation (3.10).

$$z_0 = [s^1, s^2, s^3, \dots, s^{N_s}] \cdot W_{embedding} \in \mathbb{R}^{Batch \times N_s \times dim} \quad (3.10)$$

As given in Equation (3.11), the class token  $s_{class} \in \mathbb{R}^{dim}$  extracts features from the token sequence. After the computation of the multi-head attention mechanism, the class token contains the information of all subsequences, allowing it to fuse features from all parts of the sequence. Consequently, the output of the class token is adopted as the feature map, representing the combined information from the entire sequence.

$$z_0 = [s_{class}; [s^1, s^2, s^3, \dots, s^{N_s}] \cdot W_{embedding}] \in \mathbb{R}^{Batch \times (N_s + 1) \times dim} \quad (3.11)$$

As denoted in Equation (3.12), position encoding incorporates positional information into the input data. It addresses the lack of inherent order or position in the attention mechanism. Assigning unique encoding vectors, denoted as  $E_{pos} \in \mathbb{R}^{(N_s + 1) \times dim}$  position encoding, empowers the model to differentiate tokens based on their sequence order. Consequently, the model can capture dependencies and patterns that rely on the order of elements in the sequence, leading to improved understanding and processing of time-series signals.

$$z_0 = [s_{class}; [s^1, s^2, s^3, \dots, s^{N_s}] \cdot W_{embedding}] + E_{pos} \in \mathbb{R}^{Batch \times (N_s + 1) \times dim} \quad (3.12)$$

The transformer layer is the core part of the proposed Time-Transformer for feature extraction and representation, consisting of  $N$  Transformer basic blocks. The form of the applied Time-Transformer layer is similar to the basic Transformer and mainly includes a multi-head self-attention mechanism and multilayer perceptron blocks.

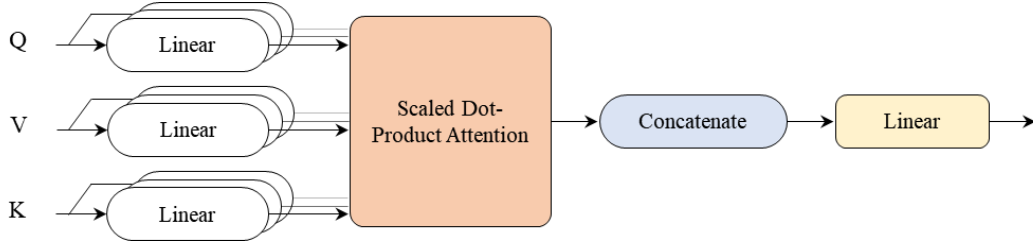


Figure 3.10 A typical structure of multi-head attention

The attention mechanism can be expressed in Figure 3.10 and Equation (3.13). The input sequence  $z_0$  is transformed to obtain query ( $Q$ ), key ( $K$ ), and value ( $V$ ) vectors using linear projections.  $VQK^T$  is applied to extract the similarity between the inputs. Then, scaling factor  $\frac{1}{\sqrt{d_k}}$  is introduced for stabilizing the gradient, where  $d_k$  is the dimension of queries and keys.

$$Attention(Q, K, V) = softmax\left(\frac{QK^T}{\sqrt{d_k}}\right)V \quad (3.13)$$

The model is expected to learn different insights based on the same attention mechanism when given the same set of queries, keys, and values. These insights are then combined as knowledge to capture dependencies of various scopes within sequences, such as short-term and long-term dependencies. To achieve this, multi-head attention is introduced, converting queries, keys, and values through  $h$  sets of linear projection. Then, the transformed queries, keys, and values are simultaneously processed. The outputs are concatenated and further transformed to produce the final output. The mechanism of multi-head attention can be given as Equation (3.14), where  $W_O \in \mathbb{R}^{hd_v \times dim}$ ,  $W_Q^i \in \mathbb{R}^{dim \times d_k}$ ,  $W_K^i \in \mathbb{R}^{dim \times d_k}$ ,  $W_V^i \in \mathbb{R}^{dim \times d_v}$ .  $h$  is the number of heads, and  $d_v$  is the dimension of values.

$$\begin{aligned} MultiHead(Q, K, V) &= \text{Concat}(Head_1, Head_2, \dots, Head_h)W_o \\ Head_i &= \text{Attention}(QW^i_Q, KW^i_K, VW^i_V) \end{aligned} \quad (3.14)$$

Multilayer Perceptron (MLP) blocks are an ML model based on the feedforward neural network. It consists of multiple layers of interconnected neurons, each fully connected to the preceding layer.

$$h^{(l)} = \text{Activation}(W^{(l)}h^{(l-1)} + b^{(l)}) \quad (3.15)$$

In Equation (3.15), the output of the hidden layers in the  $l$ -th hidden layer is denoted as  $h^{(l)}$ , while  $h^l$  represents the output of the first hidden layer. Each hidden layer is associated with a bias term,  $b$ , which can be adjusted to impact the model's output. By modifying the value of  $b$ , the model's output can be brought closer to the true values, enhancing model performance and accuracy.

Additionally, "Activation" refers to the activation functions employed in the MLP blocks. Commonly used activation functions include the Rectified Linear Unit (ReLU) (Nair & Hinton, 2010) and the Gaussian Error Linear Unit (GeLU) (Hendrycks & Gimpel, 2016). These activation functions introduce nonlinearity to the model, allowing it to learn complex relationships and capture intricate patterns in the data. By introducing nonlinearity, the Time-Transformer learns intricate patterns and extracts high-level features from the input data, enhancing the leak detection capabilities. The size and depth of the multi-layer perceptron (MLP) blocks can be adjusted as hyperparameters to suit the task and complexity of the data.

After the input time-series signals have been processed through the self-attention mechanism and other components of the Transformer, the classification layer is applied to produce the desired output. Typically, as denoted in Equation (3.16), the

classification layer consists of a fully connected layer followed by a softmax activation function, mapping the extracted features from the preceding layers to the appropriate number of output classes (leak, noleak). In Equation (3.16),  $y$  represents the input data, and  $y^{leak}$  refers to the leak conditions,  $W$  are the weights of neuron parameters and  $b$  is the bias.

$$\text{ClassLayer}(y) = y^{leak} = \text{Softmax}(y \cdot W + b) \quad (3.16)$$

During training, the classification layer is optimized using a suitable loss function. The loss function used in this study is cross-entropy (Martinez & Stiefelhagen, 2019), commonly employed in leak detection research (S. Li et al., 2018; Y. W. Nam et al., 2021). The formula is defined as Equation (3.17), where  $y_i$  represents the target label, and  $\hat{y}_i$  represents the output value.

$$\text{Loss} = -\sum_{i=1}^m y_i \log \hat{y}_i \quad (3.17)$$

Due to its capability, this study employed a Time-Transformer for leak detection to reach higher accuracy and robustness (Objective III).

### **3.3.2 Analytical and Process Tools**

#### **3.3.2.1 Short-Time Fourier Transform**

Among time-frequency transformation methods, STFT demonstrates distinct advantages when dealing with signals of short duration (Santos et al., 2009). By dividing the signal into multiple windows and applying the Fourier transform to each window, the STFT yields valuable frequency and time information. This approach facilitates a more refined analysis of the signal's spectral properties while preserving a

reasonable level of time resolution. The calculation equation of the STFT method is as Equation (3.18).

$$X(t, f) = \int_{-\infty}^{\infty} x(\tau) w(\tau - t) e^{-j2\pi f\tau} d\tau \quad (3.18)$$

where,  $X(t, f)$  is a complex-valued function in the time-frequency domain, representing the amplitude and phase information of a signal at time  $t$  and frequency  $f$ .  $x(\tau)$  is the input signal, which is a function over the entire time domain.  $w(\tau - t)$  is the window function, a non-zero function in the local time range in the time domain, and is used to extract the regional segment of the signal.  $e^{-j2\pi f\tau}$  is the complex exponential function representing the phase of a sinusoidal wave with frequency  $f$  at time  $t$ .

Among them, the type and width of the window function are the keys to the construction of the STFT time-frequency maps, and the width of the window function determines the resolution of the STFT. Meanwhile, Continuous Wavelet Transform (CWT) has better time-frequency adaptability (Qu et al., 2019). However, its resulting matrices are frequently huge, demanding substantial computational resources when dealing with many signal CWT spectrograms. Consequently, it becomes necessary to resize the CWT spectrograms for input (Shukla & Piratla, 2020a). However, this step inevitably leads to the loss of the intricate information derived from CWT, undermining its fundamental significance. Hence, this study adopts STFT as the data transformation algorithm in Objective II, as it provides a slight spectrogram matrix that is less required for the power of selected equipment.

### **3.3.2.2 Variational Mode Decomposition**

VMD is a signal analysis technique that decomposes complex signals into distinct modes based on their time-frequency characteristics (Dragomiretskiy & Zosso, 2014b).

It achieves this decomposition by formulating an optimization problem that minimizes the total variation of the decomposed modes while satisfying a constraint on the signal's energy. The optimization process iteratively updates the modes and their corresponding time-varying frequencies until convergence is reached.

The specific process of VMD decomposition can be understood as the optimal solution to a variational problem. It can be correspondingly transformed into constructing and solving a variational problem.

VMD assumed that the multi-component signal is composed of  $K$ -modal components  $v_k(t)$ , each with a finite bandwidth, and each Intrinsic Mode Function (IMF) has a central frequency of  $\omega_k(t)$ , the constraint is that the sum of all modes equals the input signal. The specific construction steps are as follows:

First, the Hilbert transform is employed to obtain the signal of  $v_k(t)$  and calculate the one-sided spectrum. Subsequently, as illustrated in Equation (3.19),  $v_k(t)$  multiply with the operator  $e^{-j\omega_k t}$  to shift the central band of  $v_k(t)$ , to the corresponding baseband:

$$\left[ \left( \delta(t) + \frac{j}{\pi t} \right) * v_k(t) \right] e^{-j\omega_k t} \quad (3.19)$$

where  $j$  is the imaginary unit.

Secondly, Equation (3.20) is applied to calculate the square norm  $L^2$  of the demodulation gradient and estimate the bandwidth of each modal component.

$$\left\{ \begin{array}{l} \min_{\{v_k\}, \{\omega_k\}} \left\{ \sum_k \partial_t \left[ \left( \delta(t) + \frac{j}{\pi t} \right) * v_k(t) \right] e^{-j\omega_k t} \right\} \\ \text{s.t. } \sum_k v_k = s(t) \end{array} \right\} \quad (3.20)$$

where  $\{v\} = \{v^1, v^2, \dots, v^K\}$  represents the decomposed IMF components, and  $\{\omega\} = \{\omega^1, \omega^2, \dots, \omega^K\}$  represents the central frequencies of each component,  $\partial_t$  is the partial derivative concerning time.

To find the optimal solution for the constrained variational problem, we first introduce the Lagrange multiplier ( $\tau$ ) and the second-order penalty factor  $\alpha$  to transform the constrained variational problem into an unconstrained variational problem. The second-order penalty factor  $\alpha$  ensures signal reconstruction accuracy in a Gaussian noise environment. The extended Lagrange expression is as Equation (3.21).

$$L(\{v_k\}, \{\omega_k\}, \tau) := \alpha \sum_k \partial_t \left[ \left( \delta(t) + \frac{j}{\pi t} \right) * v_k(t) \right] e^{-j\omega_k t^2} + s(t) - \sum_k v_k(t)^2 + \tau(t), s(t) - \sum_k v_k(t) \quad (3.21)$$

Then, the Alternating Direction Method of Multipliers (ADMM) is applied to iteratively update each component and its corresponding central frequency to obtain the unconstrained model's saddle point, representing the optimal solution to the original problem. All components can be obtained based on the frequency domain space using Equation (3.22).

$$\hat{v}_k^{n+1}(\omega) = \frac{\hat{s}(\omega) - \sum_{i \neq k} \hat{v}_i(\omega) + \hat{\tau}(\omega) / 2}{1 + 2\alpha(\omega - \omega_k)^2} \quad (3.22)$$

here  $\hat{v}_k^{n+1}(\omega)$ ,  $\hat{v}_i(\omega)$ ,  $\hat{\tau}(\omega)$  is the Fourier transformation of  $v_k^{n+1}(t)$ ,  $\hat{v}_i(t)$ ,  $\tau(t)$ .

The remaining components are used to estimate the centroid frequency  $\omega_k$  based on the power spectrum centroid for each element, using Equation (3.23) to Equation (3.24).

$$\omega_k^{n+1} = \frac{\int_0^\infty \omega |v_k^{n+1}(\omega)|^2 d\omega}{\int_0^\infty |v_k^{n+1}(\omega)|^2 d\omega} \quad (3.23)$$

$$\hat{\tau}^{n+1}(\omega) = \hat{\tau}^n(\omega) + \tau \left( \hat{s}(\omega) - \sum_k \hat{v}_k^{n+1}(\omega) \right) \quad (3.24)$$

The specific process is repeated until reaching the set condition as illustrated in Equation (3.25).

$$\sum_k \|\hat{v}_k^{n+1} - \hat{v}_k^n\|_2^2 / \|\hat{v}_k^n\|_2^2 < \varepsilon \quad (3.25)$$

One of the key advantages of VMD is its ability to handle nonstationary signals with time-varying frequency content (Yao et al., 2022). Unlike traditional Fourier-based methods, VMD simultaneously captures time and frequency variations (F. Li et al., 2019). This makes it suitable for analyzing signals with rapidly changing spectral characteristics, such as time-series energy consumption prediction (H. Song et al., 2023), biomedical signals (Smruthy & Suchetha, 2017), vibration signals in machinery (Z. Li et al., 2017) and also for acoustic leak detection (Z. Wang et al., 2022). Thus, it has also been applied to denoise signals during data preparation in Objectives II and III.

### 3.3.2.3 Gradient-weighted Class Activation Mapping

CNN is a powerful deep-learning model used for various grid-structure tasks. While they are known for their high accuracy, they are often considered black boxes, making it challenging to understand how models make their predictions (Azam et al., 2023; Szandała, 2023). Class Activation Mapping (CAM) and Grad-CAM address this issue by providing visual explanations highlighting the regions of input data that are important for the network's decision-making process and contributing to the interpretability and understanding of CNN in classification tasks (T. Liu et al., 2023).

CAM was introduced to localize the most discriminative parts of input data by leveraging the spatial information learned by the network (C. L. Choi, 2020). It

generates a heatmap that reveals the regions that contributed significantly to the predicted class. CAM provides an interpretable visualisation that highlights the important regions by focusing on the last convolutional layer and combining the feature maps with the weights of the fully connected layer. However, the original CAM technique has limitations when used with CNN architectures that employ global average pooling instead of fully connected layers and can only apply to ResNet and MobileNet. And it can't be applied to fully connected models.

To solve this limitation, Grad-CAM was proposed to utilize the gradients of the predicted class concerning the feature maps (Selvaraju et al., 2020). It computes the importance of each feature map by considering the gradients. Grad-CAM can work with any CNN architecture, providing a more flexible and general approach for generating class activation maps. The work procedures can be summarized as Equations (3.26) to (3.27).

$$L_{\text{Grad-CAM}}^c = \text{ReLU} \left( \sum_k \alpha_k^c A^k \right) \quad (3.26)$$

$$\alpha_k^c = \frac{1}{Z} \sum_i \sum_j \frac{\partial y^c}{\partial A_{ij}^k} \cdot \quad (3.27)$$

where,  $A$  represents a certain feature layer, which generally refers to the last convolutional layer.  $k$  represents the  $k$ -th channel in the feature layer.  $c$  represents the output category  $c$ .  $A^k$  represents channel  $k$  in feature layer  $A$ . data.  $\alpha_k^c$  represents the weight for  $A^k$ .  $y^c$  represents the score predicted by the network for category  $c$ .  $A_{ij}^k$  represents the data of feature layer  $A$  in channel  $k$ , with coordinates at the positions  $i, j$ .  $Z$  is equal to the width and height of the feature layer.

According to Equation (3.27), it can be determined that  $\alpha_k^c$  is obtained through backpropagation using the predicted score  $y^c$  for category  $c$ . Then, the gradient information propagated to the feature layer  $A$  is used to calculate the importance of each channel  $k$  in the feature layer  $A$ . Afterwards, the data of each channel in the feature layer  $A$  is weighted sum using  $\alpha$ , and finally, the Grad-CAM is obtained by applying the activation function. Overall, Grad-CAM represents an advancement of CAM as it provides greater flexibility and does not require modifications to the network architecture or retraining (S. Li et al., 2009). The study prioritizes the utilization of Grad-CAM due to its ease of implementation and interpretability for Objective II.

### 3.3.2.4 t-SNE analysis

Specifically, t-SNE starts by calculating pairwise similarities between high-dimension data points using a Gaussian kernel, as shown in Equations (3.28) and (3.29) capturing their relationships in the high-dimensional space.  $i$  and  $j$  represent two different samples.  $\sigma$  represents the bandwidth of the Gaussian kernel.  $N$  represents the number of samples.

$$p_{j|i} = \frac{\exp(-x_i - x_j^2 / 2\sigma_i^2)}{\sum_{k \neq i} \exp(-x_i - x_k^2 / 2\sigma_i^2)} \quad (3.28)$$

$$p_{ij} = \frac{p_{j|i} + p_{i|j}}{2N} \quad (3.29)$$

$$q_{ij} = \frac{(1 + y_i - y_j^2)^{-1}}{\sum_k \sum_{l \neq k} (1 + y_k - y_l^2)^{-1}} \quad (3.30)$$

$$KL(PQ) = \sum_{i \neq j} p_{ij} \log \frac{p_{ij}}{q_{ij}} \quad (3.31)$$

Equation (3.30) measures the similarity between samples from low-dimension samples.  $y_i$  and  $y_j$  represent the low-dimension samples. Data points are assigned to random initial positions in the lower-dimensional map. The algorithm iteratively adjusts its positions

to minimize the Kullback–Leibler divergence of the distribution  $P$  from the distribution  $Q$ , as shown in Equation (3.31). By emphasizing the preservation of the local structure, t-SNE retains the relative distances between neighboring points, effectively highlighting clusters and local patterns in the lower-dimensional representation. It is, therefore, utilized in visualizing generated samples (Objective I) and feature vectors (Objective III).

### **3.4 Chapter Summary**

This chapter provides an overview of the research framework, algorithm, and methods used. The machine learning modeling algorithms focus on leak detection and localization, incorporating state-of-the-art deep learning models such as CNN (Objectives I, II, III, and IV), LSTM (Objectives I and III), GAN (Objective I), and Transformer (Objective III). These models are applied to address the research objectives effectively. On the other hand, the analytical tools refer to techniques used for signal analysis and enhancing model performance. VMD is used for decomposition, selecting principal components to reconstruct signals, and reducing noise and outliers (Objective II and III). Grad-CAM is employed to extract the activation regions of the models, visualizing the model's emphasis and enhancing interpretability (Objective II). Additionally, t-SNE projects high-dimensional vectors into a lower-dimensional subspace, enabling effective visualization of the samples (Objective I and III). These combined methods and tools contribute to the overall effectiveness and understanding of the research outcomes.

## **CHAPTER 4 Generative Approach for Data Augmentation and Enhancement**

### **4.1 Introduction**

Generative data augmentation offers an economical and effective solution to enhance the dataset for water leak detection. This chapter proposes a long- short-term memory GAN (LSTM-GAN) approach to improve water leak detection in WDNs. The main objectives of this study are: i). propose a generative approach to enrich leak datasets, ii). improve the diversity of the dataset to enhance leak detection capability. The proposed generative methodology for enriching and diversifying the dataset contributes to advancing deep learning models for water pipe leak detection, benefiting researchers and practitioners in water infrastructure management.

### **4.2 The framework for the generative model for data augmentation**

The detailed process of the framework is shown below in Figure 4.1. The entire generative framework comprises three main parts: data collection, LSTM-GAN modeling, and model result evaluation.

First, the data collection phase requires establishing the primary acoustic leak datasets for generative models. This necessitates conducting field experiments to deploy sensors that collect acoustic signals under different scenarios, thereby enhancing the robustness of datasets. Based on the collected dataset, the generated and original data are employed for subsequent generative algorithm modeling and leak detection model evaluations.

Second, the LSTM-GAN model generates acoustic signals through an adversarial process between two neural networks. The modeling process entails establishing a generator and a discriminator. A series of model structure and hyper-parameters

experiments are required to balance the capability of two models during the training process and optimize the performance. Through an iterative process of competition and feedback between two models, the generator improves its ability to produce increasingly realistic acoustic signal data. The generated samples then undergo further evaluation and validation.

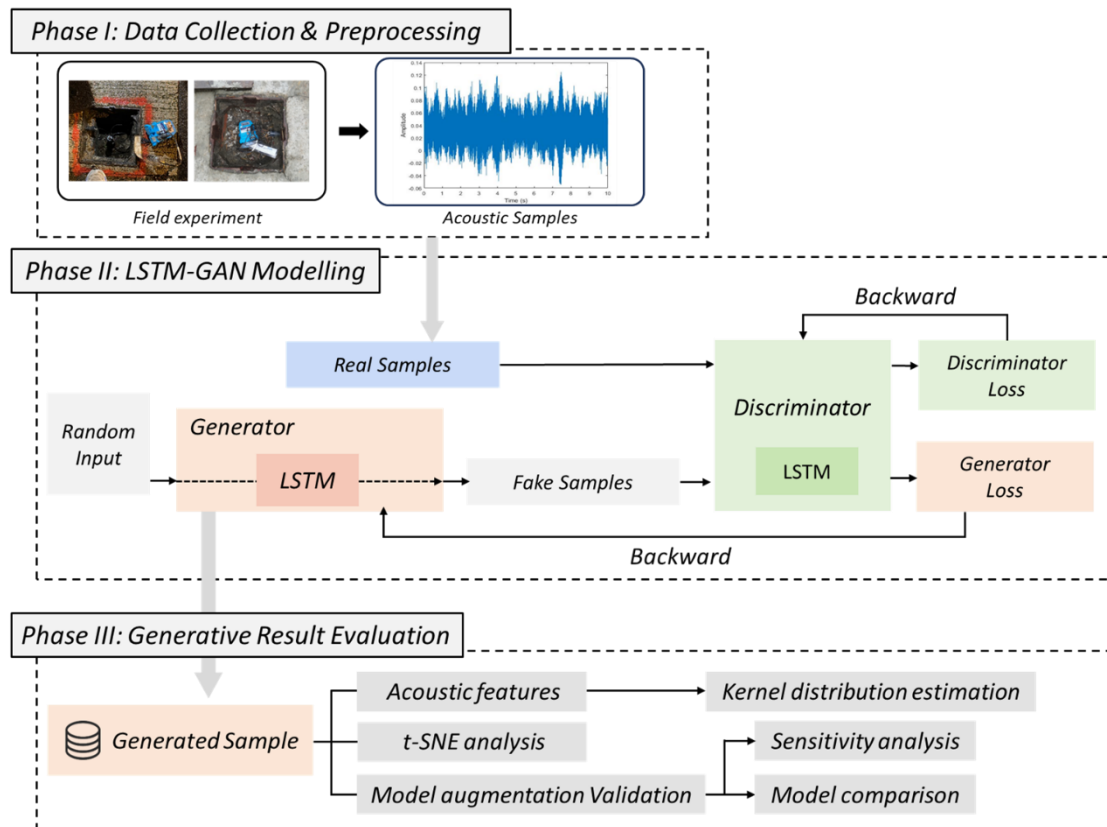


Figure 4.1 The framework of the proposed method.

Third, after generating synthetic data, the distribution of the generated and original datasets is visualized by t-SNE. Simultaneously, the acoustic features of the two datasets will be extracted and compared through kernel distribution estimation (KDE). Subsequently, the generated samples are used to enhance the original datasets. The enhanced dataset, tailored to specific objectives, will be used to train the leak detection classifier. Using the improved dataset enables evaluating the quality of the generated

acoustic signals, assessing the sensitivity of the generated samples, and comparing LSTM-GAN with other generative methods.

### 4.2.1 Data Collection

Field experiments were conducted to collect on-site signals from Hong Kong's water distribution network to assess the efficiency and practicality of the proposed framework. Meanwhile, previous generative approach is also employed to enhance the training dataset,

Figure 4.2 depicts the procedures for the data preprocessing phase, which entails acquiring representative sample signals to facilitate model training. Noise loggers were strategically placed in the on-site chamber of underground water pipelines at diverse locations within Hong Kong's water distribution network, with authorization from the local water authority. Once the leaks occur, the research team will go to the target location to deploy noise loggers to collect the signals. The noise loggers are programmed to collect signals for 10 seconds. The data collection is predominantly scheduled at midnight to minimize human activities and traffic noise influences. The signals are captured at a sampling rate of 4096Hz, ensuring a detailed representation of the acoustic data.

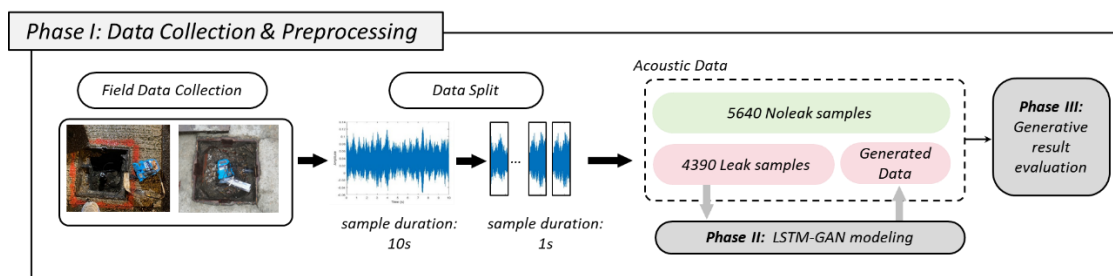


Figure 4.2 Phase I: Data Collection and Preprocessing Roadmap

Through an extensive experiment, 1003 audio signals were collected, consisting of 439 leak signals and 564 no-leak signals. The generated data is split from 10 seconds to 1 second to enrich the data volume for subsequent generative and modeling. In other words, a 1-s duration signal is defined as one sample. Ultimately, this study collects 4390 leak samples and 5640 noleak samples. The collected samples were gathered from various scenarios, covering pipe diameters ranging from DN 25 to DN 1000, pipes made from cement, iron, steel, and polyethylene, and multiple fittings, elbows, branches, etc. The STFT technique was employed to draw spectrograms of the collected signals, aiming to distinguish the differences between signals originating from leak states (G. Guo et al., 2021a). It divides the time-domain signal into smaller segments and applies the Fast Fourier Transform to each segment, capturing information based on time resolution and frequency resolution. The parameters of STFT were chosen considering the study of Yu et al. (2023). Figure 4.3 presents the spectrogram outcomes, with Figure 4.3 (a) representing the leak signal and Figure 4.3 (b) representing the normal no-leak signal. As illustrated in Figure 4.3 (a), leak signals exhibit pronounced amplitudes in the high-frequency range and noticeable distinctions among the different leakage signals. The components of the no-leak signals predominantly exhibit lower frequency content, as depicted in Figure 4.3 (b). Significantly, there are discernible differences between leak and non-leak signals, and distinct variations are also evident among different categories of leak signals.

Furthermore, given the scarcity of available leak samples in the water leak detection domain, this study emphasized explicitly generating synthetic leak samples. Therefore, the research employed a primary leak dataset comprising 4390 leak signals as the core

input for training generative neural networks and synthesizing new samples in Phase II. Furthermore, all the generated and original data were evaluated to reflect the performance of the proposed generative model in Phase III.

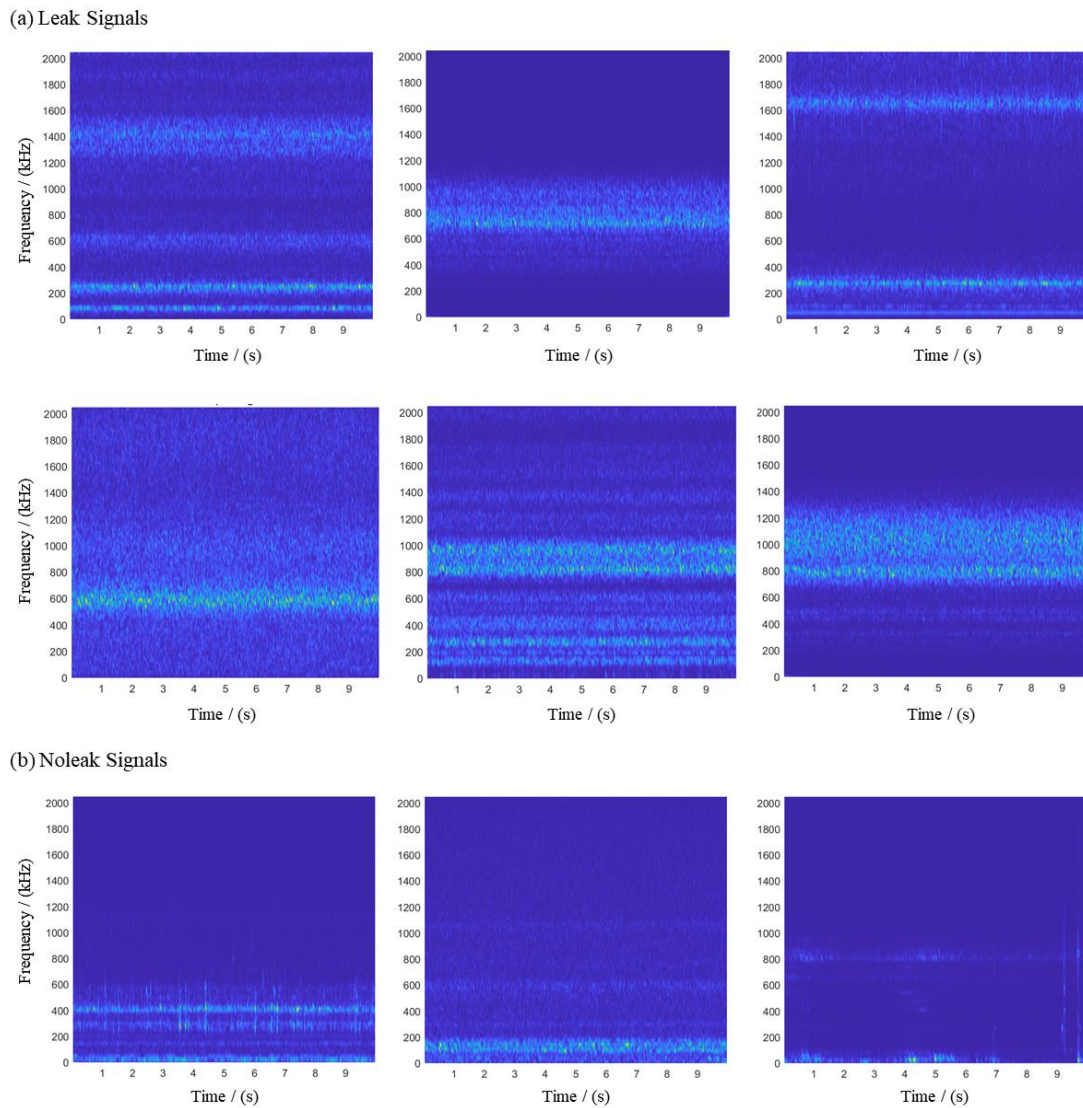


Figure 4.3 Spectrogram images of the acoustic signals from leak statuses (a) leak signals; (b) noleak signals

#### 4.2.2 LSTM-GAN for Enhancing Acoustic Dataset

This study proposes a leak signals generative model based on LSTM-GAN. The GAN model is responsible for generating the signals. Meanwhile, introducing LSTM guarantees the acoustic characteristics of generated signals. In acoustic water leak

detection, most collected signals are noleak signals, while only a tiny proportion are leak signals. Therefore, the proposed model focuses on generating the leak signals to solve the data scarcity of leak signals and enhance diversity.

The neural structures of the generator and the discriminator are shown in Figure 4.4. Four convolutional layers are the main structure of the generator. Specifically, 1-D CNN (Conv1D) is used to extract the time-series characteristics of data. Then, batch normalization is adopted to normalize the input data within a batch, stabilizing the learning process and enhancing the model generalization. Leaky Relu is adopted to realize learning under the inverse gradient of the neurons. An LSTM neural layer is appended to the discriminator network to extract the characteristics of time-series data. The generator model consists of four transposed convolutional layers. The input noise for the generator is a 500-dimensional vector with a Gaussian distribution. This input vector is projected to the length required for generating the samples through transposed convolutional layers.

Moreover, the RMSprop optimizer is utilized with a learning rate of 1e-3 for the generator and 5e-4 for the discriminator to balance the generation and discrimination capabilities of the two models. Meanwhile, the binary cross-entropy (BCE) loss function is employed and designated for binary classification problems (including leak statute identification). The calculation of BCE is shown in Equation (4.1), where  $y$  represents the actual distribution of the sample, and  $\hat{y}$  represents the output of the model;  $n$  means the number of classification classes; for binary problem,  $n$  equals 2,  $i$  represents the  $i$ -th sample in the dataset.

$$Loss = - \sum_{i=1}^n y_i \log y_i \quad (4.1)$$

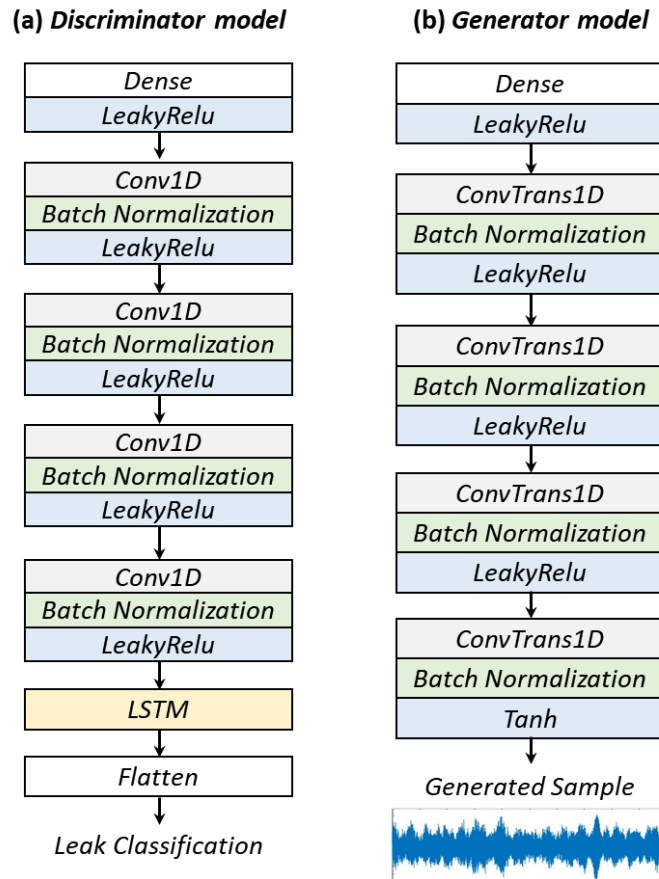


Figure 4.4 The neural structures of GAN (a) Discriminator (b) Generator

The pseudocode expresses the proposed LSTM-GAN algorithm in Table 4.1. In the Pseudocode, 'gen' and 'dis' represent the generator and the discriminator. 'z' represents the Gaussian noise with a mean of 0 and a variance of 1. During the LSTM-GAN training phase, actual data samples and the generated samples (also named fake samples) from random Gaussian noises are first used as the training data for the discriminator. Based on the empirical rules, the discriminator will be trained first, allowing the discriminator to provide accurate feedback to guide the generator toward producing more realistic samples. Then, the generator will be trained based on discriminator results. This training process will continue until the training epochs are completed. Ultimately, the generator is extracted to output the generated leak samples for subsequent model result evaluation.

Table 4.1 Pseudocode of LSTM-GAN for generating leak signals

---

**Inputs: training data, training epochs**

**Outputs: Generated Samples**

---

**LSTM-GAN Train (training data, training epochs ):**

**While** current\_epoch < training epochs **do**

z =uniform(0,1)

gen\_data ← gen(z)

dis\_real\_loss←discriminator (training\_data)

dis\_fake\_loss←discriminator (gen\_data)

dis\_loss=dis\_real\_loss+dis\_fake\_loss

**Train discriminator**

gen\_data ← genr(z)

gen\_fake\_loss←discriminator (gen\_data)

**Train generator**

**Output** Generated Leak Samples→Phase III: Model Result Evaluation

---

### 4.2.3 Generative Result Evaluation

This section evaluates the generated dataset through three indicators: t-SNE analysis, acoustic feature analysis, and model generative validation.

#### 4.2.3.1 t-SNE Analysis

Firstly, the distribution and clustering patterns of the generated samples can be assessed using t-SNE analysis, comparing the distribution of the original and the enhanced datasets. t-SNE is a widely used dimensionality reduction technique (Van der Maaten & Hinton, 2008) that visualizes high-dimensional data in lower-dimensional space. It calculates pairwise similarities between data points, constructs a probability distribution over the high-dimensional data, and optimizes the positions of points in the lower-dimensional space to preserve both local and global structure.

Overall, t-SNE enables visualization and reveals clusters, patterns, and relationships in the acoustic signals that are not apparent in the original high-dimensional space. Its capability has been widely applied across various domains, including financial data (Santoro & Grilli, 2022), machine fault diagnosis (M. Li et al., 2022), and biomedical signal processing (Svantesson et al., 2023). By leveraging t-SNE results, this study enables the identification of similarities between the generated signals and actual leak signals, providing valuable insights into the performance of the generative approach.

#### **4.2.3.2 Acoustic Characteristics Analysis**

This section objectively evaluates the quality of generated samples by comparing the acoustic characteristics. The comparison is made by extracting various time, spectral, and frequency features from both datasets. Subsequently, kernel density estimation (KDE) is employed to facilitate the comparison of these extracted features. It is a statistical technique used to provide a non-parametric, data-driven approach to estimate the probability density function of data.

KDE works by placing a kernel (e.g., Gaussian or uniform function) on each data point and summing them to create a smooth and continuous density estimate. Thus, the above acoustic features will be extracted, presented, and visualized through KDE. Specifically, given a set of observations  $x_1, x_2, \dots, x_n$ , the formula for kernel density estimation can be expressed as Equation (4.2), where  $f_n(x)$  is the probability density function estimated given the observations.  $k$  is the kernel function, usually Gaussian kernel function (normal distribution).  $n$  is the number of observations.  $x_i$  is the  $i$ -th sample in the dataset.  $h$  is the bandwidth used to control the width of the kernel function and affect the smoothness of the estimate.

$$f_n(x) = (1/n) * \sum \left[ k \left( \frac{(x-x_i)}{h} \right) \right] \quad (4.2)$$

Acoustic features play a vital role in detecting water leakage using acoustic-based methods, capturing various features associated with water leakage. Researchers and professionals can evaluate the quality and effectiveness of generated leakage signals for water leak detection by analyzing and incorporating these features into generated datasets.

A set of critical features that effectively capture the acoustic characteristics of water leakage detection were selected based on previous studies (Fan et al., 2022; Fares et al., 2022; Tariq et al., 2022). These features include spread, max amplitude, kurtosis, root mean square (RMS), energy, peak frequency, frequency spread, average amplitude in the frequency domain (FD. average amp), and frequency centroid. Then, the feature value distributions of generated and original leak samples are compared and visualized through KDE.

#### **4.2.3.3 Model Augmentation Validation**

Model augmentation validation was conducted to assess the effectiveness of the generated leak samples in enhancing the accuracy and robustness of the water leak detection models. The quality of the generated dataset is evaluated by comparing the leak detection performances of models trained on different datasets. Depending on the analysis purposes, it can be divided into i) the sensitivity analysis of generated samples, comparing the model performance with different numbers of generated samples; ii) Model comparison analysis for illustrating the superiority of LSGM-GAN compared to other generative methods.

As illustrated in Figure 4.5, sensitivity and model comparison analyses would generate the additional leak samples and employ t-SNE to capture the generated samples' distribution easily. Then, the generated samples would be used to enhance training data for subsequent modeling. Specifically, the original data is split into training (80%) and testing (20%) datasets using the hold-out method in the data preparation phase. Meanwhile, the original training dataset is enhanced by generated leak samples to form another dataset, named the enhanced training dataset. The two training datasets train models whose leak detection capability is evaluated based on testing and validation datasets. Moreover, case investigations were conducted to collect 65 new independent leak audio samples from 14 sites for further model validation.

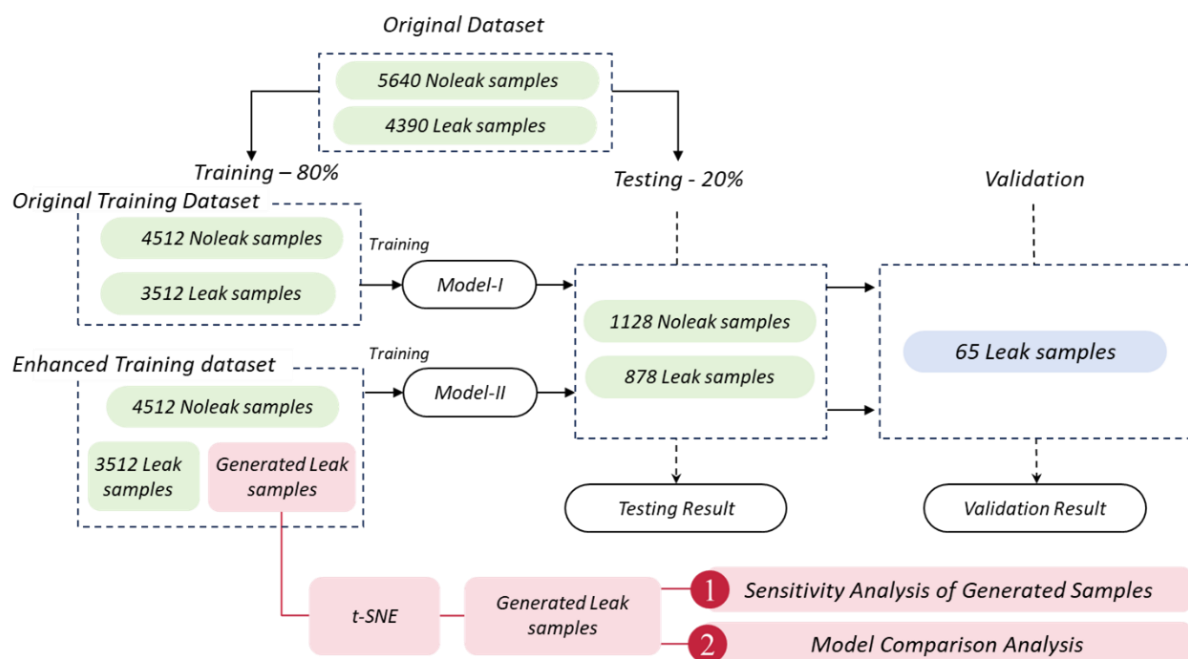


Figure 4.5 Data split for model testing and validation

In the model training and comparison phase, LSTM is chosen as the leak detection model to assess the quality of generated 1-D acoustic leak signals. The selection is made based on the capability of LSTM to process sequential data, capture temporal

dependencies, analyze variable-length acoustic signals, extract features, and learn from labeled data (X. Zhang et al., 2023). It enables accurate and effective leak detection.

As depicted in Figure 4.5, the original training dataset (containing 4512 noleak samples and 3512 leak samples) was used for training the LSTM model and regarded as the 'origin' model or baseline for subsequent comparison. Meanwhile, the enhanced training dataset was used to train another LSTM model with the same structure and hyperparameter to evaluate the effectiveness of the proposed generative method. The training epoch is 1000, and the learning rate is  $5e-4$ , using the Adam optimizer. After training, the model's performance on testing and validation datasets would be assessed and compared under different scenarios, evaluating whether the generative approach enhances the water leak detection capability.

### **4.3 Generative Results Evaluations and Discussion**

The generated dataset is extensively evaluated using t-SNE analysis, acoustic feature analysis, and model augmentation validation, which assess the generative capability of LSTM-GAN in developing realistic and representative leak samples for water leak detection.

#### **4.3.1 t-SNE Results**

Leveraging t-SNE results assists in gaining insight into the generated signal performance and identifying similarities and differences to actual leak and noleak instances through mapping the samples into the 2-D dimension. Figure 4.6 presents t-SNE visualizations of 1300 randomly generated samples (red nodes), 5640 samples from the noleak scenario (green nodes), and 4360 samples from the leak scenario (blue

nodes), showcasing the distributions and highlighting the similarities and differences among datasets.

As shown in Figure 4.6 (a), noticeable differences are observed between the noleak signals and the leak and generated samples. The noleak signals' green samples exhibit a wide distribution, suggesting distinct characteristics. On the other hand, Figure 4.6 (b) indicates that the distribution of the generated samples falls within the distribution of the original dataset. This observation highlights the effectiveness of the generated samples in preserving the overall distribution of the original data.

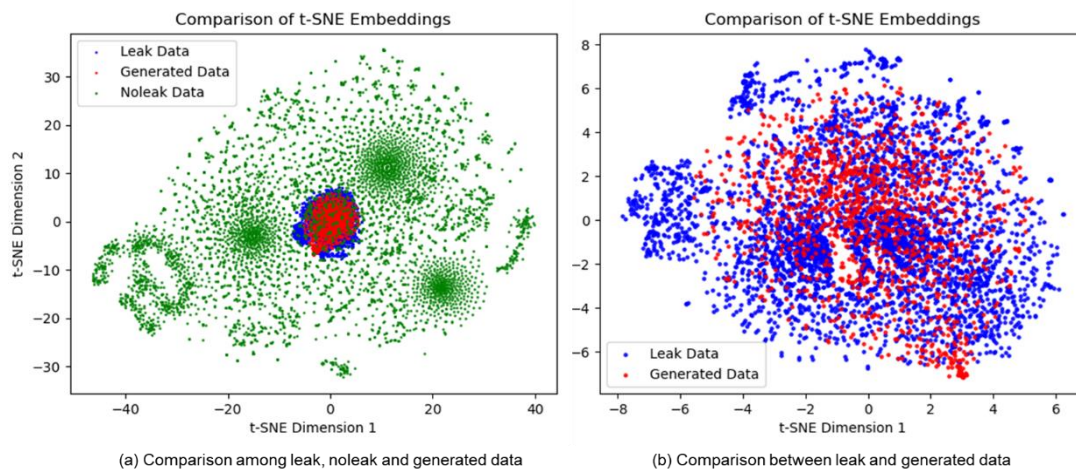


Figure 4.6 t-SNE results for comparing generated and original datasets (a) Comparison among leak, noleak, and generated data (b) Comparison between leak and generated data. Additionally, it can be found that the red points can cover voids or empty regions between the blue points. These voids might represent leak signals from other scenarios, which are not adequately represented or captured by the original dataset. Thus, red points in the void areas might represent valuable information or patterns not previously observed or captured by the original dataset. In short, the generated samples exhibit a distribution similar to the original dataset while maintaining distinct characteristics. The red points (generated samples) filling void areas suggest the potential presence of new

or previously uncollected signal points that contribute additional information to the overall data distribution.

### 4.3.2 Acoustic Characteristics Analysis Results

In Figure 4.7, the density distributions of acoustic features are depicted for three different sample sets: leak, noleak, and generated samples. Generally, the density distributions of the noleak signals (orange) exhibit distinct patterns compared to both the leak signals (green) and the generated leak signals (blue), particularly in the features of Level and FD Avg. Amp., the noleak signals exhibit significant differences from the other signals, highlighting their discriminative nature.

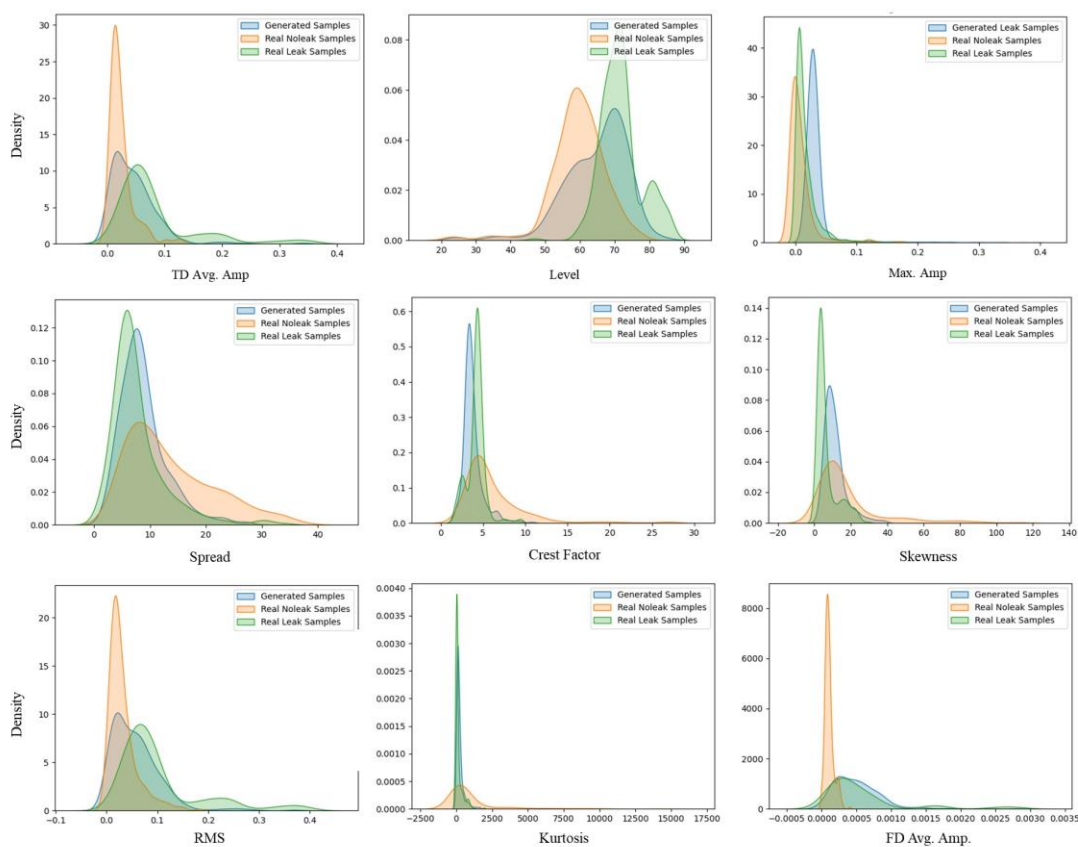


Figure 4.7 KDE results for acoustic characteristics of original and enhanced datasets

Furthermore, there is a noteworthy similarity between the leak data and the generated leak data. Features such as TD Avg. Amp, Spread, RMS, Kurtosis, and FD Avg. Amp

exhibit similar probability distributions, suggesting that the generated signals effectively capture the statistical characteristics of the original leak signals. However, certain features like Crest Factor, Skewness, and Max are observed. Amp may display slightly different maximum density values, indicating variations between the generated and original signals in these aspects.

In summary, this analysis confirms the quality of the generated leak signals by utilizing KDE results to compare the extracted features. It becomes evident that the generated signals successfully capture the essential characteristics of the original signals while preserving their statistical properties. It reaffirms the reliability and accuracy of the generated signals in capturing the crucial attributes of the original leak signals.

### **4.3.3 Model Augmentation Validation Analysis**

As discussed in Section 4.2.3.3, the effectiveness of the generative adversarial network is evaluated by examining whether the generated data can enhance the water leak detection capability.

#### **4.3.3.1 Sensitivity Analysis of Generated Samples**

The generation of samples plays a crucial role in assessing the performance and robustness of various methods and algorithms. Understanding the sensitivity of a method to the number of generated samples is essential for evaluating its reliability and generalizability. Thus, this section presents a sensitivity analysis of generated leak samples, explicitly focusing on their impact on the distribution of generated samples and the performance of the LSTM-GAN method. To further validate the performance of generated samples, the numbers of generated samples are selected as 1000, 1500, 2000, 2500, 3000, 3500, 4000, 4500, and 5000 for further sensitivity analysis.

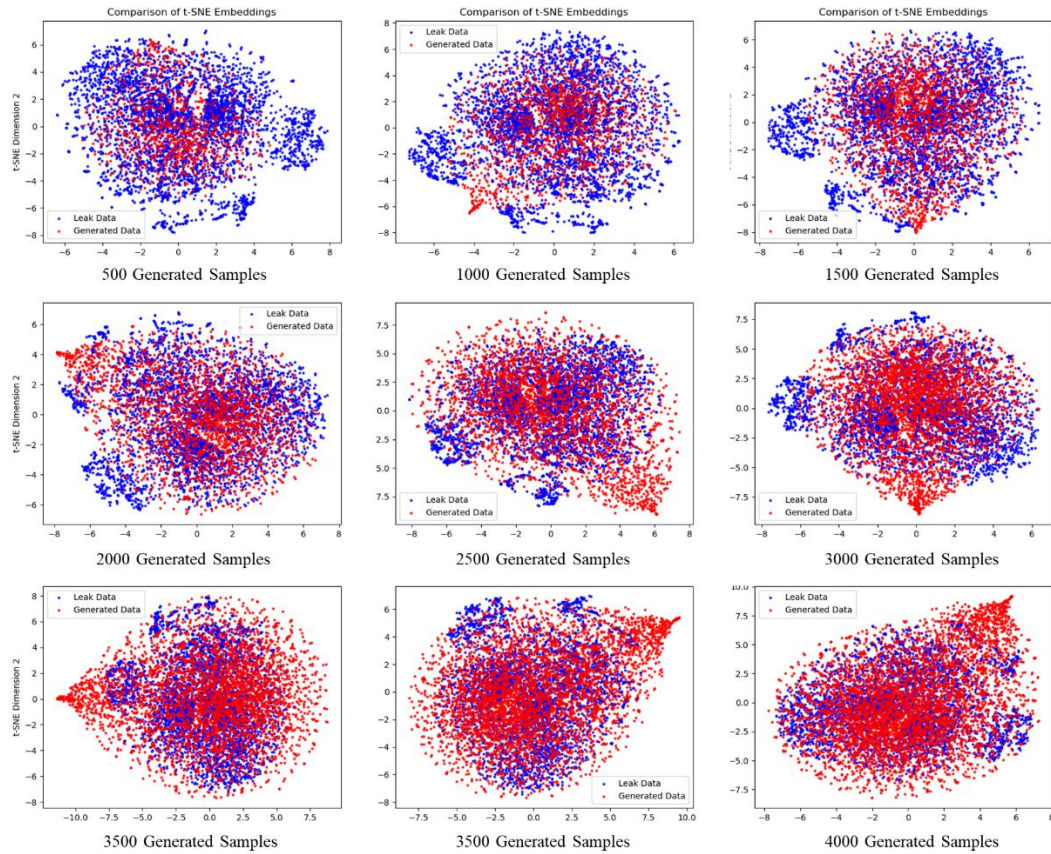


Figure 4.8 Sensitivity analysis of generated samples through t-SNE results

The generated samples were initially visually analyzed using t-SNE, as illustrated in Figure 4.8. As the number of generated samples increased, they gradually filled the gaps in the original signal distribution without exhibiting significantly concentrated points. However, with the increasing quantity, some generated points began to focus outside the original signal distribution, and this concentration became more pronounced as the number of generated samples grew. Additionally, there was a gradual increase in overlap between the generated samples and the distribution of original samples. This phenomenon indicates that there is no apparent bias within a specific range of generated sample quantities. However, as the number of generated samples increases, some outliers may potentially impact the overall training performance.

The impact of generated samples was further evaluated through model practice analysis. The testing dataset includes 2006 samples (1128 noleak samples, 878 leak samples). Furthermore, additional case investigations were employed to collect leak signals from other independent water leakage cases. The research team has cooperated with the local water supply contractor to collect new leak samples from eight leak cases and a total collection of 68 1-second leak signals. The signals are functioned as the validation set for subsequent evaluation.

Figure 4.9 depicts the testing and validation results of the model enhanced by different volumes of generated samples. Notably, the origin indicates the original data without using generated samples, and the number represents the volume of generated samples. Based on the results above, the performance of the models on both the validation and test sets demonstrates a general consistency. This consistency suggests that the model did not overfit the specific features of the validation set during training and could generalize the unseen test data effectively.

Specifically, the "origin" model represents the baseline model trained without the enhanced dataset and achieved a validation accuracy of 81.54% and a testing accuracy of 91.92%. The models' performance varies as the number of generated samples increases. For example, the model trained with 1000 generated samples showed improved validation (87.01%) and testing (92.58%) accuracies compared to the baseline model. However, the model's performance fluctuates as more generated samples are added. The model trained with 1500 generated samples had lower validation (81.07%) and testing (85.59%) accuracies than the model trained with 1000 generated samples. Meanwhile, the model trained with 2500 generated samples achieved the highest

validation accuracy of 90.61% and testing accuracy of 94.02%. Meanwhile, increasing the generated samples cannot improve the model's performance. The final model trained with 5000 generated samples had a validation accuracy of 86.15% and a testing accuracy of 90.38%, which is lower than the model trained with 2500 generated samples.

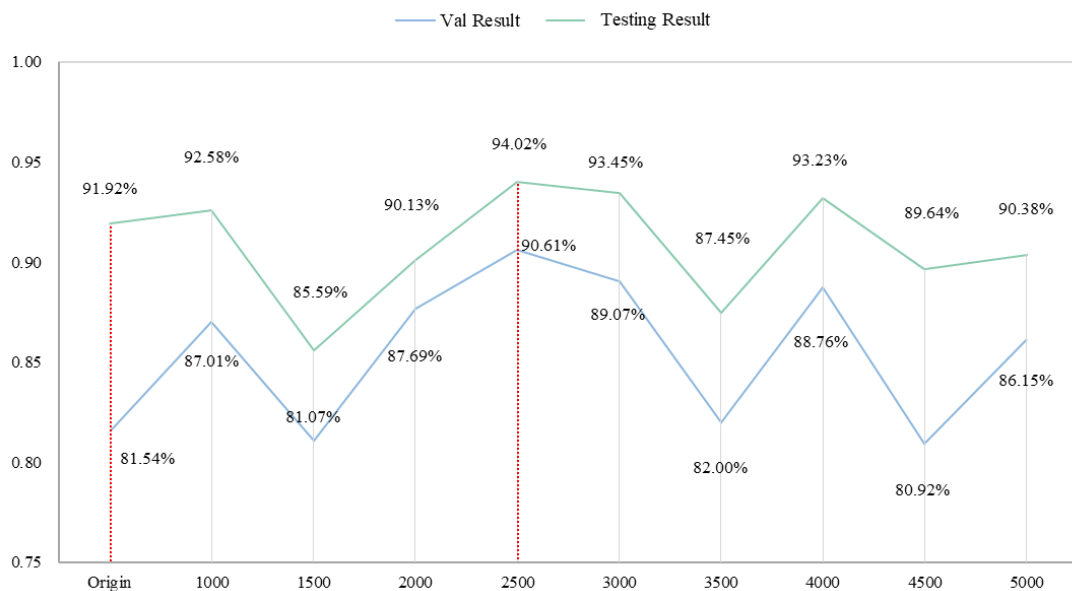


Figure 4.9 The testing and validation results of models trained with various enhanced dataset. The results demonstrate the impact of using different numbers of generated samples during training. Generally, augmenting the number of generated samples enhances model performance. However, it does not guarantee the corresponding increase in model accuracy. The model trained with 2500 generated samples achieved the optimal balance between accuracy and generalization to validation data, outperforming the other models in this evaluation. Therefore, LSTM-GAN with 2500 generated samples is selected for subsequent comparison.

## 4.4 Model Comparison

This section compares the LSTM-GAN model and other generative models to validate its effectiveness further. Specifically, three additional generative methods were employed, including i) adding noise, ii). overlapping windows, iii) SMOTE.

For adding noise, white noise was added to the original signal with the signal-to-noise ratio of 20 dB. Additionally, overlapping windows were introduced, with a start split time at 0.5 s and a window step of 1 s, to generate additional samples for data augmentation. Besides, SMOTE was employed with five nearest neighbor samples selected for subsequent enhancement. Adding noise and overlapping windows generated 3510 leak samples, while SMOTE and LSTM-GAN generated 2500 leak samples for subsequent comparison.

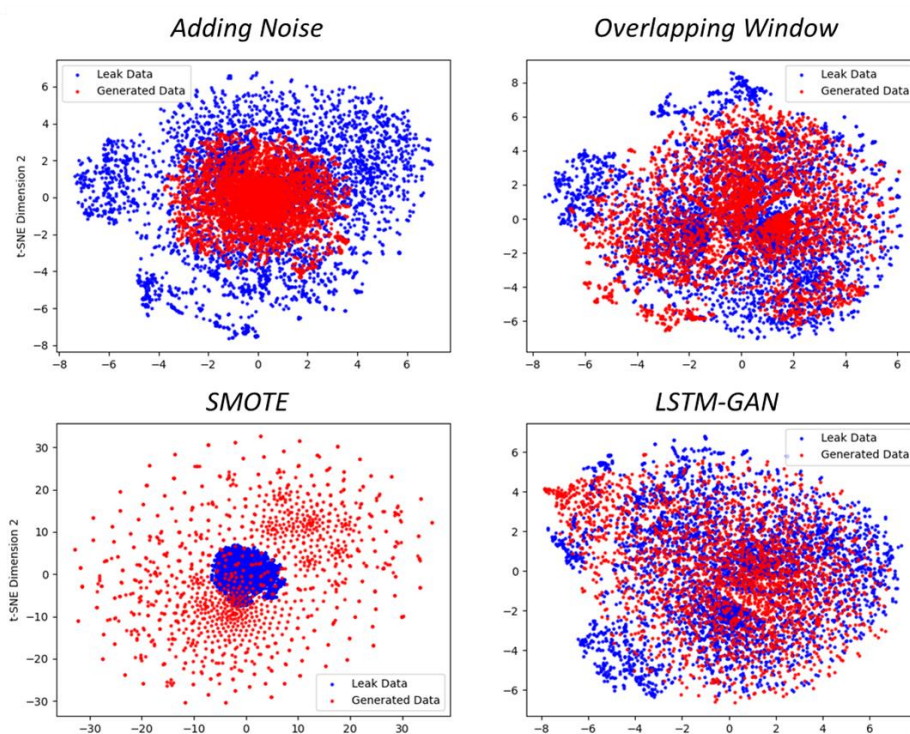


Figure 4.10 t-SNE results from various generative methods

Figure 4.10 depicts the t-SNE results of adding noise, overlapping window, SMOTE, and LSTM-GAN. The results illustrate that the samples generated by adding noise were concentrated in the center of the total distribution, potentially leading to overfitting issues. On the other hand, the samples generated by SMOTE exhibited a wider distribution compared to the original samples, suggesting that the generated samples may not align with the characteristics of real leak samples. The t-SNE result of the overlapping window technique showed a more dispersed distribution, with the generated samples located in the gaps among the red points. However, due to the nature of the overlapping window approach, where the generated and real samples originate from the same signals, there is also a potential risk of overfitting.

Subsequently, the performances of generative methods were compared through leak detection practices analysis based on testing and validation datasets. Based on Figure 4.11, LSTM-GAN achieved the highest validation accuracy (90.61%) and testing accuracy (94.02%) among all the techniques or models. The result indicates that the combination of LSTM and GAN architectures for data generation and processing has proven to be effective in improving model performance.

Meanwhile, adding noise resulted in lower accuracies compared to the baseline model. It suggests that simply adding random noise to the data may not be sufficient for improving model performance, as it can introduce unwanted variations that hinder the model's ability to generalize. SMOTE achieved similar performance on both the validation and testing datasets, with a validation accuracy of 87.61% and a testing accuracy of 87.23%. Meanwhile, the overlapping window-based model performed lower than the baseline model in the testing dataset but was better than the baseline

model and slightly lower than the LSTM-GAN model in the validation dataset. The result suggests that using overlapping windows for data processing might enhance the leak detection capability but with a higher false alarm rate.

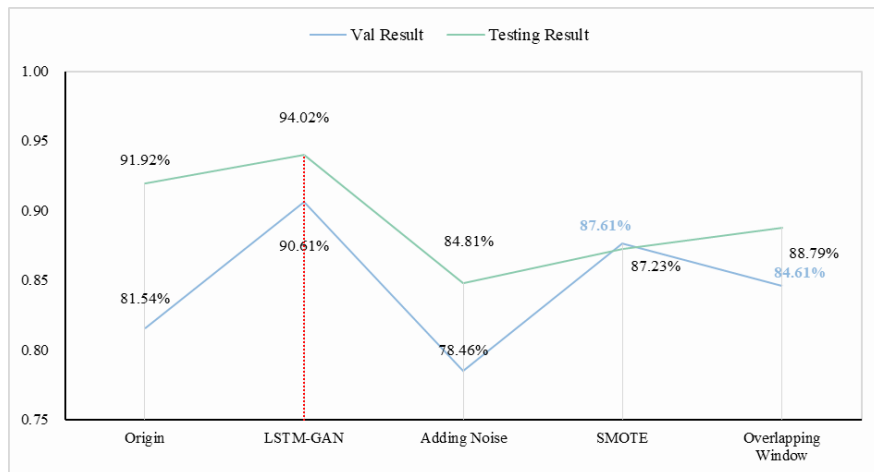


Figure 4.11 The model performances on testing and validation dataset

In summary, the above results indicate that the LSTM-GAN model outperformed other acoustic water leak detection techniques. Adding Noise did not yield significant improvements, while SMOTE helped address data imbalance. The overlapping window-based model showed moderate improvement, highlighting the importance of capturing temporal dependencies in the data.

#### 4.4.1.1 The Practicality of the Proposed Method to Real WDNs

The main contributions of this study can be summarized into two points: i) The proposal of a generative approach that can stably generate leak signals and. ii). The generated leak signals provide additional information to leak datasets, enhancing the leak detection performance.

For the first point, as illustrated in Figure 4.6, the t-SNE results illustrate that the generated signals and the original dataset share similar underlying structures from a mathematical perspective. Compared to adding noise, overlapping windows, and

SMOTE, LSTM-GAN also excels in capturing the time series structure and acoustic characteristics, enabling the generation of realistic signals.

This point is further confirmed through the acoustic characteristics analysis results in Figure 4.7, which show that the two datasets have close acoustic characteristics in time and frequency domain features. It confirms the practicality of the generated leak signals in accurately representing actual signals, thereby enhancing the quality of the associated datasets. Besides, the LSTM-GAN approach contributes to developing ML-driven water leak diagnosis models that rely heavily on ample data.

For the second point, based on the results of t-SNE (shown in Figure 4.6, Figure 4.8, and Figure 4.10) and model augmentation results (shown in Figure 4.9 and Figure 4.11), the proposed LSTM-GAN is proven to be able to generate new leak signals covering the uncollected leak scenarios with reduced bias. Specifically, the t-SNE results reveal that the generated leak signals fill voids among the mapped original signals. This observation suggests that the generated signals potentially preserve additional information that may have been absent in the original dataset, thereby mitigating the overfitting problem (Bowles et al., 2018). Furthermore, the model augmentation validation results also confirm the effectiveness of generating signals in improving the performance of water leak detection models compared with other generative methods. The model improvement can be attributed to new leakage signals generated by LSTM-GAN, potentially enhancing the dataset diversity and covering previously uncollected leakage scenarios. However, the sensitivity analysis also reveals that increasing the number of generated samples improves model performance. It is crucial to note that this enhancement does not always translate into a corresponding increase in model accuracy.

Combined with the t-SNE results, it can be explained that the increase in generated samples might also potentially introduce the outlier or noise samples and duplicated information, which might not be beneficial for model improvement. Therefore, when applying LSTM-GAN to other scenarios, it is still necessary to make appropriate adjustments based on the existing model experimental conditions and the complexity of the problem.

This study provides novel inspiration for applying the LSTM-GAN generative approach to improve water leak detection. Although previous acoustic generative methods contribute to data preprocessing and enhancement, they may struggle to capture complex patterns and lack robust generative capabilities. The research incorporates LSTM and GAN models to ensure that the model captures time series and learns the critical acoustic features of signals. LSTM retains and learns long-term dependencies, enabling it to capture critical acoustic signal features. Integrating GAN into the approach adds generative capabilities, allowing the model to generate realistic synthetic leak signals.

#### **4.5 Chapter Summary**

This chapter presents a novel approach, LSTM-GAN, designed to capture the distribution of leak signals and generate high-quality samples. The framework alleviates the inherent challenge of limited real data availability for machine learning-based leak detection in water distribution networks.

The proposed LSTM-GAN model demonstrates its capability to generate comprehensive acoustic signals that accurately simulate leak conditions in the context of WDNs. The quality of these generated signals is thoroughly evaluated through t-SNE

analysis, acoustic feature analysis, and validation using model augmentation techniques. Comparative analysis against real leak samples reveals a high degree of similarity in terms of t-SNE results and acoustic features extracted from both the time and frequency domains. Furthermore, the validation analysis conducted on model augmentation provides additional evidence of the superior performance of LSTM-GAN (94.02%) compared to other generative methods on the testing dataset.

# CHAPTER 5 Model Explanation and Interpretation

## 5.1 Introduction

This chapter presents a novel CNN-based water leak detection model that enhances interpretability by incorporating Grad-CAM. This integrated approach unveiled the detection process and improved water management practices.

## 5.2 Development of Time-Frequency Spectrum Visualization Framework

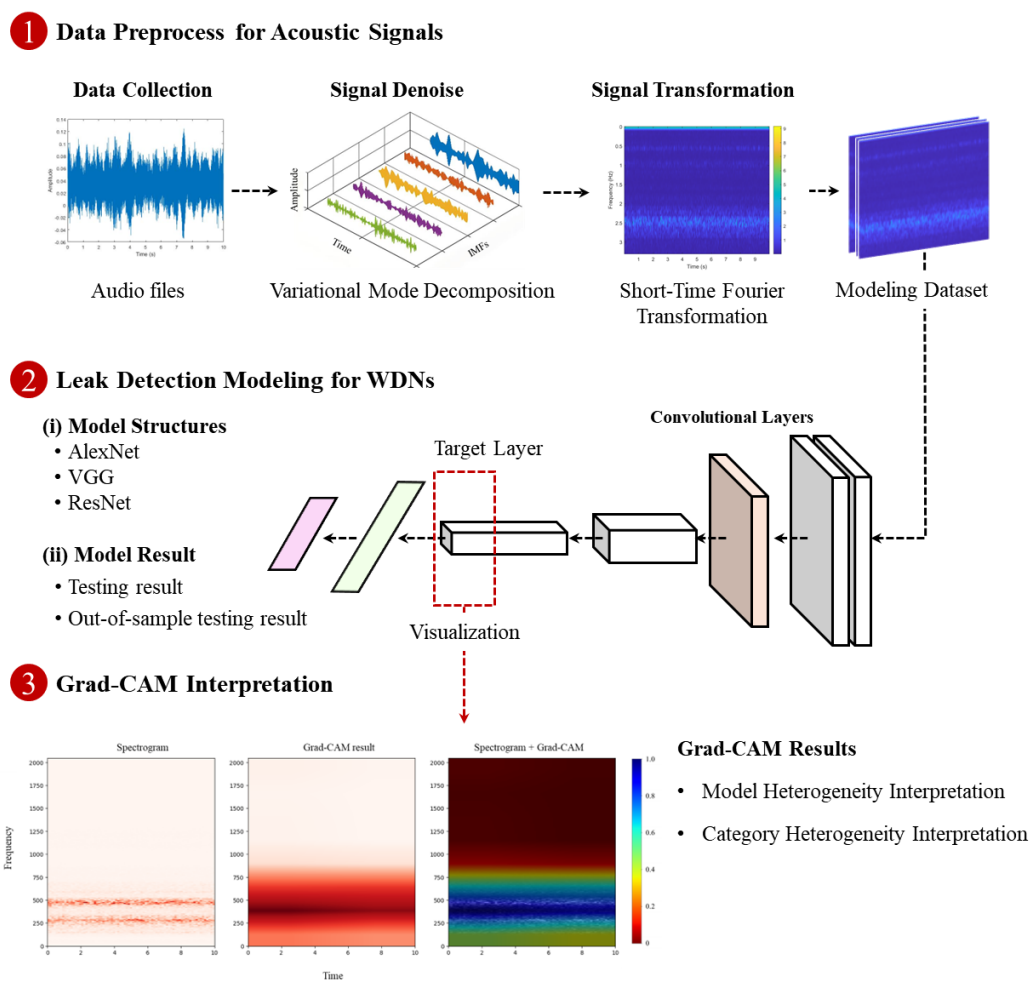


Figure 5.1 Proposed framework of explainable leak detection for WDNs.

The proposed framework for water leak detection and interpretation is shown in Figure 5.1. The framework involves obtaining vibroacoustic signals from the water system, applying VMD for noise reduction, and performing STFT to transform the signals into

spectrogram representations. The spectrogram representations are then fed into a designed CNN model. During training, the model is loaded with testing data and classified into different fault classes related to water leaks. The Grad-CAM technique is applied downstream from the neural network's classification results to identify the time and frequency regions associated with the detected fault classes. The Grad-CAM results from convolution layers are used to analyze the relationship between specific features in the acoustic characteristics of leak signals and the class-discriminative decisions made by CNNs.

## **5.2.1 Data Preprocessing**

### **5.2.1.1 Denoise for Acoustic Signals**

In the context of leak detection in WDNs, the acquired acoustic signals from sensors are often subject to significant amounts of unknown noise, rendering them stochastic signals. To mitigate the influence of noise and attenuate its adverse effects, this study employs VMD to decompose the signal into multiple IMF components. During this decomposition process, retaining the relevant components while eliminating the noise components is crucial, thereby achieving the noise reduction objective.

The number of IMFs might influence the balance between signal stability and integrity. This study takes 10 as the number of IMFs, considering the VMD setting of Liu et al. (2021a). Meanwhile, conventional approaches typically rely on empirical parameters to select the practical components and necessitate prior knowledge of the signal and noise characteristics. However, these methods are inherently limited in their applicability. To address these limitations, this study adopts correlation (B. Liu et al., 2021a; T. Xu et al., 2021) as the criterion for screening valid IMF components.

Specifically, the collected signal is decomposed into ten IMF components using the VMD method. Subsequently, the correlation of each IMF is calculated to evaluate its significance with the signal. Generally, IMFs with higher correlation represent the valid components of the signal, while those with lower correlation levels are more likely to correspond to noise components. Consequently, this study selects the key IMF components that exhibit significant energy for signal reconstruction, thereby obtaining a denoised signal.

### **5.2.1.2 Time-Frequency Transformation for Acoustic Signals**

The main goal of applying a time-frequency transformation to signals is to extract a comprehensive range of information. This transformation allows for a deeper understanding of the signal's properties by providing insights into frequency and time changes. As a result, a more holistic understanding of the signal's characteristics is achieved.

This study adopted the Short Time Fourier Transform. At the same time, the Hamming window has been selected as the window function, and it is employed with a window length of 512, an overlap of 256, and the number of Fourier transform points is 256. This configuration allows for clearly observing characteristic features associated with both leakage and non-leakage signals. The Hamming window is widely adopted in STFT applications because it suppresses spectral leakage and provides accurate frequency estimation. By applying the STFT, detailed time-frequency characteristics can be obtained, greatly facilitating further analysis and interpretation of the signals under investigation.

### **5.2.2 Leak Detection Modeling**

In the field of fault diagnosis modeling, several deep learning architectures have demonstrated remarkable performance. This section presents the structures of three adopted models: AlexNet, VGG, and ResNet. Specifically, the VGG and ResNet network architectures encompass various versions distinguished by their depth and structure. For instance, VGG-11 denotes the VGG model with 11 weighted layers, while ResNet-18 represents the ResNet model with 18 weighted layers. The choice of model depth can significantly impact the training outcomes and should be tailored based on the complexity of the problem at hand, as well as the available experimental resources such as data quantity, data quality, and computational capabilities. This study adopts multiple widely used CNN models with minor modifications for water leak detection. The main structure of the above models can be found in the following studies: i). ResNet-18, ResNet-34 (He et al., 2016), ii). VGG-11, VGG-13, VGG-16, VGG-19 (Simonyan & Zisserman, 2014), iii). AlexNet (Krizhevsky et al., 2012).

Notably, in this study, transfer learning was intentionally avoided. The main structure of the aforementioned models was adopted without incorporating any pre-trained parameters. This decision was made to ensure that the model's performance relied solely on its own learning and generalization capabilities, without any influence from prior knowledge or features extracted from pre-trained models in the context of computer vision object recognition (Z. Wang et al., 2019). Meanwhile, this study has minor changes in the input layers of the above models to meet the data structure of the input spectrogram. Specifically, the first input convolution layer is changed to one channel. The number of output neurons in the last layer within the fully connected block is

changed to two, responding to two leak statuses (leak, noleak) of water pipelines. The optimizer used in this study is Adam, with a learning rate of  $1 \times 10^{-5}$ , and the training epoch is set to 2000. The hold-out method is employed, where 80% of the data is allocated for training, while the remaining 20% is dedicated to testing. Additionally, for out-of-sample testing, the research team collected data from independent cases to ensure the robustness and generalizability of the developed models.

### 5.2.3 Grad-CAM Interpretation

Grad-CAM is a popular technique for visualizing the regions of an input grid data that contribute most to the prediction made by the CNN fault diagnosis model (Miettinen et al., 2009), providing insights into the model's decision-making process and helping understand which parts of the spectrogram are influential in the prediction. In this study, the Grad-CAM is conducted on the spectrograms of the leak and noleak signals to identify the critical regions for different leakage statuses.

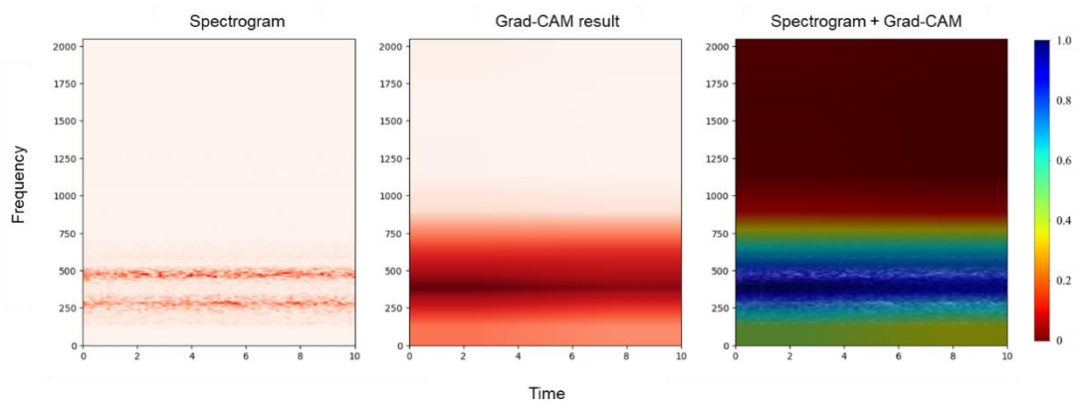


Figure 5.2 A typical Grad CAM result from the leak detection model for demonstration.

The result of Grad-CAM visualization is typically presented as a heatmap overlay on the original spectrogram, as shown in Figure 5.2, where the heatmap indicates the importance or relevance of each pixel in contributing to the model's prediction. The brighter or hotter regions in the heatmap correspond to the areas that substantially

influence the prediction, while darker or cooler regions have less significance. Meanwhile, the spectrogram and Grad-CAM are combined to provide a convenient visualization. A reverse jet colormap has been employed, wherein blue signifies regions of high importance for the models, while red represents regions of lesser significance. The result of Grad-CAM can be used for various purposes. First, it assists in model explanation and debugging by identifying regions of the spectrogram that the model may be overly reliant on or ignoring. It can also provide insights into the model's behavior, helping researchers and practitioners understand how it makes predictions and potentially uncover any biases or unexpected patterns. Furthermore, Grad-CAM points out the potential phenomenon of acoustic signals, assists in cross-validating the acoustic phenomenon, and provides insights for enriching theory research.

In conclusion, Grad-CAM results offer interpretable insights into the regions of the spectrogram that contribute most to a CNN's decision. Highlighting influential areas helps compare and understand the decision-making process of different models, distinguishing the pattern within different leak statuses.

### **5.3 Model Results Evaluation and Interpretability Discussion**

#### **5.3.1 Experiment Setup and Data Preparation**

As mentioned, the research team cooperated with the local water supply department and contractors to conduct field experiments. The 10s audio samples were split into one second. The research team has gathered signals across diverse leak scenarios, and 10030 audio samples (4390 leaks, 5640 noleaks) were collected.

Meanwhile, the previous generative approach enriches datasets for subsequent leak detection modeling. According to the last empirical rules, it would be better to establish

a dataset with equal datasets. Thus, 1250 leak samples were generated add to the dataset, which ultimately contained 5640 leak samples and 5640 noleak samples.

Meanwhile. the hold-out method divides the dataset into 80% for training (4512 leak samples, 4512 noleak samples) and 20% for testing (1128 leak samples, 1128 noleak samples). As a result, the acoustic signals collected from non-metal pipelines are excluded from the analysis. Furthermore, out-of-sample testing was conducted, involving a total of 152 audio samples. These samples consisted of 67 leaks and 85 noleak samples, enabling the evaluation of the model's effectiveness and robustness in subsequent processes.

### **5.3.2 Performances of the Proposed CNNs**

To assess the effectiveness of the proposed CNNs in leak diagnosis, their performance was evaluated using a range of metrics, where the positive class represents leaks and the negative class represents noleak. As illustrated in Equation (5.1) to Equation (5.5), accuracy, precision, recall, specificity, and F1-score have been utilized. Precision assesses the model's ability to avoid false alarms. A higher precision indicates a better ability of the model to prevent false alarms. Recall evaluates the capability to detect all leaks without missing any. A higher recall indicates fewer potential leaks. Specificity indicates the ability to identify the negative class correctly, and a higher specificity suggests that the model is effective at correctly identifying and distinguishing non-leak samples from leak samples. Besides, the F1 score is a metric that combines precision and recall into a single value, providing a measure of the binary classification model's performance in imbalanced datasets (Jeni et al., 2013). A high F1 score indicates that

the model has balanced precision and recall, signifying a more accurate and comprehensive model.

$$\text{Accuracy} = \frac{\text{True Positive} + \text{True Negative}}{\text{True Positive} + \text{True Negative} + \text{False Positive} + \text{False Negative}} \quad (5.1)$$

$$\text{Precision} = \frac{\text{True Positives}}{\text{True Positive} + \text{False Positive}} \quad (5.2)$$

$$\text{Recall} = \frac{\text{True Positive}}{\text{True Positive} + \text{False Negatives}} \quad (5.3)$$

$$\text{Specificity} = \frac{\text{True Negative}}{\text{True Negative} + \text{False Positive}} \quad (5.4)$$

$$\text{F1-score} = 2 \times \frac{\text{Precision} \times \text{Recall}}{\text{Precision} + \text{Recall}} \quad (5.5)$$

According to Figure 5.3, evaluating different CNN models for water leak detection revealed varying performance across multiple metrics. ResNet-18 and AlexNet exhibit superior precision, with ResNet-18 achieving the highest precision rate of 98.80% and closely followed by AlexNet with 98.85%. On the other hand, VGG-19 and AlexNet demonstrate promising recall rates, indicating their ability to identify all potential leak samples accurately. Additionally, VGG-13 achieved perfect specificity scores of 100.00%, showcasing the accurate classification of noleak samples.

Regarding overall accuracy, VGG-19 emerges as the top performer with an accuracy rate of 99.00%, closely followed by AlexNet with 98.01%. These results highlight the effectiveness of these CNN models in fitting the distribution of STFT-based spectrogram datasets. Their high precision, recall, and accuracy demonstrate their ability to classify and predict instances accurately.

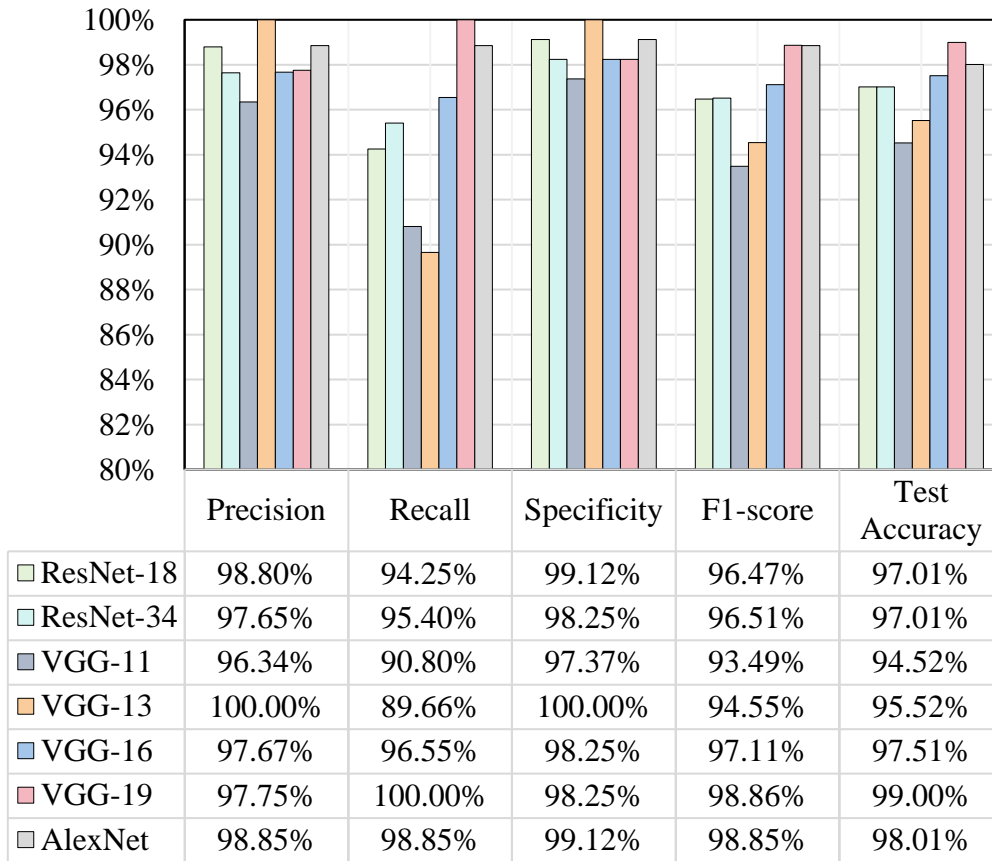


Figure 5.3 The performance of CNN models in the testing dataset.

An additional set of 67 leak samples and 85 noleak samples have been collected and regarded as the dataset for out-of-sample testing to prevent model overfitting and conduct a more thorough evaluation of the model's performance. The performances of CNN models in the out-of-sample testing are illustrated in Figure 5.4.

Compared to the testing performance, proposed CNN models achieve lower accuracy in the out-of-sample testing. The accuracies of VGG-11, VGG-13, VGG-16, and Resnet-18 are significantly decreased. It is common to witness a decline in model accuracy when the data from new cases is applied to the previously trained leak detection model (2008). From the above metrics, it can be observed that VGG-19 and AlexNet stand out with higher precision, recall, F1-score, and accuracy compared to the other models. VGG-19 achieves the highest recall rate of 88.06% and the highest F1-

score of 84.29%, indicating its effectiveness in accurately identifying leak samples with lower false alarm rate. AlexNet also demonstrates a strong balance between precision and recall, with an F1-score of 80.85%. On the other hand, VGG-11 shows lower precision and recall rates than the different models, indicating an undeveloped ability for leak detection. ResNet-18 and ResNet-34 perform consistently, with similar precision and recall rates. VGG-13 and VGG-16 exhibit moderate performance across the metrics. From testing and out-of-sample testing results, VGG-19 and AlexNet emerge as the top performers, showcasing their effectiveness in accurately identifying instances in the given dataset.

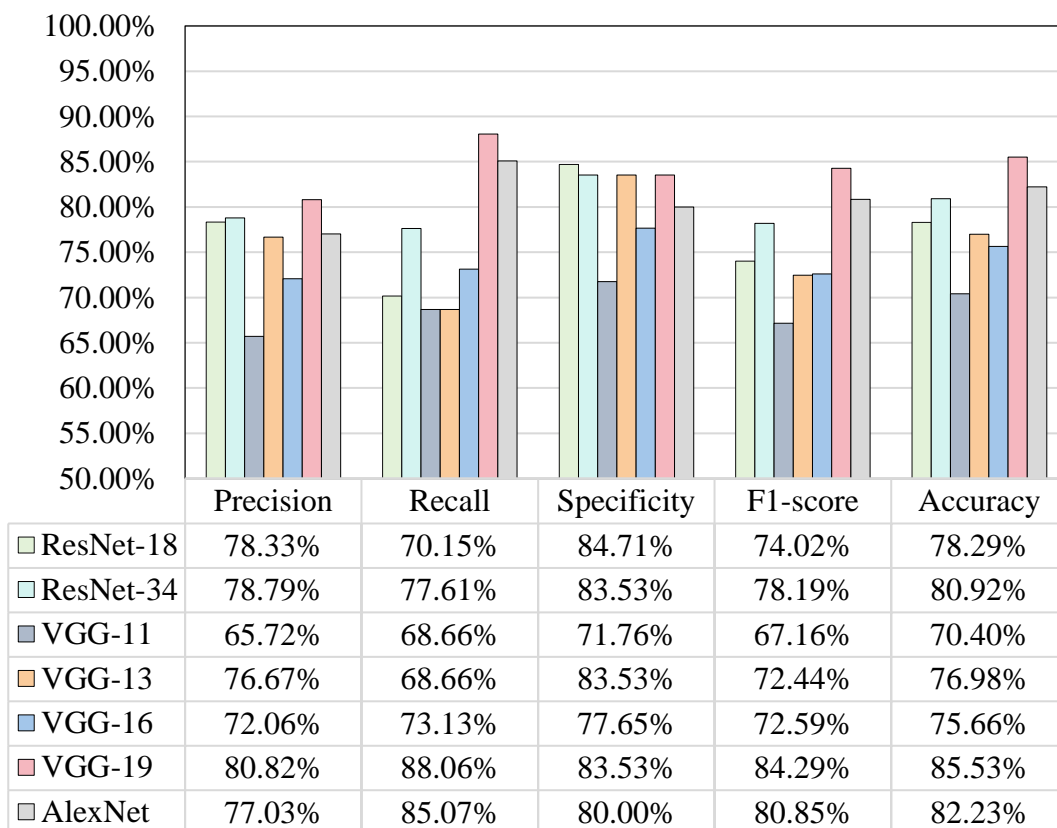


Figure 5.4 The model performance comparison between testing and out-of-sample results.

The findings demonstrate that the evaluated CNN models accurately detect and classify leaks within WDNs. However, further analysis and interpretability studies are

warranted to enhance our understanding of their decision-making processes and identify opportunities for model improvements. These additional investigations would provide valuable insights into the inner workings of the models, enabling them to refine and optimize their performance further.

### **5.3.3 Grad-CAM Interpretation Results**

Model interpretability analysis is crucial to gaining insights into the inner workings of the hidden layers in CNNs, frequently regarded as black boxes. This analysis becomes particularly valuable when applied to leak detection models. Therefore, this section applied Grad-CAM to visualize the critical convolution blocks from previously developed CNN models. The objective was to analyze the i). Model Heterogeneity, interpreting the differences between various models, and ii). Category Heterogeneity, interpreting the differences between leak statuses.

#### **5.3.3.1 Model Heterogeneity Interpretation**

Section 5.3.2 proposed several models for water leak detection, which also introduced model heterogeneity stemming from different architectures and other factors. Analyzing the Grad-CAM results of these models can provide valuable insights for model comparison and improvement. Figure 5.5 compares the Grad-CAM visualization results obtained from seven different models on leak signal (i). As depicted in Figure 5.5 (a), the spectrogram from the leak signal indicates a prominent signal within the frequency band ranging from approximately 750 Hz to 1000 Hz. A subtle signal range can also be observed between 500 Hz and 750 Hz. According to Figure 5.5 (b) to (h), models show different attention patterns when identifying a leak signal. The attention range of AlexNet shows a prominent band ranging from 740 to 1100 Hz, and attention gradually

diminishes as the frequency increases and decreases. In the case of ResNet, both ResNet-18 and ResNet-34 exhibit a relatively broad attentional scope centered around 760 Hz, with ResNet-34 displaying a more dispersed attention region compared to ResNet-18. In contrast to ResNet, VGG models demonstrate a more concentrated attention region. Specifically, VGG-11, VGG-13, and VGG-19 manifest attention within the approximate range of 500 to 1000 Hz, while the attention focus of VGG-16 is notably concentrated around 900 Hz relative to other VGG models.

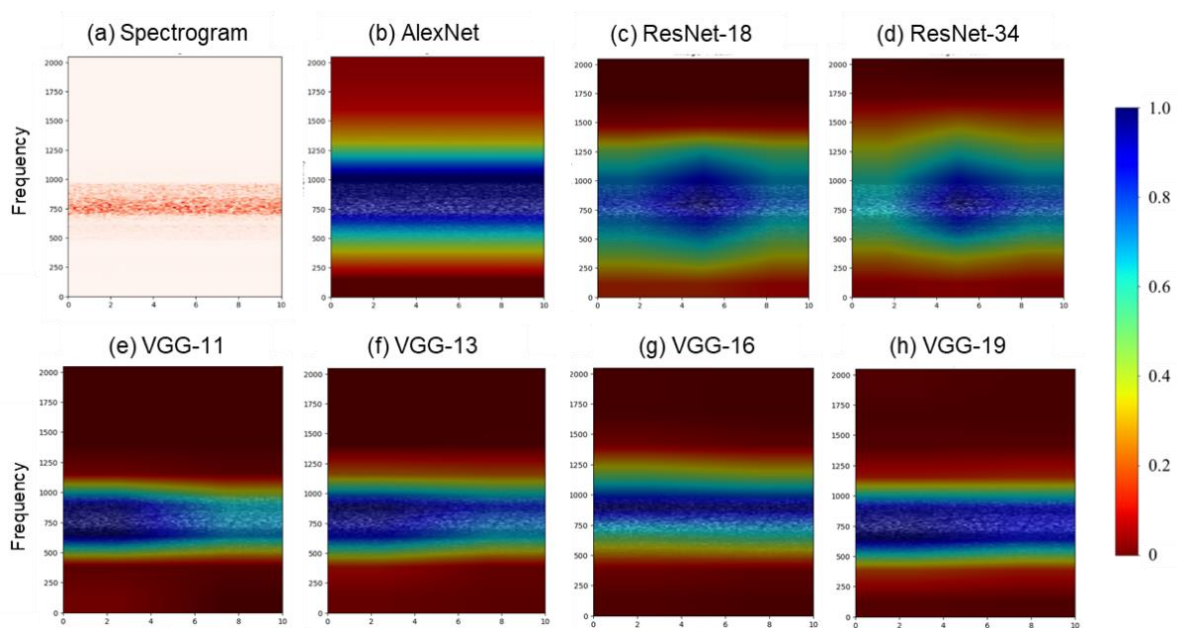


Figure 5.5 Grad-CAM visualization results comparison among various models based on leak signal (i).

Meanwhile, Figure 5.6 demonstrates the Grad-CAM results on another leak signal (ii). From Figure 5.6 (a), the spectrogram shows a distinguished signal over the 200 Hz frequency band and lower frequency band during 1250 to 1500 Hz and 600 to 700 Hz. According to the Grad-CAM analysis, AlexNet demonstrates higher attention towards signals between 1500 Hz and 1700 Hz, followed by a gradual decrease in attention towards higher and lower frequencies. Notably, it exhibits increased attention around

the frequency range of 500 Hz. On the other hand, ResNet-18 and ResNet-34 exhibit a broader distribution of attention. ResNet-18 concentrates its attention around 1250 Hz, encompassing the range of 1000 Hz to 1500 Hz, while ResNet-34 shows more concentrated attention between 750 Hz and 1250 Hz.

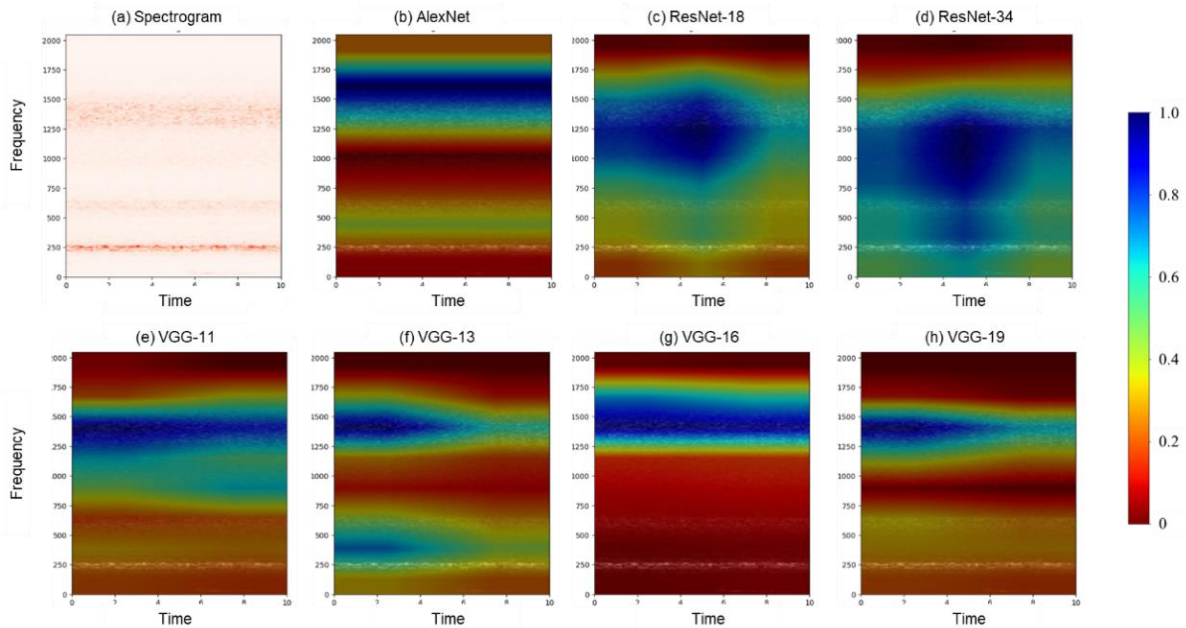


Figure 5.6 Grad-CAM visualization compares various models based on leak signal (ii).

Additionally, VGG models display evident attention around the frequency range of 1250 Hz to 1500 Hz. Specifically, VGG-11 demonstrates a higher concentration of attention between 750 Hz and 1250 Hz, with relatively less attention below 750 Hz. VGG-13, on the other hand, exhibits a stronger focus on signals between 250 Hz and 500 Hz. VGG-16 displays a higher concentration of attention towards higher frequencies, with less consideration given to signals below 1200 Hz. VGG-19, in contrast, demonstrates a more distinct attention distribution. Apart from the regions above, attention is uniformly distributed below 750 Hz.

Figure 5.7 compares the Grad-CAM visualization results obtained based on non-leak signals. As depicted in Figure 5.7 (a), the spectrogram of the non-leak signal (i) exhibits

a distinct signal close to 240 Hz, along with slight signals ranging from 130 to 510 Hz. Subsequently, the attention ranges of different models were analyzed, as shown in Figure 5.7 (b) to (h). AlexNet focuses on the frequency band ranging from 250 to 1000 Hz, particularly on 500 Hz. Conversely, ResNet-18's attention range extends from 250 to 1200 Hz, with a slight focus on the 500 to 750 Hz range. However, the attention becomes more dispersed in ResNet-34, as the model nearly encompasses the entire frequency domain, making it challenging to capture crucial information.

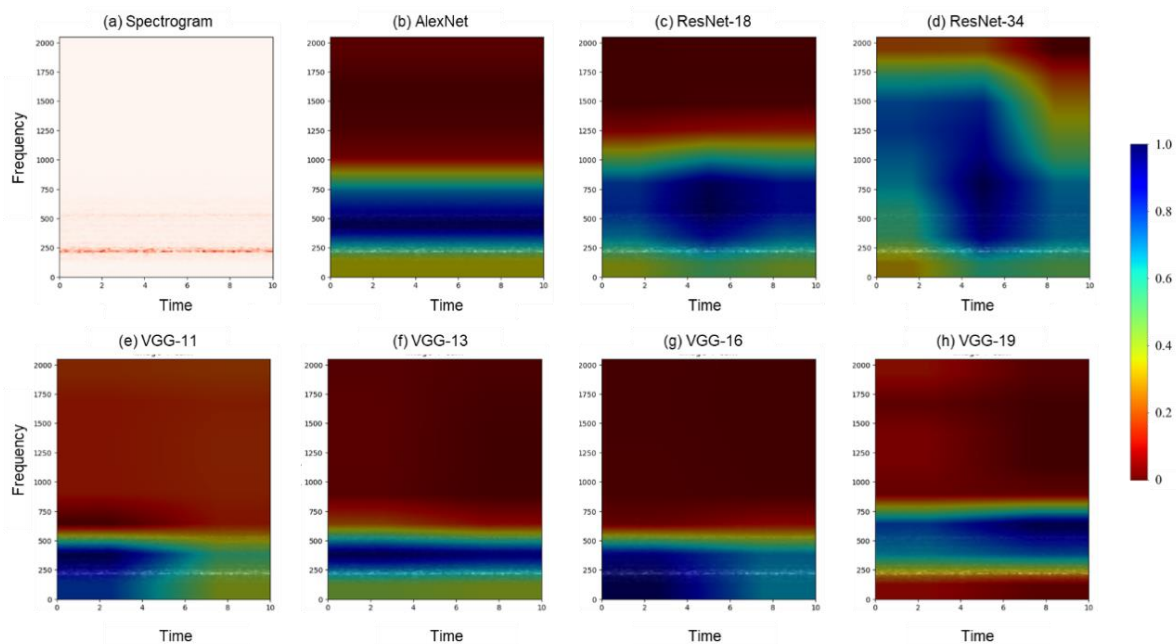


Figure 5.7 Grad-CAM visualization results in comparison among various models based on noleak signal (i).

VGG models, on the whole, exhibit similar attention patterns. VGG-11 appears to concentrate on 500 Hz and is influenced by time. VGG-13 demonstrates a clear attention region ranging from 300 to 500 Hz. In contrast, VGG-16 appears to be influenced by attention in the lower frequency band. The attention pattern of VGG-19 has notably shifted, focusing on the frequency range from 200 to 750 Hz.

Based on the analysis of model heterogeneity, it is evident that there are significant differences in attention regions among different types of models, while attention regions are relatively similar among models of the same type. However, there are slight variations in attention regions with changes in model depth.

The Grad-CAM results of AlexNet demonstrate relatively clear and concentrated attention, enabling the capture of primary input signal information, albeit with slight deviation. In contrast, VGG models can generally capture key information. However, VGG-11, VGG-13, and VGG-16 exhibit less stable attention and are more susceptible to noise interference, whereas VGG-19 displays a more apparent and stable attention pattern. In recognizing signals, ResNet demonstrates a more widely distributed attention, enabling extracting a broader range of information, which aligns with ResNet's characteristic of avoiding overfitting (Santos & Papa, 2009). On the other hand, ResNet could potentially be affected by irrelevant information from wider frequency regions. Therefore, ResNet can only achieve moderate accuracy as it encompasses comprehensive information but is susceptible to unexplored noise. Specifically, the Grad-CAM results of VGG-19 and AlexNet manifest more pronounced and stable attention regions than other models, suggesting a higher degree of discriminative decision-making. This observation provides insight into the superior performance of these models, thus offering a potential explanation for their enhanced overall efficacy relative to other counterparts.

### **5.3.3.2 Category Heterogeneity Interpretation**

In the context of leak diagnosis for WDNs, category heterogeneity arises when the heatmap visualizations vary significantly across different leak statutes. It indicates that

the model's attention and focus on relevant spectrogram regions may differ for each leak statute. The heatmap patterns can provide insights into the discriminative features learned by the model for different categories and help understand the reasoning process behind the leak detection. Therefore, this section analyzes the differences in Grad-CAM results between leak and noleak signals based on VGG-19 and AlexNet models, which have demonstrated better performance on the test and validation datasets.

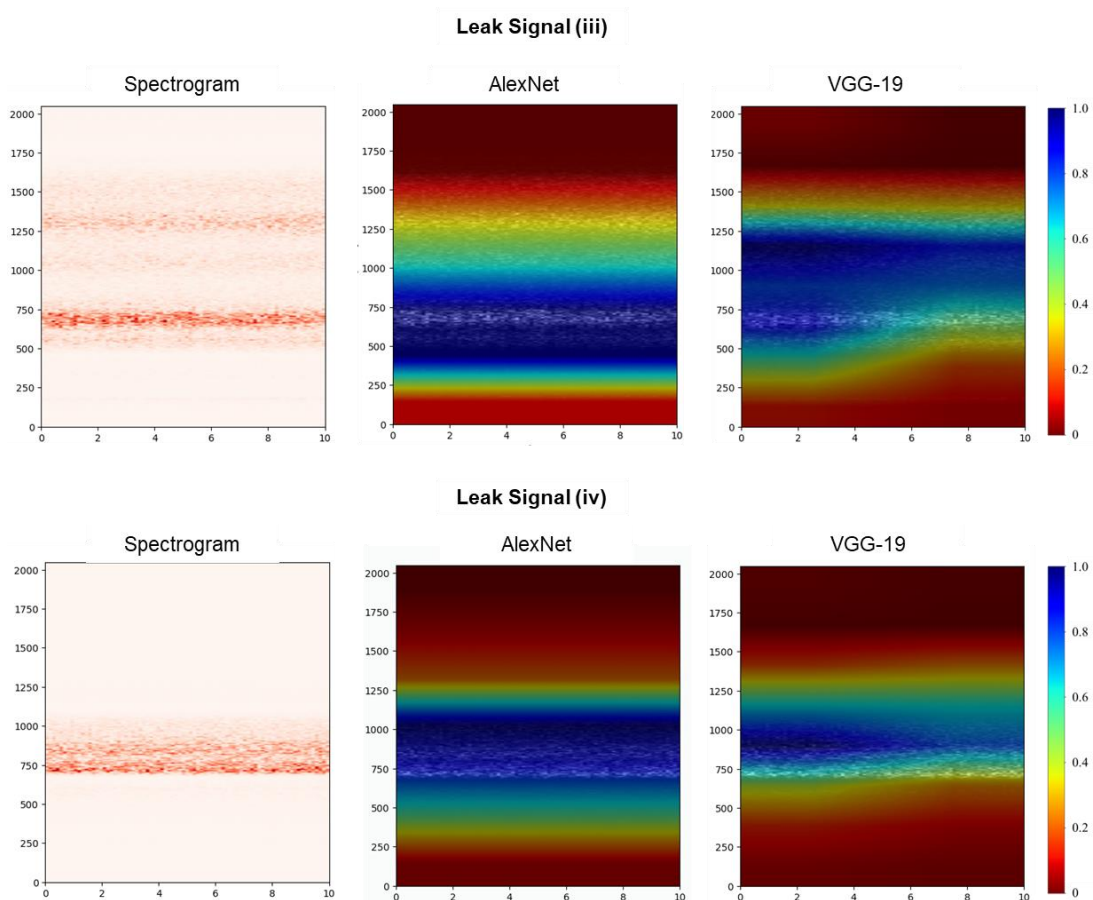


Figure 5.8 Grad-CAM results for leak signals (iii) and (iv).

Figure 5.8 primarily illustrates the Grad-CAM results for leak signals (iii) and (iv). For leak signal (iii), the spectrogram displays signals ranging from 740 Hz to 1600 Hz. It exhibits a clear signal around 700 Hz and a secondary energy peak near 1300 Hz. AlexNet and VGG-19 are strongly influenced by the frequency component ranging

from 500 Hz to 1000 Hz when making decisions regarding leak signals. In the case of leak signal (iv), both AlexNet and VGG-19 base their decisions on the presence of signals between 750 Hz and 1250 Hz, indicating the significance of this frequency range in leak detection.

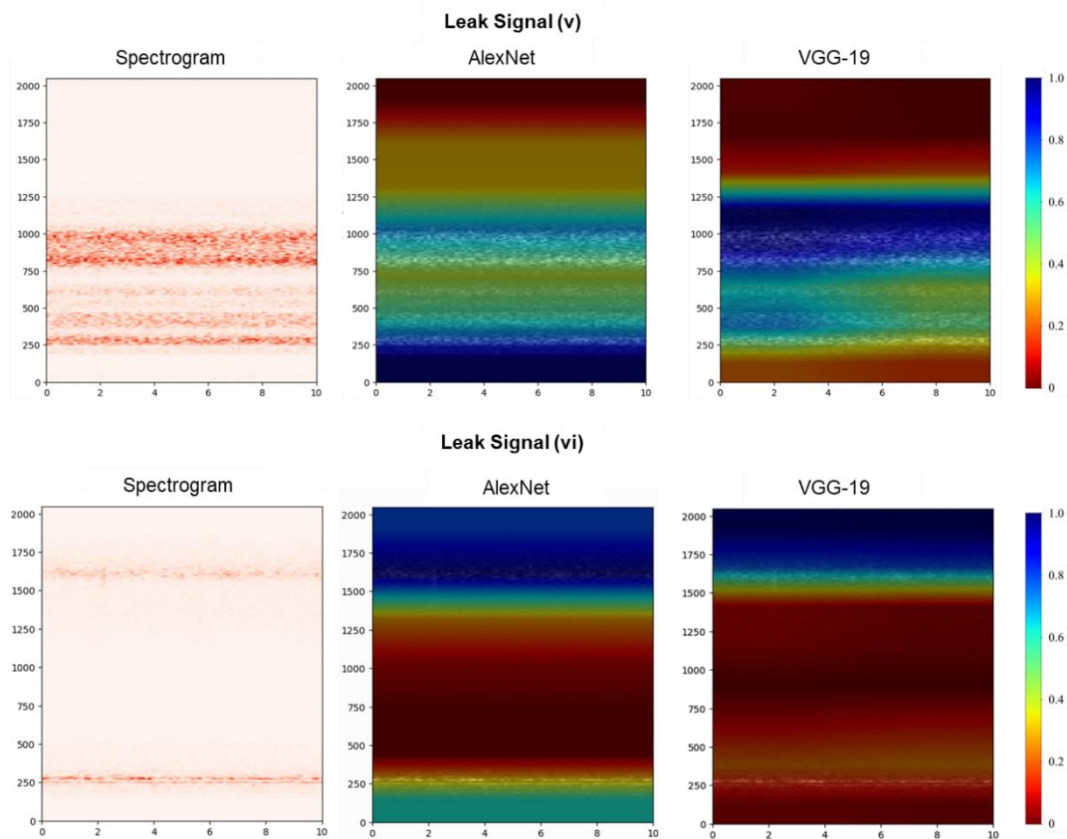


Figure 5.9 Grad-CAM results for leak signal (v) and (vi).

Meanwhile, based on Figure 5.9, the leak signals (v) and (vi) spectrograms were generated. The leak signal (v) spectrogram exhibits a prominent signal in the 800 to 1000 Hz frequency range, with varying signals observed between 250 and 750 Hz. When analyzing the Grad-CAM results, AlexNet primarily focuses on frequency components below 250 Hz and those near 1000 Hz when assessing whether a signal corresponds to a leak signal. In contrast, VGG-19 concentrate on the frequency range between 1000 Hz and 1250 Hz. Regarding leak signal (vi), significant energy is evident

around 1650 Hz. Consequently, both models are susceptible to the influence of high-frequency signals, exhibiting heightened attention beyond 1600 Hz. In addition, a blank signal within the 250Hz range can activate the region below 250Hz in AlexNet. This activation may have an impact on the accuracy of leak detection. Additionally, it should be noted that AlexNet does not perform better than VGG-19 in validation cases.

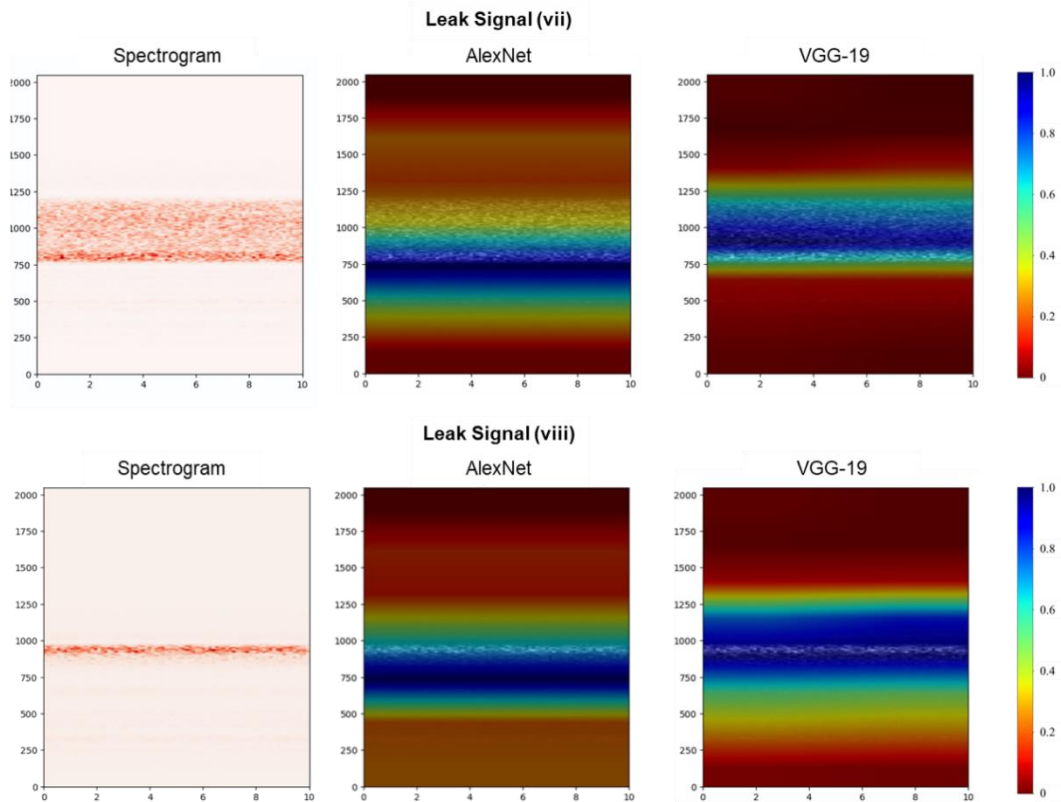


Figure 5.10 Grad-CAM results for leak signal (vii) and (viii).

From Figure 5.10, the spectrogram of the leak signal (vii) reveals the prominent frequency component between 750 Hz and 1200 Hz, with the highest intensity observed above 750 Hz. Both models are influenced by signals around 750 Hz, with AlexNet being particularly affected by signals ranging from 500 to 1000 Hz and VGG-19 being influenced by signals between 750 Hz and 1250 Hz. In the case of leak signal (viii), the signal concentrates around 900 Hz, significantly impacting the decision-making process

of both models. AlexNet is influenced by signals spanning from 500 Hz to 1000 Hz, while VGG-19 tends to be influenced by frequencies ranging from 750 Hz to 1250 Hz. During the decision-making process for identifying leak signals, high-frequency signals significantly affect the models, specifically those falling within the 750 Hz to 1250 Hz frequency band. In addition, specific models also consider signals below 250 Hz as part of their analysis.

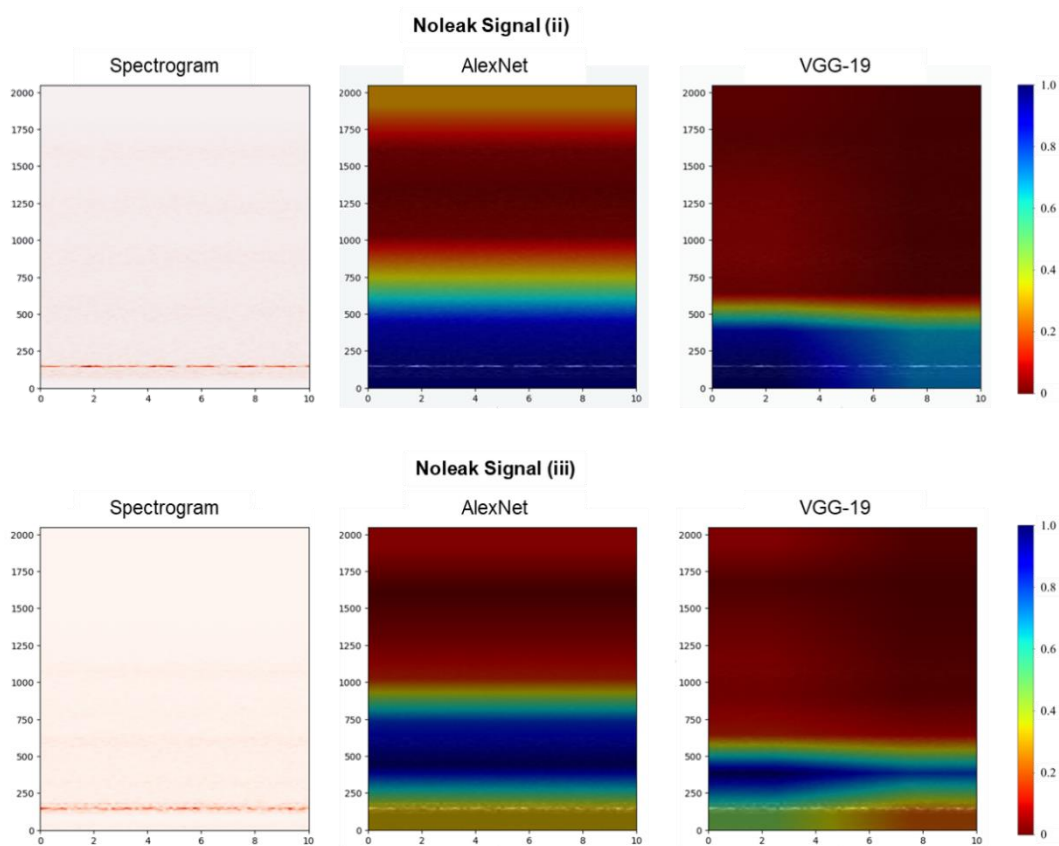


Figure 5.11 Grad-CAM results for noleak signal (ii) and (iii).

Noleak signal reveals different time-frequency characteristics. Compared to the leak signal, the noleak signal is concrete on a lower frequency band and demonstrates a different Grad-CAM pattern, as illustrated in Figure 5.11. For noleak signal (ii), the signal is clear in the frequency 120 Hz and below. The corresponding Grad-CAM result, therefore, concentrates on frequency regions below 500 Hz. Similarly, noleak signal (iii)

displays prominent spectral components above 200 Hz while exhibiting attenuated components within the 200 to 670 Hz frequency range. The Grad-CAM result depicts that both AlexNet is strongly influenced by 250 to 750 Hz signal from the region and signals from 250 to 500 Hz influence VGG-19.

Overall, Grad-CAM also demonstrates significant discrepancies across different categories. The models predominantly rely on salient features within the middle and high-frequency components (between 750 and 1250 Hz) as the basis for identifying leak signals, occasionally considering supplementary information below 250 Hz. Conversely, when discerning no-leak signals, the models primarily reference signal components in the mid-to-low frequency band (below 750 Hz), particularly emphasizing pronounced signals below 500 Hz. The above findings are aligned with the theoretical expectations that when an acoustic device is combined with the pipe effect, the system exhibits the behavior of a band-pass filter. Consequently, the collected signals are predominantly concentrated within the middle and high-frequency range (F. Almeida et al., 2014a; X. Cui et al., 2024). Meanwhile, other experiments also reveal that leak noise is concentrated at approximately 1 kHz (Gao & Liu, 2017), and noleak (interference) noise is concentrated around 500 Hz (G. Guo et al., 2021b). The proposed model's decision-making process can capture most of the general leak scenarios for WDNs, thereby indicating its enhanced robustness.

## **5.4 Chapter Summary**

This chapter presents an explainable approach providing insights into the decision rationale of CNN-based models, facilitating model improvement, and offering novel perspectives for signal analysis. Several CNN-based models, including AlexNet, VGG,

and ResNet, were employed to evaluate the performance of these models in identifying leakages in water distribution networks (WDNs). Both AlexNet and VGG-19 exhibited superior performance on both the testing dataset and out-of-sample testing.

Meanwhile, the analysis of Grad-CAM results also demonstrated that VGG-19 and Grad-CAM's attention regions captured essential components with a higher concentration level, thereby explaining the superior performance of these models. This ability enables them to capture crucial time-frequency information while disregarding irrelevant components effectively. A comparative examination of the Grad-CAM results for leakage and non-leakage signals revealed that the model primarily relied on the frequency range of 750-1250 Hz to classify signals as leaks, while frequency components below 500 Hz were the primary focus for non-leakage signals. These insights further elucidate the model's decision-making process, highlighting the frequency ranges associated with different leak conditions.

## **CHAPTER 6 Time-series-based Deep Learning Model for Leak Detection**

### **6.1 Introduction**

This chapter employs the Transformer model, which utilizes self-attention mechanisms and positional encodings to comprehensively understand temporal relationships in time-series vibroacoustic signals (Vaswani et al., 2017). The objectives of this chapter can be summarized as follows:

- i). Develop the Time-Transformer model that combines advanced temporal processing and deep learning techniques to capture temporal patterns and dependencies in acoustic leak detection signals.
- ii). Conduct comprehensive experiments to validate the performance of the Time-Transformer approach in identifying leaks within the water distribution network.
- iii). Assess the feature extraction capability of the Time-Transformer approach and demonstrate its superiority with other DL approaches employed in acoustic leak detection.

### **6.2 Development of Transformer-based Leak detection Framework**

As mentioned in previous sections, the method was evaluated based on several leak and non-leak signals collected from real WDNs in Hong Kong. The signals were preprocessed using VMD to decompose and remove unwanted noise. Unlike traditional ML algorithms that rely on extracted features and some DL algorithms that use images, this study utilizes the original time series signals as direct inputs into the time series Transformer to extract pertinent information. For comparative purposes, 1D-CNN and LSTMs were also employed. Detailed discussions have been provided to analyze the leak detection and t-SNE visualization results obtained from the Time-Transformer,

1D-CNN, and CNN-LSTM models. The proposed Transformer-based model offers promising prospects for advancing the field of leak detection in WDNs and supports efficient water management.

### 6.2.1 Data Collection & Processing

As mentioned, the research team has conducted several experiments to collect samples from field experiments in Hong Kong. Meanwhile, the developed data augmentation algorithm, GAN, was proposed to collect the signals. Meanwhile, the ten-second duration audio is divided into one-second segments, treating each segment as a unit of samples. As depicted in Table 6.1, a total of 11300 samples were ultimately collected from the site, including 5650 leak samples and 5650 noleak samples. Additionally, out-of-sample validation was conducted, involving the collection of 670 leak samples and 890 noleak samples. These samples were independent of the training and testing datasets, enabling an evaluation of the model's robustness and effectiveness.

Table 6.1 The volume of datasets for model evaluation

	Training-80%	Testing-20%	Out-of-sample validation
Leak	3512	878	670
Noleak	4520	1130	890

Overall, the data format of collected signals in the context of acoustic leak detection in WDNs is typically time-series. The collected signals cater to the context of the Time-Transformer, which is designated to capture the pattern within the 1D format signals.

#### 6.2.1.1 Signal Denoising

One inherent characteristic of on-site leak detection is background noise in the collected signals. Therefore, to improve accuracy, most studies require signal denoising before

modeling (Diao et al., 2020; Tijani & Zayed, 2022). One powerful technique that has gained significant attention in recent years is VMD (Dragomiretskiy & Zosso, 2014a). Specifically, VMD assumed that a multi-component signal can be represented as a sum of  $K$ -modal components. Each component has a finite bandwidth, and the IMF has a central frequency  $\omega_{(t)}$ , the constraint is that the sum of all modes equals the input signal. This chapter employed correlation analysis to select the most relevant IMFs for VMD (Y. Huang et al., 2018). By calculating the correlation between each IMF and the original signal, IMFs that exceeded the correlation value of 0.3 are retained for signal reconstruction (B. Liu et al., 2021b), reducing background noise's influence.

### **6.2.2 Time-series Leak Detection Modeling**

This section describes the development process of Transformer-based leak detection models. The main structure of the employed model is inspired by Vaswani et al. (Vaswani et al., 2017) and Jin et al. (2022). In this study, specific modifications have been made to the input and output layers and the hyperparameters of the previously mentioned models to align with the data structure of one-dimensional vibroacoustic signals within the domain of vibroacoustic leak detection.

Table 6.2 depicts the parameters for the Transformer. The length of the input vector layer is changed to 4096. The number of output neurons in the last layer within the fully connected block is changed to two, responding to water pipelines' leak conditions (leak, noleak). The input audio samples are embedded into 128, capturing more nuanced temporal patterns crucial for accurate predictions and analysis of time-series data. The input data were then fed into six stacked Transformer blocks. Each block contains eight attention heads. Besides, the dimension of Queries and keys is set to 64, balancing the

model's capacity to capture complex relationships while maintaining computational efficiency. The embedding dimension of 256 indicates the size of the hidden layers within the MLP component of the model. A higher embedding dimension allows the MLP to capture complex patterns and relationships within the data. A dropout rate of 0.1 is employed, meaning that each unit has a 10% probability of being randomly dropped out during training. It helps prevent overfitting by promoting the learning of more robust representations and reducing the model's reliance on specific connections. The optimizer employed in this study is Adam, with a learning rate of  $3 \times 10^{-5}$ , and the training epoch is set to 500.

Table 6.2 Parameters for the Proposed Time-Transformer

Parameter	Value
Input dimension	4096*1
Output dimension	2 (leak, noleak)
Batch size	64
Epochs	500
Optimizer	Adam
Number of sequence $N_s$	16
Time-series embedding dimension	128
Position encoding format	One dimension
The number of stacked Transformer blocks $N$	6
The number of attention heads $h$	8
The dimension of queries and keys $d_k$	64
The embedding dimension of MLP	256
Dropout rate	0.1
Learning Rate	$3 \times 10^{-5}$

### **6.2.3 Model Performance Evaluation**

After leak detection modeling, evaluating the performance of the model is crucial to determine its effectiveness and reliability. Confusion matrices have been widely used to assess the performance of leak detection models (Shukla & Piratla, 2020a; T. Yu et al., 2023). Furthermore, visualization of the feature extraction layer using t-SNE provides valuable insights into the proposed model's capability for clustering samples under different leakage conditions (Y. Jin et al., 2022). Therefore, this study has adopted confusion matrices and t-SNE visualization results for evaluation.

Confusion matrix-based metrics are designed explicitly for classification models and assess the model's outputs to the true class labels of the collected samples. Based on the confusion matrix, accuracy, precision, recall, specificity, and F1-score can be deduced, measuring the model's capability to identify the different leak conditions correctly.

In this study, leak points are considered positive, while no-leak points are considered negative. Precision measures the model's ability to minimize false alarms, with a higher score indicating a lower likelihood of false alarms. A higher recall value suggests the model's effective detection of all leaks, leading to fewer potential leaks that are overlooked. Specificity measures the model's accuracy in distinguishing non-leak samples from leak samples, with a higher score indicating better proficiency. F1-score combines precision and recall, comprehensively evaluating the model's performance, particularly in imbalanced datasets (Jeni et al., 2013). A high F1-score signifies a balanced trade-off between precision and recall, reflecting the model's accuracy and comprehensiveness.

Feature extraction transforms the raw signals into a more compact and informative representation. To facilitate clear comparisons, the high-dimensional feature vectors have been visualized using t-SNE, reducing the feature vectors' dimensionality while preserving the underlying data structure (Van der Maaten & Hinton, 2008).

## 6.3 Leak Detection Evaluation and Discussion

### 6.3.1 Parametric Experiment

In machine learning, hyperparameters play a crucial role in the modeling process. The influence of hyperparameters in ML modeling is significant and can impact various aspects of the model. Therefore, this study employed parametric experiments to assess their influence on the leak detection capability of proposed Time-Transformer models.

Specifically, considering the hyperparameters mentioned in

Table 6.3, this study considers the hyperparameters:  $N_s$ ,  $dim$ ,  $MLP_{dim}$ ,  $d_k$ ,  $h$ ,  $N$ , and dropout rate.

$N_s$  is considered an essential parameter, which significantly influences the model performance. When the  $N_s$  is relatively small, the model performance decreases rapidly.

However, as  $N_s$  increases, it does not necessarily mean that the model performance will keep increasing indefinitely. When the  $N_s$  is 8, the performance is the worst. As the  $N_s$  increases, the performance reaches a peak when  $N_s$  is 32. Then, as  $N_s$  increases further, the model performance starts to decline again. The inverse relationship between the  $N_s$  and the length of the resulting vectors can explain this. Longer audio signals may cause the model to be unable to capture the local features, leading to decreased accuracy accurately. On the other hand, shorter vectors may lose global feature information; therefore, an appropriate  $N_s$  may be able to achieve optimal performance.

Table 6.3 Influence of the hyperparameters on Time-Transformer

$N_s$	dim	MLP <sub>dim</sub>	head	N	$d_k$	dropout	Test Acc	Val Acc
32	128	256	8	5	256	0.1	<b>99.93%</b>	<b>99.02%</b>
							99.63%	91.80%
							99.84%	96.34%
							99.88%	98.83%
							99.44%	98.54%
	16	32					98.19%	97.12%
	32	64					99.20%	97.45%
	64	128					99.66%	97.71%
	256	512					100.00%	98.19%
	512	1024					99.76%	96.94%
			1				99.40%	97.48%
			2				99.33%	97.41%
			4				99.89%	98.21%
			6				99.89%	98.83%
			10				99.90%	97.88%
				1			99.49%	94.29%
				2			99.93%	97.71%
				3			99.89%	97.75%
				4			99.75%	97.53%
				6			99.94%	98.15%
				7			99.83%	97.85%
					8		99.20%	96.88%
					16		99.41%	97.51%
					32		99.34%	97.14%
					64		99.64%	97.10%
					128		99.91%	98.49%
					512		99.53%	97.62%
						0.2	99.88%	97.98%
						0.3	99.64%	97.14%

Furthermore, dim and MLP<sub>dim</sub> were the embedding lengths of the time-series tokenizer and subsequent input lengths for the final classification component. The experiments follow the empirical principles from Jin et al. (Y. Jin et al., 2022), making MLP<sub>dim</sub> equal

to two times dim. It can be found that the combination of dim-256 and  $\text{MLP}_{\text{dim}}-512$  yields higher performance compared to other settings. The higher dim and  $\text{MLP}_{\text{dim}}$  contain more parameters and better complex pattern capture capability. However, the model performance decreases when raises dim and  $\text{MLP}_{\text{dim}}$  to 512 and 1024.

Similar patterns emerged in the experiments conducted on the hyperparameters: *head*,  $N$ ,  $d_k$ . It was observed that lower values of these parameters led to diminished accuracy, while the model's performance improved as the values of the model parameters increased. However, as the values escalated excessively, the model's complexity surged, resulting in a decline in model performance. Nevertheless, regardless of changes in the model parameters, the transformer exhibited a high degree of fitting on the training set. Apart from the  $N_s$ , the model's validation accuracy was relatively less influenced by alterations in other parameters. Consequently, the head was set to 8, the number of blocks fixed at 5,  $d_k$  designated as 256, and the dropout rate established at 0.1.

### **6.3.2 Model Identification Results**

In this section, the model's performance evaluation is conducted using confusion metrics. The results are presented to provide a comprehensive understanding of the model's strengths, limitations, and implications. As depicted in Section 6.2.1, the hold-out method is employed, allocating 80% of data for training purposes, and the remaining 20% is dedicated to testing. Besides, out-of-sample validation is a crucial step in the model development process to assess the robustness and generalizability of the models. In this approach, the researchers collected independent cases not used during the model training phase. Meanwhile, alternative DL models were also incorporated and compared,

including 1D-CNN and CNN-LSTM. The explicit model structures are presented in Figure 6.1.

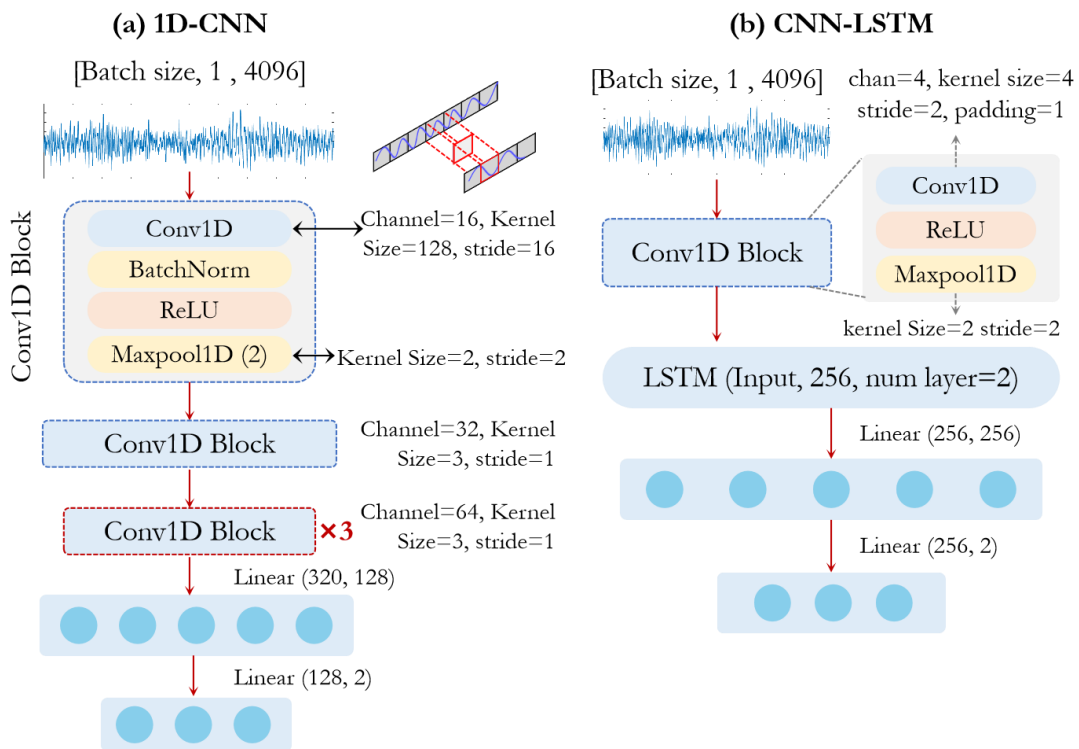


Figure 6.1 The structures of other time-series DL models

Figure 6.2 showcases the performance of models on testing datasets. Transformer achieved the highest accuracy, with 99.02%. In addition, the Transformer demonstrated a high level of specificity, scoring 98.95%, indicating the Transformer's ability to identify negative instances correctly. Regarding precision, Transformer still performed the best, with a precision score of 99.21%. This shows that when the Transformer classifies an instance as positive (leak), it is more likely to be a correct prediction. The transformer also achieved the highest recall of 99.10%, indicating its ability to identify actual leak samples correctly, with lower false alarm rate. Furthermore, the F1-score indicates the Transformer reached a balance on the leak and noleak recognition.

In the comparison, the Transformer maintains a lead over the 1D-CNN, while the CNN-LSTM demonstrates the poorest performance across all evaluated metrics. Notably, the 1D-CNN achieves a slightly lower overall leak detection accuracy of 97.06%, specificity at 97.31%, precision at 96.88%, recall at 96.78%, and an F1-score of 96.83%. Following this, CNN-LSTM achieves an accuracy of 85.48%, specificity of 89.04%, precision of 84.44%, recall of 80.65%, and an F1-score of 82.50%.

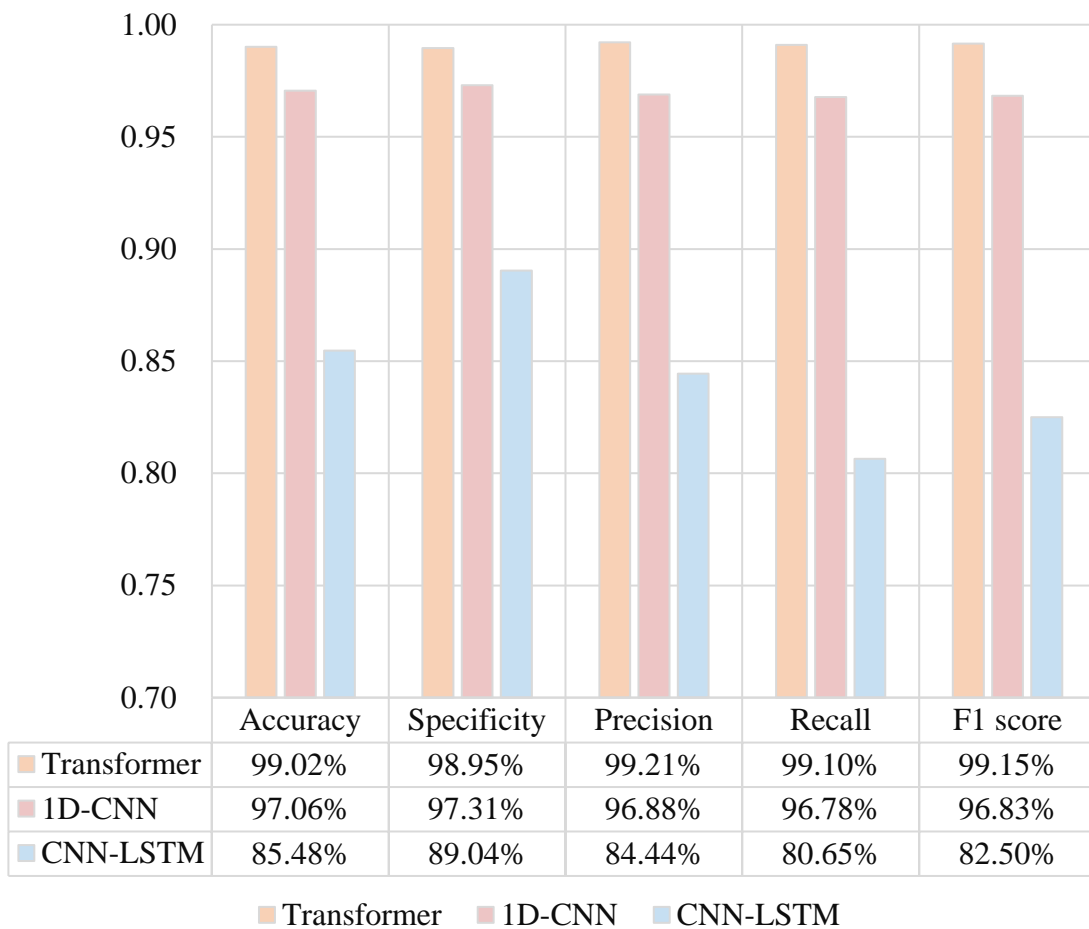


Figure 6.2 The performances of models on the testing dataset

However, the above results are specific to the testing dataset, and model performance may vary depending on the dataset's selection. Therefore, this study collects the out-of-sample datasets to evaluate the robustness and effectiveness of the model.

As illustrated in Figure 6.3, the models exhibited lower overall performance in out-of-sample validation. Transformer still achieves the highest on indicators excepting specificity, demonstrating superior capability in correctly identifying leaks and noleak samples. Similarly, the 1D-CNN slightly lagged behind the Transformer in all metrics but still exhibited reasonable classification performance, with an accuracy of 85.77%, specificity of 87.19%, and F1 score of 83.51%. However, the CNN-LSTM performed the worst in terms of accuracy (82.63%), precision (83.31%), and F1 score (78.64%) despite having the highest specificity (88.76%), indicating that its leak-free report is even more reliable.

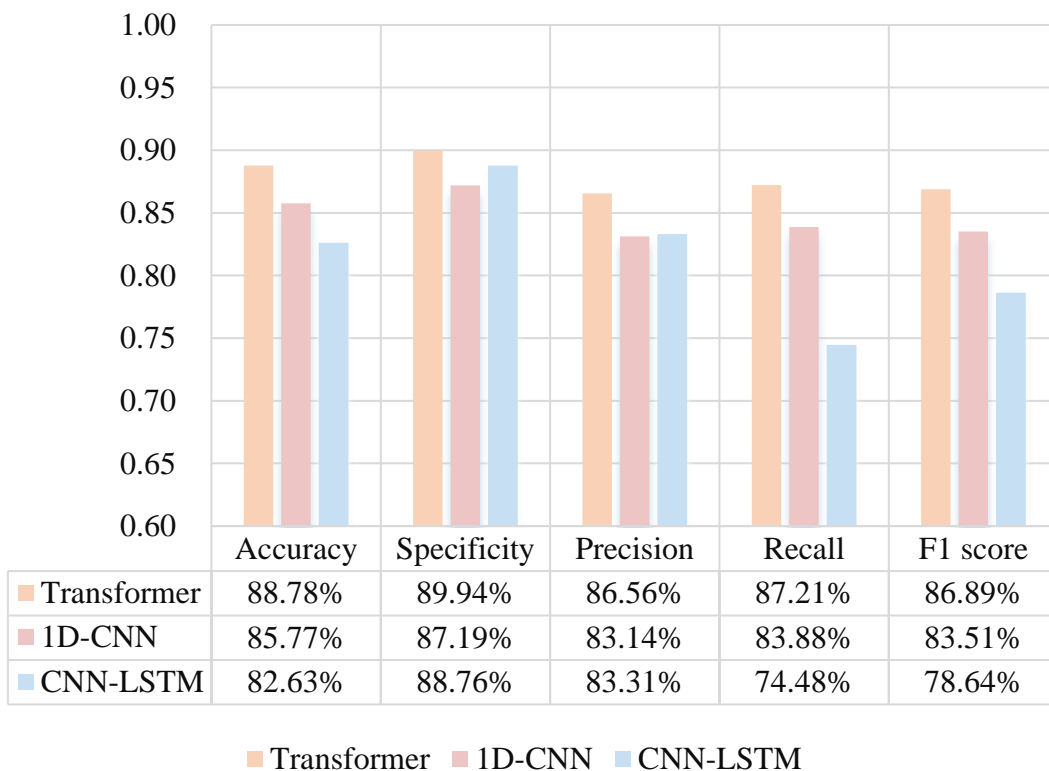


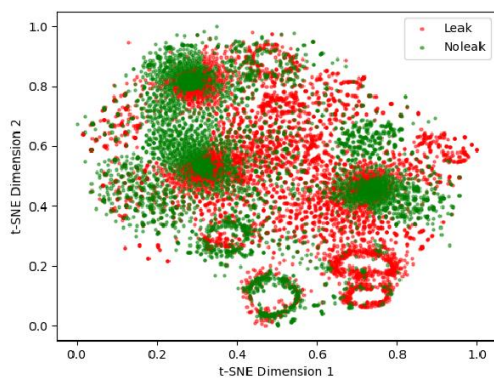
Figure 6.3 The performances of models on the out-of-sample validation dataset

Considering the testing dataset and out-of-sample validation, the comprehensive results indicate that Transformer excelled in both testing and out-of-sample validation, demonstrating high classification accuracy and generalization ability. 1D-CNN slightly

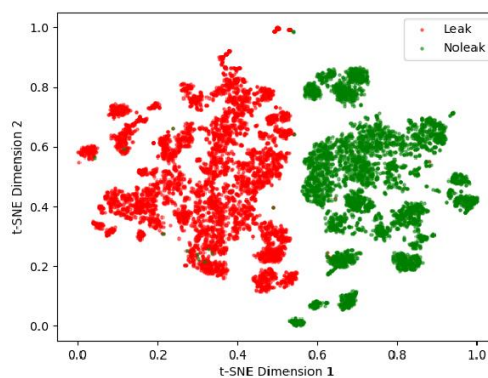
trailed behind Transformer, showing reasonable classification performance but lacking the same level of robustness. However, the CNN-LSTM performed the worst among the three, indicating its limited effectiveness in capturing the intricate patterns and dependencies required for accurate classification.

### 6.3.3 Feature Vectors Visualization

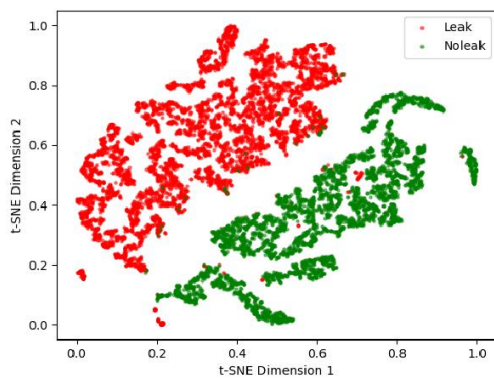
This section examines feature vector distribution within the embedding space using t-SNE to evaluate the model's generalization capacity and enhance the understanding of its operational behaviors. By analyzing the organization and clustering of feature vectors in the lower-dimensional space created by t-SNE, valuable insights are obtained regarding the model's potential to categorize acoustic samples across various fault conditions (Y. Jin et al., 2022; Pang et al., 2024).



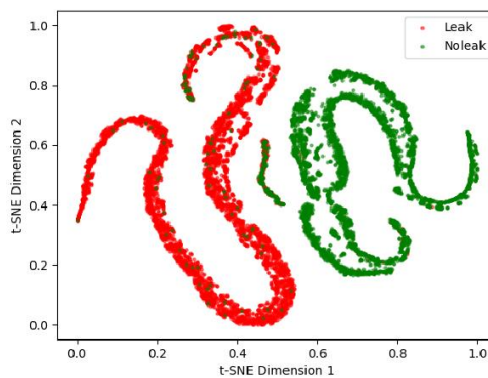
(a) Origin signals



(b) Transformer



(c) 1D-CNN



(d) CNN-LSTM

Figure 6.4 t-SNE results of the feature vectors extracted from DL models (a) Origin samples, (b) Transformer, (c) 1D-CNN, (d) CNN-LSTM

Figure 6.4 compares feature vectors derived from various DL models, Time-transformer, 1D-CNN, and CNN-LSTM. The t-SNE visualization in Figure 6.4 (a) illustrates the distribution of the signal samples in the dimensionally-reduced feature space before classification. The green data points represent the non-leakage samples, while the red points correspond to the leakage samples. Crucially, a substantial overlap is observed between the two classes. It indicates that original samples from the leak and noleak conditions shared some similar components, and it is difficult to differentiate the leakage conditions of unprocessed signals directly.

Figure 6.4 (b) and (c) visualize the extracted vector of the Transformer and 1D-CNN by projecting the vector into t-SNE space. Both the Transformer and 1D-CNN categorize the samples into two prominent clusters. This suggests that the input samples subjected to different leak conditions already exhibit distinguishing characteristics after processing by the Transformer and 1D-CNN models. This signifies the promising ability of these models to discriminate between leak and non-leak scenarios. However, it is noteworthy that the t-SNE results of the above two models also have a certain amount of outlier samples. As shown in Figure 6.4 (b), some non-leak samples are intermixed within the clustering of the leak samples. Additionally, Figure 6.4 (c) depicts that some non-leak samples are located at the edge of the leak clusters. Furthermore, the 1D-CNN model appears to have more confusing samples than the CNN-LSTM model.

Meanwhile, as illustrated in Figure 6.4 (d), the t-SNE visualization of CNN-LSTM illustrates relatively modest performance in distinguishing leak samples. A noticeable overlap is observed among the samples at the center of the t-SNE result, indicating that some samples may be complex for the CNN-LSTM model to distinguish. This suggests a potential limitation in the CNN-LSTM's ability to identify and classify leaks compared to the other models accurately.

In conclusion, the t-SNE visualization comprehensively compares the performances of Transformer, 1D-CNN, and CNN-LSTM models in leak detection within WDNs. The t-SNE results indicate that the 1D-CNN and Transformer models demonstrate distinguished sample clustering capabilities, while the cluster capability of the CNN-LSTM is comparatively lower. These findings align with the leak identification results, highlighting the superior performance of the Transformer, followed by 1D-CNN and CNN-LSTM.

#### **6.3.4 Discussion**

In this study, the structure of the Transformer model has been meticulously designed and compared with other time-series models, such as CNN-LSTM and 1D-CNN. Based on the above model performance results, it is evident that the Transformer exhibits superior capabilities in leak detection compared to CNN-LSTM and 1D-CNN.

The distinguishing factor that sets the Transformer model apart is its unique self-attention mechanism, enabling simultaneous processing of all positional information within a sequence (Ding et al., 2022). This characteristic enhances the model's ability to capture long-distance dependencies between data points, a critical aspect for identifying complex time-series patterns within leak detection scenarios. In contrast,

CNN-LSTM and 1D-CNN may struggle to capture extensive dependencies. When compared to the Transformer, CNN-LSTM's constrained structure may impede its effectiveness in handling prolonged time series dependencies (Isah et al., 2023), while 1D-CNN focuses on localized feature extraction, potentially lacking in capturing global information (Patel et al., 2018). The performance difference between CNN-LSTM and 1D-CNN can be attributed to the fact that the model efficiency of CNN-LSTM may not be consistent with the streamlined convolution process of 1D-CNN, and the complexity of CNN-LSTM may hinder its scalability and real-time applicability in scenarios where computational efficiency is a priority.

Based on the results above, the structure of the Transformer offers advantages, especially in addressing the challenges presented by leak detection tasks involving time-series data with extensive dependencies. This study has verified the proposed method's effectiveness, resilience, and generalizability for detecting water pipe leaks within the Hong Kong WDNs through model testing and out-of-sample validation. Given the inherent differences among WDNs, leak detection in each urban setting poses unique characteristics. This study proposed a Transformer-based leak detection framework that is not confined to the context of Hong Kong. It is a general framework and provides insights for other water departments that can employ this approach to collect representative acoustic samples, thereby formulating a leak detection strategy tailored to local water systems.

## **6.4 Chapter Summary**

This chapter presents a novel Transformer-based model for identifying water pipeline leaks. The model directly processes 1D vibroacoustic signals using the Transformer.

The effectiveness of the proposed model is demonstrated through experiments conducted on the signals collected from WDNs of Hong Kong.

The results demonstrate the capability of the Transformer-based model compared to other 1D DL models (ConvLSTM, 1D-CNN) through model performance comparison and evaluation of t-SNE feature vectors. Through the comparison of model accuracy, it was found that the Transformer exhibited higher leak detection accuracy in both testing (99.02%) and out-of-sample validation (88.78%) relative to the other models. The t-SNE visualizations further confirmed the exceptional pattern clustering ability of the Transformer model.

## **CHAPTER 7 Time-delay-based Leak Localization Model for WDNs**

### **7.1 Introduction**

This chapter proposed a time-delay-estimation deep learning localization method that achieves higher accuracy and robustness than basic cross-correlation. Specifically, signals are synthesized according to different physical scenarios and used for subsequent training. Res1D-CNN was developed to estimate the time delay of signal pair, enabling deducing the leak distance for leak localization. Their effectiveness at different SNRs was investigated to evaluate the performance of the developed models under the influence of background noise. Furthermore, field measurements were utilized as case studies to demonstrate the efficacy of the proposed method.

### **7.2 Framework for Time-Delay Estimation Deep Learning Model**

Figure 7.1 depicts the flowchart illustrating the workflow of the deep learning-based leak localization model. The framework comprises three phases: data preparation, leak localization model development, model experiments & discussion.

First, the empirical simulation model was proposed to generate training signals. A novel empirical model is introduced to analyze leak noise spectra, considering the attenuation of noise as it propagates along the pipes. The simulation model incorporates assumptions regarding the distribution of sensor distances, leak diameter, parameter values, and other relevant factors for generating the leak signal series. Based on the above principles, the signals can be synthesized and used for model training and validation.

Second, after establishing the leak localization modeling dataset, the residual CNN-based leak localization would be developed to estimate the time delay of two input signal pairs. Meanwhile, the leak distances can be deduced based on the estimated speed. Finally, once the initial model has been established, a series of model experiments will be conducted to evaluate the performance of the model capability from various perspectives. The sensitivity analysis is adopted to test the performances of the proposed model using signals with different signal-to-noise ratio (SNR) levels. Furthermore, to avoid overfitting problems, signals collected from field experiments would be used to validate the effectiveness of the leak localization model.

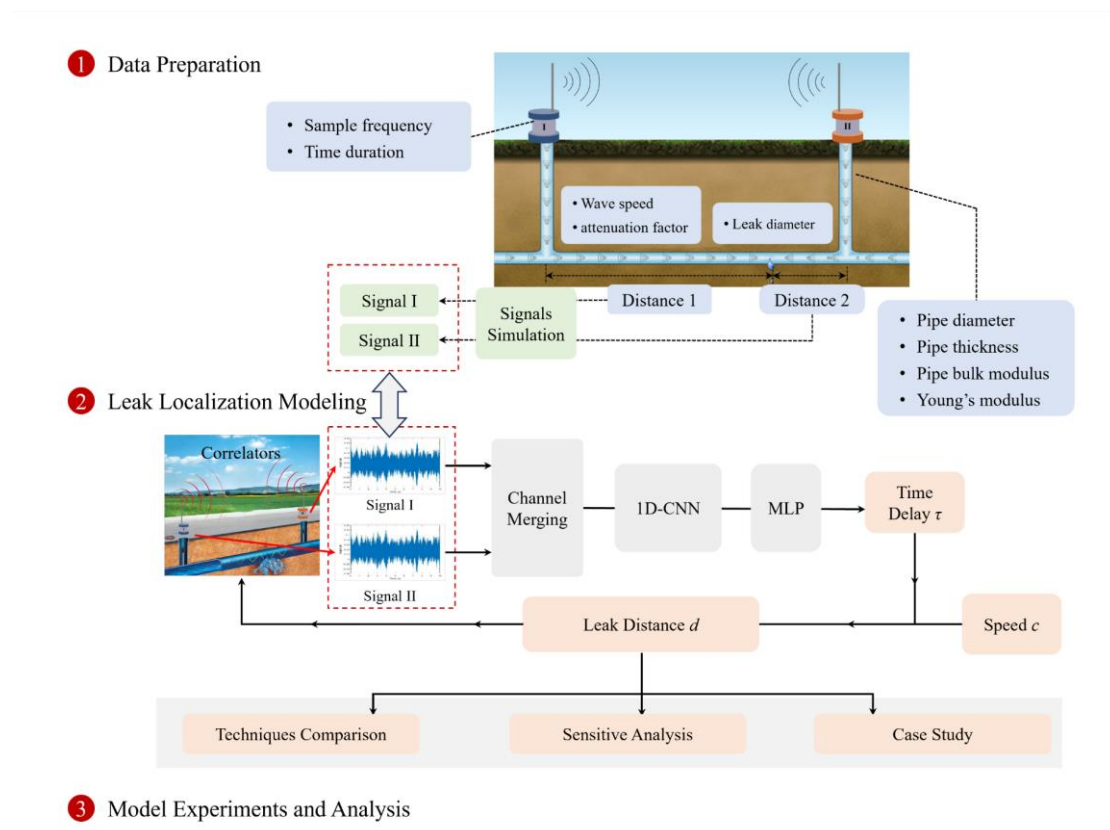


Figure 7.1 Overall framework for deep-learning-based leak localization modeling

### 7.2.1 Data Preparation

As mentioned earlier, the complex nature of pipelines and their surrounding environment, including pipe diameter, wall thickness, mechanical properties, operating pressure, and leak size, presents a significant challenge in accurately capturing all the information about leak signals through existing experimental investigations. Besides, conducting extensive field investigations to collect enough leak signals would also be time-consuming and costly, given the rarity of actual leaks. To address this challenge, this study aims to generate extensive leak signals based on a model established from experimental data.

Papastefanou et al. (2011; 2012) conducted experiments to identify the physical mechanisms of leak noise generation. The characteristics of leak noise spectra were examined with variations in the leak diameter and leak velocity. The experiments showed that cavitation is not responsible for leak noise generation and indicated that turbulence is the main mechanism. Based on the experimental results, an empirical model of the leak noise spectrum  $S_0(\omega)$  for water pipes was proposed in Equation (7.1).

$$S_0(\omega) = \begin{cases} \frac{A(V,d)}{\omega} & \omega \ll \omega_c \\ \frac{A(V,d)\omega_c^{n-1}}{\omega^n} & \omega_c < \omega < \infty \end{cases} \quad (7.1)$$

.where  $\omega_c = 2\pi St_{c,0}V/L$  is the critical frequency where the spectrum behavior changes,  $St_{c,0}$  is a diameter-independent Strouhal number, and  $L$  is a characteristic dimension associated with the turbulence generation in the leak hole. The parameter  $n$  is an integer that matches the slope of the leak spectrum and  $A(V,d)$  is a measure of the leak noise

source strength, which is a function of the hole diameter  $d$  and leak velocity  $V$ , and can be written as Equation (7.2) (Papastefanou, 21; Papastefanou et al., 2012).

$$A(V, d) = A_0 \left( d / d_{ref} \right)^3 \left( V / V_{ref} \right)^2 \left( D_{ref} / D \right)^2 \quad (7.2)$$

where  $A_0$  is a constant with appropriate dimensions, and  $d_{ref}$ ,  $D_{ref}$  and  $V_{ref}$  are reference values for the leak diameter, pipe diameter, and leak velocity, taken to be equal to 1 m, 1 m, and 1 m/s, respectively.

Equation (7.1) describes the behavior of the leak noise near the leak hole. However, since sensors are often deployed without knowing the exact location of the leak, the attenuation of leak noise during propagation along the pipes needs to be considered in the modeling. The propagation of waves along the pipes has been extensively investigated, and it has been demonstrated that the fluid-borne wave is the dominant wave responsible for the propagation of leak noise at low frequencies, with a wavenumber given by (Gao et al., 2004; J. Muggleton et al., 2002).

$$k^2 = k_f^2 \left( 1 + \frac{2Ba}{Eh + i\eta Eh} \right) \beta = \frac{1}{c_f} \left( \frac{\eta Ba / Eh}{1 + (2Ba / Eh)^{1/2}} \right) \quad (7.3)$$

$$c = c_f \left( 1 + \frac{2Ba}{Eh} \right)^{-1/2} \quad (7.4)$$

$$\beta = \frac{1}{c_f} \left( \frac{\eta Ba / Eh}{1 + (2Ba / Eh)^{1/2}} \right) \quad (7.5)$$

where  $k_f$  is the free-field fluid wavenumber,  $\eta$  is the loss factor of the pipe wall,  $a$  and  $h$  are the pipe radius and wall thickness, respectively,  $E$  is Young's modulus of the pipe wall material, and  $B$  is the fluid bulk modulus of elasticity.

The real part and imaginary part of the wavenumber give the wave speed and wave attenuation, respectively, combining Equations (7.1) and (7.5), the spectrum of leak

noise at given sensor distances,  $d_1$  and  $d_2$ , from the leak point can be obtained. This information can then be used to generate the leak signal series in the time domain using an inverse Fourier transform with random phases (Kasdin, 1995).

In this study, the distances  $d_1$  and  $d_2$  between the sensor and the leak point are assumed to follow a uniform distribution, with a maximum value of 200 m, considering the general deployment of sensors in water pipes. The leak diameter  $d$  is also assumed to follow a uniform distribution, with low and high values of 0.001 m and 0.01 m, respectively. The parameter  $n$  is assumed to follow a normal distribution with a mean of 8, and the leak velocity  $V$  is assumed to follow a normal distribution with a mean of 8 m/s. The diameter and wall thickness of the water pipes are generated based on practical experience and relevant codes. The sampling frequency is set to 4800 Hz, and the time duration for each signal is 10 seconds. We would simultaneously generate two signals from two different sensor locations for data preparation. Then, two signals would be combined into a signal pair (representing one sample) for subsequent training.

### **7.2.2 Leak Localization Model Development**

This section depicts an enhanced version of the CNN-based leak localization model by integrating residual blocks and 1D convolutional neural networks (Res1D-CNN). 1D-CNN is a specialized neural network that extracts meaningful features from one-dimensional data, such as time series or sequential data (Kiranyaz et al., 2021). It utilizes convolutional layers to capture local patterns and interactions in the input data, pooling layers to downsample and extract salient features, and fully connected layers for high-level feature extraction and prediction. Thus, 1D CNNs have found applications in various fields, including fault diagnosis (Eren et al., 2019), audio

processing (Nainan & Kulkarni, 2021), and indoor localization (X. Song et al., 2019) due to their ability to automatically learn hierarchical representations and model complex patterns in sequential data. However, the vanishing gradient problem becomes challenging as the network depth increases, hindering the learning process from long sequences.

To address this limitation, Res1D-CNN was introduced, incorporating residual connections within the convolutional layers. The residual connections allow direct information propagation from one layer to deeper layers, facilitating learning residual representations (He et al., 2016).

Figure 7.2 presents the main structure of the proposed Res1D-CNN leak localization model. The signal pairs from two sensors along the pipelines are initially fed into the model. The two signals are treated as one-dimensional tensors and placed in the two channels of the input. Subsequently, the information extraction is conducted through the convolution blocks. The Conv1d block first maps two signals to the subspace and employs kernel-based operations to extract acoustic information. Then, batch normalization is applied to enhance the network's stability and performance. After that, the ReLU activation function is employed to introduce non-linearity to the model. Additionally, the maximum pooling layer is utilized to reduce redundant information and compress the dimensionality of the feature vectors.

The residual block can be implemented in two main variants: the basic and the bottleneck blocks. In this study, due to limited graphic memory and the input signal length of 48000, the basic block was chosen as the primary building block for modeling. The basic block typically comprises two convolutional blocks for feature extraction,

and Batchnorm and ReLU are employed for their well-known benefits. The residual connections within the block facilitate the direct flow of information, connecting the input to the output of the block, enabling effective gradient propagation and improved learning of residual mappings.

After extracting the blocks above, the final extracted tensor is fed into Multi-Layer Perceptron. It is a type of neural network consisting of multiple layers of interconnected nodes, also known as neurons, and is designed to process and transform the input data non-linearly (Rumelhart et al., 1986). In the final block, the model would suppress the dense tensor into one node to output two input signals' time delay (unit: millisecond (ms)).

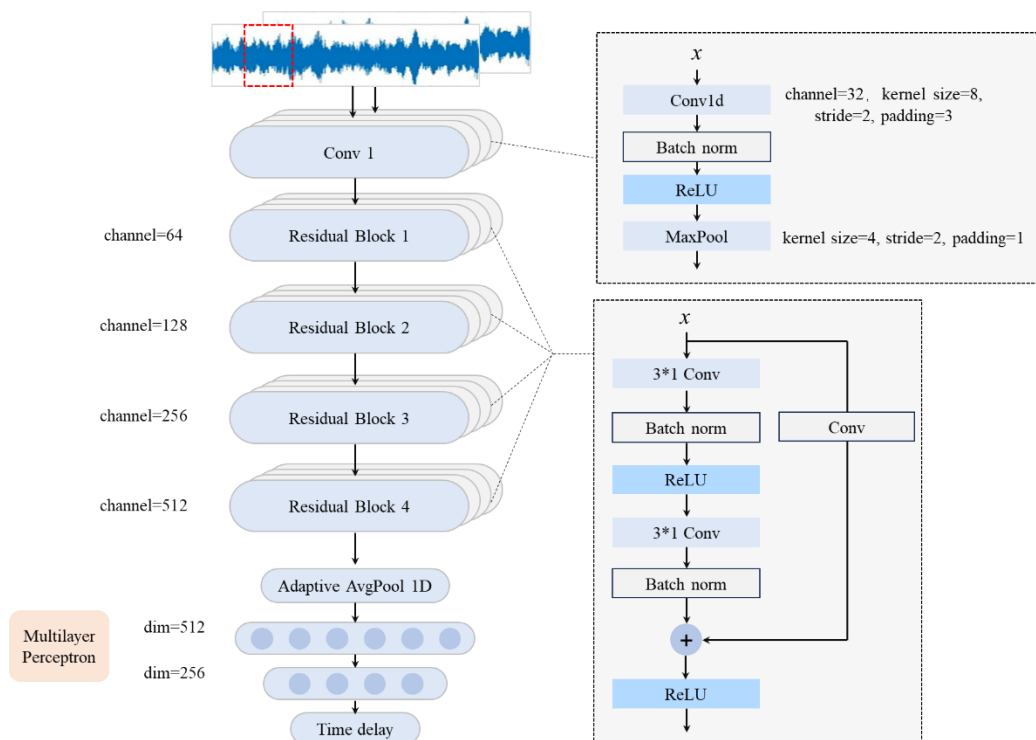


Figure 7.2 The structure of the Res1D-CNN leak localization model

Following the modeling process, the model is evaluated from different perspectives.

The training dataset is carefully regulated following the experimental objectives. The

loss function utilized is Huber loss, commonly used in regression. Compared to the Mean Squared Error (MSE), Huber loss is a mathematical function used in robust regression to strike a balance between sensitivity to outliers and robustness (Huber, 1992). The training is conducted for 1000 epochs, using the Adam optimizer with a learning rate of  $1e-4$ .

### 7.2.3 Model Experiments

Figure 7.3 outlines the method used for the model experiment, including the techniques comparison, sensitivity analysis under different SNRs, and case study validation.

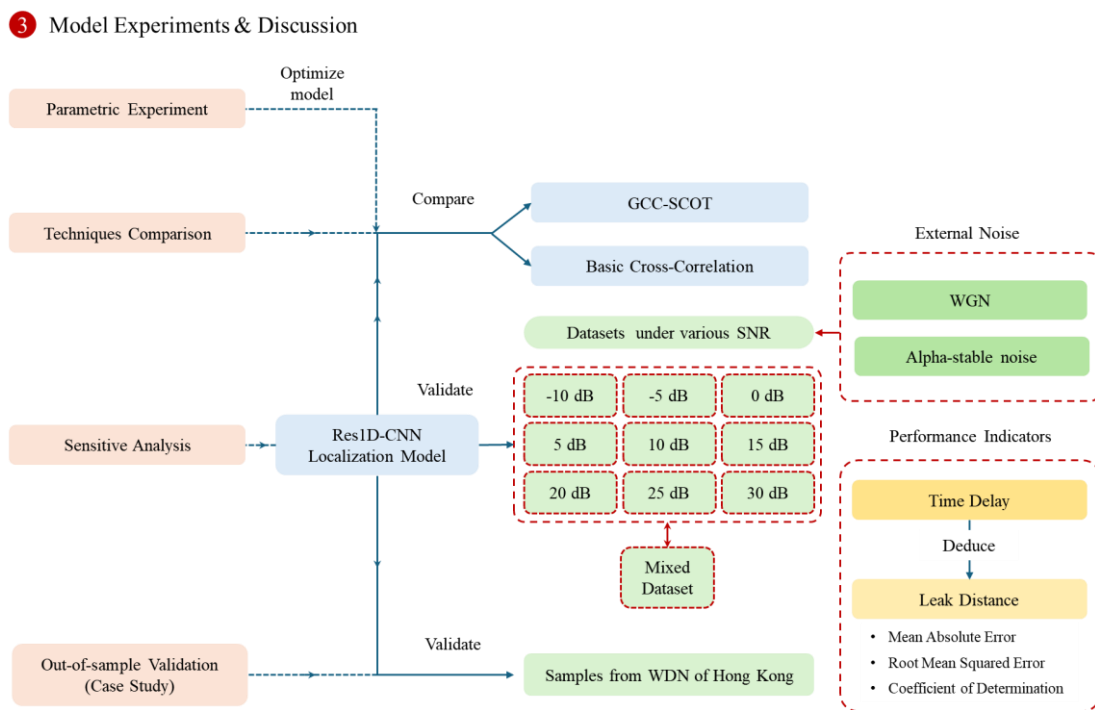


Figure 7.3 Framework for model experiments and discussion.

#### i. Model parametric experiments

The model parametric experiments focus on assessing the influence of model structure depth on the model's ability to estimate time delays. The experiments used signals at -10 dB SNR white Gaussian noise with 1,000 testing samples to identify the optimal structure that maximises accuracy and robustness. The training was carried out over 100

epochs. The study aims to improve the model's generalization ability and ensure consistent performance across diverse scenarios by fine-tuning these parameters.

## ii. Comparison of techniques

The proposed method was compared with the BCC and GCC-SCOT for technique comparison.

The BCC is a widely acknowledged signal-processing algorithm that quantifies the similarity between two signals or sequences as a function of the displacement or lags between them. Specifically, after obtaining two continuous time signals  $x(t)$  and  $y(t)$ , BCC requires selecting an appropriate range of lag values  $\tau$ . Shift the signal  $y(t)$  by a lag of  $\tau$  to obtain  $y(t+\tau)$ . The expected value can be calculated through

$$R_{xy}(\tau) = E[x(t) * y(t + \tau)] \quad (7.6)$$

where  $R_{xy}(\tau)$  is the cross-correlation function at lag  $\tau$ , and  $E$  denotes the expected value (or ensemble average) operation.

For all active lag values, repeat the calculation to obtain the complete cross-correlation function  $R_{xy}(\tau)$ . Then, BCC allows for estimating the time delay by identifying the peak value of the correlation function between the two signals. The performance of the models was evaluated through the deduction of time delay and potential leak distance and the quantification of model performance using indicators including mean absolute error (MAE), root mean squared error (RMSE), and coefficient of determination ( $R^2$ ).

Moreover, GCC-SCOT was introduced (Knapp & Carter, 1976) as it has the potential to demonstrate superior performance in real-world applications and is well-suited for leak localization (Gao et al., 2006). The GCC function is depicted as

$$R_{xy}^g(\tau) = F^{-1}\{\Psi_S(\omega)S_{xy}\} = \frac{1}{2\pi} \int_{-\infty}^{+\infty} \Psi_g(\omega) S_{xy}(\omega) e^{i\omega\tau} d\omega \quad (7.7)$$

where  $F^{-1}\{\}$  is the inverse Fourier transform,  $\Psi_g(\omega)$  is the frequency weighting function, and  $S_{xy}(\omega)$  is the cross-spectral density between two signals  $x$  and signal  $y$ .

For the SCOT estimator, the frequency weighting function of GCC-SCOT can be depicted as Equations (7.8) and (7.9)

$$\Psi_S(\omega) = \frac{\gamma_{xy}(\omega)}{|S_{xy}(\omega)|} \quad (7.8)$$

$$R_{xy}(\omega) = F^{-1}\{\Psi_S(\omega)S_{xy}\} \quad (7.9)$$

where  $\gamma_{xy}(\omega)$  is the coherence function.

Regarding time delay, the Res1D-CNN and BCC could directly output the time delay as described previously. For leak distance, after obtaining the time delay, the potential leak distance could be deduced by considering the wave speed and time delay, as illustrated by:

$$d_1 = \frac{d - c T_1}{2} \quad (7.10)$$

Where  $c$  is the propagation speed of the leakage noise,  $d$  is the total distance between the sensors, and  $T_1$  is the time delay, which is the time difference between the leakage signal generated and the signal received by the sensor.

Leveraging the values of  $c$  and  $d$ , the model can predict the distance and localize the leak point.

iii. Sensitive analysis

After confirming the efficacy of the model in evaluating the time delay of signal pairs, sensitivity analysis was conducted to further validate the effectiveness and robustness of the model in handling signals under varying SNRs of noise. This study adopted the white Gaussian noise (WGN) and Alpha-stable noise for further analysis. WGN is also referred to as normally distributed noise. The WGN simulates the diverse random interferences and measurement errors in actual measurement signals. Therefore, it has been frequently used to simulate practical noise in leak-related experiments (G. Guo et al., 2021b; W. Wang & Gao, 2023).

Alpha-stable noise refers to noise that is characterized by heavy tails (Samorodnitsky et al., 1996). The alpha-stable noise has a stability parameter ( $\alpha$ ) that determines the tail behavior of the distribution. When  $\alpha$  equals 2, the distribution is Gaussian. Besides, the parameter skewness ( $\beta$ ) controls the asymmetry of the distribution. Alpha-stable noise is extensively used to model phenomena characterized by simulating extreme events, for example, impulsive noise in signal processing (W. Cui et al., 2024; Nguyen et al., 2020). In this study, the  $\alpha$  is set as 1.2,  $\beta$  is set as 0.

For sensitivity analysis, related leak localization studies generally consider the noise ranging from -10 dB to 30 dB (Lu et al., 2016; F. Wang et al., 2017; X. Wang & Ghidaoui, 2018). The datasets were established under 9 SNR scenarios (-10 dB, -5 dB, 0 dB, 5 dB, 10 dB, 15 dB, 20 dB, 25 dB, 30 dB). The model was then solely trained with different datasets to assess its resilience to external noise. Furthermore, a comprehensive model based on the mixed dataset incorporating all 9 datasets was established to enhance the model's robustness and effectiveness.

#### iv. Out-of-sample validation

The out-of-sample signals were collected from field experiments to verify the model's capacity to analyze complex situations in the domain of leak localization. Specifically, the acoustic signals were obtained from WDN of Hong Kong using the correlators, representing actual operating conditions and system dynamics. The comprehensive model developed was adopted to analyze the field signals, predict the related results, and evaluate the accuracy and reliability. The case study aims to gain insight into the model's performance in a real-world scenario and validate its applicability in the industrial setting.

### **7.3 Leak Localization Experiments & Evaluation**

#### **7.3.1 Model Parametric Experiments**

In machine learning, hyperparameters play a crucial role in the modeling process. Thus, this study employed parametric experiments to assess their influence on the leak localization capability of Res1D-CNN. Specifically, this study considers the number of residual blocks ( $N_{res}$ ), activation function ( $\sigma$ ), and selection of normalization (Norm) for experiments and considers MAE and RMSE as the leading indicators.

Table 7.1 depicts the influence of hyperparameters on the Res1D-CNN. The experiment reveals that the number of residual layers significantly affects the performance of the Res1D-CNN; simply increasing the depth of the model does not guarantee improvement. Additionally, the selection of normalization techniques also significantly impacts model performance. Batch normalization aims to normalize the values in the feature domain of inputs within a batch, but it may lead to the loss of local time features. In contrast, layer normalization focuses on normalizing the values within a sample, making it more

suitable for the data processing in this study. Therefore, this study employed four residual blocks, layer normalization, and ReLU for subsequent analysis.

Table 7.1 Influence of the hyperparameters on Res1D-CNN

$\sigma$	Norm	$N_{res}$	MAE	RMSE
<b>ReLU</b>	<b>Layer norm</b>	<b>4</b>	<b>5.4433</b>	<b>7.3138</b>
Leaky-ReLU			5.7765	7.1569
	Batch norm		8.4231	11.5192
		5	7.1542	9.6332
		3	9.7303	12.3280
		2	11.2295	14.5786

### 7.3.2 Comparison of Techniques

The effectiveness of the proposed model is evaluated using the simulated dataset that excludes external noise, with 2000 signal pairs for training and 200 signal pairs for testing. The testing experiment was repeated 50 times to reduce randomness, generating new data each time. To establish a comparative baseline, the performance of Res1D-CNN is juxtaposed with that of the BCC and GCC-SCOT, widely acknowledged leak localization techniques (Gao et al., 2006).

Figure 7.4 displays a scatter plot comparing the performance of the Res1D-CNN (blue nodes) against BCC (red nodes) and GCC-SCOT (yellow nodes). The x-axis represents the predicted distance, while the y-axis represents the actual distance. The marginal histogram depicts the distribution of predicted values for the three methods and label values. The figure shows that the Res1D-CNN, BCC, and GCC-SCOT scatters are aligned with the diagonal line. The distribution of predicted values is similar to that of label distribution. The visualization results indicate that the three methods accurately

evaluate the time delay between the two signals on the clean dataset. Consistent with this, the  $R^2$  results show that all three methods have an  $R^2$  greater than 0.99, with GCC-SCOT (0.99989) outperforming the other methods, followed by BCC (0.99971) and Res1D-CNN (0.99890).

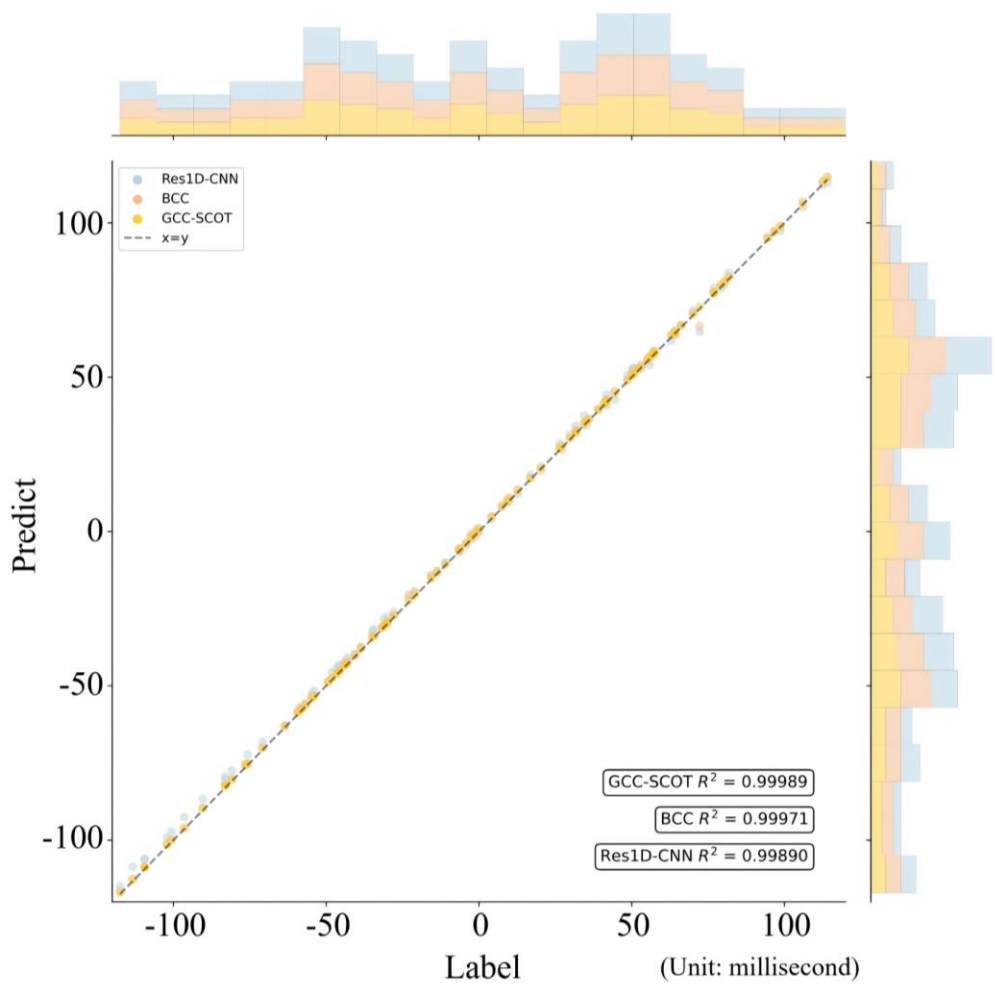


Figure 7.4 The scatter plot of the time-delay result based on clean data

Figure 7.5 presents the distribution of the MAE for the Res1D-CNN, BCC, and GCC-SCOT methods based on 50 independent testing experiments. The results indicate that GCC-SCOT produces clustered predictions, as evidenced by the narrow distribution and the center located at lower MAE values. This suggests that GCC-SCOT demonstrates a higher degree of precision in estimating time delays, likely contributing

to its superior performance in leak localization. The MAE distributions for BCC and Res1D-CNN exhibit a wider spread, indicating greater variability in their predictions. The central value of BCC's MAE distribution remains lower than that of Res1D-CNN, implying that BCC provides more accurate results than Res1D-CNN.

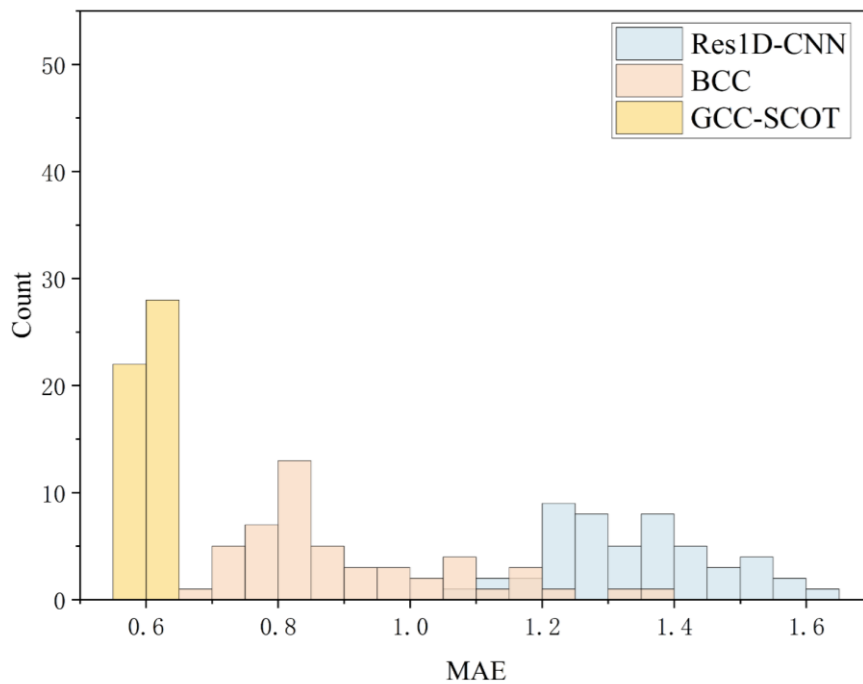


Figure 7.5 The distribution of MAE of time-delay results

Besides, Figure 7.6 illustrates the distribution of the RMSE for all three methods. Consistent with the MAE distribution results, the center of distribution indicates that GCC-SCOT outperforms both BCC and Res1D-CNN. Although the central values for BCC and GCC-SCOT are close, the RMSE for BCC exhibits greater dispersion. Additionally, Res1D-CNN consistently demonstrates lower RMSE values compared to GCC-SCOT.

These observations highlight that GCC-SCOT demonstrates the highest accuracy and consistency with clean signal pairs, followed by BCC. Although slightly less precise,

BCC achieves better overall accuracy than Res1D-CNN. However, Res1D-CNN has the potential to surpass both BCC and GCC-SCOT in more complex scenarios and under low SNR conditions (Y. Chen et al., 2019), owing to its ability to extract intricate pattern features. Consequently, further evaluation and analysis of Res1D-CNN's performance are necessary to fully understand its potential and limitations across a broader range of application contexts.

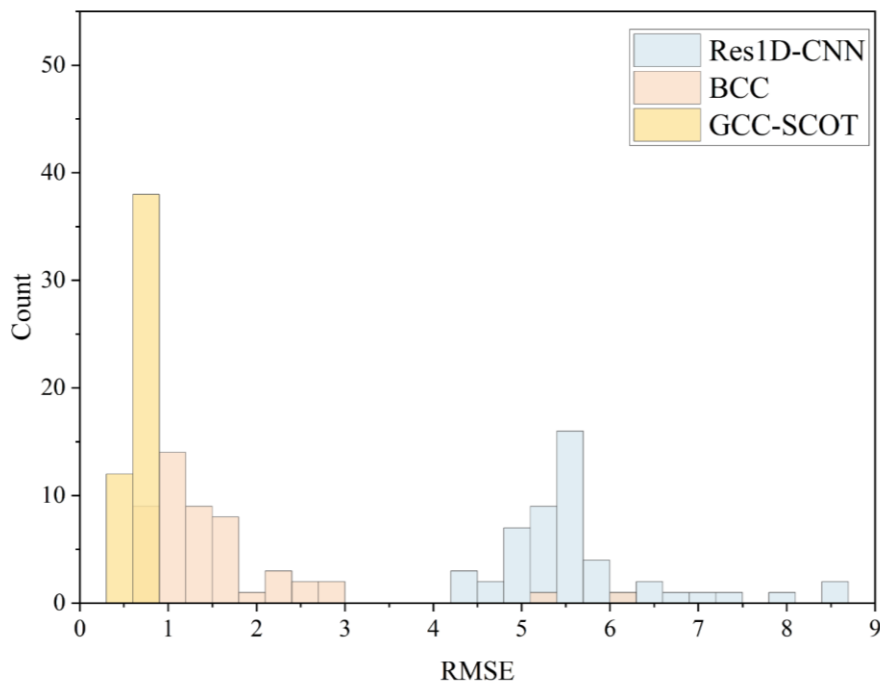


Figure 7.6 The distribution of RMSE of time-delay results

### 7.3.3 Sensitivity Analysis

This section evaluates the proposed model based on the datasets under different SNRs. For each dataset under SNR, 2000 signal pairs (samples) were collected for training and 200 samples for testing, evaluating the effectiveness of the model restricted to external WGN and Alpha-stable noise. Furthermore, the Res1D-CNN was validated through a comprehensive mixed dataset, consisting of 1000 samples of nine SNR scenarios (total

of 9000 signal pairs) for training and 100 samples of each SNR (total of 900 signal pairs) for testing. Similarly, the testing process was repeated 50 times, with a new dataset generated each time.

i). White Gaussian Noise

First, GCC-SCOT, BCC, and Res1D-CNN were compared under WGN. Figure 7.7 shows the scatter of time-delay results under different SNRs. The figure highlights five key scenarios (-10 dB, 0 dB, 10 dB, 20 dB, 30 dB) to demonstrate the observed significant changes effectively. Overall, the figure shows that all three methods were influenced by external noise, with sample distributions observed at -10 dB and 0 dB. As the SNR increased, the performances of the three methods showed varying degrees of improvement. Specifically, BCC and GCC-SCOT displayed a more dispersed sample distribution at 10 dB. When the SNR reached 0 dB, BCC demonstrated significant improvement. Furthermore, between 10 dB and 30 dB, BCC and GCC-SCOT converged towards the centerline, whereas Res1D-CNN still exhibited some outliers outside the centerline. The performance of the GCC-SCOT and BCC techniques is notably affected by scenarios with -10 dB WGN. Nevertheless, this influence of WGN is relatively constrained. As the SNR increases, there is a marked improvement in the performance of these techniques.

Figure 7.8 depicts the performance metrics of GCC-SCOT, BCC, and Res1D-CNN. Following the scatter results, the metrics indicate that Res1D-CNN outperforms the other methods at the -10 dB and -5 dB scenarios. The performance of Res1D-CNN shows fluctuating improvements as the SNR increases. Meanwhile, BCC and GCC-SCOT achieve rapid and substantial improvements, surpassing Res1D-CNN after 0 dB.

Although all methods plateau in high SNRs, the GCC-SCOT and BCC metrics remain higher than those of Res1D-CNN regarding MAE, RMSE, and  $R^2$ .

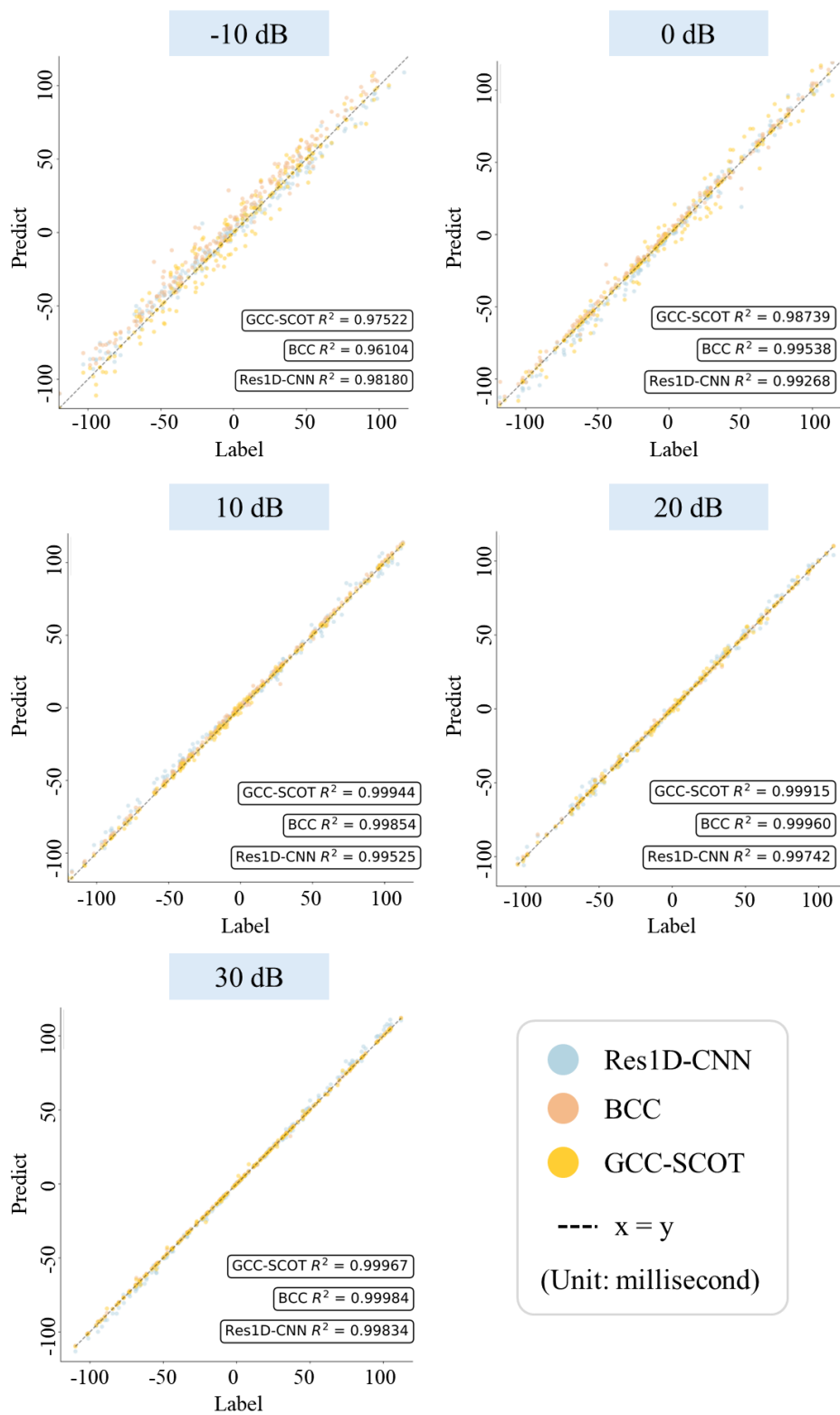


Figure 7.7 The scatter plot of the time-delay results under WGN

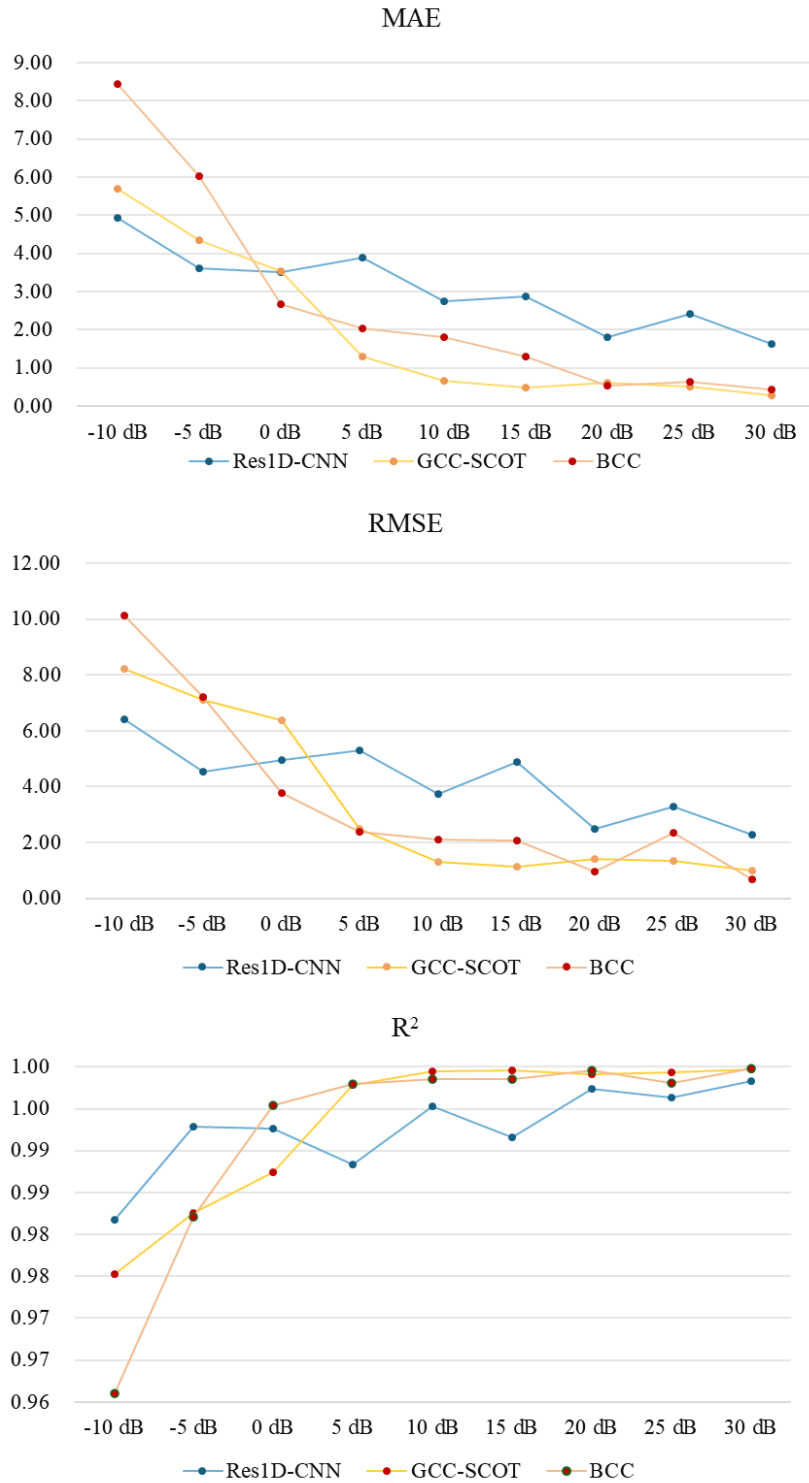


Figure 7.8 The performance metrics of time-delay results under WGN

Furthermore, comprehensive evaluations have been conducted based on the samples from 9 SNR scenarios under WGN to assess the effectiveness and robustness of Res1D-CNN further. Figure 7.9 depicts the time-delay results based on the mixed dataset under

WGN. The samples associated with GCC-SCOT BCC share similar distributions that are more dispersed. The proposed method focuses on the center line, with fewer outliers. The  $R^2$  also demonstrated the consistent point that the Res1D-CNN (0.99387) has superior robustness than GCC-SCOT (0.96238) and BCC (0.95999).

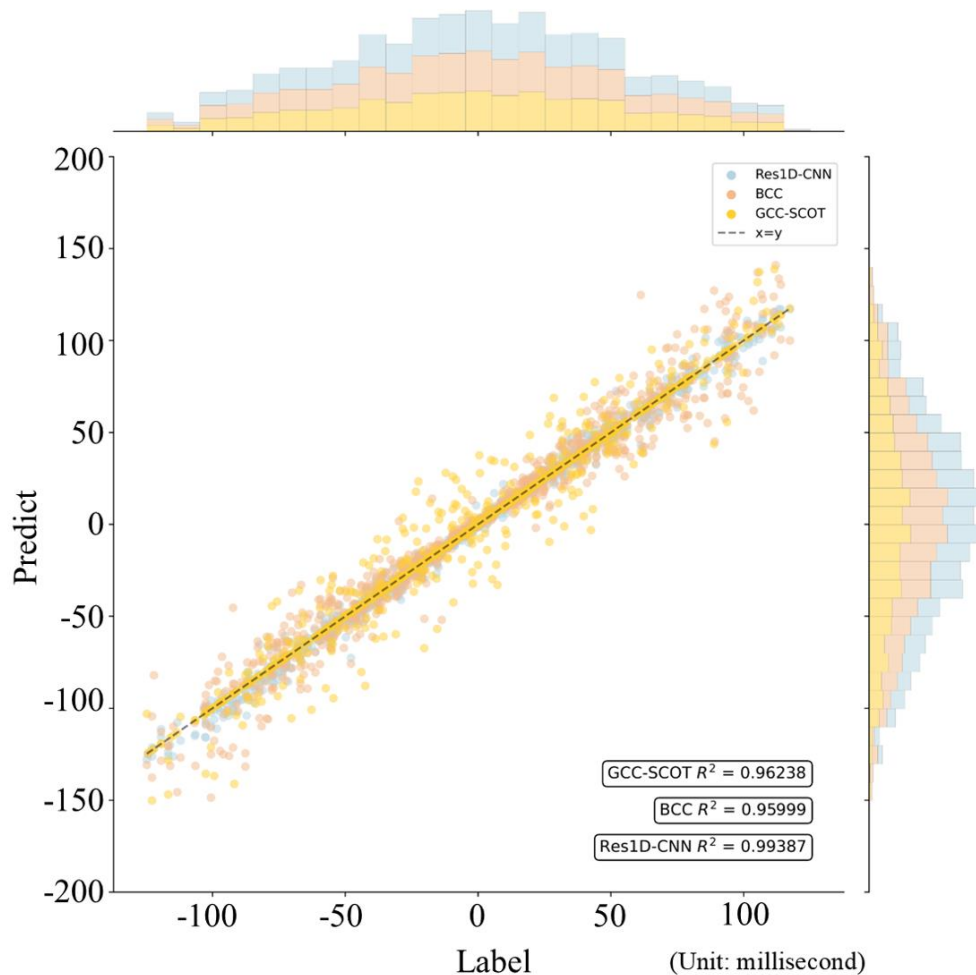


Figure 7.9 The scatter plot of time-delay results for mixed datasets under WGN

Figure 7.10 illustrates the distribution of RMSE and MAE for the mixed dataset under white Gaussian noise (WGN). The results indicate that Res1D-CNN outperforms the other methods, achieving the most accurate time delay estimations. It is followed by GCC-SCOT and BCC, which show slightly lower accuracy. The close RMSE values for GCC-SCOT and BCC suggest their predictions exhibit similar variability in

estimating time delay. It indicates that Res1D-CNN demonstrates a clear advantage, particularly in handling the WGN environment, while GCC-SCOT and BCC share close time delay estimation inability in WGN.

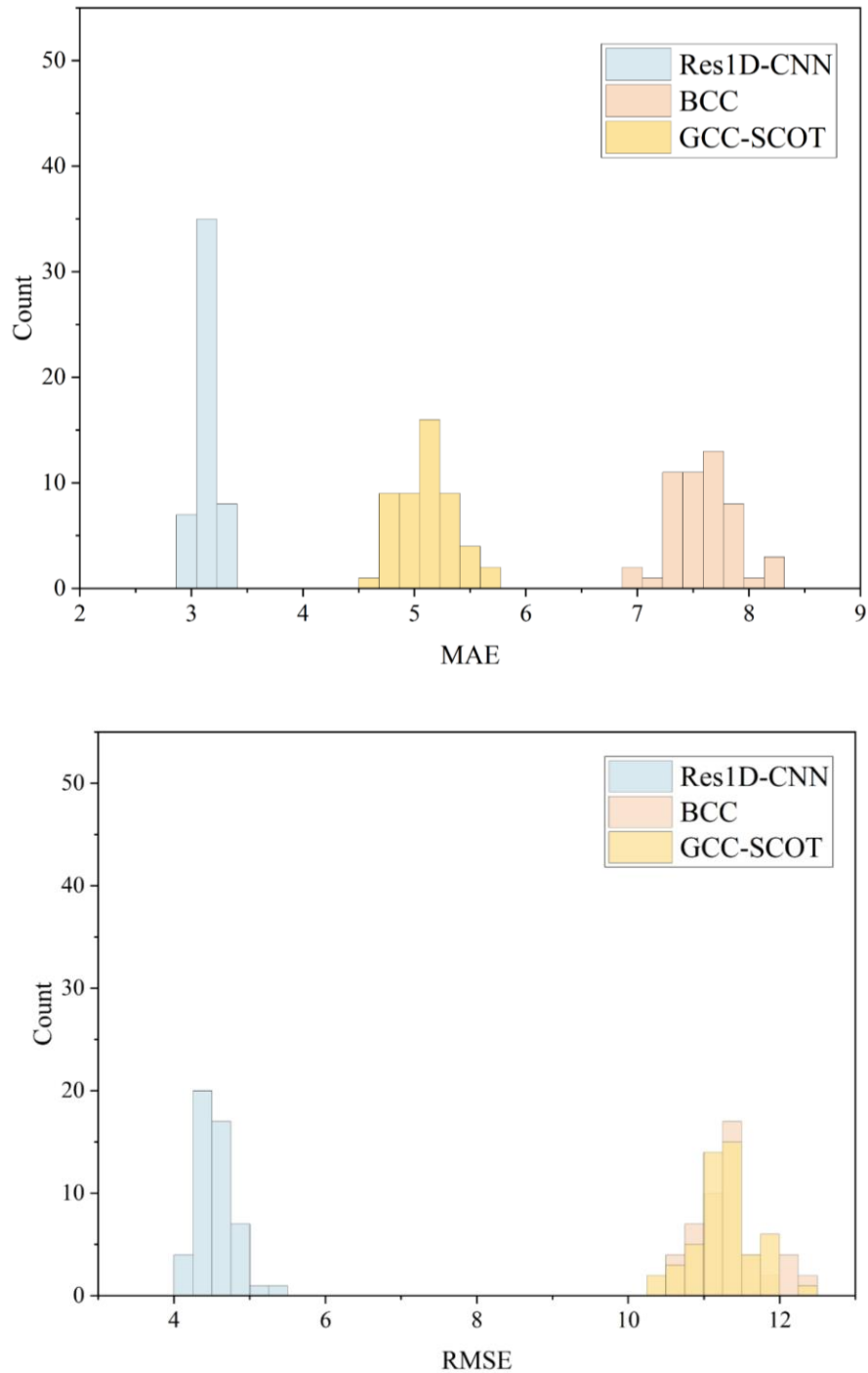


Figure 7.10 The distribution of RMSE and MAE based on the mixed dataset under WGN

Furthermore, Res1D-CNN, GCC-SCOT, and BCC were also evaluated by comparing the leak distance deduced by considering wave speed and time delay in Figure 7.11. Res1D-CNN ( $\pm 2.2701$  m) demonstrates significantly lower absolute distance bias compared to the GCC-SCOT ( $\pm 3.3975$  m) and BCC ( $\pm 5.6637$  m). Meanwhile, the predicted distance of the Res1D-CNN also demonstrated a lower RMSE, indicating it has fewer instances of large outliers when localizing the leak points. Consistent with previous points, the Res1D-CNN model has a higher  $R^2$  of 0.997, while the GCC-SCOT and BCC have lower  $R^2$ , with 0.9837 and 0.9795. It indicates that both modeling approaches enable highly accurate leak localization performance.

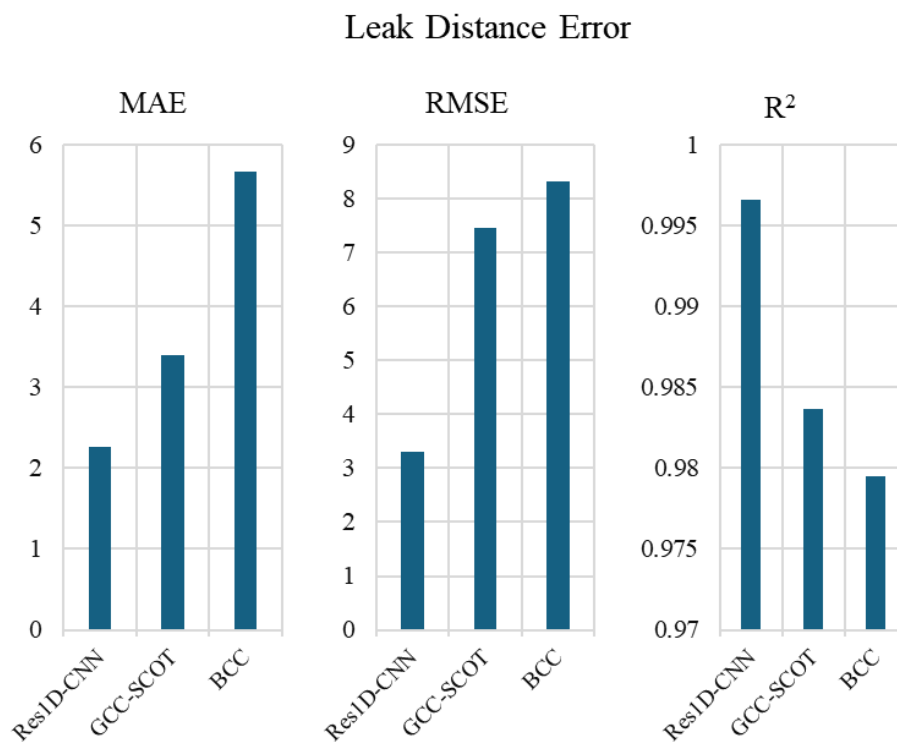


Figure 7.11 The leak distance error under WGN

Based on sensitivity analysis, GCC-SCOT and BCC outperform the Res1D-CNN in high SNR scenarios (ranging from 0 dB to 30 dB). However, Res1D-CNN demonstrates

robust noise leak localization capabilities, especially in low SNR WGN environments and complex scenarios.

ii). Alpha-stable noise

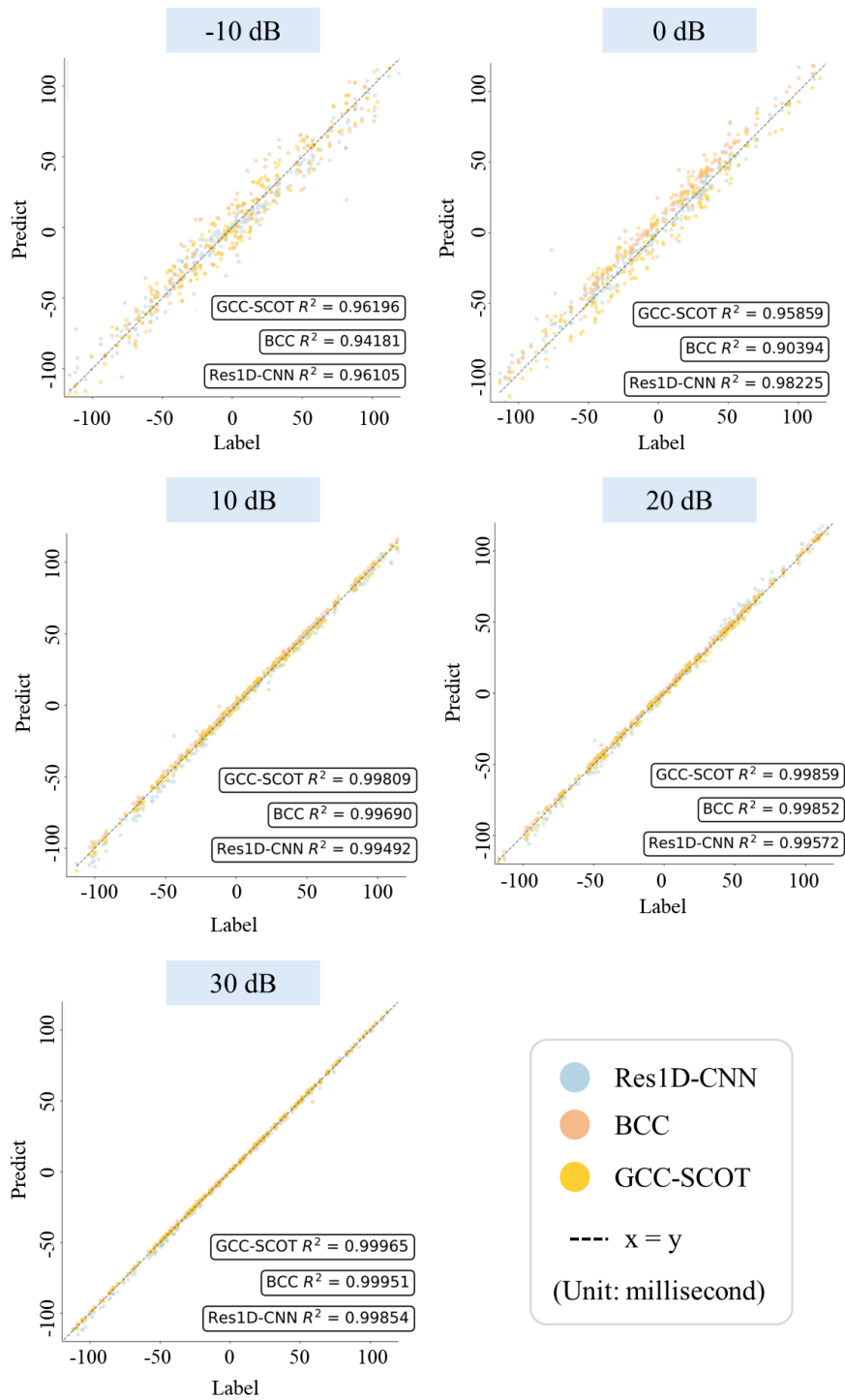


Figure 7.12 The scatter plot of the time-delay results under alpha-stable noise

The leak localization methods were also evaluated under alpha-stable noise. Figure 7.13 illustrates the outputs of the Res1D-CNN, BCC, and GCC-SCOT across various SNRs through scatter plots. The results indicate that the degree of noise significantly influences the performance of both the GCC-SCOT and BCC, while the Res1D-CNN demonstrates robust capabilities in external noise. Specifically, the data points associated with the BCC show a wider distribution ranging from -10 dB to 0 dB, and the distribution of samples becomes increasingly concentrated around the center line as the level of external noise reduces. In contrast, the Res1D-CNN demonstrates robust performance. Although a slight separation of samples is observed at -10 dB of noise, most data points remain concentrated around the center line under most conditions. Ranging from 0 to 0 dB, the wider spread of prediction of GCC-SCOT and BCC suggests that both methods are sensitive to outliers or noise in the input data, compared to the Res1D-CNN approach in the low SNRs scenario. As the SNR increases, GCC-SCOT and BCC exhibit an apparent convergence towards the centerline, beginning at 10 dB. Conversely, Res1D-CNN continues to display several outliers in the SNR ranges from 10 dB to 30 dB.

Figure 7.13 provides a detailed comparison of GCC-SCOT, BCC, and Res1D-CNN through evaluation metrics. Overall, similar to the previous results, as the SNR of signals decreases, the performance metrics of the GCC-SCOT and BCC methods tend to drop. In contrast, the performance of the Res1D-CNN remains relatively stable. Compared to WGN, alpha-stable noise appears to impact the leak localization performance of GCC-SCOT and BCC significantly. The overall performance of these

techniques under alpha-stable noise (in the range of -10 dB to 0 dB) is inferior to their performance under WGN under the same SNR.

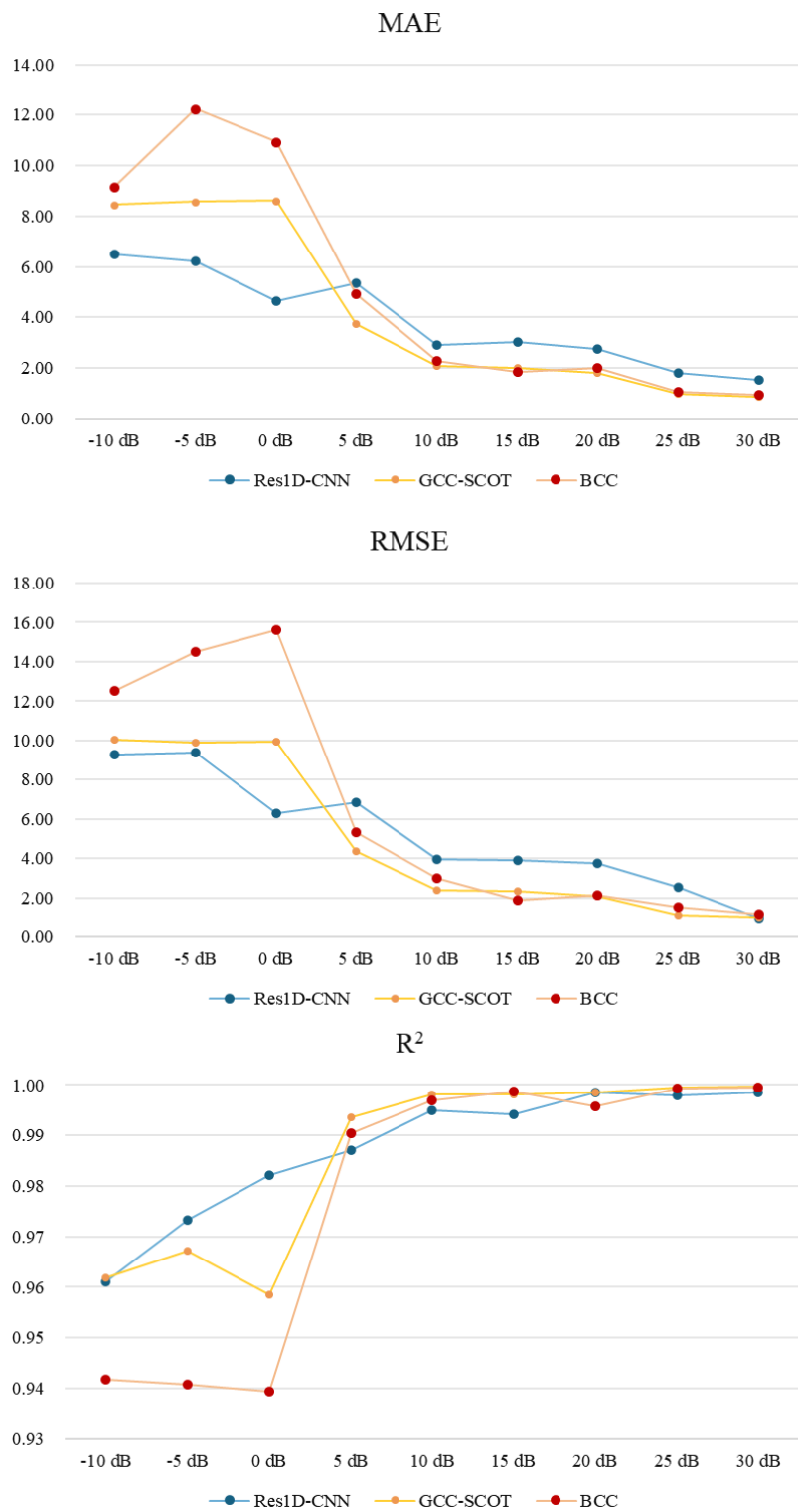


Figure 7.13 The performance metrics of time-delay results under alpha-stable noise

For SNR ranging from -10 dB to 5 dB, the Res1D-CNN outperforms the BCC and GCC-SCOT. The Res1D-CNN exhibits lower MAE, RMSE, and higher  $R^2$ , indicating better localization performance. However, as the SNR increases, after reaching 5 dB or 15 dB, the GCC-SCOT and BCC appear to perform better than the Res1D-CNN in higher SNR. Meanwhile, Figure 7.14 draws the time-delay distributions of three methods in the mixed dataset under alpha-stable noise. Compared to the scatter observed under WGN (Figure 7.9), the sample distributions of GCC-SCOT and BCC under alpha-stable noise are noticeably wider. At the same time, Res1D-CNN still exhibits a more pronounced concentration along the central axis. According to  $R^2$ , Res1D-CNN achieved the highest performance, followed by GCC-SCOT and BCC, similar to the results under WGN. Notably, BCC is significantly impacted by its lower  $R^2$  value of 0.76864.

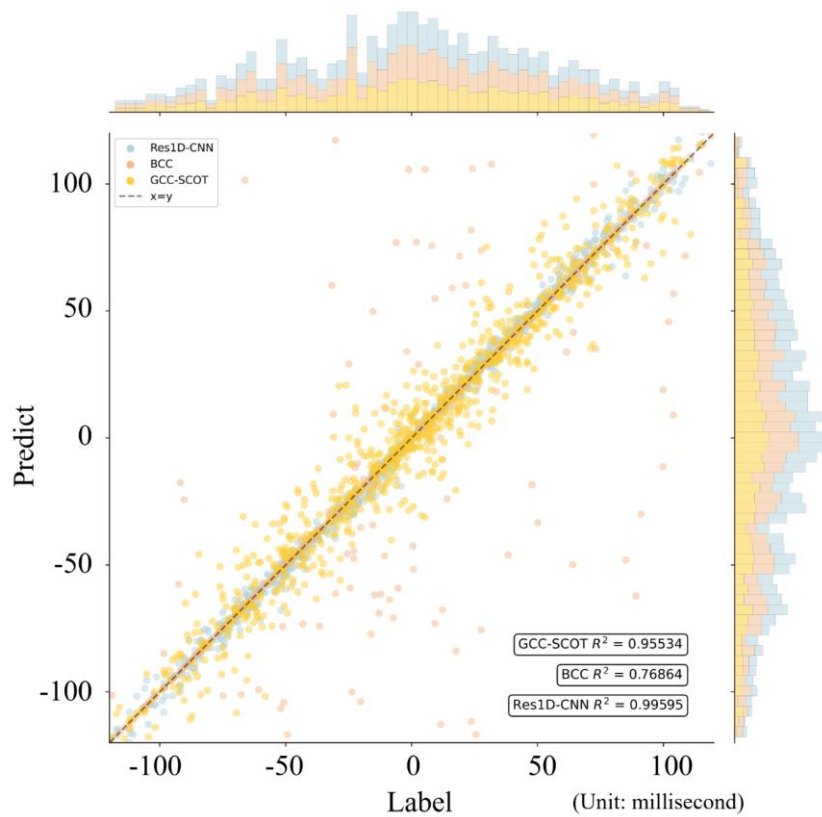


Figure 7.14 The scatter plot of time-delay results for mixed datasets under alpha-stable noise

The results of each method are quantified and visualized in Figure 7.15. Unlike the WGN scenario, the MAE distributions of GCC-SCOT and BCC are relatively similar, though GCC-SCOT exhibits a slightly lower MAE than BCC. Regarding RMSE, GCC-SCOT demonstrates greater resistance to complex noise (alpha-stable noise), with a significantly lower RMSE than BCC. In contrast, BCC shows a much higher RMSE and produces several outliers.

Meanwhile, leak distance prediction experiments were also conducted on alpha-stable noise. Figure 7.16 depicts the leak distance error of each method through performance metrics. Compared to WGN, it can be found that alpha-stable noise imposes a greater influence on GCC-SCOT and BCC, and their MAE is significantly larger than Res1D-CNN. The BCC might output more extreme leak distances than the other two through RMSE. Thus, the Res1D-CNN reaches the optimal model to locate the leaks under alpha-stable noise based on the  $R^2$ .

The findings suggest the Res1D-CNN demonstrates promising performance, particularly in low SNR scenarios. However, the applicability of the Res1D-CNN, GCC-SCOT, and BCC appears contingent on the specific context, as GCC-SCOT and BCC exhibited superior performance in higher SNR conditions. Consequently, further empirical investigation is required to comprehensively elucidate the strengths and limitations of each approach across operational settings.

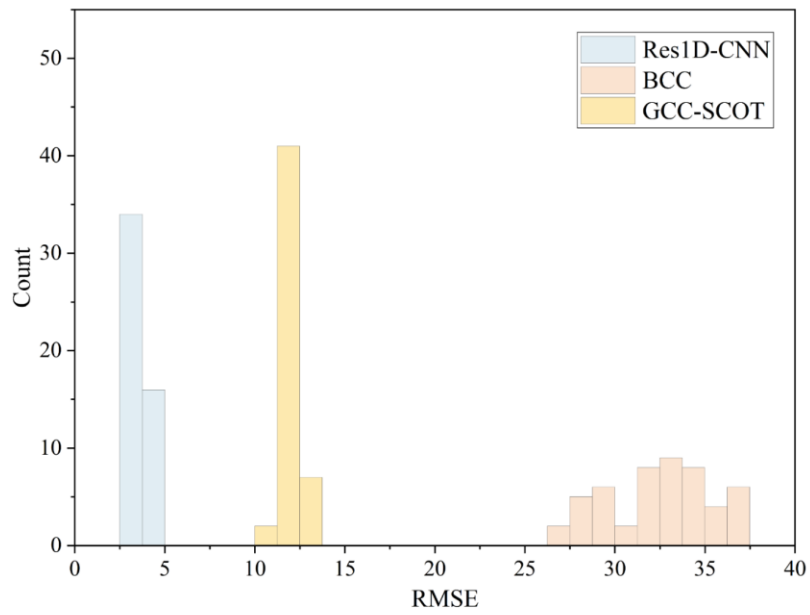
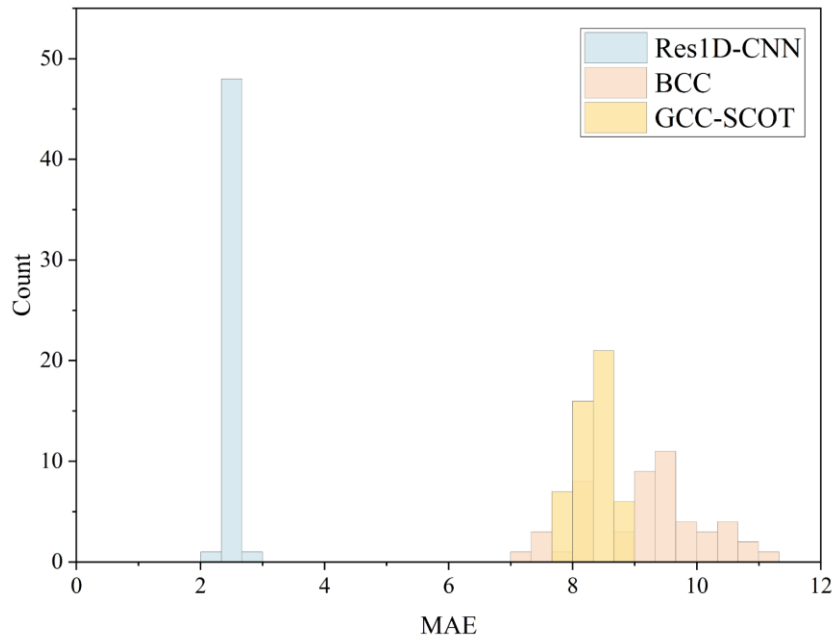


Figure 7.15 The distribution of RMSE and MAE based on the mixed dataset under Alpha-stable noise

## Leak Distance Error

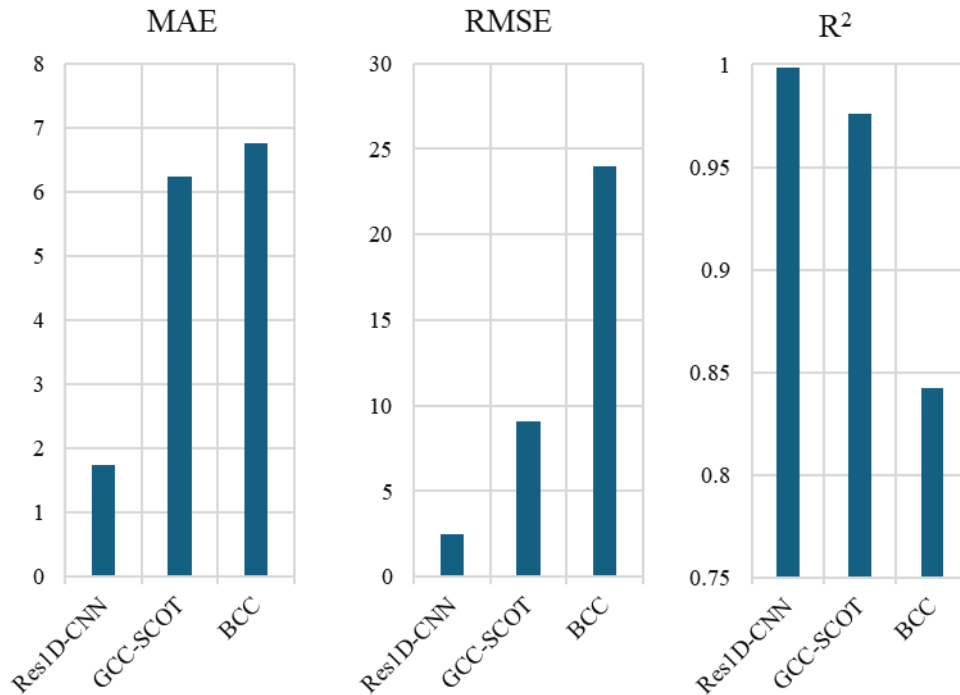


Figure 7.16 The leak distance error under alpha-stable noise

### 7.4 Case Study for Leak Localization

The model's capability to capture the time delay of two signals has been validated in previous procedures. To avoid overfitting risk and evaluate the practical effectiveness of the proposed model, case study experiments were conducted to provide further validation. The research team has contacted the Hong Kong water distribution network contractor to obtain field samples for further analysis. By collaborating with the contractor, the research team obtained two signal pairs deemed suitable for in-depth analysis.

As illustrated in Figure 7.17, two correlators were deployed on the chambers located within the respective sections of the leaking pipelines. The signal was collected under 4096 Hz sampling rate, and the collected duration was ten seconds. The collection

occurs at midnight to minimize the influence of external noise, including traffic and pedestrian noise. The actual distances of the two sensors were verified and measured through excavation and on-site inspection. Subsequently, three signal pairs were collected from two correlators. The total length between the two points is 36 m. The sound velocity is 530 m/s, and the leak point is closer to the Chamber I, with  $d_1$  equal to 14.69 m.

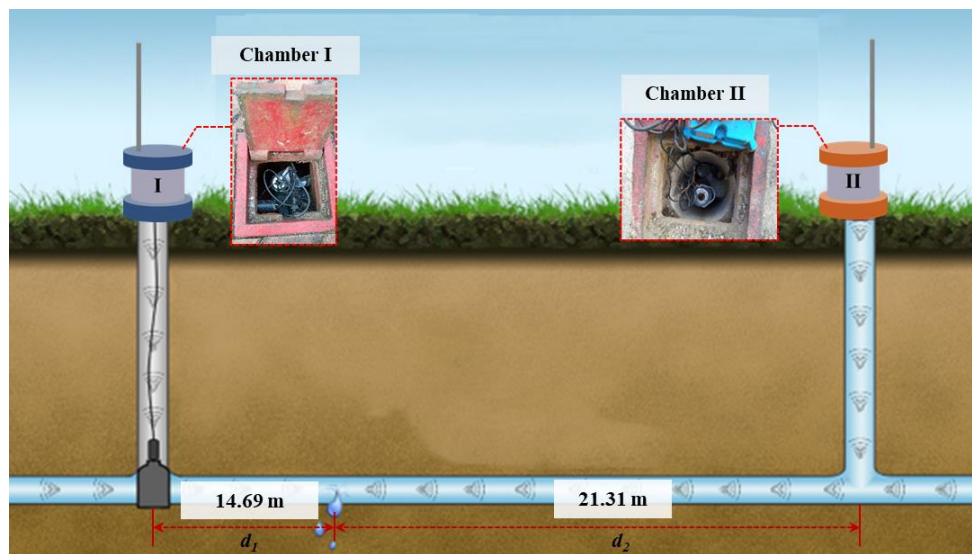


Figure 7.17 The deployment diagram of field experiments

The BCC and GCC-SCOT results show a significant decrease, indicating the time delay is 9.883 seconds and 2.6246 seconds. The BCC and GCC-SCOT exceed the maximum time required for sound waves to propagate through the entire pipe. The intense external noise in the experiment environment might cause the invalid of BCC and GCC-SCOT. Although the experiments were conducted at midnight, traffic and environmental noise could not be avoided. This result demonstrates that the BCC method might not be well-suited to the field environment of WDNs. In contrast, the Res1D-CNN predicts a time delay of -16.7173 ms and estimates the distance  $d_1$  to be 13.5718 meters. This model-predicted location is within a 1-meter bias of the actual leak point. Overall, the findings

suggest the Res1D-CNN appears to outperform the BCC method in the context of field experiments, demonstrating its suitability and effectiveness for leak localization applications in water distribution networks.

## **7.5 Discussion**

The mentioned results provide a comprehensive evaluation of the Res1D-CNN in the context of leak localization and a comparison to the GCC-SCOT and BCC. This evaluation process has provided valuable insights into the performance and effectiveness of both approaches.

First, the BCC nearly correctly predicted all time delays in the clean dataset without any noise, showcasing its effectiveness. Meanwhile, the Res1D-CNN also demonstrated solid time estimation ability, although slightly inferior to the performance of BCC. This discrepancy can be attributed to the information feature extraction process employed by the Res1D-CNN.

During the convolution operation, the applied kernel moves with a certain stride, projecting the input vector into subspaces. The convolution operation along the signals is similar to the short-time Fourier transform (STFT). Specifically, the window in STFT is analogous to the convolution kernel in CNN, moving through the signals and extracting in-depth information through transformation. However, the STFT operation may lose precision in the time dimension (Kıymık et al., 2005). Similarly, while removing the information, the convolution operation in CNN may also suppress detailed temporal information and alter the phase characteristics of the time series data (L. Zhao & Zhang, 2024). Furthermore, while enhancing the model's robustness to small input variations, max-pooling may inadvertently ignore certain fine-grained features,

resulting in a loss of resolution during feature extraction. The above limitations may restrict the maximum achievable accuracy of the proposed method.

However, the convolution block of the Res1D-CNN has its advantage, which assists in extracting the information and enhances the model's robustness and effectiveness. In the experiments conducted with various SNRs, Res1D-CNN exhibited greater robustness performance than BCC, particularly in low SNR conditions. This can also be attributed to the convolution blocks in Res1D-CNN, which function as encoders or feature extractors (B. Zhao et al., 2017). These blocks encode the input data into compact representations and emphasize critical features, aiding in identifying and filtering abnormal noise. Therefore, the model is resistant to outliers or noise.

Although GCC-SCOT and BCC demonstrated higher accuracy than Res1D-CNN in high SNR conditions, it is crucial to consider realistic pipeline localization scenarios wherein the presence of surrounding noise, such as traffic or pedestrians, simulates low SNR conditions (Fan et al., 2022). Consequently, Res1D-CNN emerges as a more practical choice in such contexts. The case study further supports this viewpoint. In the context of field experiments, BCC has limited predicted performance and suffers from the impact of external noise (Gao et al., 2004). On the other hand, Res1D-CNN yields notably improved accuracy, exhibiting a location bias of lower than 3 meters. This disparity highlights the potential of Res1D-CNN in accurately estimating pipeline locations, further reinforcing its practical applicability in real-world scenarios.

The comprehensive evaluation and comparison of Res1D-CNN with GCC-SCOT and BCC have provided valuable insights. Res1D-CNN has proven a highly effective method for accurately estimating time delay and localizing leaks in low SNR conditions.

However, its performance is less advantageous in ideal scenarios characterized by high SNR with limited noise than GCC-SCOT and BCC. These findings contribute to a deeper understanding of the inherent characteristics of both methods and highlight the potential effectiveness of Res1D-CNN for acoustic water leak localization. Nevertheless, the applicability of Res1D-CNN was not entirely unexplored due to the lack of additional data for further validation. Future research is expected to collect sufficient data to evaluate the proposed framework thoroughly.

## **7.6 Chapter Summary**

This chapter introduces Res1D-CNN as a novel approach for localizing water leaks by leveraging time-delay information. The model is trained using simulated data to predict the time delay and corresponding leak locations accurately. Evaluation results demonstrate that Res1D-CNN exhibits greater robustness and effectiveness in low SNR scenarios and field experiments compared to the benchmark method BCC and GCC-SCOT. The experiments conducted on both simulated and real-world data provide substantial evidence supporting the efficacy of Res1D-CNN, showcasing its high degree of robustness and potential to significantly improve operational efficiency and sustainable water management by precisely identifying leak locations.

## **CHAPTER 8 Conclusions and Recommendations**

### **8.1 Introduction**

This chapter begins by critically reassessing the original research objectives to evaluate the extent to which they have been addressed within the study's scope. It then provides a comprehensive analysis of key findings, highlighting their significance. The substantial contributions of this work to the academic literature and knowledge advancement in the field are emphasized. Additionally, the chapter discusses the research's inherent limitations and identifies potential areas for future investigations that can build on the foundations established by this study.

### **8.2 Summary of Findings**

Objective I: Generative approach to augment leak diagnosis dataset

This study proposes LSTM-GAN, a novel approach for using machine learning to address the challenge of limited real leak detection data in WDN. Our approach aims to capture leak signal distribution and consistently generate high-quality samples. By applying LSTM-GAN to WDNs in Hong Kong, the proposed method successfully generates a sufficient number of acoustic signals representative of leak conditions. Through rigorous evaluation using t-SNE analysis, acoustic feature analysis, and model augmentation validation, the findings demonstrate that the generated samples exhibit a high level of consistency with real leak samples regarding t-SNE results and acoustic features. Moreover, the validation study reveals that LSTM-GAN outperforms other generative methods, significantly enhancing water leak detection performance. Overall, the study highlights the effectiveness and potential of LSTM-GAN for improving water leak detection in WDNs by addressing the limitations of real data availability.

Objective II: Establish an explainable deep-learning model enhancing the interpretability and feature visualization

This study introduces explainable deep-learning models that utilize time-frequency spectrograms for water leak detection. The Grad-CAM technique generates attention maps of time-frequency components, providing novel insights for signal analysis. Specifically, the method is applied to visualize the operational mechanisms of CNNs, including AlexNet, VGGs, and ResNet, explaining the variation in model capabilities and leak detection performance across different leak types. The analysis of Grad-CAM results demonstrates that VGG-19 and Grad-CAM's attention regions effectively capture essential signals with a higher concentration level, elucidating their superior performance by accurately capturing relevant time-frequency information. Furthermore, a comparative investigation of Grad-CAM results between leakage and non-leakage signals reveals that the model primarily relies on the frequency range of 750-1250 Hz for leak detection, while frequencies below 500 Hz play a crucial role in noleak signal classification. These insights helped the researchers reveal the model's decision-making process and highlighted specific frequency ranges associated with different signal classifications.

Objective III: Develop an effective time-series leak detection model for WDN

This study employs the Time-transformer model for in-depth analysis of acoustic signals, specifically the total signals. The model directly processes 1D vibroacoustic signals using the Transformer architecture. The effectiveness of the Transformer-based model is demonstrated through experiments conducted on signals collected from water distribution networks in Hong Kong. Comparative analysis with other time-series deep

learning models (ConvLSTM and 1D-CNN) reveals the superior performance of the Transformer model in leak detection. The Time-transformer achieved a higher accuracy in testing and out-of-sample validation. Besides, t-SNE visualizations confirm the exceptional pattern clustering ability of the Transformer model, with transformer blocks contributing to enhanced leak detection capabilities. These findings demonstrated the effectiveness and practicality of the Time-Transformer model for water leak detection in distribution networks.

Objective IV: Develop a robust time-delay deep learning leak localization model for WDN.

This study introduces a novel approach, Res1D CNN, to analyse time delays between signal pairs. Using simulated data, the proposed model can estimate time delays. It is trained and compared with the conventional GCC-SCOT and BCC methods. The experimental results showcase the effectiveness of the proposed method, particularly in low SNR scenarios. This outcome highlights the potential value of applying deep learning techniques for accurately localizing leak points.

### **8.3 Contribution of the Research**

This research provides original contributions to ML-based acoustic leak detection from theoretical and practical perspectives. In terms of the theoretical perspective, this study expands the knowledge of water leak diagnosis by:

- i. Providing a comprehensive review of the trends and developments in the modeling of acoustic leak diagnosis.
- ii. Proposing an advanced generative approach, LSTM-GAN, enables data augmentation to enrich the training dataset, laying the foundation for machine

learning training and promoting the training performance.

- iii. Enhancing model interpretability, visualization algorithms can explain the model's features and provide insights into the decision-making process of leak detection models, enabling targeted measures to improve the model internally and enhance its accuracy.
- iv. The feature interpretability results also provide insights into the leak-related time-frequency components, contributing to acoustic wave theory and noise reduction research.
- v. Validate the effectiveness of utilizing multi-dimension data (time-series model or time-frequency spectrum) to establish a robust leak detection model for water distribution networks.
- vi. Proposed a deep learning model for estimating time delay to deduce the leak distance, promoting the development of deep learning on capturing the time-temporal in signal pairs.

As for the practical perspective, this research provides the following:

- i. Development of a practical and effective acoustic leak detection system. This study contributes to developing a real-world acoustic leak diagnosis system, which can be implemented in water distribution networks to detect and locate leaks accurately and efficiently.
- ii. Improving accuracy and reliability of leak detection. By utilizing advanced machine learning techniques and multi-dimensional data analysis, the study enhances the accuracy and reliability of leak detection, reducing false positives and false negatives in the maintenance process.

- iii. Cost and resource savings. The model needs less data by employing the proposed GAN data augmentation technique, and field experiments and associated costs are reduced. Also, deep learning models for leak distance estimation lead to substantial cost and resource savings. Accurate leak detection and localization help minimize water loss, reduce operational expenses, and preserve valuable water resources.
- iv. Enhanced the development and acceptance of machine learning leak detection. This study enables a better understanding and interpretation of the leak detection model's decision-making process. It offers valuable insights that can help maintenance teams and infrastructure managers better understand and increase their trust in ML techniques.
- v. Advancing smart leak management. This study proposes a deep learning model to estimate time delays, enhance the leak localization process, and advance intelligent leak detection systems. This technology reduces the need for prior knowledge, quickly identifies and locates leaks, and paves the way for smarter and more sustainable ways to address water infrastructure leaks through timely intervention.

## **8.4 Limitations and Future Research**

### **8.4.1 Limitations**

Despite achieving the research objectives, this study acknowledges the existence of certain limitations that warrant further attention and improvement. The identified constraints are outlined as follows:

For generative modeling for data augmentation, a significant limitation arises from the lack of consideration for the impact of acoustic properties, leak types, and physical factors on the generated samples. Presently, the generated samples primarily focus on a

singular scenario, failing to account for the influence of these influential factors. This oversight restricts the comprehensive representation of real-world variations and hinders the feasibility and effectiveness of the data augmentation approach.

For model interpretability and explainable enhancement, the applied Grad-CAM algorithm does not inherently consider the uncertainty or confidence levels associated with its visual explanations. It may present saliency maps or heatmaps without quantifying the certainty of the highlighted regions, which can be misleading in scenarios where uncertainty estimation is critical. Furthermore, the interpretability analysis and enhancement techniques primarily examine time-frequency components, neglecting to uncover and consider the underlying physical principles governing these components.

For the time-series leak detection model, the applied transformer model imposes a higher requirement on the computation resource. Transformers are computationally demanding models, requiring significant computational resources and longer training times than traditional machine learning algorithms. It poses practical challenges for deploying transformer-based leak detection models, particularly in resource-constrained environments or real-time applications where quick response times are crucial. The limitations of time-delay-based deep learning leak localization models include the reliance on simulated data, which introduces uncertainties regarding the accuracy and robustness of the model in real-world leak detection scenarios. Additionally, the assumption of a single leak point restricts the applicability of the model to scenarios involving multiple leak locations. These factors might hinder the practicality of the applied method in field experiments.

## 8.4.2 Future Studies

This section outlines the potential improvements to the current studies.

### **Enhancement of the existing research:**

-The acoustic generative model can be enhanced by utilizing the advancing model (e.g., transformer model) as the backbone, which possesses a robust capacity for capturing time-series features.

-In terms of model interpretability, incorporating physical information as input can enhance interpretability and leverage the benefits of deep learning. For instance, this physical information can be encoded into the vector and input into the model. Utilizing feature importance algorithms, including Shapley and Grad-CAM, can aid in determining the importance of various features and formalizing the underlying physical principles.

-Regarding leak detection modeling, the current model relies exclusively on vibroacoustic data. However, integrating additional data sources, such as pressure and volume measurements, could provide valuable information to improve the model's performance.

-Regarding leak localization modelling, future studies can combine with contrastive learning, which provides a self-supervised training algorithm that reduces the burden on labeled leak localization datasets.

### **Extension of the existing research:**

-The proposed GAN model can be extended to generate leak signals with varying physical characteristics by employing the concept of conditional GAN. This method

allows for the incorporation of label information (leak conditions) and the adjustment of output signals based on different internal features by manipulating hyperparameters.

- Research on model interpretability focused on the time-frequency spectrum but can be extended to other two-dimensional data formats such as recurrent plots or Mel plots.

The explainable technique can also be applied to one-dimensional time series data.

- The applied leak detection transformer model is running in lab-based devices. Researchers can try to deploy the model on resource-constrained equipment like mobile devices for practical usage.

- The leak localization model relies on simulated data. Future studies need to incorporate field experiments. By conducting experiments in real-world environments and collecting data under diverse conditions, researchers can effectively evaluate and develop a comprehensive leak localization that caters to different conditions with higher robustness and effectiveness.

## References

- Abdulshaheed, A., Mustapha, F., & Anuar, M. (2018). Pipe Material Effect on Water Network Leak Detection Using a Pressure Residual Vector Method. *Journal of Water Resources Planning and Management*, *144*(4), 05018006. [https://doi.org/10.1061/\(ASCE\)WR.1943-5452.0000798](https://doi.org/10.1061/(ASCE)WR.1943-5452.0000798)
- Aghashahi, M., Sela, L., & Banks, M. K. (2023). Benchmarking dataset for leak detection and localization in water distribution systems. *Data in Brief*, *48*, 109148. <https://doi.org/10.1016/j.dib.2023.109148>
- Ahmad, S., Ahmad, Z., Kim, C.-H., & Kim, J.-M. (2022). A Method for Pipeline Leak Detection Based on Acoustic Imaging and Deep Learning. *Sensors*, *22*(4), 1562. <https://doi.org/10.3390/s22041562>
- Ahmad, Z., Nguyen, T.-K., & Kim, J.-M. (2023). Leak detection and size identification in fluid pipelines using a novel vulnerability index and 1-D convolutional neural network. *Engineering Applications of Computational Fluid Mechanics*, *17*(1), 2165159. <https://doi.org/10.1080/19942060.2023.2165159>
- Ahmad, Z., Nguyen, T.-K., Rai, A., & Kim, J.-M. (2023). Industrial fluid pipeline leak detection and localization based on a multiscale Mann-Whitney test and acoustic emission event tracking. *Mechanical Systems and Signal Processing*, *189*, 110067. <https://doi.org/10.1016/j.ymsp.2022.110067>
- Almeida, F., Brennan, M., Joseph, P., Whitfield, S., Dray, S., & Paschoalini, A. (2014a). On the Acoustic Filtering of the Pipe and Sensor in a Buried Plastic Water Pipe and its Effect on Leak Detection: An Experimental Investigation. *Sensors*, *14*(3), 5595–5610. <https://doi.org/10.3390/s140305595>
- Almeida, F., Brennan, M., Joseph, P., Whitfield, S., Dray, S., & Paschoalini, A. (2014b). On the Acoustic Filtering of the Pipe and Sensor in a Buried Plastic Water Pipe and its Effect on Leak Detection: An Experimental Investigation. *Sensors*, *14*(3), 5595–5610. <https://doi.org/10.3390/s140305595>

- Almeida, F. C. L., Brennan, M. J., Joseph, P. F., Gao, Y., & Paschoalini, A. T. (2018). The effects of resonances on time delay estimation for water leak detection in plastic pipes. *Journal of Sound and Vibration*, *420*, 315–329. <https://doi.org/10.1016/j.jsv.2017.06.025>
- Alzubaidi, L., Zhang, J., Humaidi, A. J., Al-Dujaili, A., Duan, Y., Al-Shamma, O., Santamaría, J., Fadhel, M. A., Al-Amidie, M., & Farhan, L. (2021). Review of deep learning: Concepts, CNN architectures, challenges, applications, future directions. *Journal of Big Data*, *8*(1), 1–74. <https://doi.org/10.1186/s40537-021-00444-8>
- Ayati, A. H., Haghghi, A., & Ghafouri, H. R. (2022). Machine learning approach to transient-based leak detection of pressurized pipelines: Classification vs Regression. *Journal of Civil Structural Health Monitoring*, *12*(3), 611–628. <https://doi.org/10.1007/s13349-022-00568-2>
- Azam, S., Montaha, S., Fahim, K. U., Rafid, A. K. M. R. H., Mukta, Md. S. H., & Jonkman, M. (2023). Using feature maps to unpack the CNN ‘Black box’ theory with two medical datasets of different modality. *Intelligent Systems with Applications*, *18*, 200233. <https://doi.org/10.1016/j.iswa.2023.200233>
- Azaria, M., & Hertz, D. (1984). Time delay estimation by generalized cross correlation methods. *IEEE Transactions on Acoustics, Speech, and Signal Processing*, *32*(2), 280–285. <https://doi.org/10.1109/TASSP.1984.1164314>
- Bai, M. R., Lan, S.-S., & Huang, J.-Y. (2018). *Time difference of arrival (TDOA)-based acoustic source localization and signal extraction for intelligent audio classification*. 632–636. <https://doi.org/10.1109/SAM.2018.8448583>
- Banjara, N. K., Sasmal, S., & Voggu, S. (2020). Machine learning supported acoustic emission technique for leakage detection in pipelines. *International Journal of Pressure Vessels and Piping*, *188*, 104243. <https://doi.org/10.1016/j.ijpvp.2020.104243>
- Bashir, T., Haoyong, C., Tahir, M. F., & Liqiang, Z. (2022). Short term electricity load forecasting using hybrid prophet-LSTM model optimized by BPNN. *Energy Reports*, *8*, 1678–1686. <https://doi.org/10.1016/j.egyr.2021.12.067>

- Basu, J., & RoyChaudhuri, C. (2016). Graphene Nanogrids FET Immunosensor: Signal to Noise Ratio Enhancement. *Sensors*, *16*(10), Article 10. <https://doi.org/10.3390/s16101481>
- Bellot, D., Boyer, A., & Charpillat, F. (2002). *A new definition of qualified gain in a data fusion process: Application to telemedicine*. *2*, 865–872. <https://doi.org/10.1109/ICIF.2002.1020898>
- Berkhin, P. (2006). A Survey of Clustering Data Mining Techniques. In J. Kogan, C. Nicholas, & M. Teboulle (Eds.), *Grouping Multidimensional Data: Recent Advances in Clustering* (pp. 25–71). Springer. [https://doi.org/10.1007/3-540-28349-8\\_2](https://doi.org/10.1007/3-540-28349-8_2)
- Boashash, B. (2016). *Time frequency signal analysis and processing: A comprehensive reference* (Second edition). Academic Press.
- Bohorquez, J., Alexander, B., Simpson, A. R., & Lambert, M. F. (2020). Leak Detection and Topology Identification in Pipelines Using Fluid Transients and Artificial Neural Networks. *Journal of Water Resources Planning and Management*, *146*(6), 04020040. [https://doi.org/10.1061/\(ASCE\)WR.1943-5452.0001187](https://doi.org/10.1061/(ASCE)WR.1943-5452.0001187)
- Boretti, A., & Rosa, L. (2019). Reassessing the projections of the World Water Development Report. *Npj Clean Water*, *2*(1), 15. <https://doi.org/10.1038/s41545-019-0039-9>
- Boujelben, M., Benmessaoud, Z., Abid, M., & Elleuchi, M. (2023). An efficient system for water leak detection and localization based on IoT and lightweight deep learning. *Internet of Things*, *24*, 100995. <https://doi.org/10.1016/j.iot.2023.100995>
- Bowles, C., Chen, L., Guerrero, R., Bentley, P., Gunn, R., Hammers, A., Dickie, D. A., Hernández, M. V., Wardlaw, J., & Rueckert, D. (2018). Gan augmentation: Augmenting training data using generative adversarial networks. *arXiv Preprint arXiv:1810.10863*. <https://doi.org/10.48550/arXiv.1810.10863>
- Brennan, M. J., Karimi, M., Muggleton, J. M., Almeida, F. C. L., Kroll de Lima, F., Ayala, P. C., Obata, D., Paschoalini, A. T., & Kessissoglou, N. (2018a). On the effects of soil properties on leak noise propagation in plastic water distribution pipes. *Journal of Sound and Vibration*, *427*, 120–133. <https://doi.org/10.1016/j.jsv.2018.03.027>

- Brennan, M. J., Karimi, M., Muggleton, J. M., Almeida, F. C. L., Kroll de Lima, F., Ayala, P. C., Obata, D., Paschoalini, A. T., & Kessissoglou, N. (2018b). On the effects of soil properties on leak noise propagation in plastic water distribution pipes. *Journal of Sound and Vibration*, *427*, 120–133. <https://doi.org/10.1016/j.jsv.2018.03.027>
- Brito, L. C., Susto, G. A., Brito, J. N., & Duarte, M. A. V. (2022). An explainable artificial intelligence approach for unsupervised fault detection and diagnosis in rotating machinery. *Mechanical Systems and Signal Processing*, *163*, 108105. <https://doi.org/10.1016/j.ymsp.2021.108105>
- Brophy, E., Wang, Z., She, Q., & Ward, T. (2023). Generative Adversarial Networks in Time Series: A Systematic Literature Review. *ACM Computing Surveys*, *55*(10), 1–31. <https://doi.org/10.1145/3559540>
- Butterfield, J. D., Collins, R. P., & Beck, S. B. M. (2018). Influence of Pipe Material on the Transmission of Vibroacoustic Leak Signals in Real Complex Water Distribution Systems: Case Study. *Journal of Pipeline Systems Engineering and Practice*, *9*(3), 05018003. [https://doi.org/10.1061/\(ASCE\)PS.1949-1204.0000321](https://doi.org/10.1061/(ASCE)PS.1949-1204.0000321)
- Butterfield, J. D., Krynkin, A., Collins, R. P., & Beck, S. B. M. (2017). Experimental investigation into vibro-acoustic emission signal processing techniques to quantify leak flow rate in plastic water distribution pipes. *Applied Acoustics*, *119*, 146–155. <https://doi.org/10.1016/j.apacoust.2017.01.002>
- Butterfield, J., Meyers, G., Meruane, V., Collins, R., & Beck, S. (2018). Experimental investigation into techniques to predict leak shapes in water distribution systems using vibration measurements. *Journal of Hydraulic Research*, *20*(4), 815–828. <https://doi.org/10.2166/hydro.2018.117>
- Bykerk, L., & Valls Miro, J. (2022). Vibro-Acoustic Distributed Sensing for Large-Scale Data-Driven Leak Detection on Urban Distribution Mains. *Sensors*, *22*(18), 6897. <https://doi.org/10.3390/s22186897>
- Castanedo, F. (2013). A Review of Data Fusion Techniques. *The Scientific World Journal*, *2013*, 1–19. <https://doi.org/10.1155/2013/704504>

- Chandrashekar, G., & Sahin, F. (2014). A survey on feature selection methods. *Computers & Electrical Engineering*, *40*(1), 16–28. <https://doi.org/10.1016/j.compeleceng.2013.11.024>
- Chawla, N. V., Bowyer, K. W., Hall, L. O., & Kegelmeyer, W. P. (2002). SMOTE: Synthetic minority over-sampling technique. *Journal of Artificial Intelligence Research*, *16*, 321–357. <https://doi.org/10.1613/jair.953>
- Chen, T., & Guestrin, C. (2016). *Xgboost: A scalable tree boosting system*. 785–794. <https://doi.org/10.1145/2939672.2939785>
- Chen, Y., Zhang, M., Bai, M., & Chen, W. (2019). Improving the Signal-to-Noise Ratio of Seismological Datasets by Unsupervised Machine Learning. *Seismological Research Letters*, *90*(4), 1552–1564. <https://doi.org/10.1785/0220190028>
- Chi, Z., Jiang, J., Diao, X., Chen, Q., Ni, L., Wang, Z., & Shen, G. (2022). Novel Leakage Detection Method by Improved Adaptive Filtering and Pattern Recognition based on Acoustic Waves. *International Journal of Pattern Recognition and Artificial Intelligence*, *36*(02), 2259001. <https://doi.org/10.1142/S0218001422590017>
- Chimmula, V. K. R., & Zhang, L. (2020). Time series forecasting of COVID-19 transmission in Canada using LSTM networks. *Chaos, Solitons & Fractals*, *135*, 109864. <https://doi.org/10.1016/j.chaos.2020.109864>
- Choi, C. L. (2020, March 18). *Learning Deep Features for Discriminative Localization: Class Activation Mapping*. Medium. <https://towardsdatascience.com/learning-deep-features-for-discriminative-localization-class-activation-mapping-2a653572be7f>
- Choi, J., & Im, S. (2023). Application of CNN Models to Detect and Classify Leakages in Water Pipelines Using Magnitude Spectra of Vibration Sound. *Applied Sciences*, *13*(5), 2845. <https://doi.org/10.3390/app13052845>
- Chuang, W.-Y., Tsai, Y.-L., & Wang, L.-H. (2019). Leak Detection in Water Distribution Pipes Based on CNN with Mel Frequency Cepstral Coefficients. *Proceedings of the 2019 3rd International Conference on Innovation in Artificial Intelligence*, 83–86. <https://doi.org/10.1145/3319921.3319926>

- Cody, R. A., & Narasimhan, S. (2020). A field implementation of linear prediction for leak-monitoring in water distribution networks. *Advanced Engineering Informatics*, 45, 101103. <https://doi.org/10.1016/j.aei.2020.101103>
- Cody, R. A., Tolson, B. A., & Orchard, J. (2020). Detecting Leaks in Water Distribution Pipes Using a Deep Autoencoder and Hydroacoustic Spectrograms. *Journal of Computing in Civil Engineering*, 34(2), 04020001. [https://doi.org/10.1061/\(ASCE\)CP.1943-5487.0000881](https://doi.org/10.1061/(ASCE)CP.1943-5487.0000881)
- Cody, R., Harmouche, J., & Narasimhan, S. (2018). Leak detection in water distribution pipes using singular spectrum analysis. *Urban Water Journal*, 15(7), 636–644. <https://doi.org/10.1080/1573062X.2018.1532016>
- Cody, R., Narasimhan, S., & Tolson, B. (2017). One-class SVM–Leak detection in water distribution systems. *Proc., Computing and Control for the Water Industry, CCWI*.
- Cortes, C., & Vapnik, V. (1995). Support-vector networks. *Machine Learning*, 20, 273–297.
- Creswell, A., White, T., Dumoulin, V., Arulkumaran, K., Sengupta, B., & Bharath, A. A. (2018). Generative Adversarial Networks: An Overview. *IEEE Signal Processing Magazine*, 35(1), 53–65. <https://doi.org/10.1109/MSP.2017.2765202>
- Cui, W., Jiao, S., Zhang, Q., Hou, T., Xue, Q., Zhu, Y., & Li, Z. (2024). Dual-channel two-dimensional stochastic resonance and its application in bearing fault detection under alpha-stable noise. *Chinese Journal of Physics*, 88, 922–937. <https://doi.org/10.1016/j.cjph.2023.12.006>
- Cui, X., Gao, Y., & Han, X. (2024). On the mixed acoustic and vibration sensors for the cross-correlation analysis of pipe leakage signals. *Applied Acoustics*, 216, 109798. <https://doi.org/10.1016/j.apacoust.2023.109798>
- Cui, X., Gao, Y., Ma, Y., Liu, F., & Wang, H. (2023). Time delay estimation using cascaded LMS filters fused by correlation coefficient for pipeline leak localization. *Mechanical Systems and Signal Processing*, 199, 110500. <https://doi.org/10.1016/j.ymsp.2023.110500>

- Cui, X., Gao, Y., Ma, Y., Liu, Y., & Jin, B. (2022). Variable Step Normalized LMS Adaptive Filter for Leak Localization in Water-Filled Plastic Pipes. *IEEE Transactions on Instrumentation and Measurement*, 71, 1–11. <https://doi.org/10.1109/TIM.2022.3169526>
- Daubechies, I. (1992). *Ten lectures on wavelets*. Society for Industrial and Applied Mathematics.
- Dawood, T., Elwakil, E., Novoa, H. M., & Delgado, J. F. G. (2020). Artificial intelligence for the modeling of water pipes deterioration mechanisms. *Automation in Construction*, 120, 103398. <https://doi.org/10.1016/j.autcon.2020.103398>
- Diao, X., Jiang, J., Shen, G., Chi, Z., Wang, Z., Ni, L., Mebarki, A., Bian, H., & Hao, Y. (2020). An improved variational mode decomposition method based on particle swarm optimization for leak detection of liquid pipelines. *Mechanical Systems and Signal Processing*, 143. <https://doi.org/10.1016/j.ymssp.2020.106787>
- Ding, Y., Jia, M., Miao, Q., & Cao, Y. (2022). A novel time–frequency Transformer based on self–attention mechanism and its application in fault diagnosis of rolling bearings. *Mechanical Systems and Signal Processing*, 168, 108616. <https://doi.org/10.1016/j.ymssp.2021.108616>
- Doersch, C. (2016). Tutorial on variational autoencoders. *arXiv Preprint arXiv:1606.05908*.
- Domingos, P., & Pazzani, M. (1997). On the optimality of the simple Bayesian classifier under zero-one loss. *Machine Learning*, 29, 103–130. <https://doi.org/10.1023/A:1007413511361>
- Dong, L., Xu, S., & Xu, B. (2018). *Speech-transformer: A no-recurrence sequence-to-sequence model for speech recognition*. 5884–5888. <https://doi.org/10.1109/ICASSP.2018.8462506>
- Dragomiretskiy, K., & Zosso, D. (2014a). Variational Mode Decomposition. *IEEE Transactions on Signal Processing*, 62(3), 531–544. <https://doi.org/10.1109/TSP.2013.2288675>

- Dragomiretskiy, K., & Zosso, D. (2014b). Variational Mode Decomposition. *IEEE Transactions on Signal Processing*, 62(3), 531–544. <https://doi.org/10.1109/TSP.2013.2288675>
- Duong, B., & Kim, J. (2018). *Pipeline Fault Diagnosis Using Wavelet Entropy and Ensemble Deep Neural Technique* (A. Mansouri, A. ElMoataz, F. Nouboud, & D. Mammass, Eds.; 4 ; Vol. 10884, pp. 292–300). [https://doi.org/10.1007/978-3-319-94211-7\\_32](https://doi.org/10.1007/978-3-319-94211-7_32)
- ECKMANN, J.-P., KAMPHORST, S. O., & RUELLE, D. (1995). Recurrence Plots of Dynamical Systems. *Turbulence, Strange Attractors and Chaos*, 16, 441–445. [https://doi.org/10.1142/9789812833709\\_0030](https://doi.org/10.1142/9789812833709_0030)
- El-Abbasy, M. S., Mosleh, F., Senouci, A., Zayed, T., & Al-Derham, H. (2016). Locating Leaks in Water Mains Using Noise Loggers. *Journal of Infrastructure Systems*, 22(3). [https://doi.org/10.1061/\(ASCE\)IS.1943-555X.0000305](https://doi.org/10.1061/(ASCE)IS.1943-555X.0000305)
- El-Zahab, S., Al-Sakkaf, A., Mohammed Abdelkader, E., & Zayed, T. (2022). A machine learning-based model for real-time leak pinpointing in buildings using accelerometers. *Journal of Vibration and Control*, 10775463211066247. <https://doi.org/10.1177/10775463211066247>
- El-Zahab, S., Asaad, A., Mohammed Abdelkader, E., & Zayed, T. (2016). Collective thinking approach for improving leak detection systems. *Smart Water*, 2, 1–10. <https://doi.org/10.1186/s40713-017-0007-9>
- El-Zahab, S., Asaad, A., Mohammed Abdelkader, E., & Zayed, T. (2019). Development of a clustering-based model for enhancing acoustic leak detection. *Canadian Journal of Civil Engineering*, 46(4), 278–286. <https://doi.org/10.1139/cjce-2018-0229>
- El-Zahab, S., Mohammed Abdelkader, E., & Zayed, T. (2018). An accelerometer-based leak detection system. *Mechanical Systems and Signal Processing*, 108, 276–291. <https://doi.org/10.1016/j.ymssp.2018.02.030>
- Eren, L., Ince, T., & Kiranyaz, S. (2019). A Generic Intelligent Bearing Fault Diagnosis System Using Compact Adaptive 1D CNN Classifier. *Journal of Signal Processing Systems*, 91(2), 179–189. <https://doi.org/10.1007/s11265-018-1378-3>

- Fabbiano, L., Vacca, G., & Dinardo, G. (2020). Smart water grid: A smart methodology to detect leaks in water distribution networks. *Measurement*, *151*, 107260. <https://doi.org/10.1016/j.measurement.2019.107260>
- Falagas, M. E., Pitsouni, E. I., Malietzis, G. A., & Pappas, G. (2008). Comparison of PubMed, Scopus, web of science, and Google scholar: Strengths and weaknesses. *The FASEB Journal*, *22*(2), 338–342. <https://doi.org/10.1096/fj.07-9492LSF>
- Fan, H., Tariq, S., & Zayed, T. (2022). Acoustic leak detection approaches for water pipelines. *Automation in Construction*, *138*, 104226. <https://doi.org/10.1016/j.autcon.2022.104226>
- Farah, E., & Shahrour, I. (2017). Leakage Detection Using Smart Water System: Combination of Water Balance and Automated Minimum Night Flow. *Water Resources Management*, *31*(15), 4821–4833. <https://doi.org/10.1007/s11269-017-1780-9>
- Fares, A., Tijani, I. A., Rui, Z., & Zayed, T. (2022). Leak detection in real water distribution networks based on acoustic emission and machine learning. *Environmental Technology*, *0*(0), 1–17. <https://doi.org/10.1080/09593330.2022.2074320>
- Friedman, J. H. (2001). Greedy function approximation: A gradient boosting machine. *Annals of Statistics*, 1189–1232.
- Gao, Y., Brennan, M. J., & Joseph, P. F. (2006). A comparison of time delay estimators for the detection of leak noise signals in plastic water distribution pipes. *Journal of Sound and Vibration*, *292*(3–5), 552–570. <https://doi.org/10.1016/j.jsv.2005.08.014>
- Gao, Y., Brennan, M. J., Joseph, P. F., Muggleton, J. M., & Hunaidi, O. (2004). A model of the correlation function of leak noise in buried plastic pipes. *Journal of Sound and Vibration*, *277*(1–2), 133–148. <https://doi.org/10.1016/j.jsv.2003.08.045>
- Gao, Y., & Liu, Y. (2017). Theoretical and experimental investigation into structural and fluid motions at low frequencies in water distribution pipes. *Mechanical Systems and Signal Processing*, *90*, 126–140. <https://doi.org/10.1016/j.ymssp.2016.12.018>
- Goldstein, A., Kapelner, A., Bleich, J., & Pitkin, E. (2015). Peeking Inside the Black Box: Visualizing Statistical Learning With Plots of Individual Conditional Expectation.

*Journal of Computational and Graphical Statistics*, 24(1), 44–65.  
<https://doi.org/10.1080/10618600.2014.907095>

Gong, J., Lambert, M. F., Stephens, M. L., Cazzolato, B. S., & Zhang, C. (2020). Detection of Emerging through-Wall Cracks for Pipe Break Early Warning in Water Distribution Systems Using Permanent Acoustic Monitoring and Acoustic Wave Analysis. *Water Resources Management*, 34(8), 2419–2432.  
<https://doi.org/10.1007/s11269-020-02560-1>

Goodfellow, I., Bengio, Y., & Courville, A. (2016). *Deep learning*. MIT press.

Goodfellow, I., Pouget-Abadie, J., Mirza, M., Xu, B., Warde-Farley, D., Ozair, S., Courville, A., & Bengio, Y. (2014). Generative adversarial nets. *Advances in Neural Information Processing Systems*, 27.

Guidotti, R., Monreale, A., Ruggieri, S., Turini, F., Giannotti, F., Pedreschi, D., Zuo, Z., Shuai, B., Wang, G., Liu, X., Wang, X., Wang, B., & Chen, Y. (2016). Learning Contextual Dependence With Convolutional Hierarchical Recurrent Neural Networks. *IEEE Transactions on Image Processing*, 25(7), 2983–2996.  
<https://doi.org/10.1109/TIP.2016.2548241>

Guidotti, R., Monreale, A., Ruggieri, S., Turini, F., Giannotti, F., Pedreschi, D., Zuo, Z., Shuai, B., Wang, G., Liu, X., Wang, X., Wang, B., & Chen, Y. (2019). A Survey of Methods for Explaining Black Box Models. *IEEE Transactions on Image Processing*, 51(5), 1–42. <https://doi.org/10.1145/3236009>

Guo, G., Yu, X., Liu, S., Ma, Z., Wu, Y., Xu, X., Wang, X., Smith, K., & Wu, X. (2021a). Leakage Detection in Water Distribution Systems Based on Time–Frequency Convolutional Neural Network. *Journal of Water Resources Planning and Management*, 147(2), 04020101. [https://doi.org/10.1061/\(ASCE\)WR.1943-5452.0001317](https://doi.org/10.1061/(ASCE)WR.1943-5452.0001317)

Guo, G., Yu, X., Liu, S., Ma, Z., Wu, Y., Xu, X., Wang, X., Smith, K., & Wu, X. (2021b). Leakage Detection in Water Distribution Systems Based on Time-Frequency Convolutional Neural Network. *Journal of Water Resources Planning and Management*, 147(2). [https://doi.org/10.1061/\(ASCE\)WR.1943-5452.0001317](https://doi.org/10.1061/(ASCE)WR.1943-5452.0001317)

- Guo, G., Yu, X., Liu, S., Xu, X., Ma, Z., Wang, X., Huang, Y., & Smith, K. (2020). Novel Leakage Detection and Localization Method Based on Line Spectrum Pair and Cubic Interpolation Search. *Water Resources Management*, *34*(12), 3895–3911. <https://doi.org/10.1007/s11269-020-02651-z>
- Guo, X., Song, H., Zeng, Y., Chen, H., Hu, W., & Liu, G. (2024). An intelligent water supply pipeline leakage detection method based on SV-WTBSVM. *Measurement Science and Technology*, *35*(4), 046125. <https://doi.org/10.1088/1361-6501/ad21d7>
- Haibo He, & Garcia, E. A. (2009a). Learning from Imbalanced Data. *IEEE Transactions on Knowledge and Data Engineering*, *21*(9), 1263–1284. <https://doi.org/10.1109/TKDE.2008.239>
- Haibo He, & Garcia, E. A. (2009b). Learning from Imbalanced Data. *IEEE Transactions on Knowledge and Data Engineering*, *21*(9), 1263–1284. <https://doi.org/10.1109/TKDE.2008.239>
- Harmouche, J., & Narasimhan, S. (2020). Long-Term Monitoring for Leaks in Water Distribution Networks Using Association Rules Mining. *IEEE TRANSACTIONS ON INDUSTRIAL INFORMATICS*, *16*(1), 258–266. <https://doi.org/10.1109/TII.2019.2911064>
- Haykin, S., & Network, N. (2004). A comprehensive foundation. *Neural Networks*, *2*(2004), 41.
- He, K., Zhang, X., Ren, S., & Sun, J. (2016). *Deep residual learning for image recognition*. 770–778.
- Hema, C., & Garcia Marquez, F. P. (2023). Emotional speech Recognition using CNN and Deep learning techniques. *Applied Acoustics*, *211*, 109492. <https://doi.org/10.1016/j.apacoust.2023.109492>
- Hendrycks, D., & Gimpel, K. (2016). Gaussian error linear units (gelus). *arXiv Preprint arXiv:1606.08415*.
- Hershey, S., Chaudhuri, S., Ellis, D. P., Gemmeke, J. F., Jansen, A., Moore, R. C., Plakal, M., Platt, D., Saurous, R. A., & Seybold, B. (2017). *CNN architectures for large-scale audio classification*. 131–135. <https://doi.org/10.1109/ICASSP.2017.7952132>

- Hochreiter, S., & Schmidhuber, J. (1997). Long Short-Term Memory. *Neural Computation*, 9(8), 1735–1780. <https://doi.org/10.1162/neco.1997.9.8.1735>
- Hoffer, E., & Ailon, N. (2015). *Deep metric learning using triplet network*. 84–92.
- Homma, T., & Saltelli, A. (1996). Importance measures in global sensitivity analysis of nonlinear models. *Reliability Engineering & System Safety*, 52(1), 1–17. [https://doi.org/10.1016/0951-8320\(96\)00002-6](https://doi.org/10.1016/0951-8320(96)00002-6)
- Hu, Z., Tariq, S., & Zayed, T. (2021). A comprehensive review of acoustic based leak localization method in pressurized pipelines. *Mechanical Systems and Signal Processing*, 161, 107994. <https://doi.org/10.1016/j.ymssp.2021.107994>
- Huang, N. E., Shen, Z., Long, S. R., Wu, M. C., Shih, H. H., Zheng, Q., Yen, N.-C., Tung, C. C., & Liu, H. H. (1998). The empirical mode decomposition and the Hilbert spectrum for nonlinear and non-stationary time series analysis. *Proceedings of the Royal Society of London. Series A: Mathematical, Physical and Engineering Sciences*, 454(1971), 903–995. <https://doi.org/10.1098/rspa.1998.0193>
- Huang, Y., Bao, H., & Qi, X. (2018). Seismic Random Noise Attenuation Method Based on Variational Mode Decomposition and Correlation Coefficients. *Electronics*, 7(11), 280. <https://doi.org/10.3390/electronics7110280>
- Huber, P. J. (1992). Robust estimation of a location parameter. In *Breakthroughs in statistics: Methodology and distribution* (pp. 492–518). Springer.
- Hunaidi, O., & Chu, W. T. (1999). Acoustical characteristics of leak signals in plastic water distribution pipes. *Applied Acoustics*, 58(3), 235–254. [https://doi.org/10.1016/S0003-682X\(99\)00013-4](https://doi.org/10.1016/S0003-682X(99)00013-4)
- Iandola, F. N., Han, S., Moskewicz, M. W., Ashraf, K., Dally, W. J., & Keutzer, K. (2016). SqueezeNet: AlexNet-level accuracy with 50x fewer parameters and < 0.5 MB model size. *arXiv Preprint arXiv:1602.07360*.
- Isah, A., Shin, H., Oh, S., Oh, S., Aliyu, I., Um, T., & Kim, J. (2023). Digital Twins Temporal Dependencies-Based on Time Series Using Multivariate Long Short-Term Memory. *Electronics*, 12(19), 4187. <https://doi.org/10.3390/electronics12194187>

- Jara-Arriagada, C., Ulusoy, A.-J., & Stoianov, I. (2024). Localization of Transient Pressure Sources in Water Supply Networks with Connectivity Uncertainty. *Journal of Water Resources Planning and Management*, 150(4), 04024002. <https://doi.org/10.1061/JWRMD5.WRENG-6235>
- Jeni, L. A., Cohn, J. F., & De La Torre, F. (2013). Facing Imbalanced Data—Recommendations for the Use of Performance Metrics. *2013 Humaine Association Conference on Affective Computing and Intelligent Interaction*, 245–251. <https://doi.org/10.1109/ACII.2013.47>
- Jiao, J., Zhao, M., Lin, J., & Liang, K. (2020). A comprehensive review on convolutional neural network in machine fault diagnosis. *Neurocomputing*, 417, 36–63. <https://doi.org/10.1016/j.neucom.2020.07.088>
- Jin, H., Zhang, L., Liang, W., & Ding, Q. (2014). Integrated leakage detection and localization model for gas pipelines based on the acoustic wave method. *Journal of Loss Prevention in the Process Industries*, 27, 74–88. <https://doi.org/10.1016/j.jlp.2013.11.006>
- Jin, Y., Hou, L., & Chen, Y. (2022). A Time Series Transformer based method for the rotating machinery fault diagnosis. *Neurocomputing*, 494, 379–395. <https://doi.org/10.1016/j.neucom.2022.04.111>
- Kammoun, M., Kammoun, A., & Abid, M. (2022). Leak Detection Methods in Water Distribution Networks: A Comparative Survey on Artificial Intelligence Applications. *Journal of Pipeline Systems Engineering and Practice*, 13(3), 04022024. [https://doi.org/10.1061/\(ASCE\)PS.1949-1204.0000646](https://doi.org/10.1061/(ASCE)PS.1949-1204.0000646)
- Kang, J., Park, Y.-J., Lee, J., Wang, S.-H., & Eom, D.-S. (2018). Novel Leakage Detection by Ensemble CNN-SVM and Graph-Based Localization in Water Distribution Systems. *IEEE Transactions on Industrial Electronics*, 65(5), 4279–4289. *IEEE Transactions on Industrial Electronics*. <https://doi.org/10.1109/TIE.2017.2764861>

- Kasdin, N. J. (1995). Discrete simulation of colored noise and stochastic processes and  $1/f$  power law noise generation. *Proceedings of the IEEE*, 83(5), 802–827. <https://doi.org/10.1109/5.381848>
- Khulief, Y. A., Khalifa, A., Mansour, R. B., & Habib, M. A. (2012a). Acoustic Detection of Leaks in Water Pipelines Using Measurements inside Pipe. *Journal of Pipeline Systems Engineering and Practice*, 3(2), 47–54. [https://doi.org/10.1061/\(ASCE\)PS.1949-1204.0000089](https://doi.org/10.1061/(ASCE)PS.1949-1204.0000089)
- Khulief, Y. A., Khalifa, A., Mansour, R. B., & Habib, M. A. (2012b). Acoustic Detection of Leaks in Water Pipelines Using Measurements inside Pipe. *Journal of Pipeline Systems Engineering and Practice*, 3(2), 47–54. [https://doi.org/10.1061/\(ASCE\)PS.1949-1204.0000089](https://doi.org/10.1061/(ASCE)PS.1949-1204.0000089)
- Kingma, D. P., & Welling, M. (2013). Auto-encoding variational bayes. *arXiv Preprint arXiv:1312.6114*.
- Kiranyaz, S., Avci, O., Abdeljaber, O., Ince, T., Gabbouj, M., & Inman, D. J. (2021). 1D convolutional neural networks and applications: A survey. *Mechanical Systems and Signal Processing*, 151, 107398. <https://doi.org/10.1016/j.ymsp.2020.107398>
- Kıymık, M. K., Güler, İ., Dizibüyük, A., & Akın, M. (2005). Comparison of STFT and wavelet transform methods in determining epileptic seizure activity in EEG signals for real-time application. *Computers in Biology and Medicine*, 35(7), 603–616. <https://doi.org/10.1016/j.combiomed.2004.05.001>
- Klema, V., & Laub, A. (1980). The singular value decomposition: Its computation and some applications. *IEEE Transactions on Automatic Control*, 25(2), 164–176. <https://doi.org/10.1109/TAC.1980.1102314>
- Knapp, C., & Carter, G. (1976). The generalized correlation method for estimation of time delay. *IEEE Transactions on Acoustics, Speech, and Signal Processing*, 24(4), 320–327. <https://doi.org/10.1109/TASSP.1976.1162830>
- Koch, G., Zemel, R., & Salakhutdinov, R. (2015). *Siamese neural networks for one-shot image recognition*. 2(1), 1–30.

- Kong, Q., Cao, Y., Iqbal, T., Xu, Y., Wang, W., & Plumbley, M. D. (2019). Cross-task learning for audio tagging, sound event detection and spatial localization: DCASE 2019 baseline systems. *arXiv Preprint arXiv:1904.03476*.
- Krizhevsky, A., Sutskever, I., & Hinton, G. E. (2012). Imagenet classification with deep convolutional neural networks. *Advances in Neural Information Processing Systems*, 25.
- Krizhevsky, A., Sutskever, I., & Hinton, G. E. (2017). ImageNet classification with deep convolutional neural networks. *Communications of the ACM*, 60(6), 84–90. <https://doi.org/10.1145/3065386>
- Krogh, A. (2008). What are artificial neural networks? *Nature Biotechnology*, 26(2), Article 2. <https://doi.org/10.1038/nbt1386>
- Kumar, D., Tu, D., Zhu, N., Hou, D., & Zhang, H. (2017). In-Line Acoustic Device Inspection of Leakage in Water Distribution Pipes Based on Wavelet and Neural Network. *Journal of Sensors*, 2017. <https://doi.org/10.1155/2017/5789510>
- Leak Detection Systems Home*. (2023). Aquarius Spectrum. <https://aqs-systems.com/>
- LeCun, Y., Bengio, Y., & Hinton, G. (2015). Deep learning. *Nature*, 521(7553), 436–444.
- LeCun, Y., Bottou, L., Bengio, Y., & Haffner, P. (1998). Gradient-based learning applied to document recognition. *Proceedings of the IEEE*, 86(11), 2278–2324. <https://doi.org/10.1109/5.726791>
- Levinas, D., Perelman, G., & Ostfeld, A. (2021). Water Leak Localization Using High-Resolution Pressure Sensors. *Water*, 13(5), Article 5. <https://doi.org/10.3390/w13050591>
- Li, F., Li, R., Tian, L., Chen, L., & Liu, J. (2019). Data-driven time-frequency analysis method based on variational mode decomposition and its application to gear fault diagnosis in variable working conditions. *Mechanical Systems and Signal Processing*, 116, 462–479. <https://doi.org/10.1016/j.ymssp.2018.06.055>

- Li, J., Liu, Z., He, C., Yue, H., & Gou, S. (2017). Water shortages raised a legitimate concern over the sustainable development of the drylands of northern China: Evidence from the water stress index. *Science of The Total Environment*, 590–591, 739–750. <https://doi.org/10.1016/j.scitotenv.2017.03.037>
- Li, J., Zheng, W., & Lu, C. (2022). An Accurate Leakage Localization Method for Water Supply Network Based on Deep Learning Network. *Water Resources Management*, 36(7), 2309–2325. <https://doi.org/10.1007/s11269-022-03144-x>
- Li, M., Zou, D., Luo, S., Zhou, Q., Cao, L., & Liu, H. (2022). A new generative adversarial network based imbalanced fault diagnosis method. *Measurement*, 194, 111045. <https://doi.org/10.1016/j.measurement.2022.111045>
- Li, R., Huang, H., Xin, K., & Tao, T. (2015). A review of methods for burst/leakage detection and location in water distribution systems. *WATER SCIENCE AND TECHNOLOGY-WATER SUPPLY*, 15(3), 429–441. <https://doi.org/10.2166/ws.2014.131>
- Li, S., Li, T., Sun, C., Yan, R., & Chen, X. (2009). Multilayer Grad-CAM: An effective tool towards explainable deep neural networks for intelligent fault diagnosis. *Digital Signal Processing*, 19(1), 153–183. <https://doi.org/10.1016/j.jmsy.2023.05.027>
- Li, S., Song, Y., & Zhou, G. (2018). Leak detection of water distribution pipeline subject to failure of socket joint based on acoustic emission and pattern recognition. *Measurement*, 115, 39–44. <https://doi.org/10.1016/j.measurement.2017.10.021>
- LI, Y., & LIU, C. (2017). Advances in leak detection and location based on acoustic wave for gas pipelines. *Chinese Science Bulletin*, 62(7), 650–658. <https://doi.org/10.1360/N972015-01452>
- Li, Z., Chen, J., Zi, Y., Pan, J., Xu, T., Zeng, Z., Huang, X., Li, J., & Feng, H. (2017). Independence-oriented VMD to identify fault feature for wheel set bearing fault diagnosis of high speed locomotive. *Mechanical Systems and Signal Processing*, 85, 512–529. <https://doi.org/10.1016/j.ymsp.2016.08.042>
- Liu, B., Jiang, Z., Nie, W., Ran, Y., & Lin, H. (2021a). Research on leak location method of water supply pipeline based on negative pressure wave technology and VMD

algorithm. *Measurement*, 186, 110235.  
<https://doi.org/10.1016/j.measurement.2021.110235>

Liu, B., Jiang, Z., Nie, W., Ran, Y., & Lin, H. (2021b). Research on leak location method of water supply pipeline based on negative pressure wave technology and VMD algorithm. *Measurement*, 186, 110235.  
<https://doi.org/10.1016/j.measurement.2021.110235>

Liu, J., Wang, J., Liu, S., & Qian, X. (2018). Feature extraction and identification of leak acoustic signal in water supply pipelines using correlation analysis and Lyapunov exponent. *Vibroengineering PROCEDIA*, 19, 182–187.  
<https://doi.org/10.21595/vp.2018.20113>

Liu, M., He, J., Huang, Y., Tang, T., Hu, J., & Xiao, X. (2022). Algal bloom forecasting with time-frequency analysis: A hybrid deep learning approach. *Water Research*, 219, 118591. <https://doi.org/10.1016/j.watres.2022.118591>

Liu, M., Yang, J., Li, S., Zhou, Z., Fan, E., & Zheng, W. (2022). Robust GMM least square twin K-class support vector machine for urban water pipe leak recognition. *Expert Systems with Applications*, 195, 116525.  
<https://doi.org/10.1016/j.eswa.2022.116525>

Liu, M., Yang, J., Zheng, W., & Fan, E. (2021). Using Novel Complex-Efficient FastICA Blind Deconvolution Method for Urban Water Pipe Leak Localization in the Presence of Branch Noise. *Journal of Water Resources Planning and Management*, 147(10), 04021072. [https://doi.org/10.1061/\(ASCE\)WR.1943-5452.0001453](https://doi.org/10.1061/(ASCE)WR.1943-5452.0001453)

Liu, P., Xu, C., Xie, J., Fu, M., Chen, Y., Liu, Z., & Zhang, Z. (2023). A CNN-based transfer learning method for leakage detection of pipeline under multiple working conditions with AE signals. *Process Safety and Environmental Protection*, 170, 1161–1172. <https://doi.org/10.1016/j.psep.2022.12.070>

Liu, T., Zheng, H., Zheng, P., Bao, J., Wang, J., Liu, X., & Yang, C. (2023). An expert knowledge-empowered CNN approach for welding radiographic image recognition. *Advanced Engineering Informatics*, 56, 101963.  
<https://doi.org/10.1016/j.aei.2023.101963>

- Liu, Y., Ma, X., Li, Y., Tie, Y., Zhang, Y., & Gao, J. (2019). Water Pipeline Leakage Detection Based on Machine Learning and Wireless Sensor Networks. *Sensors*, *19*(23), Article 23. <https://doi.org/10.3390/s19235086>
- López, V., Fernández, A., García, S., Palade, V., & Herrera, F. (2013). An insight into classification with imbalanced data: Empirical results and current trends on using data intrinsic characteristics. *Information Sciences*, *250*, 113–141. <https://doi.org/10.1016/j.ins.2013.07.007>
- Lu, W., Zhang, L., Liang, W., & Yu, X. (2016). Research on a small-noise reduction method based on EMD and its application in pipeline leakage detection. *Journal of Loss Prevention in the Process Industries*, *41*, 282–293.
- Luong, T., & Kim, J. (2020). The Enhancement of Leak Detection Performance for Water Pipelines through the Renovation of Training Data. *Sensors*, *20*(9). <https://doi.org/10.3390/s20092542>
- Lyu, P., Chen, N., Mao, S., & Li, M. (2020). LSTM based encoder-decoder for short-term predictions of gas concentration using multi-sensor fusion. *Process Safety and Environmental Protection*, *137*, 93–105. <https://doi.org/10.1016/j.psep.2020.02.021>
- MacQueen, J. (1967). *Classification and analysis of multivariate observations*. 281–297.
- Mallat, S. G. (2009). *A wavelet tour of signal processing: The sparse way* (3rd ed). Elsevier/Academic Press.
- Martinez, M., & Stiefelhagen, R. (2019). *Taming the cross entropy loss*. 628–637.
- Martini, A., Troncossi, M., & Rivola, A. (2015). Automatic Leak Detection in Buried Plastic Pipes of Water Supply Networks by Means of Vibration Measurements. *Shock and Vibration*, *2015*, 1–13. <https://doi.org/10.1155/2015/165304>
- Martini, A., Troncossi, M., & Rivola, A. (2017). Vibroacoustic Measurements for Detecting Water Leaks in Buried Small-Diameter Plastic Pipes. *Journal of Pipeline Systems Engineering and Practice*, *8*(4), 04017022. [https://doi.org/10.1061/\(ASCE\)PS.1949-1204.0000287](https://doi.org/10.1061/(ASCE)PS.1949-1204.0000287)

- McCulloch, W. S., & Pitts, W. (1943). A logical calculus of the ideas immanent in nervous activity. *The Bulletin of Mathematical Biophysics*, 5(4), 115–133. <https://doi.org/10.1007/BF02478259>
- Mei, L., Zhou, J., Li, S., Cai, M., & Li, T. (2022). Leak Identification Based on CS-ResNet Under Different Leakage Apertures for Water-Supply Pipeline. *IEEE Access*, 10, 57783–57795. <https://doi.org/10.1109/ACCESS.2022.3177595>
- Meng, L., Tan, W., Ma, J., Wang, R., Yin, X., & Zhang, Y. (2022). Enhancing dynamic ECG heartbeat classification with lightweight transformer model. *Artificial Intelligence in Medicine*, 124, 102236. <https://doi.org/10.1016/j.artmed.2022.102236>
- Meng, Z., Guo, X., Pan, Z., Sun, D., & Liu, S. (2019). Data Segmentation and Augmentation Methods Based on Raw Data Using Deep Neural Networks Approach for Rotating Machinery Fault Diagnosis. *IEEE Access*, 7, 79510–79522. [IEEE Access. https://doi.org/10.1109/ACCESS.2019.2923417](https://doi.org/10.1109/ACCESS.2019.2923417)
- Miettinen, J., Haikonen, S., Koene, I., Keski-Rahkonen, J., & Viitala, R. (2009). Comparing torsional and lateral vibration data for deep learning-based drive train gear diagnosis. *Digital Signal Processing*, 19(1), 153–183. <https://doi.org/10.1016/j.ymsp.2023.110710>
- Misiunas, D., Vítkovský, J., Olsson, G., Simpson, A., & Lambert, M. (2005). Pipeline Break Detection Using Pressure Transient Monitoring. *Journal of Water Resources Planning and Management*, 131(4), 316–325. [https://doi.org/10.1061/\(ASCE\)0733-9496\(2005\)131:4\(316\)](https://doi.org/10.1061/(ASCE)0733-9496(2005)131:4(316))
- Moghar, A., & Hamiche, M. (2020). Stock Market Prediction Using LSTM Recurrent Neural Network. *Procedia Computer Science*, 170, 1168–1173. <https://doi.org/10.1016/j.procs.2020.03.049>
- Mongeon, P., & Paul-Hus, A. (2016). The journal coverage of Web of Science and Scopus: A comparative analysis. *Scientometrics*, 106(1), 213–228. <https://doi.org/10.1007/s11192-015-1765-5>

- Muggleton, J., Brennan, M., & Pinnington, R. (2002). Wavenumber prediction of waves in buried pipes for water leak detection. *Journal of Sound and Vibration*, 249(5), 939–954.
- Muggleton, J. M., Brennan, M. J., & Linford, P. W. (2004). Axisymmetric wave propagation in fluid-filled pipes: Wavenumber measurements in in vacuo and buried pipes. *Journal of Sound and Vibration*, 270(1–2), 171–190. [https://doi.org/10.1016/S0022-460X\(03\)00489-9](https://doi.org/10.1016/S0022-460X(03)00489-9)
- Muller, R., Illium, S., Ritz, F., Schroder, T., Platschek, C., Ochs, J., & Linnhoff-Popien, C. (2021). *Acoustic Leak Detection in Water Networks* (A. Rocha, L. Steels, & J. VandenHerik, Eds.; 9 ; pp. 306–313). <https://doi.org/10.5220/0010295403060313>
- Murvay, P.-S., & Silea, I. (2012). A survey on gas leak detection and localization techniques. *Journal of Loss Prevention in the Process Industries*, 25(6), 966–973. <https://doi.org/10.1016/j.jlp.2012.05.010>
- Mwelase, L. T. (2016). *Non-revenue water: Most suitable business model for water services authorities in South Africa: Ugu District Municipality* [Theses and dissertations]. Durban University of Technology.
- Nainan, S., & Kulkarni, V. (2021). Enhancement in speaker recognition for optimized speech features using GMM, SVM and 1-D CNN. *International Journal of Speech Technology*, 24(4), 809–822. <https://doi.org/10.1007/s10772-020-09771-2>
- Nair, V., & Hinton, G. E. (2010). *Rectified linear units improve restricted boltzmann machines*. 807–814.
- Nam, H., Kim, S.-H., & Park, Y.-H. (2022). Filteraugument: An Acoustic Environmental Data Augmentation Method. *ICASSP 2022 - 2022 IEEE International Conference on Acoustics, Speech and Signal Processing (ICASSP)*, 4308–4312. <https://doi.org/10.1109/ICASSP43922.2022.9747680>
- Nam, Y., Arai, Y., Kunizane, T., & Koizumi, A. (2021). Water leak detection based on convolutional neural network (CNN) using actual leak sounds and the hold-out method. *Water Supply*, 21(7), 3477–3485. <https://doi.org/10.2166/ws.2021.109>

- Nam, Y. W., Arai, Y., Kunizane, T., & Koizumi, A. (2021). Water leak detection based on convolutional neural network (CNN) using actual leak sounds and the hold-out method. *Water Supply*, 9.
- Nguyen, N. H., Doğançay, K., & Wang, W. (2020). Adaptive estimation and sparse sampling for graph signals in alpha-stable noise. *Digital Signal Processing*, 105, 102782. <https://doi.org/10.1016/j.dsp.2020.102782>
- Nikos Fakotakis, D., Nousias, S., Arvanitis, G., Zacharaki, E. I., & Moustakas, K. (2023). AI Sound Recognition on Asthma Medication Adherence: Evaluation With the RDA Benchmark Suite. *IEEE Access*, 11, 13810–13829. <https://doi.org/10.1109/ACCESS.2023.3243547>
- Nishizaki, H. (2017). *Data augmentation and feature extraction using variational autoencoder for acoustic modeling*. 1222–1227. <https://doi.org/10.1109/APSIPA.2017.8282225>
- Oord, A. van den, Dieleman, S., Zen, H., Simonyan, K., Vinyals, O., Graves, A., Kalchbrenner, N., Senior, A., & Kavukcuoglu, K. (2016). Wavenet: A generative model for raw audio. *arXiv Preprint arXiv:1609.03499*.
- Ozevin, D., & Harding, J. (2012). Novel leak localization in pressurized pipeline networks using acoustic emission and geometric connectivity. *International Journal of Pressure Vessels and Piping*, 92, 63–69. <https://doi.org/10.1016/j.ijpvp.2012.01.001>
- Pan, S., Xu, Z., Li, D., & Lu, D. (2018). Research on Detection and Location of Fluid-Filled Pipeline Leakage Based on Acoustic Emission Technology. *Sensors*, 18(11), Article 11. <https://doi.org/10.3390/s18113628>
- Pang, B., Liu, Q., Sun, Z., Xu, Z., & Hao, Z. (2024). Time-frequency supervised contrastive learning via pseudo-labeling: An unsupervised domain adaptation network for rolling bearing fault diagnosis under time-varying speeds. *Advanced Engineering Informatics*, 59, 102304. <https://doi.org/10.1016/j.aei.2023.102304>
- Papastefanou, A. (2011). *An experimental investigation of leak noise from water filled plastic pipes (Doctoral dissertation)*. University of Southampton.

- Papastefanou, A. S., Joseph, P. F., & Brennan, M. J. (2012). Experimental Investigation into the Characteristics of In-Pipe Leak Noise in Plastic Water Filled Pipes. *Acta Acustica United with Acustica*, 98(6), 847–856. <https://doi.org/10.3813/AAA.918568>
- Park, D. S., Chan, W., Zhang, Y., Chiu, C.-C., Zoph, B., Cubuk, E. D., & Le, Q. V. (2019). Specaugment: A simple data augmentation method for automatic speech recognition. *arXiv Preprint arXiv:1904.08779*.
- Patel, M., Patel, A., & Ghosh, D. R. (2018). Precipitation nowcasting: Leveraging bidirectional lstm and 1d cnn. *arXiv Preprint arXiv:1810.10485*.
- Peng, L., Zhang, J., Lu, S., Li, Y., & Du, G. (2023). One-dimensional residual convolutional neural network and percussion-based method for pipeline leakage and water deposit detection. *Process Safety and Environmental Protection*, 177, 1142–1153. <https://doi.org/10.1016/j.psep.2023.07.059>
- Pincus, S. (1995). Approximate entropy (ApEn) as a complexity measure. *Chaos: An Interdisciplinary Journal of Nonlinear Science*, 5(1), 110–117. <https://doi.org/10.1063/1.166092>
- Provost, F., & Fawcett, T. (2013). *Data Science for Business: What you need to know about data mining and data-analytic thinking*. O'Reilly Media, Inc.
- Puust, R., Kapelan, Z., Savic, D. A., & Koppel, T. (2010). A review of methods for leakage management in pipe networks. *Urban Water Journal*, 7(1), 25–45. <https://doi.org/10.1080/15730621003610878>
- Qu, H., Li, T., & Chen, G. (2019). Synchro-squeezed adaptive wavelet transform with optimum parameters for arbitrary time series. *Mechanical Systems and Signal Processing*, 114, 366–377. <https://doi.org/10.1016/j.ymsp.2018.05.020>
- Quy, T. B., Muhammad, S., & Kim, J.-M. (2019). A Reliable Acoustic EMISSION Based Technique for the Detection of a Small Leak in a Pipeline System. *Energies*, 12(8), Article 8. <https://doi.org/10.3390/en12081472>

- Quy, T., & Kim, J. (2019). *Leakage Detection of Water-Induced Pipelines Using Hybrid Features and Support Vector Machines* (S. Bhatia, S. Tiwari, K. Mishra, & M. Trivedi, Eds.; 0 ; Vol. 924, pp. 377–387). [https://doi.org/10.1007/978-981-13-6861-5\\_33](https://doi.org/10.1007/978-981-13-6861-5_33)
- Rai, A., & Kim, J.-M. (2021). A novel pipeline leak detection approach independent of prior failure information. *Measurement*, *167*, 108284. <https://doi.org/10.1016/j.measurement.2020.108284>
- Rajani, B., & Kleiner, Y. (2001). Comprehensive review of structural deterioration of water mains: Physically based models. *Urban Water*, *3*(3), 151–164. [https://doi.org/10.1016/S1462-0758\(01\)00032-2](https://doi.org/10.1016/S1462-0758(01)00032-2)
- Rashid, S., Akram, U., Qaisar, S., Khan, S. A., & Felemban, E. (2014). Wireless Sensor Network for Distributed Event Detection Based on Machine Learning. *2014 IEEE International Conference on Internet of Things(iThings), and IEEE Green Computing and Communications (GreenCom) and IEEE Cyber, Physical and Social Computing (CPSCom)*, 540–545. <https://doi.org/10.1109/iThings.2014.93>
- Ravichandran, T., Gavahi, K., Ponnambalam, K., Burtea, V., & Mousavi, S. (2021). Ensemble-based machine learning approach for improved leak detection in water mains. *Journal of Hydraulic Research*, *23*(2), 307–323. <https://doi.org/10.2166/hydro.2021.093>
- Ravichandran, T., Gavahi, K., Ponnambalam, K., Burtea, V., Mousavi, S. J., Ahmad, S., Ahmad, Z., Kim, C.-H., & Kim, J.-M. (2021). A Method for Pipeline Leak Detection Based on Acoustic Imaging and Deep Learning. *Sensors*, *22*(4), Article 4. <https://doi.org/10.3390/s22041562>
- Rayaroth, R., & G, S. (2019). Random Bagging Classifier and Shuffled Frog Leaping Based Optimal Sensor Placement for Leakage Detection in WDS. *Water Resources Management*, *33*(9), 3111–3125. <https://doi.org/10.1007/s11269-019-02296-7>
- Richman, J. S., & Moorman, J. R. (2000). Physiological time-series analysis using approximate entropy and sample entropy. *American Journal of Physiology-Heart and Circulatory Physiology*, *278*(6), H2039–H2049. <https://doi.org/10.1152/ajpheart.2000.278.6.H2039>

- Ruan, D., Wang, J., Yan, J., & Gühmann, C. (2023). CNN parameter design based on fault signal analysis and its application in bearing fault diagnosis. *Advanced Engineering Informatics*, 55, 101877. <https://doi.org/10.1016/j.aei.2023.101877>
- Rumelhart, D. E., Hinton, G. E., & Williams, R. J. (1986). Learning representations by back-propagating errors. *Nature*, 323(6088), 533–536. <https://doi.org/10.1038/323533a0>
- Samorodnitsky, G., Taqqu, M. S., & Linde, R. (1996). Stable non-gaussian random processes: Stochastic models with infinite variance. *Bulletin of the London Mathematical Society*, 28(134), 554–555.
- Santoro, D., & Grilli, L. (2022). Generative Adversarial Network to evaluate quantity of information in financial markets. *Neural Computing and Applications*, 34(20), 17473–17490. <https://doi.org/10.1007/s00521-022-07401-3>
- Santos, C. F. G. D., & Papa, J. P. (2009). Avoiding Overfitting: A Survey on Regularization Methods for Convolutional Neural Networks. *Digital Signal Processing*, 19(1), 153–183. <https://doi.org/10.1145/3510413>
- Santos, C. F. G. D., Papa, J. P., Li, S., Li, T., Sun, C., Yan, R., Chen, X., Sejdić, E., Djurović, I., & Jiang, J. (2009). Time–frequency feature representation using energy concentration: An overview of recent advances. *Digital Signal Processing*, 19(1), 153–183. <https://doi.org/10.1016/j.dsp.2007.12.004>
- Saravanabalaji, M., Sivakumaran, N., Ranganthan, S., & Athappan, V. (2023). Acoustic signal based water leakage detection system using hybrid machine learning model. *Urban Water Journal*, 20(9), 1123–1139. <https://doi.org/10.1080/1573062X.2023.2239782>
- Scherer, D., Müller, A., & Behnke, S. (2010). Evaluation of Pooling Operations in Convolutional Architectures for Object Recognition. In K. Diamantaras, W. Duch, & L. S. Iliadis (Eds.), *Artificial Neural Networks – ICANN 2010* (1482 ; pp. 92–101). Springer. [https://doi.org/10.1007/978-3-642-15825-4\\_10](https://doi.org/10.1007/978-3-642-15825-4_10)
- Scussel, O., Brennan, M. J., De Almeida, F. C. L., Iwanaga, M. K., Muggleton, J. M., Joseph, P. F., & Gao, Y. (2023). Key Factors That Influence the Frequency Range of

Measured Leak Noise in Buried Plastic Water Pipes: Theory and Experiment. *Acoustics*, 5(2), 490–508. <https://doi.org/10.3390/acoustics5020029>

Selvaraju, R. R., Cogswell, M., Das, A., Vedantam, R., Parikh, D., & Batra, D. (2020). Grad-CAM: Visual Explanations from Deep Networks via Gradient-Based Localization. *International Journal of Computer Vision*, 128(2), 336–359. <https://doi.org/10.1007/s11263-019-01228-7>

Shukla, H., & Piratla, K. (2019). *An Automated Leakage Detection Model for Water Distribution System*.

Shukla, H., & Piratla, K. (2020a). Leakage detection in water pipelines using supervised classification of acceleration signals. *Automation in Construction*, 117. <https://doi.org/10.1016/j.autcon.2020.103256>

Shukla, H., & Piratla, K. R. (2020b). Unsupervised Classification of Flow-Induced Vibration Signals to Detect Leakages in Water Distribution Pipelines. In J. F. Pulido & M. Poppe (Eds.), *Pipelines 2020: Planning and Design* (pp. 437–444). Amer Soc Civil Engineers. <https://www.webofscience.com/wos/woscc/full-record/WOS:000614861000048>

Shukla, H., Piratla, K. R., & Atamturktur, S. (2020). Influence of Soil Backfill on Vibration-Based Pipeline Leakage Detection. *Journal of Pipeline Systems Engineering and Practice*, 11(1), 04019055. [https://doi.org/10.1061/\(ASCE\)PS.1949-1204.0000435](https://doi.org/10.1061/(ASCE)PS.1949-1204.0000435)

Siddique, M. F., Ahmad, Z., & Kim, J.-M. (2023). Pipeline leak diagnosis based on leak-augmented scalograms and deep learning. *Engineering Applications of Computational Fluid Mechanics*, 17(1), 2225577. <https://doi.org/10.1080/19942060.2023.2225577>

Siddique, M. F., Ahmad, Z., Ullah, N., & Kim, J. (2023). A Hybrid Deep Learning Approach: Integrating Short-Time Fourier Transform and Continuous Wavelet Transform for Improved Pipeline Leak Detection. *Sensors*, 23(19), Article 19. <https://doi.org/10.3390/s23198079>

- Simonyan, K., & Zisserman, A. (2014, September 4). *Very Deep Convolutional Networks for Large-Scale Image Recognition*. arXiv.Org. <https://arxiv.org/abs/1409.1556v6>
- Singh, S., Agrawal, S., Sahu, T., & Das, D. (2021). *iPipe: Water pipeline monitoring and leakage detection*. 367–372.
- Sitaropoulos, K., Salamone, S., & Sela, L. (2023a). Frequency-based leak signature investigation using acoustic sensors in urban water distribution networks. *Advanced Engineering Informatics*, 55, 101905. <https://doi.org/10.1016/j.aei.2023.101905>
- Sitaropoulos, K., Salamone, S., & Sela, L. (2023b). Frequency-based leak signature investigation using acoustic sensors in urban water distribution networks. *Advanced Engineering Informatics*, 55, 101905. <https://doi.org/10.1016/j.aei.2023.101905>
- Smruthy, A., & Suchetha, M. (2017). Real-Time Classification of Healthy and Apnea Subjects Using ECG Signals With Variational Mode Decomposition. *IEEE Sensors Journal*, 17(10), 3092–3099. <https://doi.org/10.1109/JSEN.2017.2690805>
- Song, H., Li, G., Li, X., Xiong, X., Qin, Q., & Mitrouchev, P. (2023). Developing a data-driven hydraulic excavator fuel consumption prediction system based on deep learning. *Advanced Engineering Informatics*, 57, 102063. <https://doi.org/10.1016/j.aei.2023.102063>
- Song, X., Fan, X., Xiang, C., Ye, Q., Liu, L., Wang, Z., He, X., Yang, N., & Fang, G. (2019). A Novel Convolutional Neural Network Based Indoor Localization Framework With WiFi Fingerprinting. *IEEE Access*, 7, 110698–110709. <https://doi.org/10.1109/ACCESS.2019.2933921>
- Sousa, D. P., Du, R., Mairton Barros da Silva Jr, J., Cavalcante, C. C., & Fischione, C. (2023). Leakage detection in water distribution networks using machine-learning strategies. *Water Supply*, 23(3), 1115–1126. <https://doi.org/10.2166/ws.2023.054>
- Srirangarajan, S., Iqbal, M., Lim, H. B., Allen, M., Preis, A., & Whittle, A. J. (2010). Water main burst event detection and localization. *Water Distribution Systems Analysis 2010*, 1324–1335. [https://doi.org/10.1061/41203\(425\)119](https://doi.org/10.1061/41203(425)119)

- Stieglitz, S., Wilms, K., Mirbabaie, M., Hofeditz, L., Brenger, B., López, A., & Rehwald, S. (2020). When are researchers willing to share their data? – Impacts of values and uncertainty on open data in academia. *PLOS ONE*, *15*(7), e0234172. <https://doi.org/10.1371/journal.pone.0234172>
- Sun, J., Xiao, Q., Wen, J., & Zhang, Y. (2016). Natural gas pipeline leak aperture identification and location based on local mean decomposition analysis. *Measurement*, *79*, 147–157. <https://doi.org/10.1016/j.measurement.2015.10.015>
- Svantesson, M., Olausson, H., Eklund, A., & Thordstein, M. (2023). Get a New Perspective on EEG: Convolutional Neural Network Encoders for Parametric t-SNE. *Brain Sciences*, *13*(3), 453. <https://doi.org/10.3390/brainsci13030453>
- Szandała, T. (2023). Unlocking the black box of CNNs: Visualising the decision-making process with PRISM. *Information Sciences*, *642*, 119162. <https://doi.org/10.1016/j.ins.2023.119162>
- Tariq, S., Bakhtawar, B., & Zayed, T. (2021). Data-driven application of MEMS-based accelerometers for leak detection in water distribution networks. *Science of The Total Environment*, *151110*. <https://doi.org/10.1016/j.scitotenv.2021.151110>
- Tariq, S., Bakhtawar, B., & Zayed, T. (2022). Data-driven application of MEMS-based accelerometers for leak detection in water distribution networks. *Science of The Total Environment*, *809*, 151110. <https://doi.org/10.1016/j.scitotenv.2021.151110>
- Taylor, R. G., Scanlon, B., Döll, P., Rodell, M., van Beek, R., Wada, Y., Longuevergne, L., Leblanc, M., Famiglietti, J. S., Edmunds, M., Konikow, L., Green, T. R., Chen, J., Taniguchi, M., Bierkens, M. F. P., MacDonald, A., Fan, Y., Maxwell, R. M., Yechieli, Y., ... Treidel, H. (2013). Ground water and climate change. *Nature Climate Change*, *3*(4), 322–329. <https://doi.org/10.1038/nclimate1744>
- Tijani, I., Abdelmageed, S., Fares, A., Fan, K., Hu, Z., & Zayed, T. (2022). Improving the leak detection efficiency in water distribution networks using noise loggers. *Science of The Total Environment*, *821*. <https://doi.org/10.1016/j.scitotenv.2022.153530>

- Tijani, I., & Zayed, T. (2022). Gene expression programming based mathematical modeling for leak detection of water distribution networks. *Measurement*, 188. <https://doi.org/10.1016/j.measurement.2021.110611>
- Tin Kam Ho. (1998). The random subspace method for constructing decision forests. *IEEE Transactions on Pattern Analysis and Machine Intelligence*, 20(8), 832–844. <https://doi.org/10.1109/34.709601>
- Tsai, Y., Chang, H., Lin, S., Chiou, A., & Lee, T. (2022). Using Convolutional Neural Networks in the Development of a Water Pipe Leakage and Location Identification System. *APPLIED SCIENCES-BASEL*, 12(16). <https://doi.org/10.3390/app12168034>
- Ullah, N., Ahmed, Z., & Kim, J.-M. (2023). Pipeline Leakage Detection Using Acoustic Emission and Machine Learning Algorithms. *Sensors*, 23(6), 3226. <https://doi.org/10.3390/s23063226>
- Van der Maaten, L., & Hinton, G. (2008). Visualizing data using t-SNE. *Journal of Machine Learning Research*, 9(11).
- van Eck, N. J., & Waltman, L. (2010). Software survey: VOSviewer, a computer program for bibliometric mapping. *Scientometrics*, 84(2), 523–538. <https://doi.org/10.1007/s11192-009-0146-3>
- Vanijjirattikhan, R., Khomsay, S., Kitbutrawat, N., Khomsay, K., Supakchukul, U., Udomsuk, S., Suwatthikul, J., Oumtrakul, N., & Anusart, K. (2022). AI-based acoustic leak detection in water distribution systems. *RESULTS IN ENGINEERING*, 15. <https://doi.org/10.1016/j.rineng.2022.100557>
- Vankov, Y., Rumyantsev, A., Ziganshin, S., Politova, T., Minyazev, R., & Zagretdinov, A. (2020). Assessment of the Condition of Pipelines Using Convolutional Neural Networks. *Energies*, 13(3), Article 3. <https://doi.org/10.3390/en13030618>
- Vaswani, A., Shazeer, N., Parmar, N., Uszkoreit, J., Jones, L., Gomez, A. N., Kaiser, Ł., & Polosukhin, I. (2017). Attention is all you need. *Advances in Neural Information Processing Systems*, 30.

- Vera-Diaz, J. M., Pizarro, D., & Macias-Guarasa, J. (2021). Acoustic source localization with deep generalized cross correlations. *Signal Processing*, *187*, 108169. <https://doi.org/10.1016/j.sigpro.2021.108169>
- Virk, M., Mysorewala, M., Cheded, L., & Ali, I. (2020). Leak Detection Using Flow-Induced Vibrations in Pressurized Wall-Mounted Water Pipelines. *IEEE Access*, *8*, 188673–188687. <https://doi.org/10.1109/ACCESS.2020.3032319>
- Vrachimis, S. G., Eliades, D. G., Taormina, R., Kapelan, Z., Ostfeld, A., Liu, S., Kyriakou, M., Pavlou, P., Qiu, M., & Polycarpou, M. M. (2022). Battle of the Leakage Detection and Isolation Methods. *Journal of Water Resources Planning and Management*, *148*(12), 04022068. [https://doi.org/10.1061/\(ASCE\)WR.1943-5452.0001601](https://doi.org/10.1061/(ASCE)WR.1943-5452.0001601)
- Vrachimis, S. G., Timotheou, S., Eliades, D. G., & Polycarpou, M. M. (2021). Leakage detection and localization in water distribution systems: A model invalidation approach. *Control Engineering Practice*, *110*, 104755. <https://doi.org/10.1016/j.conengprac.2021.104755>
- Wang, F., Lin, W., Liu, Z., Wu, S., & Qiu, X. (2017). Pipeline leak detection by using time-domain statistical features. *IEEE Sensors Journal*, *17*(19), 6431–6442. <https://doi.org/10.1109/JSEN.2017.2740220>
- Wang, J., Yu, L., Zhang, W., Gong, Y., Xu, Y., Wang, B., Zhang, P., & Zhang, D. (2017). *Irgan: A minimax game for unifying generative and discriminative information retrieval models*. 515–524. <https://doi.org/10.1145/3077136.3080786>
- Wang, W., & Gao, Y. (2023). Pipeline leak detection method based on acoustic-pressure information fusion. *Measurement*, *212*, 112691. <https://doi.org/10.1016/j.measurement.2023.112691>
- Wang, W., Sun, H., Guo, J., Lao, L., Wu, S., & Zhang, J. (2021). Experimental study on water pipeline leak using In-Pipe acoustic signal analysis and artificial neural network prediction. *Measurement*, *186*. <https://doi.org/10.1016/j.measurement.2021.110094>

Wang, X., & Ghidaoui, M. S. (2018). Pipeline Leak Detection Using the Matched-Field Processing Method. *Journal of Hydraulic Engineering*, 144(6), 04018030. [https://doi.org/10.1061/\(ASCE\)HY.1943-7900.0001476](https://doi.org/10.1061/(ASCE)HY.1943-7900.0001476)

Wang, Y., Yao, Q., Kwok, J. T., & Ni, L. M. (2020). Generalizing from a few examples: A survey on few-shot learning. *ACM Computing Surveys (Csur)*, 53(3), 1–34. <https://doi.org/10.1145/3386252>

Wang, Z., Dai, Z., Póczos, B., & Carbonell, J. (2019). *Characterizing and avoiding negative transfer*. 11293–11302.

Wang, Z., He, X., Shen, H., Fan, S., & Zeng, Y. (2022). Multi-source information fusion to identify water supply pipe leakage based on SVM and VMD. *INFORMATION PROCESSING & MANAGEMENT*, 59(2). <https://doi.org/10.1016/j.ipm.2021.102819>

Wang, Z.-Q., Zhang, X., & Wang, D. (2018). *Robust TDOA Estimation Based on Time-Frequency Masking and Deep Neural Networks*. 322–326.

*Water Leak Detection Technology and Products*. (2023). Gutermann. <https://en.gutermann-water.com/products/>

Wen, L., Li, X., & Gao, L. (2020). A transfer convolutional neural network for fault diagnosis based on ResNet-50. *Neural Computing and Applications*, 32(10), 6111–6124. <https://doi.org/10.1007/s00521-019-04097-w>

Wu, Y., Ma, X., Guo, G., Huang, Y., Liu, M., Liu, S., Zhang, J., & Fan, J. (2023). Hybrid method for enhancing acoustic leak detection in water distribution systems: Integration of handcrafted features and deep learning approaches. *Process Safety and Environmental Protection*, 177, 1366–1376. <https://doi.org/10.1016/j.psep.2023.08.011>

Xu, M., Duan, L.-Y., Cai, J., Chia, L.-T., Xu, C., & Tian, Q. (2005). *HMM-based audio keyword generation*. 566–574.

Xu, T., Zeng, Z., Huang, X., Li, J., & Feng, H. (2021). Pipeline leak detection based on variational mode decomposition and support vector machine using an interior spherical detector. *Process Safety and Environmental Protection*, 153, 167–177. <https://doi.org/10.1016/j.psep.2021.07.024>

- Xu, W., Fan, S., Wang, C., Wu, J., Yao, Y., & Wu, J. (2022). Leakage identification in water pipes using explainable ensemble tree model of vibration signals. *Measurement*, *194*, 110996. <https://doi.org/10.1016/j.measurement.2022.110996>
- Yang, J., Wen, Y., & Li, P. (2008). *Leak acoustic detection in water distribution pipelines*. 3057–3061.
- Yang, J., Wen, Y., Li, P., & IEEE. (2010). *Approximate Entropy-based Leak Detection Using Artificial Neural Network in Water Distribution Pipelines* (WOS:000291559800178). 1029–1034.
- Yang, J., Wen, Y., Li, P., & Wang, X. (2013). Study on an improved acoustic leak detection method for water distribution systems. *Urban Water Journal*, *10*(2), 71–84. <https://doi.org/10.1080/1573062X.2012.699071>
- Yao, X.-J., Yi, T.-H., & Qu, C.-X. (2022). Autoregressive spectrum-guided variational mode decomposition for time-varying modal identification under nonstationary conditions. *Engineering Structures*, *251*, 113543. <https://doi.org/10.1016/j.engstruct.2021.113543>
- Yazdekhesti, S., Piratla, K. R., Atamturktur, S., & Khan, A. (2018). Experimental evaluation of a vibration-based leak detection technique for water pipelines. *Structure and Infrastructure Engineering*, *14*(1), 46–55. <https://doi.org/10.1080/15732479.2017.1327544>
- Yin, Y., Tang, Q., Liu, X., & Zhang, X. (2017). Water scarcity under various socio-economic pathways and its potential effects on food production in the Yellow River basin. *Hydrology and Earth System Sciences*, *21*(2), 791–804. <https://doi.org/10.5194/hess-21-791-2017>
- Yu, T., Chen, X., Yan, W., Xu, Z., & Ye, M. (2023). Leak detection in water distribution systems by classifying vibration signals. *Mechanical Systems and Signal Processing*, *185*, 109810. 2022-12-01. <https://doi.org/10.1016/j.ymsp.2022.109810>
- Yu, Y., Srivastava, A., & Canales, S. (2021). Conditional lstm-gan for melody generation from lyrics. *ACM Transactions on Multimedia Computing, Communications, and Applications (TOMM)*, *17*(1), 1–20.

- Yuriko Terao & Akira Mita. (2008). Robust water leakage detection approach using the sound signals and pattern recognition. *SPIE Proceedings*, 6932, 69322D. <https://doi.org/10.1117/12.775968>
- Zeng, W., Cazzolato, B., Lambert, M., Stephens, M., & Gong, J. (2022). Coherenceogram for leak detection in water pipes. *Journal of Sound and Vibration*, 530, 116979. <https://doi.org/10.1016/j.jsv.2022.116979>
- Zhang, C., Alexander, B. J., Stephens, M. L., Lambert, M. F., & Gong, J. (2023). A convolutional neural network for pipe crack and leak detection in smart water network. *Structural Health Monitoring*, 22(1), 232–244. <https://doi.org/10.1177/14759217221080198>
- Zhang, C., Alexander, B., Stephens, M., Lambert, M., & Gong, J. (n.d.). A convolutional neural network for pipe crack and leak detection in smart water network. *STRUCTURAL HEALTH MONITORING-AN INTERNATIONAL JOURNAL*. <https://doi.org/10.1177/14759217221080198>
- Zhang, C., Stephens, M., Lambert, M., Alexander, B., & Gong, J. (2022). Acoustic Signal Classification by Support Vector Machine for Pipe Crack Early Warning in Smart Water Networks. *Journal of Water Resources Planning and Management*, 148(7). [https://doi.org/10.1061/\(ASCE\)WR.1943-5452.0001570](https://doi.org/10.1061/(ASCE)WR.1943-5452.0001570)
- Zhang, G. P. (2003). Time series forecasting using a hybrid ARIMA and neural network model. *Neurocomputing*, 50, 159–175. [https://doi.org/10.1016/S0925-2312\(01\)00702-0](https://doi.org/10.1016/S0925-2312(01)00702-0)
- Zhang, H. (2004). The optimality of naive Bayes. *Aa*, 1(2), 3.
- Zhang, P., He, J., Huang, W., Zhang, J., Yuan, Y., Chen, B., Yang, Z., Xiao, Y., Yuan, Y., Wu, C., Cui, H., & Zhang, L. (2023). Water Pipeline Leak Detection Based on a Pseudo-Siamese Convolutional Neural Network: Integrating Handcrafted Features and Deep Representations. *Water*, 15(6), Article 6. <https://doi.org/10.3390/w15061088>
- Zhang, Q., Wu, Y. N., & Zhu, S.-C. (2018). Interpretable Convolutional Neural Networks. *2018 IEEE/CVF Conference on Computer Vision and Pattern Recognition*, 8827–8836. <https://doi.org/10.1109/CVPR.2018.00920>

- Zhang, X., Shi, J., Yang, M., Huang, X., Usmani, A. S., Chen, G., Fu, J., Huang, J., & Li, J. (2023). Real-time pipeline leak detection and localization using an attention-based LSTM approach. *Process Safety and Environmental Protection*, 174, 460–472. <https://doi.org/10.1016/j.psep.2023.04.020>
- Zhang, Y., Han, D., Tian, J., & Shi, P. (2023). Domain adaptation meta-learning network with discard-supplement module for few-shot cross-domain rotating machinery fault diagnosis. *Knowledge-Based Systems*, 268, 110484. <https://doi.org/10.1016/j.knosys.2023.110484>
- Zhao, B., Lu, H., Chen, S., Liu, J., & Wu, D. (2017). Convolutional neural networks for time series classification. *Journal of Systems Engineering and Electronics*, 28(1), 162–169. <https://doi.org/10.21629/JSEE.2017.01.18>
- Zhao, H., Qu, S., Liu, Y., Guo, S., Zhao, H., Chiu, A. C. F., Liang, S., Zou, J.-P., & Xu, M. (2020). Virtual water scarcity risk in China. *Resources, Conservation and Recycling*, 160, 104886. <https://doi.org/10.1016/j.resconrec.2020.104886>
- Zhao, L., & Zhang, Z. (2024). A improved pooling method for convolutional neural networks. *Scientific Reports*, 14(1), 1589. <https://doi.org/10.1038/s41598-024-51258-6>
- Zhao, S.-L., Liu, S.-G., Qiu, B., Hong, Z., Zhao, D., & Dong, L.-Q. (2023). Leak detection method of liquid-filled pipeline based on VMD and SVM. *Urban Water Journal*, 20(9), 1169–1182. <https://doi.org/10.1080/1573062X.2023.2251952>
- Zhou, B., Lau, V., & Wang, X. (2020). Machine-Learning-Based Leakage-Event Identification for Smart Water Supply Systems. *IEEE INTERNET OF THINGS JOURNAL*, 7(3), 2277–2292. <https://doi.org/10.1109/JIOT.2019.2958920>
- Zhou, M., Yang, Y., Xu, Y., Hu, Y., Cai, Y., Lin, J., & Pan, H. (2021). A Pipeline Leak Detection and Localization Approach Based on Ensemble TL1DCNN. *IEEE Access*, 9, 47565–47578. IEEE Access. <https://doi.org/10.1109/ACCESS.2021.3068292>